



**Carlos André
Soares Couto**

**Verificação da resistência ao fogo de elementos
metálicos com secção transversal de classe 4**

**Fire design of steel members with class 4
cross-section**



**Carlos André
Soares Couto**

**Verificação da resistência ao fogo de elementos
metálicos com secção transversal de classe 4**

Dissertação apresentada à Universidade de Aveiro para cumprimento dos requisitos necessários à obtenção do grau de Doutor em Engenharia Civil, realizada sob a orientação científica do Doutor Paulo Jorge de Melo Matias Faria de Vila Real, Professor Catedrático do Departamento de Engenharia Civil da Universidade de Aveiro e coorientação científica do Doutor Nuno Filipe Ferreira Soares Borges Lopes, Professor Auxiliar do Departamento de Engenharia Civil da Universidade de Aveiro e do Doutor Bin Zhao, Director do Research and Valorisation Department no Centre Technique Industriel de la Construction Métallique (CTICM), França.



**Carlos André
Soares Couto**

**Fire design of steel members with class 4
cross-section**

Thesis submitted to the University of Aveiro to fulfil the necessary requirements for the degree of Doctor of Philosophy in Civil Engineering, made under the scientific supervision of Doctor Paulo Jorge de Melo Matias Faria de Vila Real, Full Professor at the University of Aveiro and co-supervision of Doctor Nuno Filipe Ferreira Soares Borges Lopes, Assistant Professor at the University of Aveiro and Doctor Bin Zhao, Director of the Research and Valorisation Department at the Centre Technique Industriel de la Construction Métallique (CTICM), France.

A Deus
Aos meus Pais
À Sónia

Pelo amor incondicional

To God
To my Parents
To Sónia

For the unconditional love

o júri

presidente

Prof. Doutor Vitor Brás de Sequeira Amaral
professor catedrático da Universidade de Aveiro

Prof. Doutor Luís Alberto Proença Simões da Silva
professor catedrático da Faculdade de Ciências e Tecnologia, Universidade de Coimbra

Prof. Doutor Dinar Reis Zamith Camotim
professor catedrático do Instituto Superior Técnico, Universidade de Lisboa

Prof. Doutor František Wald
professor catedrático da Czech Technical University de Praga

Prof. Doutor Jean-Marc Franssen
professor catedrático Institut de Mécanique et Génie Civil, Universidade de Liège

Prof. Doutor Enrique Mirambell Arrizabalaga
professor catedrático da Escuela Técnica Superior de Ingenieros de Caminos, Canales y Puertos de Barcelona, Universidade Politècnica da Catalunya

Prof. Doutor Paulo Jorge de Melo Matias Faria de Vila Real
professor catedrático da Universidade de Aveiro

Prof. Doutor Nuno Miguel Rosa Pereira Silvestre
professor associado do Instituto Superior Técnico, Universidade de Lisboa

the jury

chairman

Prof. Doctor Vitor Brás de Sequeira Amaral
full professor at University of Aveiro

Prof. Doctor Luís Alberto Proença Simões da Silva
full professor at the Faculty of Science and Technology of the University of Coimbra

Prof. Doctor Dinar Reis Zamith Camotim
full professor at Superior Technical Institute at University of Lisbon

Prof. Doctor František Wald
full professor at Czech Technical University of Prague

Prof. Doctor Jean-Marc Franssen
full professor at Institut de Mécanique et Génie Civil, at University of Liege

Prof. Doctor Enrique Mirambell Arrizabalaga
full professor at Escuela Técnica Superior de Ingenieros de Caminos, Canales y Puertos de Barcelona, at Polytechnic University of Catalonia

Prof. Doctor Paulo Jorge de Melo Matias Faria de Vila Real
full professor at University of Aveiro

Prof. Doctor Nuno Miguel Rosa Pereira Silvestre
associate professor at Superior Technical Institute at University of Lisbon

agradecimentos

O trabalho realizado nesta dissertação não seria possível sem o apoio ímpar do Professor Doutor Paulo Vila Real, meu orientador, a quem estou profundamente grato pela excelência da sua supervisão. A partilha do seu saber e dos seus princípios morais, a sempre pronta disponibilidade e motivação, o compromisso e a dedicação a este trabalho foram um contributo imensurável para o desenvolvimento desta dissertação.

Ao Professor Doutor Nuno Lopes, meu coorientador, agradeço toda a disponibilidade e apoio, o sentido crítico que entregou a este trabalho permitiram elevar a sua qualidade e polir o seu resultado.

Ao Doutor Bin Zhao, coorientador deste trabalho, expresso igualmente a minha gratidão, pelas suas sugestões e recomendações que contribuíram de forma valiosa para este trabalho. Agradeço também o seu apoio nas condições oferecidas durante a estadia no CTICM.

Ao Departamento de Engenharia Civil da Universidade de Aveiro, nas pessoas dos seus diretores durante o desenvolvimento deste trabalho, Professor Doutor Paulo Cachim e Professor Doutor Paulo Vila Real, a quem agradeço pelas condições proporcionadas para a realização desta tese.

Aos colegas do CTICM pela simpatia e amizade com que fui recebido expresso a minha gratidão. Em particular, à Gisèle Bihina pelos importantes conhecimentos partilhados sobre o Cast3M e ao Arnaud Sanzel por toda a sua disponibilidade e ajuda na comparação dos modelos numéricos durante a estadia no CTICM e apoio prestado no decurso do projeto FIDESC4.

Ao Marc Braham, a quem agradeço a sempre agradável troca de ideias, tantas vezes além da engenharia, e que permitiram um conhecimento maior sobre as estruturas metálicas e a sua aplicação prática mas também sobre a vida.

Aos meus colegas de trabalho João Ferreira, Cláudia Amaral, Élio Maia, Thiago Silva, André Reis, Flávio Arrais, Pedro Duarte e Hugo Rodrigues, fico grato por toda a indispensável ajuda e constante incentivo.

Aos meus tios, José Manuel e Launay Mireille, pela hospitalidade e amizade com que me receberam em sua casa durante a estadia no CTICM em Paris. Os laços que se fortaleceram vão muito para além do propósito deste trabalho dando-lhe um outro significado, muito especial e enriquecedor.

À minha família e amigos que com assinalável compreensão aceitaram a minha frequente ausência durante o desenvolvimento desta dissertação. A sua amizade foi tantas vezes a energia que precisava e que agradeço. Em especial, aos meus irmãos Pedro e Mário, expresso o meu profundo agradecimento por todo o apoio e afeto inestimável.

Aos meus pais João Carlos e Maria Celeste, que graças aos seus bondosos valores são, e serão sempre, uma fonte de inspiração e exemplo. Agradeço do coração o amor incondicional que me presenteiam diariamente e que me motiva para superar os obstáculos deste caminho, e também todos os ensinamentos que me transmitem e que permitem crescer como pessoa e como homem.

À Sónia, por ser o pilar. O seu amor, apoio e compreensão foram os alicerces que ajudaram a que tudo isto acontecesse e fizesse sentido. As suas palavras conselheiras e de incentivo foram um suporte constante fazendo-me acreditar e manter o foco nos objetivos. A amizade, a dedicação e carinho sempre presentes deram um contributo muito especial para que esta obra se concretizasse. O meu sincero agradecimento por tudo isto e pelo somatório de todas as outras pequenas coisas.

Muito obrigado.

acknowledgements

The work done in this thesis would not be possible without the unique support of Professor Paulo Vila Real, my supervisor, to whom I am deeply grateful for the excellence of his supervision. The sharing about his knowledge and his moral principles, the always prompt availability and motivation, commitment and dedication to this work were an immeasurable contribution to the development of this thesis.

To Professor Nuno Lopes, my co-supervisor, I thank all the availability and support, the critical sense employed in this thesis allowed to raise its quality and polish its result.

To Dr. Bin Zhao, co-supervisor of this work, I wish also to express my gratitude for his suggestions and recommendations that have contributed in a valuable way for this work. I also wish to express my gratitude for his support in the conditions offered during the stay at CTICM.

The Department of Civil Engineering at the University of Aveiro, in the persons of its directors during the development of this work, Professor Paulo Cachim and Professor Paulo Vila Real, whom I thank for the conditions provided to carry out this thesis.

To the colleagues from CTICM for the sympathy and friendship with which I was received I want to express my gratitude. In particular, to Gisèle Bihina for the important knowledge shared about Cast3M and to Arnaud Sanzel throughout his availability and help in the comparison of numerical models during the stay at CTICM and support provided during the development of FIDESC4 project.

To Marc Braham, whom I thank for the pleasant exchange of ideas, often beyond engineering and which enabled a better understanding about steel structures and their practical application but also about life.

To my colleagues João Ferreira, Claudia Amaral, Élio Maia, Thiago Silva, André Reis, Flávio Arrais, Pedro Duarte and Hugo Rodrigues, I am grateful for all their indispensable help and constant encouragement.

To my uncles, José Manuel and Launay Mireille, for the hospitality and friendship that welcomed into their home while staying at the CTICM in Paris. The bonds that have been strengthened extend far beyond the scope of this work giving it another meaning, very special and enriching.

To my family and friends with remarkable understanding they accepted my frequent absence during the development of this thesis. Their friendship was so often the energy needed and for which I express my gratitude. In particular, my brothers Pedro and Mário, I express my deep thankfulness for all the support and inestimable affection.

To my parents João Carlos and Maria Celeste, who thanks to their benevolent values are, and always will be, a source of inspiration and example. I thank them from the heart for their unconditional love in every day that motivates me to overcome all the obstacles of the journey, and also all the teachings that allow me to grow as a person and as a man.

To Sónia, for being the pillar. Her love, support and understanding were the foundations that helped all this happen and have meaning. Her counsellor's words and encouragement have been a constant support, making me believe and stay focused on the objectives. The friendship, dedication and always present affection gave a very special contribution to this work and made it a reality. My sincere thanks for all this and the sum of all the other little things.

Thank you.

palavras-chave

Classe 4, secções transversais de parede fina, secções esbeltas, encurvadura local, encurvadura lateral, flexão composta com compressão, viga, viga-coluna, comportamento ao fogo, Eurocódigos.

resumo

A presente tese resulta de um trabalho de investigação com o propósito de aumentar o conhecimento do comportamento ao fogo de elementos metálicos com secção transversal de Classe 4, ou seja, suscetíveis à ocorrência de fenómenos de encurvadura local.

Os elementos metálicos com secção transversal de Classe 4 são amplamente utilizados na construção metálica por serem soluções bastante atrativas em termos de eficiência e economia de material. No entanto, a verificação da resistência ao fogo destes elementos carece de fórmulas simplificadas que se adequem à mais-valia proporcionada por este tipo de solução.

O principal objetivo desta dissertação foca-se no desenvolvimento de metodologias de cálculo para verificação da resistência ao fogo de elementos metálicos com secção transversal de Classe 4 com base em estudos numéricos realizados com elementos finitos de casca recorrendo ao programa SAFIR através de análises material e geometricamente não lineares (GMNIA - geometrically and material non-linear analysis with imperfections).

É demonstrado nesta tese que, as fórmulas atualmente propostas no Eurocódigo 3 para verificação da resistência ao fogo de elementos de Classe 4 em situação de incêndio podem ser melhoradas.

No que diz respeito à capacidade resistente da secção transversal, a metodologia atual do Eurocódigo 3 subestima a resistência das secções quando constituídas simultaneamente por placas de Classe 4 e de outras classes. Por outro lado, mostra-se que os fenómenos de encurvadura local afetam também as secções de Classe 3 a altas temperaturas. Neste trabalho, ambas as classes foram tratadas como secções transversais esbeltas, tendo sido propostas novas fórmulas para o seu cálculo em situação de incêndio.

No caso de vigas com secção transversal esbelta, observa-se que as formulações preconizadas no Eurocódigo 3 são também inadequadas. A proposta para o cálculo da resistência da secção transversal desenvolvida neste trabalho conduz a melhorias na verificação da segurança ao fogo destes elementos mas, não obstante, propõe-se novas expressões que consideram a interação entre a encurvadura local e o fenómeno de encurvadura lateral que ocorre nestas vigas. Assim desenvolveu-se um parâmetro de secção efetiva cuja utilização permite uma verificação ao fogo da encurvadura lateral mais eficiente.

Por fim, estudam-se as vigas-coluna com secção transversal esbelta, concluindo-se que as fórmulas de interação do Eurocódigo 3 conduzem simultaneamente a resultados muito conservativos ou fora da segurança. Observou-se que este comportamento se deve essencialmente ao cálculo dos fatores de redução para o comportamento de coluna e viga, mas por outro lado, houve a necessidade de alterar os fatores de interação das curvas para que a verificação da resistência ao fogo destes elementos fosse mais segura.

keywords

Class 4, thin-walled steel sections, slender cross-sections, local buckling, lateral-torsional buckling, combined bending and compression, beam, beam-column, fire behaviour, Eurocodes

abstract

This thesis is the result of a research work with the purpose of increasing the knowledge on the fire behaviour of steel members with Class 4 cross-section, that is, prone to the occurrence of local buckling phenomena.

Steel members with Class 4 cross-section due to their advantages regarding their lightness and efficiency are widely used in steel constructions. However, the verification of the fire resistance of these elements lacks simplified formulas that are in agreement with the added value provided by this type of solutions.

The main objective of this thesis aims to develop improved structural fire design rules for the stability check of steel members with Class 4 cross-section based on numerical investigation with shell finite elements carried out with the software SAFIR by performing geometrically and material non-linear analysis with imperfections (GMNIA).

It is demonstrated in this work that, the existing design rules preconized proposed in Eurocode 3 for the design of steel members with Class 4 cross-section in case of fire could be improved.

In what concerns the cross-sectional capacity, the present methodology of Eurocode 3 underestimates the resistance of the sections when they are built up simultaneous of Class 4 plates and plates of other classes. Moreover, it is demonstrated that local buckling affects also Class 3 cross-sections in case of fire. Thus, in this work, both classes are treated as slender cross-sections and proposals are made for new rules to calculate their capacity in fire situation.

For beams with slender cross-sections, it is concluded that the formulae available in Eurocode 3 are also inadequate. The new proposal for the cross-sectional resistance calculation leads to improvements in terms of the fire design of these members but, nonetheless, new expressions are proposed that account for the interaction between local buckling and lateral-torsional buckling that occurs in these beams. Accordingly, the effective section factor was developed allowing a better design against lateral-torsional buckling of on beams with slender cross-sections in case of fire.

Finally, beam-columns with slender cross-sections are studied, and it is concluded that the present interaction formulae provided by Eurocode 3 leads simultaneous to very conservative or unsafe results. It was observed that this was mainly due to the calculation of the reduction factors for the beam and column behaviour, but besides that, there was the need to change the interaction factors so that the design rules to assess the mechanical resistance of beam-columns in case of fire be safer.

Contents

Chapter 1	Introduction.....	1
1.1	Background and motivation	3
1.2	Objectives and Research Programme.....	4
1.3	Outline of the Thesis.....	6
1.4	List of publications resulting from the thesis.....	10
	References	11
Chapter 2	Plates	13
2.1	Introduction.....	15
2.2	Actual design provisions of Eurocode 3 to take into account local buckling.....	17
2.2.1	Effective width method	17
2.2.2	Cross-section classification.....	19
2.2.2.1	At normal temperature	19
2.2.2.2	In fire situation	20
2.2.3	Code provisions for local buckling at elevated temperatures.....	21
2.3	Numerical study of plates	23
2.3.1	Numerical model	23
2.3.1.1	Validation of the numerical model with experimental results.....	25
2.3.2	Results at normal temperature.....	28
2.3.2.1	Elements under compression	28
2.3.2.2	Elements under bending.....	33
2.3.3	Results at elevated temperatures	36
2.3.3.1	Elements under compression	36
2.3.3.2	Elements under bending.....	41
2.4	New proposal.....	44
2.4.1	Results for plates under compression.....	49
2.4.2	Results for plates under bending	52
2.5	Conclusions	54
	References	56
Chapter 3	Cross-sections.....	59
3.1	Introduction.....	61

3.2	Design provisions to take local buckling into account in the cross-sectional resistance according to Eurocode 3	63
3.2.1	Cross-section classification	63
3.2.2	The effective width method from Eurocode 3	67
3.2.3	Code provisions for local buckling at elevated temperatures	68
3.3	New proposal to calculate the effective width at elevated temperatures	70
3.4	Simple design methods to calculate the cross-sectional resistance at elevated temperatures	73
3.5	Numerical model	75
3.5.1	Material properties	75
3.5.2	Support conditions	76
3.5.3	Loading	76
3.5.4	Imperfections	77
3.6	Numerical study	77
3.6.1	Cross-sections	78
3.6.2	Results and comparison to simple design methods	80
3.6.2.1	Elements in compression	80
3.6.2.2	Elements in bending about the major-axis	84
3.6.3	Statistical investigation of the proposed methodologies	90
3.7	Comparison with experimental results	92
3.8	Conclusions.....	95
	References	97
Chapter 4	Beams.....	101
4.1	Introduction	103
4.2	Lateral-torsional buckling of beams with Class 3 and 4 cross-section at elevated temperatures	106
4.2.1	Eurocode 3 Part 1-2.....	106
4.2.2	Using a new methodology to calculate the cross-sectional resistance.....	107
4.3	Numerical model	109
4.4	Comparison of FEA results with current beam design curve of the Eurocode 3.....	112
4.5	Parametric Study.....	116
4.5.1	The Effective Section Factor concept and its influence	116
4.5.2	Temperature influence.....	119
4.5.3	Residual stresses influence	122

4.5.4	Steel grade influence	123
4.5.5	Depth-to-width ratio influence	125
4.6	New design curve	127
4.7	Non-uniform bending diagrams	133
4.7.1	Uniformly distributed load.....	134
4.7.2	End-moments.....	136
4.8	Statistical evaluation.....	140
4.9	Conclusions	142
References		144
Chapter 5 Beam-columns		149
5.1	Introduction.....	151
5.2	The code provisions of Part 1-2 of Eurocode 3	152
5.3	Numerical study.....	154
5.3.1	Numeric model.....	155
5.3.2	Geometric and material imperfections	155
5.3.3	Cases studied	157
5.4	Results.....	158
5.4.1	In-plane behaviour	158
5.4.2	Calibration of in-plane interaction factor.....	162
5.4.3	Out-of-plane behaviour	167
5.4.4	Calibration of out-of-plane interaction factor	170
5.5	Statistical evaluation.....	175
5.6	New proposal according to the developments of this thesis.....	176
5.7	Conclusions	178
References		180
Chapter 6 Conclusions		183
6.1	General description of the work developed	185
6.2	Chapter 2 – Plates.....	186
6.3	Chapter 3 – Cross-sections	188
6.4	Chapter 4 – Beams.....	190
6.5	Chapter 5 – Beam-Columns	191
6.6	Future developments.....	193
References		195

List of figures

Figure 1.1: Example of local buckling of a beam after an experimental test at 450°C carried out at Czech Technical University [1.3].	4
Figure 1.2: Local and global buckling on a beam-column tested at elevated temperatures carried out at University of Liège [1.3].	5
Figure 2.1: Stress distribution on a rectangular plate in the post-buckling regime.	17
Figure 2.2: Effective width b_{eff} concept.	18
Figure 2.3: Ratio $\sqrt{k_{E,\theta}/k_{y,\theta}}$ as a function of the temperature.	21
Figure 2.4: Reductions factors for the mechanical properties of carbon steel at elevated temperatures according to Part 1-2 of Eurocode 3.	22
Figure 2.5: Example of the numerical model used to calculate the ultimate strength of a simply-supported plate in 3 sides – outstand element.	24
Figure 2.6: Pattern of the residual stresses considered.	25
Figure 2.7: Comparison between the results obtained with the numerical model and the experimental results of other authors [2.10, 2.23, 2.25, 2.26].	27
Figure 2.8: Comparison between the results predicted by the Eurocode 3 and the experimental results of other authors [2.10, 2.23, 2.25, 2.26].	28
Figure 2.9: Ultimate strength of plates simply supported in 3 sides (outstand element) at normal temperature under compression.	29
Figure 2.10: Influence of the residual stresses in the ultimate strength of a simply supported plate in 3 sides (outstand element) under compression at normal temperature.	30
Figure 2.11: Ultimate strength of a plate simply supported in 4 sides (internal element) at normal temperature submitted to compression.	31
Figure 2.12: Ultimate strength of a plate simply supported in 4 sides (internal element) under compression at normal temperature using a less severe geometrical imperfection.	32
Figure 2.13: Influence of the residual stresses in the ultimate strength of simply supported plate in 4 sides (internal element) under compression at normal temperature.	33
Figure 2.14: Deformed shape at the collapse of simply supported plates.	33
Figure 2.15: Ultimate strength of a plate simply supported in 4 sides at normal temperature under bending.	34

Figure 2.16: Influence of the residual stresses in the ultimate strength of stiffened plates under bending at normal temperature.	35
Figure 2.17: Ultimate strength of a plate simply supported in 3 sides (outstand element) at elevated temperatures under compression.	38
Figure 2.18: Ultimate strength of a plate simply supported in 4 sides (internal element) at elevated temperatures under compression.	40
Figure 2.19: Influence of the residual stresses in the ultimate strength of outstand plates under compression at elevated temperature for steel grade S355.	41
Figure 2.20: Ultimate strength of a plate simply supported in 4 sides at elevated temperatures under bending.	43
Figure 2.21: New proposed design curves for outstand elements under compression for steel grade S355.	46
Figure 2.22: New proposed design curves for internal elements under compression for steel grade S355.	46
Figure 2.23: New proposed design curves for internal elements under bending for steel grade S355.	47
Figure 2.24: Comparison of the new simplified proposal with the actual design curves of Eurocode 3 for outstand elements under compression for steel grade S355.	47
Figure 2.25: Comparison of the new simplified proposal with the actual design curves of Eurocode 3 for internal elements under compression for steel grade S355.	48
Figure 2.26: Comparison of the new simplified proposal with the actual design curves of Eurocode 3 for internal elements under bending for steel grade S355.	48
Figure 2.27: Results of numerical study of simply supported plates on 3 sides at elevated temperature for steel grade S235 under compression and comparison to the new proposal.	49
Figure 2.28: Results of numerical study of simply supported plates on 3 sides at elevated temperature for steel grade S355 under compression and comparison to the new proposal.	49
Figure 2.29: Results of numerical study of simply supported plates on 3 sides at elevated temperature for steel grade S460 under compression and comparison to the new proposal.	50
Figure 2.30: Results of numerical study of simply supported plates on 4 sides at elevated temperature for steel grade S235 under compression and comparison to the new proposal.	50

Figure 2.31: Results of numerical study of simply supported plates on 4 sides at elevated temperature for steel grade S355 under compression and comparison to the new proposal..... 51

Figure 2.32: Results of numerical study of simply supported plates on 4 sides at elevated temperature for steel grade S460 under compression and comparison to the new proposal..... 51

Figure 2.33: Results of numerical study of simply supported plates on 4 sides at elevated temperature for steel grade S235 under bending and comparison to the new proposal. 52

Figure 2.34: Results of numerical study of simply supported plates on 4 sides at elevated temperature for steel grade S355 under bending and comparison to the new proposal. 53

Figure 2.35: Results of numerical study of simply supported plates on 4 sides at elevated temperature for steel grade S460 under bending and comparison to the new proposal. 53

Figure 3.1: Stress-strain relationship for carbon steel at elevated temperatures [3.4]. 61

Figure 3.2: Example of column showing local buckling from a test performed at elevated temperatures at the University of Liège (taken from[3.13])...... 62

Figure 3.3: Moment-rotation curves for different cross-section classification (adapted from [3.4])..... 64

Figure 3.4: Ratios $\sqrt{k_{E,\theta}/k_{y,\theta}}$ and $\sqrt{k_{0.2p,\theta}/k_{E,\theta}}$ as a function of the temperature. 66

Figure 3.5: Plate reduction factor for internal and outstand elements. 68

Figure 3.6: Comparison between the Full proposal and Simple proposal for internal elements (steel grade S355)..... 72

Figure 3.7: Comparison between the Full proposal and Simple proposal for outstand elements (steel grade S355)..... 72

Figure 3.8: Illustration of the numerical model..... 76

Figure 3.9: Load modelling..... 77

Figure 3.10: Different combinations of the cross-section dimensions (in mm) analysed under compression at elevated temperatures (o – S235; × – S355; □ – S460)..... 79

Figure 3.11: Different combinations of the cross-section dimensions (in mm) analysed under bending about the major-axis at elevated temperatures (o – S235; × – S355; □ – S460). 79

Figure 3.12: Number and classification of cross-sections used in the numerical study. .. 80

Figure 3.13: Cross-sectional resistance of Class 3 and Class 4 members submitted to compression at elevated temperatures. Comparison between FEA and Part 1-2 of Eurocode 3.....	81
Figure 3.14: Deformed shape ($\times 5$) at the collapse for a Class 3 profile (I450 \times 18+450 \times 30, steel grade S460) at 450°C.....	82
Figure 3.15: Deformed shape ($\times 5$) at the collapse for a Class 4 cross-section but with Class 1 flanges (I450 \times 4+150 \times 11, steel grade S235) at 450°C.....	83
Figure 3.16: Cross-sectional resistance of Class 3 and Class 4 members submitted to compression at elevated temperatures. Comparison between FEA and the Full Proposal.....	83
Figure 3.17: Cross-sectional resistance of Class 3 and Class 4 members submitted to compression at elevated temperatures. Comparison between FEA and the Simple Proposal.....	84
Figure 3.18: Cross-sectional resistance of Class 3 and Class 4 I-shaped profiles under bending about the major axis at elevated temperatures. Comparison between FEA and Part 1-2 of Eurocode 3.....	85
Figure 3.19: Moment-rotation curve at elevated temperatures for an element submitted to bending about the major-axis with a cross-section classified as Class 4 with a fully effective flange (with $h_w = 450$ mm, $b_f = 150$ mm, $t_w = 3.5$ mm and $t_f = 11$ mm). Steel grade S355.....	87
Figure 3.20: Moment-rotation curve at high temperatures for an element submitted to bending about major-axis with Class 3 cross-section ($h_w=450$ mm, $b_f=150$ mm, $t_w=6$ mm and $t_f=11$ mm). Steel grade S355.	88
Figure 3.21: Cross-sectional resistance of Class 3 and Class 4 I-shaped profiles under bending about the major axis at elevated temperatures. Comparison between FEA and the Full Proposal.	89
Figure 3.22: Cross-sectional resistance of Class 3 and Class 4 I-shaped profiles under bending about the major axis at elevated temperatures. Comparison between FEA and the Simple Proposal.	89
Figure 3.23: Comparison between the New proposal (Full and Simple) and experimental results from other authors [3.27, 3.28].	93
Figure 3.24: Comparison between Part 1-2 of Eurocode 3 (EN1993-1-2) provisions and experimental results from other authors [3.27, 3.28].....	94
Figure 4.1: Stress-strain relationship for carbon steel at elevated temperatures [4.14]..	105
Figure 4.2: Illustration of the boundary conditions in the numerical model.	110

Figure 4.3: Shape of eigenmodes for imperfection consideration. 111

Figure 4.4: Pattern of the residual stresses considered in this study. 111

Figure 4.5: Comparison of actual LTB design curve of EN1993-1-2 and FEA simulations.
..... 113

Figure 4.6: Accuracy of the LTB design curve from EN1993-1-2 compared to FEA results
with cross-sectional resistance calculated according to EN1993-1-2..... 114

Figure 4.7: Comparison of actual LTB design curve of EN1993-1-2 with cross-sectional
calculated according to Simple proposal from Chapter 3 (see equation (4.9)) and FEA
simulations..... 115

Figure 4.8: Accuracy of the LTB design curve from EN1993-1-2 compared to FEA results
with cross-sectional resistance calculated according to Simple proposal from Chapter
3..... 115

Figure 4.9: LTB behaviour of beams with effective section factor of $W_{eff,y}/W_{el,y} \leq 0.8$ 117

Figure 4.10: LTB behaviour of beams with effective section factor of $0.8 < W_{eff,y}/W_{el,y} \leq 0.9$.
..... 117

Figure 4.11: LTB behaviour of beams with effective section factor of $W_{eff,y}/W_{el,y} > 0.9$.. 118

Figure 4.12: Influence of the temperature on the LTB resistance of the beams with cross-
section 450×6+150×15, effective section factor $W_{eff,y}/W_{el,y} = 0.96$ 120

Figure 4.13: Influence of the temperature on the LTB resistance of the beams with cross-
section 450×4+150×10, effective section factor $W_{eff,y}/W_{el,y} = 0.85$ 120

Figure 4.14: Influence of the temperature on the LTB resistance of the beams with cross-
section 450×6+150×8, effective section factor $W_{eff,y}/W_{el,y} = 0.73$ 121

Figure 4.15: Influence of the temperature on the LTB resistance of the beams with cross-
section 450×4+150×5, effective section factor $W_{eff,y}/W_{el,y} = 0.60$ 121

Figure 4.16: Influence of the residual stresses on the LTB resistance of a) hot-rolled and
b) welded beams with slender cross-section. 122

Figure 4.17: LTB behaviour of beams with effective section factor of $W_{eff,y}/W_{el,y} \leq 0.8$ for
different steel grades. 125

Figure 4.18: Influence of the depth-to-width ratio on the LTB resistance of beams with
different effective section factor. Steel grade S355. 127

Figure 4.19: New design curve for beams with slender cross-sections at elevated
temperatures (S235)..... 129

Figure 4.20: Variation of new design curve (L1) with the steel grade..... 129

Figure 4.21: Comparison between the new design curve the beam with cross-section 450×6+150×15, effective section factor $W_{eff,y}/W_{el,y} = 0.96$	130
Figure 4.22: Comparison between the new design curve the beam with cross-section 450×4+150×10, effective section factor $W_{eff,y}/W_{el,y} = 0.85$	130
Figure 4.23: Comparison between the new design curve the beam with cross-section 450×6+150×8, effective section factor $W_{eff,y}/W_{el,y} = 0.73$	131
Figure 4.24: Comparison between the new design curve the beam with cross-section 450×4+150×5, effective section factor $W_{eff,y}/W_{el,y} = 0.60$	131
Figure 4.25: Accuracy of the new design curve compared to FEA results with cross-sectional resistance calculated according to Simple proposal from Chapter 3.	132
Figure 4.26: Comparison of the new proposal with factor “ ρ ” for distributed load.....	135
Figure 4.27: Comparison of the new proposal with factor “ ρ ” for triangular bending moment.	137
Figure 4.28: Comparison of the new proposal with factor “ ρ ” for bi-triangular bending moment.	138
Figure 4.29: Comparison of the new proposal with factor “ ρ ” modified for the bi-triangular bending moment case using equation (4.20).	140
Figure 5.1: Buckling modes in a laterally unrestrained steel beam-column with Class 4 cross-section subjected to in-plane bending moment.	156
Figure 5.2: Pattern of the residual stresses considered in this study for welded profiles.	157
Figure 5.3: Additional lateral restraints added to the model to prevent the out-of-plane displacements.	159
Figure 5.4: Comparison of interaction curve and the numerical cases studied for the in-plane behaviour in terms of non-dimensional slenderness.	159
Figure 5.5: Comparison of interaction curve and the numerical cases studied for the in-plane behaviour in terms of the applied bending moment.	160
Figure 5.6: Comparison of the reduction factor for the column behaviour obtained numerically and according to EN1993-1-2.	160
Figure 5.7: Comparison of interaction curves and the numerical cases studied.....	161
Figure 5.8: Calibration of the factor μ_y for the in-plane behaviour of beam-columns considering different loading cases at 450°C.....	163

Figure 5.9: Interaction curves for a beam-column with $L=18\text{m}$ ($\bar{\lambda}_{y,\theta} \approx 1.0$) and cross-section I450×4+150×5 at elevated temperatures. 164

Figure 5.10: Interaction curves for different moment distribution for in-plane buckling. . 165

Figure 5.11: Improvement of the in-plane interaction curve for the bi-triangular cases.. 166

Figure 5.12: Comparison of interaction curves and the numerical cases studied considering μ_y from equation (5.9). 166

Figure 5.13: Comparison of interaction curve and the numerical cases studied for the out-of-plane behaviour in terms of non-dimensional slenderness. 167

Figure 5.14: Comparison of interaction curve and the numerical cases studied for the out-of-plane behaviour in terms of the applied bending moment. 168

Figure 5.15: Comparison of the numerical results with the reduction factor for flexural buckling about the minor-axis. 168

Figure 5.16: Comparison of the numerical results with the reduction factor for lateral-torsional buckling a) function of the temperature and b) function of the moment distribution. 169

Figure 5.17: Comparison of interaction curves and the numerical cases studied with reduction factors according to equations (5.10) and (5.11). 170

Figure 5.18: Calibration of the factor μ_{LT} for the out-of-plane behaviour of beam-columns considering different loading cases for different temperatures. 172

Figure 5.19: Interaction curves for a beam-column with $L=1.5\text{m}$ ($\bar{\lambda}_{z,\theta} \approx 0.50$) and cross-section I450×4+150×5 at elevated temperatures. 173

Figure 5.20: Interaction curves for different moment distribution for out-of-plane buckling. 173

Figure 5.21: Improvements of the out-of-plane interaction curve for the bi-triangular cases. 174

Figure 5.22: Comparison of interaction curve and the numerical cases studied using μ_{LT} from equation (5.13). 174

List of tables

Table 2.1: Slenderness limits (b/t) for the plates for cross-sectional classification at normal temperature.....	20
Table 2.2: Non-dimensional slenderness limits of the plates for cross-sectional classification at normal and elevated temperature.....	21
Table 2.3: Comparison of experimental results on the ultimate compressive strength of steel sections with thin-plates with the values predicted by the numerical model and the Eurocode 3 for a different set of temperatures.....	26
Table 2.4: Comparison of experimental results on the ultimate bending strength of steel sections with thin-plates with the values predicted by the numerical model and the Eurocode 3 for a different set of temperatures.....	27
Table 2.5: Coefficients to be used in equations (2.13) and (2.14).....	44
Table 2.6: Coefficients to be used in equations (2.13) and (2.14) by conservatively adopting a steel temperature of $\theta_a = 700^\circ\text{C}$	45
Table 3.1: Slenderness limits (b/t) for the plates for cross-sectional classification at normal temperature.....	65
Table 3.2: Coefficients to be used in equations (3.8) and (3.9).....	70
Table 3.3: Summary of methodologies to calculate the cross-sectional compression resistance at elevated temperatures.	73
Table 3.4: Summary of methodologies to calculate the cross-sectional bending resistance at elevated temperatures.	74
Table 3.5: Statistical results for each of the methodologies.....	91
Table 3.6: Comparison of the proposed methodologies against experimental results [3.27] for compression.....	92
Table 3.7: Comparison of the proposed methodologies against experimental results [3.28] for bending about major-axis.....	93
Table 4.1: Cases considered in the numerical study.....	112
Table 4.2: Geometry and classification of cross-sections in fire.	113
Table 4.3: Cross-sections considered in the study of the influence of the temperature on the LTB resistance.	119
Table 4.4: Parameters for the new design curve of beams with slender cross-sections and criteria for selection.	128
Table 4.5: Correction factors k_c	133

Table 4.6: Statistical results of beams submitted to uniform bending diagrams.	141
Table 4.7: Statistical results of beams submitted to non-uniform bending diagrams.	142
Table 5.1: Equivalent uniform moment factor for the cases studied.	154
Table 5.2: Summary of the cases analysed (steel grade S355).	158
Table 5.3: Statistical results of beam-columns in fire situation	176
Table 5.4: Statistical results for the new proposals.....	177
Table 5.5: Statistical results according to Eurocode 3 Part 1-2	178

Chapter 1 Introduction

Chapter outline

- 1.1 Background and motivation
 - 1.2 Objectives and research Programme
 - 1.3 Outline of the thesis
 - 1.4 List of publications resulting from the thesis
- References

Abstract This chapter presents the introductory aspects of the research conducted within the PhD work. The background and the motivation are firstly addressed followed by the objectives and some key aspects of the research programme that was undertaken. The final part of the chapter is reserved to the outline of the whole document and a brief description about each chapter organization.

1.1 Background and motivation

Steel members with H or I shape Class 4 cross-sections are widely used in steel constructions due to their advantages regarding their lightness and efficiency. In terms of its design in case of fire, the Eurocode 3 Part 1-2 [1.1] provides simple calculation rules for the determination of the mechanical resistance. However, according to recent numerical investigations [1.2], these rules for Class 4 members with H and I shape proved to be not very accurate and too conservative. The main reason for that lies in the fact that these rules were developed for Class 1 or 2 members in case of fire and its accuracy for the fire design of Class 4 members still needs to be checked or improvements of those rules can still be developed.

Nevertheless, some recommendations are given for the fire design of Class 4 cross-sections in the informative Annex E of Part 1-2 of Eurocode 3 in order to account for local buckling. In this annex, it is suggested that the design yield strength of steel should be taken as the 0.2% proof strength instead of the stress at 2% total strain as for the other classes design and that the effective cross-section be determined as for normal temperature, that is with the properties at normal temperature. However, as mentioned before, it has been demonstrated through numerical investigations [1.2], that this methodology is conservative and leads to uneconomical results. Moreover, the fire regulations of certain European countries have a fire resistance requirement of 15 minutes under ISO fire condition for buildings with large spans (for example, industrial halls) where Class 4 steel members are mostly used [1.3]. Part 1-2 of Eurocode 3 suggests a default critical temperature of 350 °C if no fire design is made, which means that even for a requirement of 15 minutes of fire resistance, passive fire protection must be used. The use of such prescriptive rules should be replaced with much more realistic fire design rules to allow real fire safety engineering.

Some studies have been done previously within the scope of one research project [1.4], for welded or hot-rolled Class 4 steel members. This type of study is very limited and cover only, for example, the buckling of Class 4 steel columns [1.5–1.8] or is related to other types of steel, for example stainless steels [1.9], for which the constitutive laws differ from carbon steel. Thus, more studies must be carried out and practical and precise design rules be developed.

1.2 Objectives and Research Programme

The main objective of this thesis is to study and to develop simple rules for fire design of steel members with Class 4 cross-sections, in particular for beams and beam-columns as close as possible to the principles of design rules of Eurocode 3 at room temperature.

The influence of local buckling (see Figures 1.1-1.2) on the capacity of the members is investigated and addressed. For that purpose, the work has been divided according to the scale of the elements by its increasing dimension or complexity: thin plates, cross-sections, beams and finally beam-columns, which are analysed separately and constitute the subject of chapter's two to five. Columns have not been incorporated in this work since this thesis was developed within the scope of the EU research project FIDESC4 being this particular subject addressed by other project partners. Albeit the author did not contribute directly to this study, the contributions highlighted in this thesis regarding the calculation of thin-plates and the cross-section capacity together with the existing formulae of the Eurocode 3 Part 1-2 demonstrated to be sufficient to address the resistance of the columns with slender cross-sections in case of fire.



Figure 1.1: Example of local buckling of a beam after an experimental test at 450°C carried out at Czech Technical University [1.3].



Figure 1.2: Local and global buckling on a beam-column tested at elevated temperatures carried out at University of Liège [1.3].

More particularly, the study of thin-plates in case of fire has the objective of studying the influence of local buckling on the reduction of the plate capacity at high temperature and, thus, to determine if the existing rules to calculate the effective width of the plates at normal temperature can be used under fire situation and adapt those rules as necessary to account for the effect of the temperature. Following, the study is directed to the cross-section behaviour in case of fire. The objective is to study cross-sections prone to local buckling at elevated temperature and establish a methodology to assess its capacity under fire situation. For the resistance of members with Class 4 cross-sections, this thesis addresses beams and beams-columns. For the first, the accuracy of existing design rules of Eurocode 3 is identified. The influence of local buckling in the response of laterally unrestrained steel beams against lateral-torsional buckling is study in order to develop more accurate design rules. Secondly, the determination of the accuracy of existing interaction curve of Eurocode 3 to the fire design of steel beam-columns in case of fire is investigated so that the accuracy is established and more accurate design rules are developed.

To accomplish these objectives, first a literature review is made. However, the subject of this thesis has not been addressed by many researchers in the past and therefore the existing literature is noticeably scarce. After, a numerical investigation is performed to assess the validity of existing design rules and to serve as the basis of the development of new rules. GMNIA (geometrical and material non-linear analysis with imperfections) analyses are carried out with the finite element software SAFIR [1.10] using shell finite elements. The definition of the numerical model, namely the material model, the boundary conditions, the geometric and material imperfections and the model for the application of the loads is made

according to the literature. The validation of the numerical model is based on reference results (both numerical and experimental) found in the literature and on the fire tests developed within the European Research Project FIDESC4 “Fire Design of Steel Members with Welded or Hot-Rolled Class 4 Cross-Section” as this thesis is under the scope of that project. Finally, new rules are developed and validated against numerical and experimental results available.

1.3 Outline of the Thesis

This thesis is organized into six chapters describing the research conducted in this PhD thesis. A first introductory chapter is followed by four chapters with the subject addressed within each of which increases in scale gradually: Chapter 2 presents a study at elevated temperatures on the thin plates that form slender cross-section, followed by the study of the capacity of slender cross-sections under fire situation (Chapter 3), and then, on a member level by the study of the beams (Chapter 4) and finally the study of the beam-columns (Chapter 5). General conclusions and final remarks are presented in the last chapter of this work. The organization of each chapter is presented next in more detail.

The **first chapter** serves as the introduction to the thematic addressed in this work. The purpose, meaning and objectives are highlighted, as well as brief description of the research programmed that was followed in order to accomplish those objectives. In the final part, the outline and organization of the thesis is detailed.

The **second chapter** corresponds to the study of individual thin steel plates that form the slender cross-sections and how local buckling influences its capacity at elevated temperature. A revision on the existing literature to account for the effect of local buckling at elevated temperature is presented and the methods to design against local buckling in fire are presented. This last sentence can be rewritten as stating that the design methods for Class 4 cross-sections in fire are also presented. In this sense, the design provisions against local buckling of the Eurocode 3 are highlighted: firstly the cross-section classification and then the effective width method as given in Part 1-5 of the Eurocode 3 [1.11] both at normal and the respective nuances at elevated temperatures. This is followed by the description of the numerical model used in this chapter as well as its validation based on experimental results

available in the literature. The aim is to study at high temperature the capacity of simply supported internal and outstand thin-plates, that correspond respectively to the web and the flange of H or I shaped cross-sections and compare the results with the design provisions of the Eurocode 3. Outstand plates (flange) are analysed under compression while internal plates (web) are studied both in compression and in bending. The comparison of the results with Eurocode 3 philosophy uncover its inconsistencies and the need to have a better methodology to calculate the resistance against local buckling in case of fire. Therefore, an effective width method to better account with the unfavourable effect of local buckling in case of fire, based on a shell finite element numerical investigation, is defined and new expressions to calculate the plate effective width are presented following the same principles as the ones existing at normal temperature. The method presented in this part of the work is used in Chapter 3 as the basis of a methodology to calculate the resistance of slender cross-sections.

The **third chapter** is reserved for the study of H and I shaped slender cross-sections where local buckling has a predominant role in the ultimate capacity at elevated temperatures, several cross-sections submitted to compression or bending about the major-axis are investigated. In the begin of the chapter, the bibliography available on the subject is revisited, some duplication exists with the literature review made in Chapter 2, due to the scarce existence of studies within the scope of this thesis. Next, the Eurocode 3 design provisions to take local buckling into account in the cross-sectional resistance are highlighted. The new proposal developed in Chapter 2 is again revisited and a simplification of the initial proposal is also presented followed by a summary of the simplified methods to calculate the cross-sectional resistance at elevated temperatures. The numerical model used to determine the capacity of the cross-sections is presented next, with the focus on the definition of material properties, support conditions, loading model and the geometric and material imperfections. The numerical study on several cross-sections with different web height and flange width and respective thickness is presented. The objective is to cover different groups of cross-section classifications which are then submitted to pure compression and also to bending about the major-axis. The results are compared with the existing methodology of Eurocode 3 and also with the new proposed methodology showing the inconsistencies of the Eurocode method and the improvements of the new proposal also supported by the statistical

investigation presented. The chapter is closed with a comparison with experimental results found in the literature.

The **fourth chapter** presents the study on the lateral-torsional buckling of beams with slender cross-sections. The chapter begins with a literature review about the current design methods against lateral-torsional buckling in case of fire, with the focus on Part 1-2 of Eurocode 3. The numerical model used to perform the numerical investigation is then described: the mesh, the boundary conditions, the material model, the geometric and material imperfections (residual stresses) and some considerations on how the loads are applied to the model. After a comparison between the results of the numerical investigation and the existing beam design curve of Part 1-2 of Eurocode 3 is made. The aim is to demonstrate that the current provisions of Eurocode 3 are unreliable for slender cross-sections mainly due to influence of local buckling not being satisfactorily taken into account. The methodology presented in Chapter 3 is then used to calculate the capacity of the cross-sections and to analyse the accuracy of the existing beam design curve, and although improvements are observed, it is noticeable the need of an improved design curve against lateral-torsional buckling for beams with slender cross-sections in case of fire. For the purpose of developing new design curves against lateral-torsional buckling, a parametric study is presented where the influence of several parameters on the resistance of laterally unrestrained steel beams is investigated. Based on the results of the parametric study a proposal for a new design curve is made for beams with slender cross-sections in case of fire that allows for a better prediction of the influence of local buckling and, thus, leads to an improved yet safe design method when compared to the results of the finite element analysis. In the end of the chapter it is also demonstrated that the new proposal could be used together with a factor (factor “ f ”, but limited to $f \geq 0.8$) to account for the non-uniform bending diagrams. The chapter ends with a statistical investigation that support the withdrawn conclusions.

A **fifth chapter** related to the study of beam-columns with Class 4 cross-section has been included. The chapter starts with a literature review on the topic of beam-columns in case of fire, with special attention on how the existing interaction curve of Part 1-2 of Eurocode 3 was established which was developed for Class 1 and 2 cross-sections. The interaction curve for the design of beam-columns with Class 4 cross-sections is then presented by making the

necessary modifications to account for the effective area and effective section modulus to the existing expressions on the Eurocode 3. This is followed by the description of the numerical study: first the numerical model is presented followed by the geometric and material imperfections and the definition of the cases studied. The different cross-sections and loading distributions cases are highlighted. Results of the numerical investigation are then presented for two situations, namely in-plane buckling representing the buckling about the major-axis of the cross-section and the out-of-plane buckling representing the buckling about the minor-axis of the cross-section. The aim is to establish the safety level of the current design formulation. The inconsistencies of the existing design formulae are pointed out and rely mainly on the fact that the reduction factors for the column case and for the beam case, on which the interaction formulae is dependent, are not accurate enough. For each buckling direction, the calibration of the interaction factors is also presented and the improvements to the original proposal of Eurocode 3 Part 1-2 are highlighted. This study is complemented with a statistical investigation that is performed in the final part of the chapter and the formulation of the interaction curve accounting to the developments of this thesis.

The final chapter, the **sixth chapter**, presents the general conclusions for the present work as well as a critical review and thoughts on future developments.

1.4 List of publications resulting from the thesis

The publications submitted to peer-reviewed journals and resulting from this thesis are listed below. The correspondence between the publications and the chapters is also highlighted.

Chapter 2: Couto C., Vila Real P., Lopes N., Zhao B., “Effective width method to account for the local buckling of steel thin plates at elevated temperatures,” *Thin-Walled Structures*, vol. 84, pp. 134–149, November 2014. DOI: 10.1016/j.tws.2014.06.003.

Chapter 3: Couto, C., Vila Real, P.; Lopes, N.; Zhao B. “Resistance of steel cross-sections with local buckling at elevated temperatures”, *Journal of Constructional Steel Research*, vol. 109, pp. 101–114, June 2015. DOI: 10.1016/j.jcsr.2015.03.005.

Chapter 4: Couto C., Vila Real P., Lopes N., Zhao B., “Numerical investigation of the lateral-torsional buckling of beams with slender cross-sections for the case of fire”.

Chapter 5: Couto C., Vila Real P., Lopes N., Zhao B., “Steel beam-columns with slender cross-sections in case of fire”.

References

- [1.1] CEN, “EN 1993-1-2, Eurocode 3: Design of steel structures - Part 1-2: General rules - Structural fire design.” European Committee for Standardisation, Brussels, Belgium, 2005.
- [1.2] Renaud C., Zhao B., “Investigation of simple calculation method in EN 1993-1-2 for buckling of hot rolled class 4 steel members exposed to fire,” in *Fourth International Workshop “Structures in Fire,”* Aveiro, Portugal, 2006.
- [1.3] FIDESC4, “Fire Design of Steel Members with Welded or Hot-Rolled Class 4 Cross-Section, RFCS-CT-2011-00030, 2011-2014,” 2014.
- [1.4] Directorate-General for Research and Innovation, “Fire safety of industrial halls and low-rise industrial buildings, Contract No 7210-PR/378,” European Commission, Brussels, Belgium, 2005.
- [1.5] Fontana M., Knobloch M., “Local buckling behaviour and strain-based effective widths of steel structures subjected to fire,” in *Third International Workshop “Structures in Fire,”* Ottawa, Canada, 2004.
- [1.6] Knobloch M., Fontana M., “Strain-based approach to local buckling of steel sections subjected to fire,” *Journal of Constructional Steel Research*, vol. 62, no. 1–2, pp. 44–67, January 2006.
- [1.7] Fontana M., Knobloch M., “Elements with nonlinear stress-strain relationships subjected to local buckling,” in *Proceedings of ICMS 2006 Conference*, 2006.
- [1.8] Pauli J., Knobloch M., Fontana M., “On the local buckling behaviour of steel columns in fire,” in *8th fib PhD Symposium in Kgs. Lyngby, Denmark*, 2010, vol. 1.
- [1.9] Lopes N., Vila Real P., Simões da Silva L., Franssen J.-M., “Numerical Modelling of Thin-Walled Stainless Steel Structural Elements in Case of Fire,” *Fire Technology*, vol. 46, pp. 91–108, 2010.
- [1.10] Franssen J.-M., “SAFIR, A Thermal/Structural Program for Modelling Structures under Fire,” *Engineering Journal, A.I.S.C.*, vol. 42, no. 3, pp. 143–158, 2005.

[1.11] CEN, “EN 1993-1-5, Eurocode 3 - Design of steel structures - Part 1-5: Plated structural elements.” European Committee for Standardisation, Brussels, Belgium, 2006.

Chapter 2 Plates

Chapter outline

- 2.1 Introduction
- 2.2 Actual design provisions of Eurocode 3 to take into account local buckling
 - 2.2.1 Effective width method
 - 2.2.2 Cross-section classification
 - 2.2.2.1 At normal temperature
 - 2.2.2.2 In fire situation
 - 2.2.3 Code provisions for local buckling at elevated temperatures
- 2.3 Numerical study of plates
 - 2.3.1 Numerical model
 - 2.3.1.1 Validation of the numerical model with experimental results
 - 2.3.2 Results at normal temperature
 - 2.3.2.1 Elements under compression
 - 2.3.2.2 Elements under bending
 - 2.3.3 Results at elevated temperatures
 - 2.3.3.1 Elements under compression
 - 2.3.3.2 Elements under bending
- 2.4 New proposal
 - 2.4.1 Results for plates under compression
 - 2.4.2 Results for plates under bending
- 2.5 Conclusions
- References

Abstract In this chapter, the local buckling of thin steel plates exposed to fire is investigated using a shell finite element model. The reduction of strength and stiffness that occurs at elevated temperatures needs to be taken into account in the design, as it increases the susceptibility to local buckling of the plates thus affecting their load carrying capacity. The obtained results show that the current design method of Eurocode 3 to take into consideration the local buckling in the calculation of the ultimate strength of steel thin plates at elevated temperatures needs to be improved. These methods are based on the same principles as for normal temperature but using for the design yield strength of steel, at elevated temperatures, the 0.2% proof strength of the steel instead of its strength at 2% total strain as for the cases where the local buckling is not limiting the ultimate strength of the plates. This consideration, however, leads to an inconsistency if cross-sections are composed simultaneous of plates susceptible and not to local buckling. To address this issue, new expressions for calculating the effective width of internal compressed elements (webs) and outstand elements (flanges) are proposed, which have been derived from the actual expressions of the Part 1-5 of the Eurocode 3 and validated against numerical results. It is also demonstrated that it is not necessary to use for the yield stress at elevated temperatures the 0.2% proof strength of the steel instead of the yield stress at 2% total strain, given that the necessary allowances are considered in these new expressions, thus leading to a more economic design.

2.1 Introduction

In steel construction, the engineering challenge of having the most economic structural elements demands the use of slender cross-sections. Moreover, cross-sections can be considered as an assembly of plates which are often referred as internal (webs) and outstand (flange) elements and if these plates are thin, with an high width-to-thickness ratio, they may buckle when submitted to compression preventing the attainment of the yield stress in one or more parts of the cross-section, thus affecting the ultimate load bearing capacity of the structural members. According to Eurocode 3 [2.1], this type of cross-sections where local buckling governs the ultimate limit state are classified as being of Class 4 and their design rules at normal temperature are well established. Under fire conditions, however, the recent investigations of Fontana and Knobloch [2.2], Renaud and Zhao [2.3] and Quiel and Garlock [2.4] have shown that the existing design rules are too conservative for Class 4 cross-sections and hence the need to have more realistic formulae to account for the local buckling at elevated temperatures, mainly because consistency between the rules at normal temperature and in fire situation has prevailed.

At normal temperature, the Eurocode 3 gives in its Part 1-5 [2.5] two methods to account for the effects of local buckling in the design, namely the effective width method and the reduced stress method. At elevated temperatures, the same concepts are used, and in the informative Annex E of the Part 1-2 of the Eurocode 3 [2.6] some recommendations are given for the fire design of steel members with Class 4 cross-sections. In this annex, it is suggested to use the simple calculation methods with the design value for the steel yield strength as the 0.2% proof strength instead of the strength at 2% total strain as normally done in the fire design of the other cross-sectional classes. In addition, it is stated that the effective cross-section can be determined with the effective width method as for normal temperature, i.e. the effective widths of the different elements that constitute the cross-section are determined on the basis of the material properties at normal temperature. The early work of Ranby [2.7] has demonstrated that this methodology is safe and leads to accurate results for determining the ultimate load of plates susceptible to local buckling at elevated temperatures. Nevertheless, it must be noted that, if a cross-section is built up of plates of which some are with and others are without local buckling, using the 0.2% proof strength of steel as the design strength underestimates the cross-sectional resistance. Take, for example, an element

submitted to pure bending about the major-axis with a regular I-shaped cross-section with Class 1 or 2 flanges and Class 4 web, and therefore the overall cross-section classification is Class 4. Since the cross-section is Class 4, the designer is forced to use the 0.2% proof stress as the design yield strength, even for the flanges that are classified as Class 1 (or 2). This is very much conservative because in these type of cross-sections it is usual that around 80% of the bending resistance is provided by the flanges that will have no local buckling problems, in that case.

The limits of the width-to-thickness ratio from which the plates are susceptible to local buckling at normal temperature are defined in the Eurocode 3 Part 1-1. Under fire conditions these limits are the same as for normal temperature but the value $\varepsilon = 0.85\sqrt{235/f_y}$ is used instead of $\varepsilon = \sqrt{235/f_y}$. Using a reduced value of ε in fire situation can lead to a higher classification but prevents that classification changes for each temperature, as it will be justified in the next section. It worth be mentioned that on this subject, Renaud and Zhao [2.3] point out that it would be more consistent to classify the cross-sections as for normal temperature, instead of those recommendations, since the square root of the reduction factors for the steel strength $k_{0.2p,\theta}$ and for the *Young modulus* $k_{E,\theta}$ at elevated temperatures is close to one, in accordance with the recommendation of calculating the effective cross-section to be used at elevated temperatures on the basis of the material properties at normal temperature. On the other hand, the experimental results of Ala-Outinen and Myllymäki [2.8] and Yang et al. [2.9–2.11], show that local buckling occurs even for cross-sections with plates that are classified as Class 1 or Class 2 for temperatures above 500°C.

Quiel and Garlock [2.4] calculated the buckling strength of steel plates exposed to fire and proposed new expressions for calculating the effective widths and account for the local buckling, however, these expressions are codified in a more similar manner to North American standards than to the Eurocodes and the effect of the steel grade has not been taken into account. Fontana and Knobloch [2.2] have developed a strain-based approach for calculating ultimate strength of steel plates at elevated temperatures and expressions to calculate the effective cross-section, however those expressions vary for various ranges of strain at each increment of temperature and are only for outstand elements. Both works show

that an improved method is needed in order to obtain a more realistic cross-sectional resistance at elevated temperatures taking into account the local buckling.

In this chapter, a parametric study with the help of the finite element method (FEM) software SAFIR [2.12] has been performed to assess the ultimate strength of steel plates with different support conditions and load patterns at elevated temperatures. Comparisons of the numerical results with the existing formulae demonstrate the need of new expressions to determine the effective width of the steel plates at elevated temperatures which have been derived accordingly and are herein presented. The necessary allowances for the local buckling is taken into account in the determination of the effective width of the plates and as a result using these new expressions it is not necessary to use the 0.2% proof strength of steel at elevated temperatures and therefore the yield stress at a total strain of 2% can be used to calculate the resistance of Class 4 cross-sections.

2.2 Actual design provisions of Eurocode 3 to take into account local buckling

2.2.1 Effective width method

Thin plates when submitted to in-plane compressive stresses may buckle. The stress distribution on a plate after buckling is clearly non-linear as shown in Figure 2.1, with lower values on the central part and maximum stresses at the edges of the plate equal to the yield stress f_y .

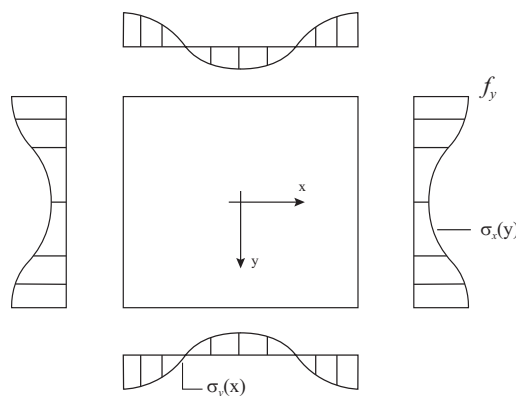


Figure 2.1: Stress distribution on a rectangular plate in the post-buckling regime.

The effective width method originally developed by von Karman [2.13] and then adapted by Winter [2.14] to account for the influence of the geometrical imperfections and the residual stresses, translates this concept into a “fictitious plate” with an effective width of b_{eff} and a uniform stress distribution equal to the yield stress, as shown in Figure 2.2.

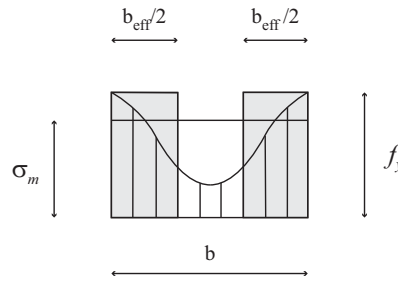


Figure 2.2: Effective width b_{eff} concept.

The effective width can then be determined as the ratio between the mean value of the stresses along the plate $\sigma_m = \frac{1}{b} \int \sigma(x) dx$ and the maximum stress on the edge of the plate f_y multiplied by the total width of the plate

$$\rho = \frac{\sigma_m}{f_y} = \frac{b_{eff}}{b} \quad (2.1)$$

being ρ the reduction factor for the plate buckling resistance.

According to Part 1-5 of Eurocode 3 this reduction factor is calculated by [2.15] for internal elements in compression

$$\rho = \begin{cases} \rho = 1 & \text{for } \bar{\lambda}_p \leq 0.5 + \sqrt{0.085 - 0.055\psi} \\ \frac{\bar{\lambda}_p - 0.055(3 + \psi)}{\bar{\lambda}_p^2} & \text{for } \bar{\lambda}_p > 0.5 + \sqrt{0.085 - 0.055\psi} \end{cases} \quad (2.2)$$

and for outstand elements under compression by

$$\rho = \begin{cases} 1 & \text{for } \bar{\lambda}_p \leq 0.748 \\ \frac{\bar{\lambda}_p - 0.188}{\bar{\lambda}_p^2} & \text{for } \bar{\lambda}_p > 0.748 \end{cases} \quad (2.3)$$

where ψ is the stress ratio and $\bar{\lambda}_p$ is the non-dimensional slenderness of a plate given by

$$\bar{\lambda}_p = \frac{b/t}{28.4\varepsilon\sqrt{k_\sigma}} \quad (2.4)$$

where, k_σ is the buckling coefficient of the plates which takes into account the different boundary conditions and the stress pattern applied to the plates and

$$\varepsilon = \sqrt{\frac{235}{f_y}} \sqrt{\frac{E}{210000}} \quad \text{with } f_y \text{ and } E \text{ in MPa} \quad (2.5)$$

2.2.2 Cross-section classification

2.2.2.1 At normal temperature

Albeit the scope of this work is to study the local buckling in steel plates at elevated temperatures, it is important to mention the limits defined in Part 1-1 of Eurocode 3 [2.1] regarding the four different classes of the cross-sections concerning the resistance and rotation capacity as a function of the local buckling resistance of their elementary plates. The limit width-to-thickness ratio (b/t), i.e. the plate slenderness, for a steel plate to belong to a certain class is shown in Table 2.1, where at normal temperature for carbon steel, substituting $E = 210000$ MPa in equation (2.5), the parameter ε is defined by:

$$\varepsilon = \sqrt{235/f_y} \quad \text{with } f_y \text{ in MPa.} \quad (2.6)$$

Table 2.1: Slenderness limits (b/t) for the plates for cross-sectional classification at normal temperature.

Element	Class 1	Class 2	Class 3
Outstand element (flange) submitted to compression	9ε	10ε	14ε
Internal element (web) submitted to compression	33ε	38ε	42ε
Internal element (web) submitted to bending	72ε	83ε	124ε

2.2.2.2 In fire situation

In case of fire, the cross-section classification follows the same procedure and width-to-thickness limits as for normal temperature, but as the Young's modulus and the yield strength are dependent of the temperature equation (2.5) must be used instead of equation (2.6), resulting for carbon steel in [2.17]:

$$\begin{aligned}
 \varepsilon &= \sqrt{\frac{235}{f_{y,\theta}}} \sqrt{\frac{E_\theta}{210000}} = \sqrt{\frac{k_{E,\theta}}{k_{y,\theta}}} \sqrt{\frac{235}{f_y}} \sqrt{\frac{E}{210000}} \quad \text{with } f_y \text{ in MPa.} \\
 &= \sqrt{\frac{k_{E,\theta}}{k_{y,\theta}}} \sqrt{\frac{235}{f_y}} \approx 0.85 \sqrt{\frac{235}{f_y}}
 \end{aligned} \tag{2.7}$$

The ratio $\sqrt{k_{E,\theta}/k_{y,\theta}}$ is a function of the temperature and is depicted in Figure 2.3. Eurocode 3 recommends that the ratio $\sqrt{k_{E,\theta}/k_{y,\theta}}$ is replaced by a constant value of 0.85, which is a kind of a mean value of that ratio as shown in Figure 2.3.

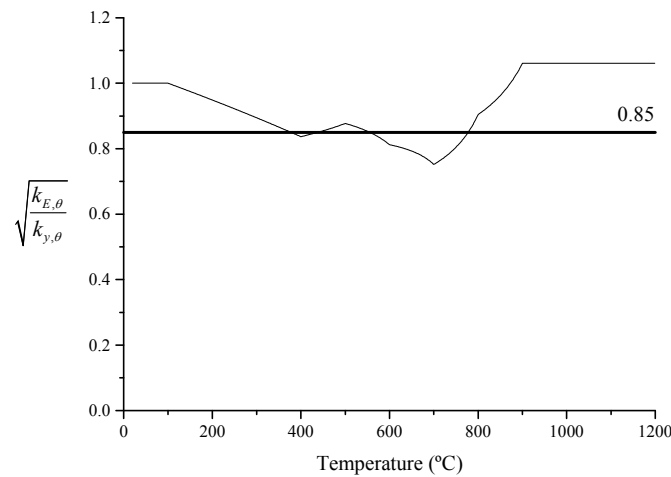


Figure 2.3: Ratio $\sqrt{k_{E,\theta}/k_{y,\theta}}$ as a function of the temperature.

The advantage of using this simplification as opposed to the temperature dependent classification model is that it prevents changes of a cross-sectional classification for each temperature. In this work the classification of the plates is referred also in terms of the non-dimensional slenderness limits and these values are given in Table 2.2 for normal temperature and elevated temperatures.

Table 2.2: Non-dimensional slenderness limits of the plates for cross-sectional classification at normal and elevated temperature.

Element	Normal temperature ($\bar{\lambda}_p$)			Elevated temperature ($\bar{\lambda}_{p,\theta}$)		
	Class 1	Class 2	Class 3	Class 1	Class 2	Class 3
Outstand (flange) in compression	0.483	0.537	0.752	0.411	0.456	0.639
Internal (web) in compression	0.581	0.669	0.739	0.494	0.569	0.629
Internal (web) in bending	0.519	0.598	0.893	0.441	0.508	0.759

2.2.3 Code provisions for local buckling at elevated temperatures

In Part 1-2 of the Eurocode 3, for Class 4 cross-sections it is suggested to adopt a default critical temperature of 350°C if no other calculation is made. Nonetheless, this is very

conservative and some further guidance is given in the Annex E for the fire design of this type of cross-sections. According to this annex, when using simple design models the same principles apply as for the other cross-section classes but effective cross-sections properties need to be determined based on the material properties at normal temperature. For Class 4 cross-sections, it is suggested to use the simple calculation methods with the design value for the steel yield strength as the 0.2% proof strength instead of the stress at 2% total strain as for the other classes.

In fact, at elevated temperatures, the reduction factor for plate buckling would be, according to equations (2.5) and (2.6), $\rho_\theta = \rho_\theta(\bar{\lambda}_{p,\theta})$ with the corresponding non-dimensional slenderness at elevated temperatures, given by

$$\bar{\lambda}_{p,\theta} = \sqrt{\frac{f_{y,\theta}}{\sigma_{cr,\theta}}} = \sqrt{\frac{k_{0.2p,\theta}}{k_{E,\theta}}} \sqrt{\frac{f_y}{\sigma_{cr}}} \cong 1.0 \sqrt{\frac{f_y}{\sigma_{cr}}} = \bar{\lambda}_p \quad (2.8)$$

The ratio $\sqrt{k_{0.2p,\theta} / k_{E,\theta}}$ is almost equal to 1.0 as shown in Figure 2.4, and since $\bar{\lambda}_{p,\theta} \cong \bar{\lambda}_p$, equations (2.2) and (2.3) show that it can be considered $\rho_\theta = \rho$.

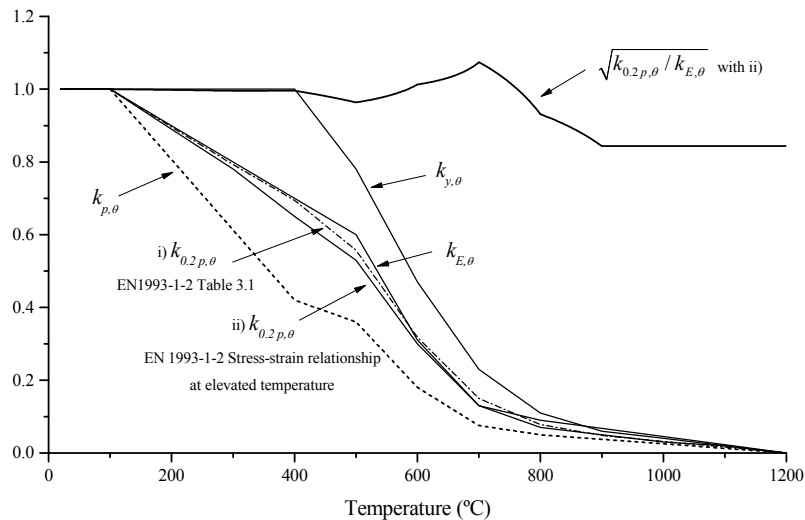


Figure 2.4: Reductions factors for the mechanical properties of carbon steel at elevated temperatures according to Part 1-2 of Eurocode 3.

This methodology however, has the disadvantage of underestimating the cross-sectional resistance if only some of the plates of the cross-section are susceptible to local buckling. In this case, using the 0.2% proof strength for the whole cross-section is, thus, very limiting, as already mentioned.

The reduction factors for the mechanical properties of carbon steel at elevated temperatures according to Part 1-2 of Eurocode 3 are shown in Figure 2.4. There is an inconsistency pointed out by Renaud and Zhao [2.3] regarding the reduction factors for the 0.2% proof strength at elevated temperatures, $k_{0.2p,\theta}$, since these values are not calculated according to the stress-strain relationship of steel at elevated temperatures, and it is unknown to the author where the values given in the Part 1-2 of Eurocode 3 come from (see in Figure 2.4). In this study the values of $k_{0.2p,\theta}$ used are those calculated according to the stress-strain relationship of carbon steel at elevated temperatures for the case of the steel grade S355, as adopted in the French National Annex of the Eurocode.

2.3 Numerical study of plates

2.3.1 Numerical model

To calculate the ultimate strength of rectangular plates ($a \times b$ with $a > b$) the FEM software SAFIR [2.12] has been used. The plates were discretized into several quadrangular shell elements with four nodes and six degrees of freedom (3 translations and 3 rotations). These shell elements adopt the Kirchoff's theory formulation with a total co-rotational description and have been previously validated by Talamona and Franssen [2.16]. The steel material law is a two-dimensional constitutive relation with the von Mises yield surface according to the non-linear stress-strain formulae of the Eurocode 3 and the respective reduction factors at elevated temperatures ($k_{y,\theta}$, $k_{p,\theta}$ and $k_{E,\theta}$) as plotted in Figure 2.4. The integration on the shell element follows a Gauss scheme with 2×2 points on the surface and 4 points through the thickness.

A mesh density study has been performed and the solution converged for rectangular plates with the dimensions of $a=1.6\text{ m}$ and $b=0.4\text{ m}$ using 80 elements along the length a and 20 elements along the width b . These dimensions and mesh have been adopted in this study (see Figure 2.5).

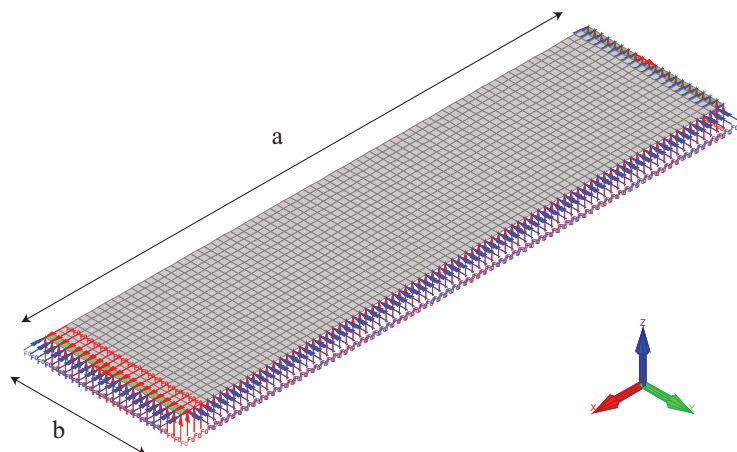


Figure 2.5: Example of the numerical model used to calculate the ultimate strength of a simply-supported plate in 3 sides – outstand element.

The boundary conditions taken into consideration as a restraint to the vertical displacements (U_z) and rotations (R_y on edge a and R_x on edge b) on the plate edges, displacements in the plane of the plate were also restrained (U_x and U_y). Loads were applied to the model as forces and a layer of shells with increased thickness was used on the edges of the plate to avoid numerical problems. The numerical model used to calculate the ultimate strength of a simply-supported plate on 3 sides is shown in Figure 2.5.

Geometrical imperfections were introduced into the model by modifying the nodal coordinates. The shape for the geometrical imperfections was considered as the first eigenmode of a linear buckling analysis and the amplitude of the imperfections has been considered as 80% of $b/50$ for plates corresponding to the flanges and 80% of $b/100$ for plates corresponding to the webs, following the recommendations of Part 1-5 of the Eurocode to use 80% of the fabrication tolerances as given in [2.17]. A procedure written in Cast3M [2.18] has been used to obtain the eigenmodes [2.19]. Residual stresses at normal temperature affect the ultimate strength of the plates but at elevated temperatures have a negligible effect on resistance of the plates because a relaxation of initial residual stresses is likely to occur due to an increase of the steel temperature [2.4]. In this study, the residual

stresses when considered have the pattern [2.20] depicted in Figure 2.6 with the values of the residual stresses according to [2.20, 2.21] as used in [2.22].

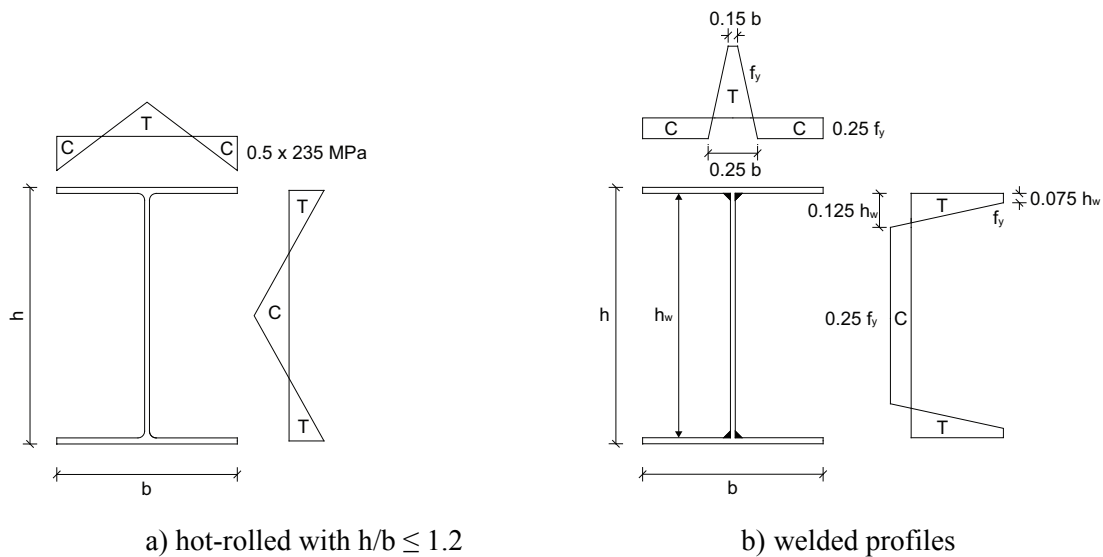


Figure 2.6: Pattern of the residual stresses considered.

2.3.1.1 Validation of the numerical model with experimental results

In this section, validation of the numerical model is made by comparing the predicted results with the experimental results by other researchers at both normal and elevated temperatures. At present, few studies exist on the ultimate strength of compressed thin-plate steel sections exposed to fire. Tests by Pauli *et al.* [2.23] focus on the investigation of the local buckling behaviour and cross-sectional resistance of heated steel members at elevated temperatures on stub columns of square and rectangular hollow sections (internal elements in compression). Yang *et al.* [2.10] carried out experimental investigations on the buckling strength of wide-flanged steel sections with local flange buckling (outstand elements in compression) at elevated temperatures. On the scope of the European Research Project FIDESC4 [2.24], Hricák *et al.* [2.25] tested two laterally restrained steel beams with Class 4 cross-sections heated at two different temperatures. More recently, Wang *et al.* [2.26] also carried out experiments to investigate the local buckling behaviour of H stub columns at elevated temperatures. In Tables 2.3 and 2.4, the section dimensions, the steel yield strength at normal temperature and the results obtained in the experiments for the specimens of each study and predicted with numerical models are compared for different temperatures. A

comparison between the results predicted with Eurocode 3 is also shown in these tables. In the numerical model, the residual stresses and geometric imperfections were considered as described in section 3.1.

Table 2.3: Comparison of experimental results on the ultimate compressive strength of steel sections with thin-plates with the values predicted by the numerical model and the Eurocode 3 for a different set of temperatures.

Source	Section	$f_{y,20^{\circ}\text{C}}$ (MPa)	Temp. (°C)	Exp. F_{ULT} [kN]	EC3 F_{ULT} [kN]	SAFIR F_{ULT} [kN]	EC3 /Exp.	SAFIR /Exp.
[2.23]	SHS160×160×5	370	20°C	1225	1214	1221	0.99	1.00
			400°C	795	841	776	1.06	0.98
			550°C	468	531	491	1.13	1.05
			700°C	138	182	166	1.32	1.21
[2.23]	RHS120×60×3.6	385	20°C	483	505	499	1.05	1.03
			400°C	408	347	360	0.85	0.88
			550°C	257	220	227	0.86	0.88
			700°C	74	76	81	1.03	1.10
[2.10]	H175×175×6.5×11	243	20°C	(¹)	(¹)	(¹)	(¹)	(¹)
			400°C	1033	850	997	0.82	0.96
			500°C	843	682	786	0.81	0.93
			600°C	392	389	465	0.99	1.19
[2.10]	H300×300×10×15	306.3	20°C	4615	4013	4103	0.87	0.89
			300°C	4384	3182	3522	0.73	0.80
			400°C	4107	2785	3341	0.68	0.81
			450°C	3692	2512	2992	0.68	0.81
			500°C	3323	2235	2657	0.67	0.80
			550°C	2492	1758	2102	0.71	0.84
			600°C	1984	1276	1549	0.64	0.78
[2.26]	H250×250×6×8	306.3	20°C	1375	1603	1265	1.17	0.92
			450°C	930	946	847	1.02	0.91
			650°C	295	345	330	1.17	1.12
[2.26]	H316×200×6×8	321.9	20°C	1247	1473	1247	1.18	1.00
			450°C	830	869	835	1.05	1.01
			650°C	280	317	326	1.13	1.16

(¹) The failure in this case was a global mode (flexural buckling), so this test result was disregarded.

Table 2.4: Comparison of experimental results on the ultimate bending strength of steel sections with thin-plates with the values predicted by the numerical model and the Eurocode 3 for a different set of temperatures.

Source	Section	$f_{y,20^{\circ}\text{C}}$ (MPa)	Temp. ($^{\circ}\text{C}$)	Exp. F_{ULT} [kNm]	EC3 F_{ULT} [kNm]	SAFIR F_{ULT} [kNm]	EC3 /Exp.	SAFIR /Exp.
[2.25]	H680×250×4×12	424/392 (flange/web)	450°C	558	567	570	1.02	1.02
			650°C	202	212	212	1.05	1.05
[2.25]	H846×300×5×8	338/378 (flange/web)	450°C	424	441	411	1.04	0.97
			650°C	176	165	157	0.94	0.89

In Figures 2.7 and 2.8, results are plotted for the comparison between the experimental results and the numerical model and the Eurocode 3 respectively, with the points below the solid line that divides the chart meaning the predicted results are conservative and non-conservative otherwise.

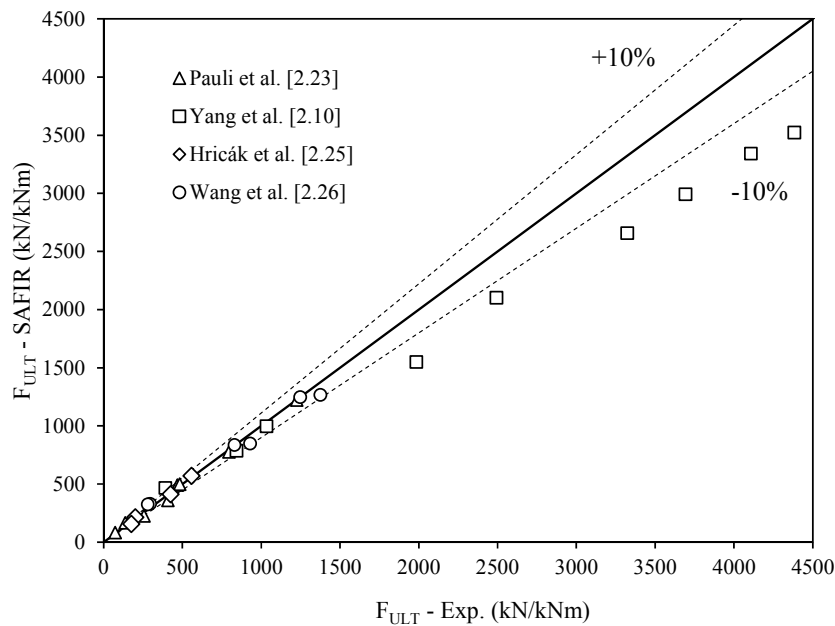


Figure 2.7: Comparison between the results obtained with the numerical model and the experimental results of other authors [2.10, 2.23, 2.25, 2.26].

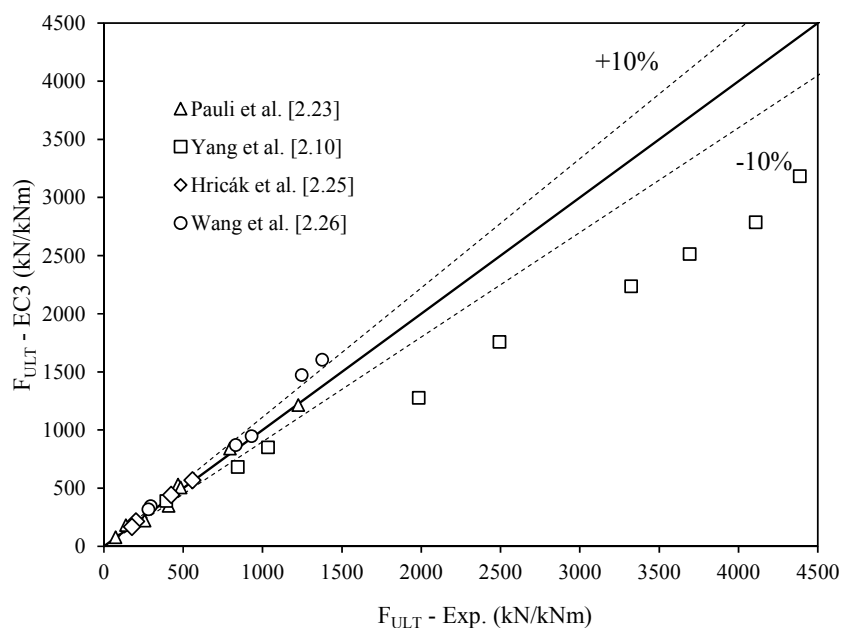


Figure 2.8: Comparison between the results predicted by the Eurocode 3 and the experimental results of other authors [2.10, 2.23, 2.25, 2.26].

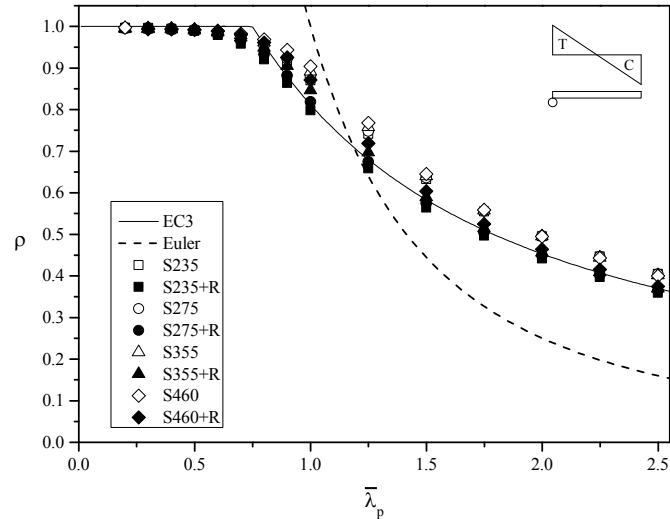
A total of 28 different results were analysed, both at normal temperature (5 cases) and at elevated temperatures (23 cases). Results show a good correlation between the experimental results and the results calculated with SAFIR. At normal temperature, the differences between the numerical model and the experimental results are small except for two test results where 8% and 11% difference was obtained although on the safe side. At elevated temperatures, the predicted results were mainly conservative. Only four of the cases show significant differences (more than 10% on the unsafe side) but they refer to tests where the specimens were heated at more than 600°C and where it is more difficult to control the tests for such temperature levels. Nevertheless, the numerical model used in this study has proven to be capable of predicting the local buckling influence on the ultimate strength of cross-sections at normal and elevated temperature.

2.3.2 Results at normal temperature

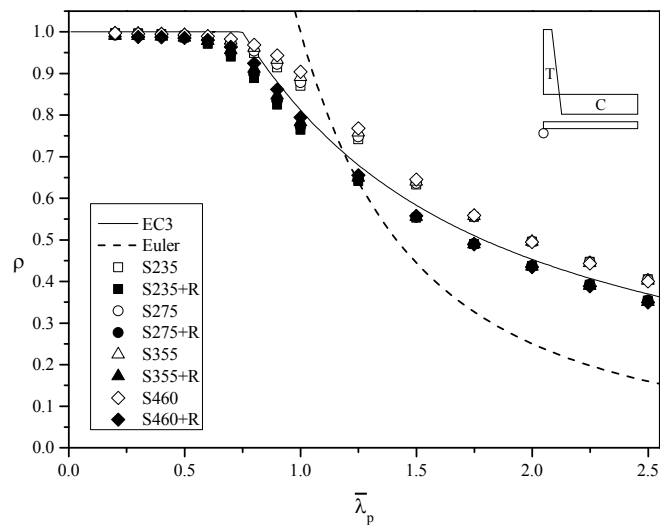
2.3.2.1 Elements under compression

At normal temperature, the ultimate strength of an outstand element (flange) under compression for various steel grades is shown in Figure 2.9 for hot-rolled and welded

residual stress pattern. In this figure the numerical results are determined according to equation (2.1) by taking $\sigma_m = \sigma_{\text{Numeric}}$, where σ_{Numeric} is the value obtained with SAFIR for the ultimate strength of the plate.



a) hot-rolled residual stresses



b) welded residual stresses.

Figure 2.9: Ultimate strength of plates simply supported in 3 sides (outstand element) at normal temperature under compression.

It can be seen that the numerical results obtained are in accordance with the design curve of the Eurocode 3 given by equation (2.3), in this figure the notation “+R” means that residual stresses have been considered. It is also evident the influence of the residual stresses on the

results by reducing the plate ultimate strength and therefore need to be taken into account at normal temperature, this aspect is highlighted in the Figure 2.10.

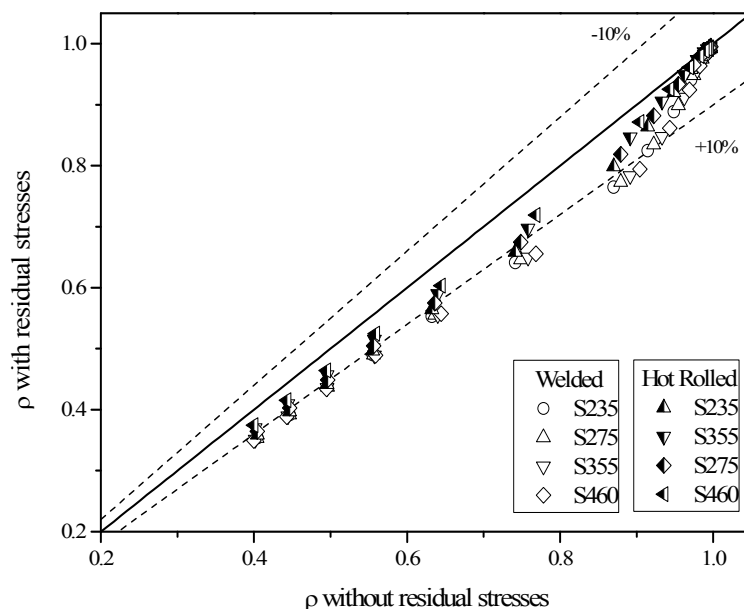
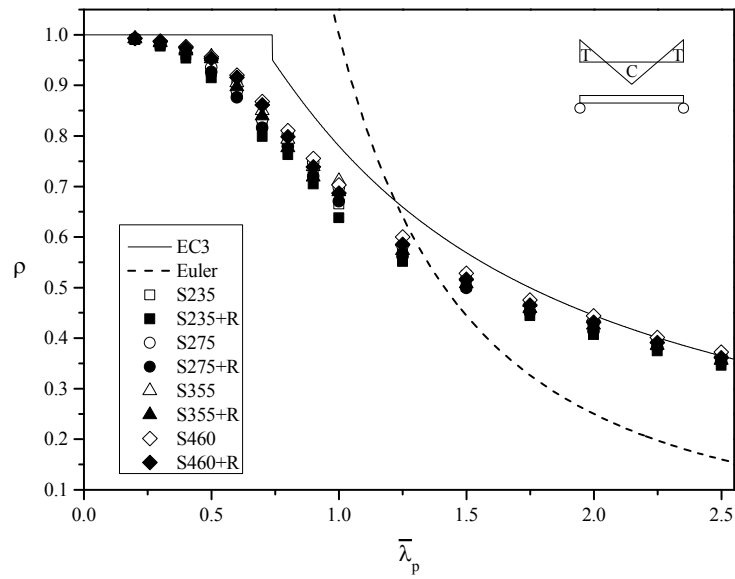


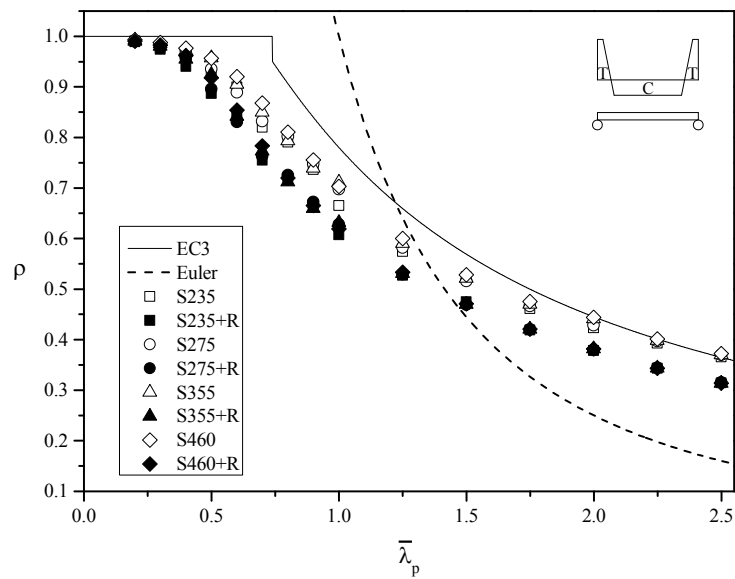
Figure 2.10: Influence of the residual stresses in the ultimate strength of a simply supported plate in 3 sides (outstand element) under compression at normal temperature.

The so-called post-buckling behaviour is also noticeable given that the numerical results are above the elastic buckling curve (Euler) for non-dimensional slenderness higher than $\bar{\lambda}_p \approx 1.25$.

The ultimate strength of an internal element (web) under compression for various steel grades is shown in Figure 2.11 for hot-rolled and welded residual stress patterns. It worth mention that the discontinuity that exists in the Eurocode 3 (EC3) curve in this figure is due to the fact that the plate buckling resistance starts to decrease for $\bar{\lambda}_p = 0.673$ (see Equation (2.2)) but the Class 4 limit is set at $\bar{\lambda}_p = 0.739$ (see Table 2.2).



a) hot-rolled residual stresses



b) welded residual stresses.

Figure 2.11: Ultimate strength of a plate simply supported in 4 sides (internal element) at normal temperature submitted to compression.

The numerical analyses for internal elements under compression show that there is some difference in the results. A possible explanation for this fact is that the design curves were obtained on the basis of experimental results of different cross-sections and the geometrical

imperfections were not as severe as the ones considered in this study, in the Figure 2.12 it is exemplified the use of a less severe geometrical imperfection.

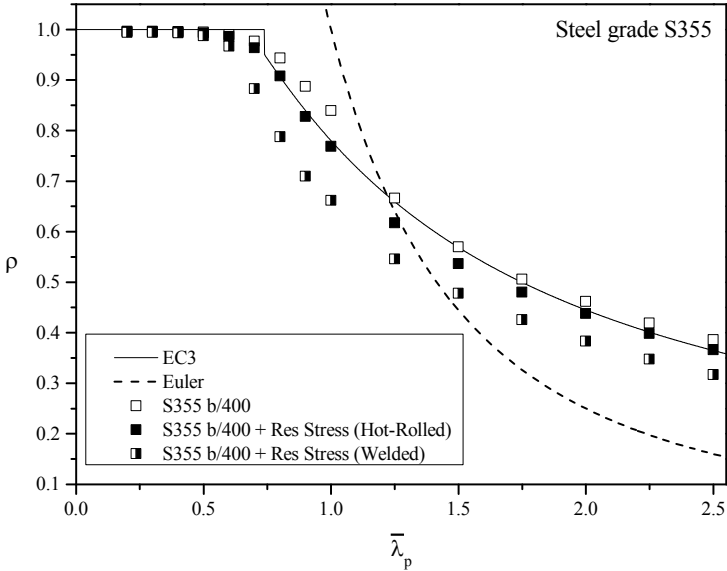


Figure 2.12: Ultimate strength of a plate simply supported in 4 sides (internal element) under compression at normal temperature using a less severe geometrical imperfection.

In this case the maximum displacement of the eigenmodes has been scaled to an arbitrary value of $b/400$ instead of the 80% of $b/100$, i.e. $b/125$, used in the remaining cases as recommend in the EN1993-1-5. From this figure it can be seen that there is a better agreement between the numerical results and the design curve of the Eurocode 3 when considering residual stresses with the pattern of the Hot-Rolled profiles of Figure 2.6 and a lower value for the geometrical imperfections. In this study the recommendations of EN1993-1-5 for the geometrical imperfections were followed.

The influence of the residual stress pattern in the ultimate load bearing capacity of internal elements under compression is shown in Figure 2.13 and it can be seen that considering hot-rolled residual stresses pattern has almost no influence in the ultimate strength of the internal plate, while for welded residual stresses pattern has a considerable influence.

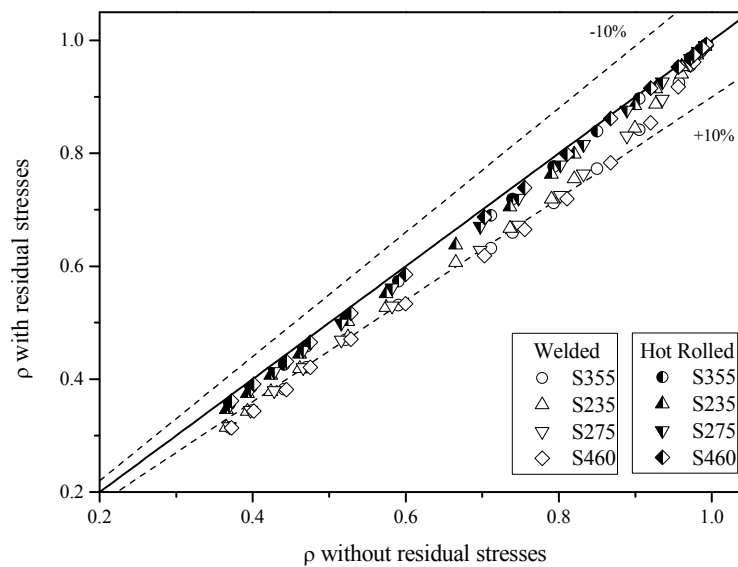


Figure 2.13: Influence of the residual stresses in the ultimate strength of simply supported plate in 4 sides (internal element) under compression at normal temperature.

In Figure 2.14 the typical deformed shape obtained at collapse for a simply supported plate in 3 and 4 sides is shown.

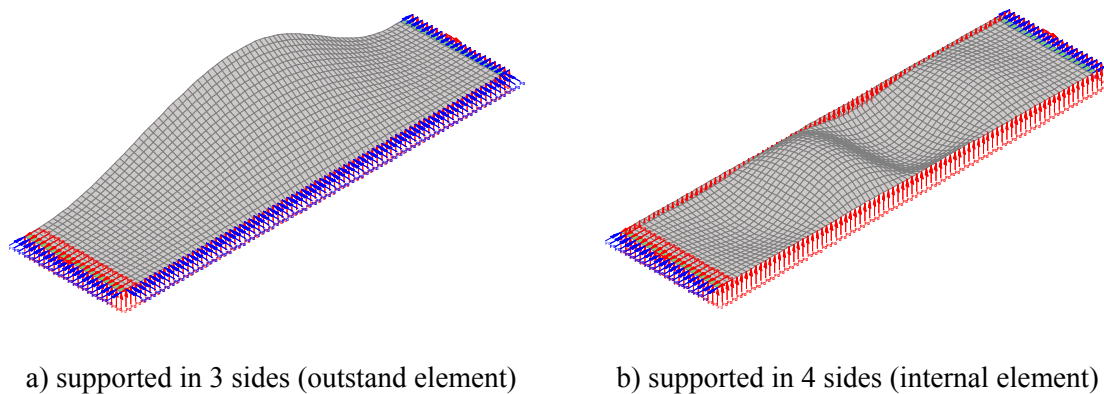
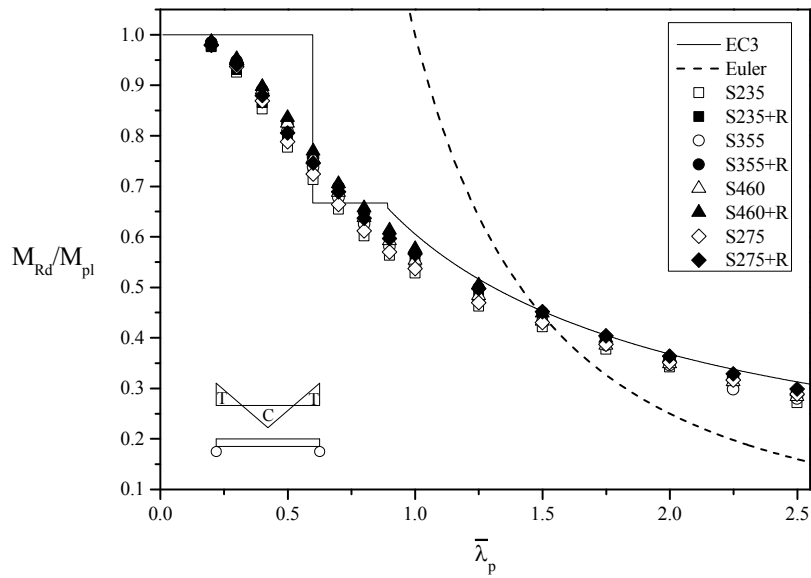


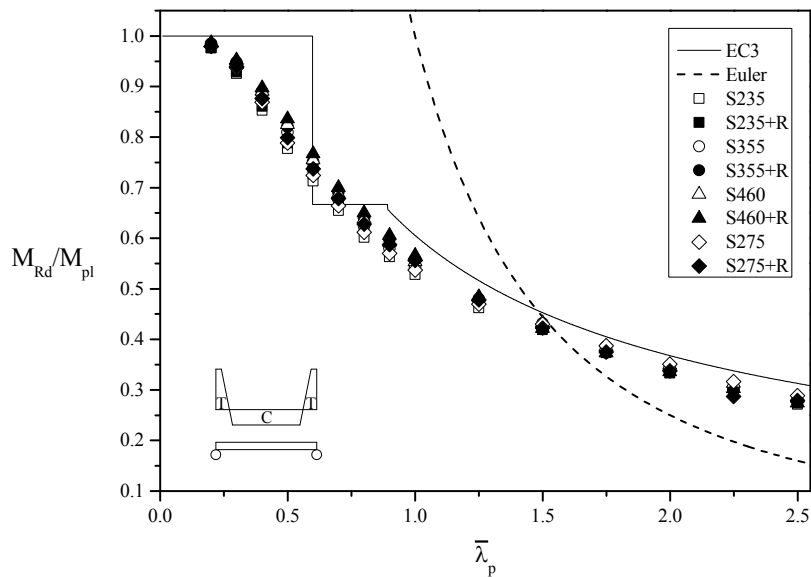
Figure 2.14: Deformed shape at the collapse of simply supported plates.

2.3.2.2 Elements under bending

The plate ultimate resistance of internal elements (web) submitted to bending is shown in Figure 2.15 for different steel grades and considering hot-rolled and welded residual stresses pattern.



a) hot-rolled residual stresses



b) welded residual stresses.

Figure 2.15: Ultimate strength of a plate simply supported in 4 sides at normal temperature under bending.

Since the bending resistance of the plate varies with its classification regarding local buckling according to the Eurocode 3

$$M_{Rd} = \begin{cases} M_{pl,Rd} = W_{pl,y} f_y / \gamma_{M0} & \bar{\lambda}_p \leq 0.598 \\ M_{el,Rd} = W_{el,y} f_y / \gamma_{M0} & 0.598 < \bar{\lambda}_p \leq 0.893 \\ M_{eff,Rd} = W_{eff,y} f_y / \gamma_{M0} & \bar{\lambda}_p > 0.893 \end{cases} \quad (2.9)$$

where $M_{pl,Rd}$, $M_{el,Rd}$ and $M_{eff,Rd}$ are the plastic bending resistance, elastic bending resistance and the effective bending resistance respectively for a plate, a discontinuous curve is presented in these figures. At $\bar{\lambda}_p = 0.893$ there is also a small discontinuity in the EC3 curve due to the fact that in Equation (2.3) the plate buckling resistance starts to decrease at $\bar{\lambda}_p = 0.748$.

From Figure 2.15 it can be seen that numerical results are close to the design curve provided by the Eurocode 3 for plates classified as Class 4 ($\bar{\lambda}_p > 0.893$) and that for the remaining classes the numerical results show that the transition from Class 1 to Class 3 is naturally more smoother than the design curve predicts, being the Eurocode non-conservative for a certain range of small values of slenderness.

In Figure 2.16 the influence of the residual stresses is shown. It can be seen that the influence of the residual stresses in the ultimate strength of plates submitted to bending is small.

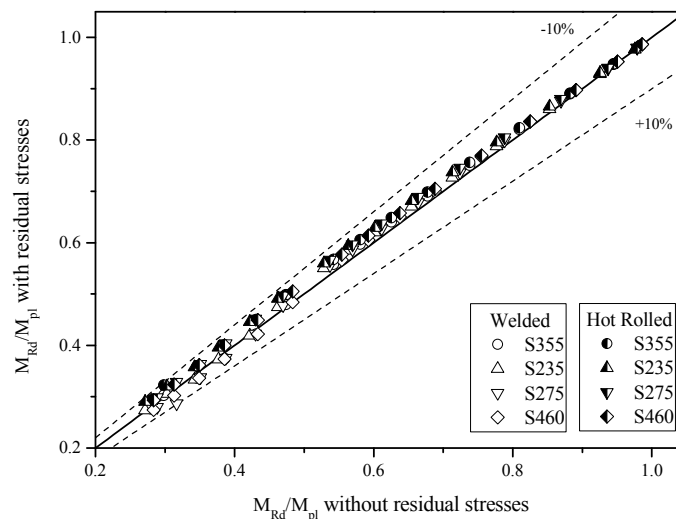


Figure 2.16: Influence of the residual stresses in the ultimate strength of stiffened plates under bending at normal temperature.

2.3.3 Results at elevated temperatures

2.3.3.1 Elements under compression

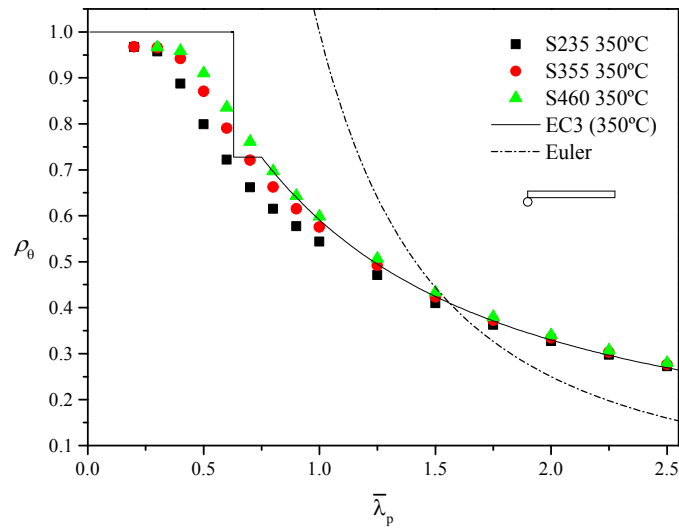
At elevated temperatures, the equations (2.2) and (2.3) to calculate the reduction factor for the plate buckling need to be adapted to account for the transition that occurs when passing from Class 3 to Class 4 elements, since at this point ($\bar{\lambda}_p = \bar{\lambda}_{p,\theta} = 0.629$ for internal elements and $\bar{\lambda}_p = \bar{\lambda}_{p,\theta} = 0.639$ for outstand elements, see Table 2.2) the steel yield strength to be considered equals to the 0.2% proof strength instead of the strength at 2% total strain, leading to a discontinuity in the formulation and, additionally, to the appearance of a plateau because the reduction factor for the plate buckling only starts to decrease at higher values of the non-dimensional slenderness, for instance, in compression ($\psi = 1$) for internal elements $\bar{\lambda}_p = 0.5 + \sqrt{0.085 - 0.055\psi} = 0.673$ and $\bar{\lambda}_p = 0.748$ for outstand elements. Therefore, the reduction factor for the plate buckling at elevated temperatures can be written, for internal elements under compression as:

$$\begin{aligned} \rho_\theta &= 1 && \text{for } \bar{\lambda}_p \leq 0.629 \\ \rho_\theta &= \left(\frac{k_{0.2p,\theta}}{k_{y,\theta}} \right) && \text{for } 0.629 < \bar{\lambda}_p \leq 0.5 + \sqrt{0.085 - 0.055\psi} \quad (2.10) \\ \rho_\theta &= \left(\frac{k_{0.2p,\theta}}{k_{y,\theta}} \right) \left(\frac{\bar{\lambda}_p - 0.055(3 + \psi)}{\bar{\lambda}_p^2} \right) && \text{for } \bar{\lambda}_p > 0.5 + \sqrt{0.085 - 0.055\psi} \end{aligned}$$

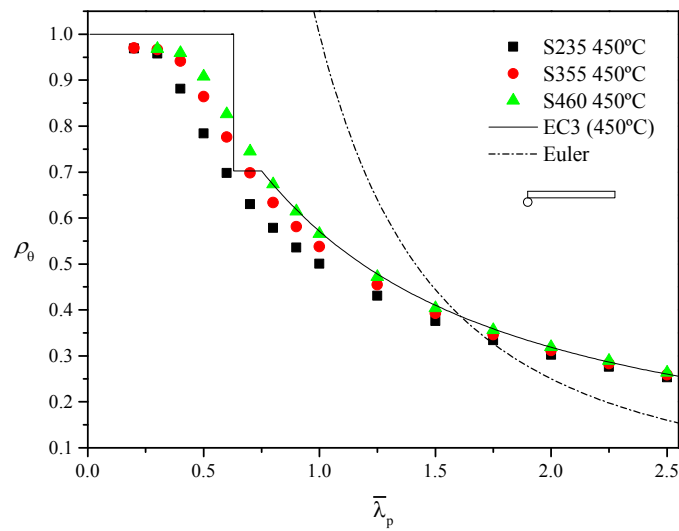
and for outstand elements under compression as

$$\begin{aligned} \rho_\theta &= 1 && \text{for } \bar{\lambda}_p \leq 0.639 \\ \rho_\theta &= \left(\frac{k_{0.2p,\theta}}{k_{y,\theta}} \right) && \text{for } 0.639 < \bar{\lambda}_p \leq 0.748 \quad (2.11) \\ \rho_\theta &= \left(\frac{k_{0.2p,\theta}}{k_{y,\theta}} \right) \left(\frac{\bar{\lambda}_p - 0.188}{\bar{\lambda}_p^2} \right) && \text{for } \bar{\lambda}_p > 0.748 \end{aligned}$$

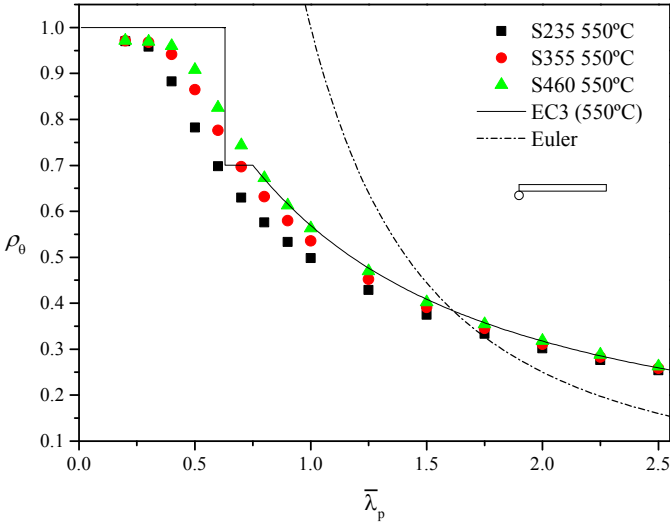
In Figure 2.17 and Figure 2.18 the ultimate strength of outstand elements and internal elements under compression obtained with the FEM calculations is shown for different temperatures and steel grades respectively and compared with the Eurocode 3 (EC3) formulae defined in equations (2.10) and (2.11).



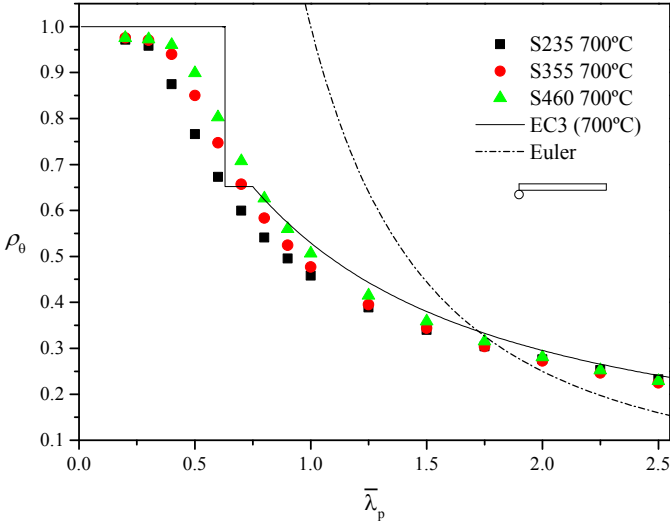
a) 350°C



b) 450°C

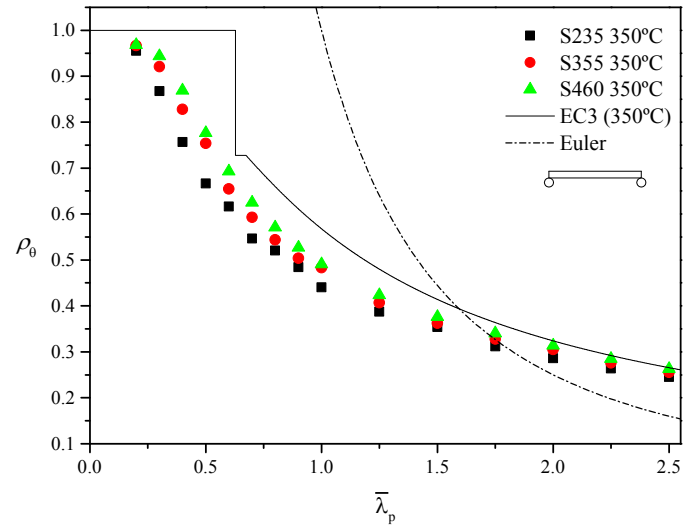


c) 550°C

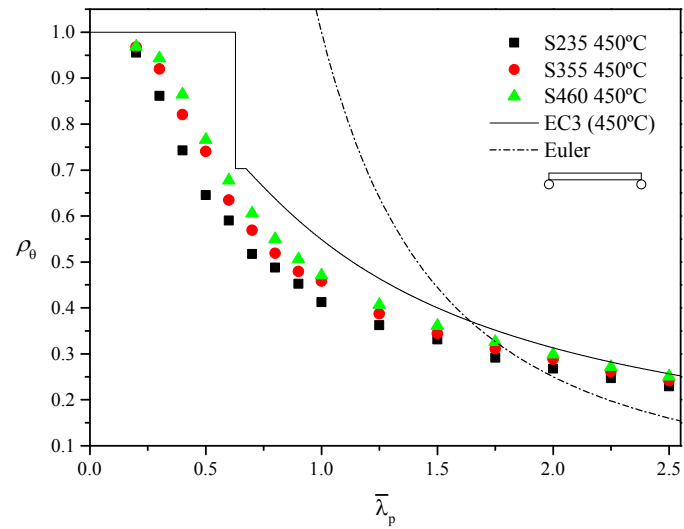


d) 700°C

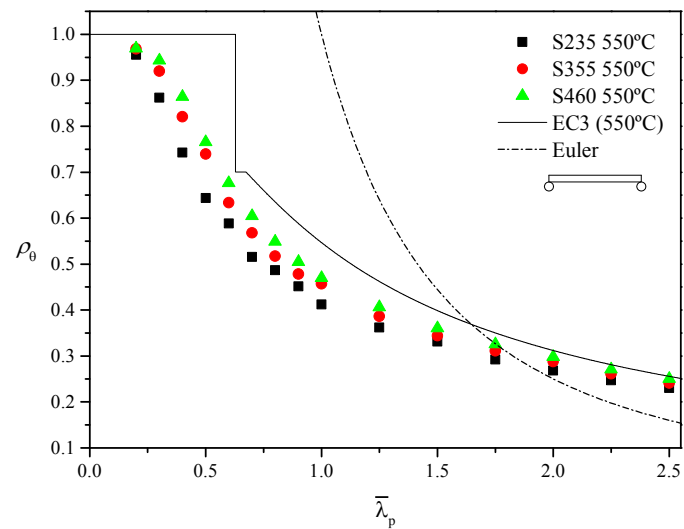
Figure 2.17: Ultimate strength of a plate simply supported in 3 sides (outstand element) at elevated temperatures under compression.



a) 350°C



b) 450°C



c) 550°C

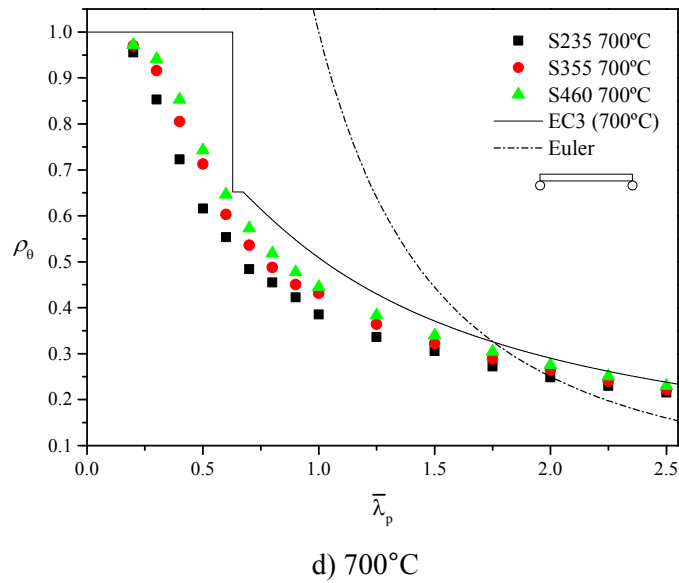


Figure 2.18: Ultimate strength of a plate simply supported in 4 sides (internal element) at elevated temperatures under compression.

For outstand elements under compression, it can be observed that at elevated temperatures the steel grade has some influence on the ultimate strength of the plates, while at normal temperature this is not the case (see Figure 2.9), mainly because at elevated temperatures the stress-strain diagram of steel is non-linear and at normal temperature a bi-linear stress-strain diagram is used. It can be seen that there is a good agreement for the plates classified as Class 4 at elevated temperatures ($\bar{\lambda}_p = \bar{\lambda}_{p,\theta} \geq 0.639$) and for steel grade S460 but the Eurocode 3 gives higher values for plates with lower non-dimensional slenderness and for different steel grades, being considerably un-conservative for the non-dimensional slenderness lower than $\bar{\lambda}_p = \bar{\lambda}_{p,\theta} < 0.639$.

For internal plates under compression, it is observed that the numerical results obtained are below the design curve of the Eurocode 3, meaning that it is not on the safe side, as it is also observed at normal temperature and also justified by the more severe geometrical imperfections used in this study. Nevertheless the differences in this case are greater than at normal temperature, as expected, since the design curve adopted at elevated temperatures is the same as at normal temperature, where additional post-critical reserve has been taken into account as mentioned in section §2.3.2.1, however at elevated temperatures the reduction of stiffness and strength that occurs due to the thermal effects, is not accounted for, therefore bigger differences exist between the two situations. In both cases, it can be seen that the steel

grade has some influence in the ultimate plate strength and this has not been taken into account in the design curve of the Eurocode 3. It is also noticeable, from Figure 2.17 and Figure 2.18 that the post-critical resistance decrease at elevated temperature compared with the behaviour at normal temperature.

At elevated temperatures, as mentioned before, the residual stresses have little or no influence in the plate ultimate strength. In Figure 2.19 this is observed with the comparison of the numerical results obtained with and without residual stresses. Therefore in this study the residual stresses have not been taken into account at elevated temperatures.

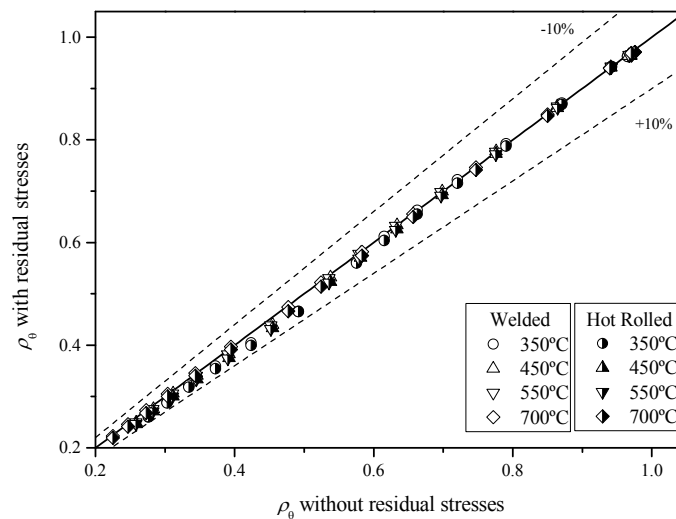
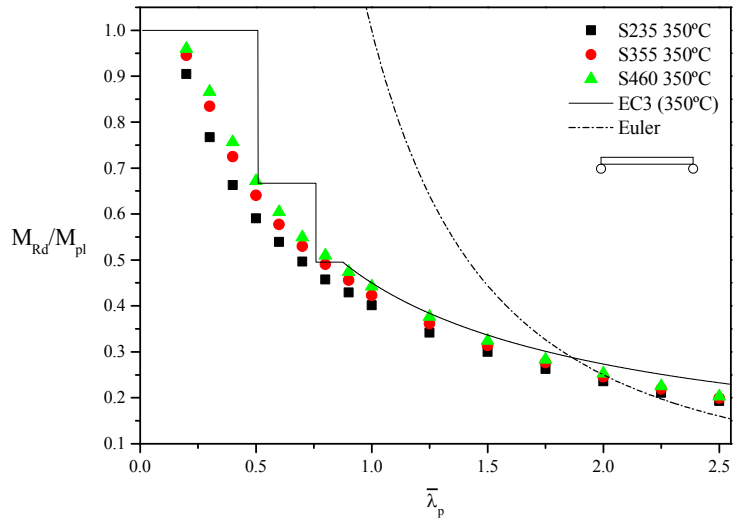


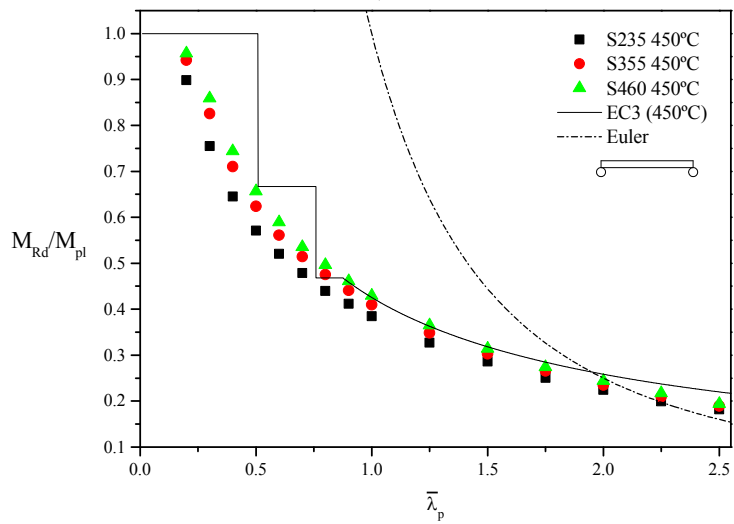
Figure 2.19: Influence of the residual stresses in the ultimate strength of outstand plates under compression at elevated temperature for steel grade S355.

2.3.3.2 Elements under bending

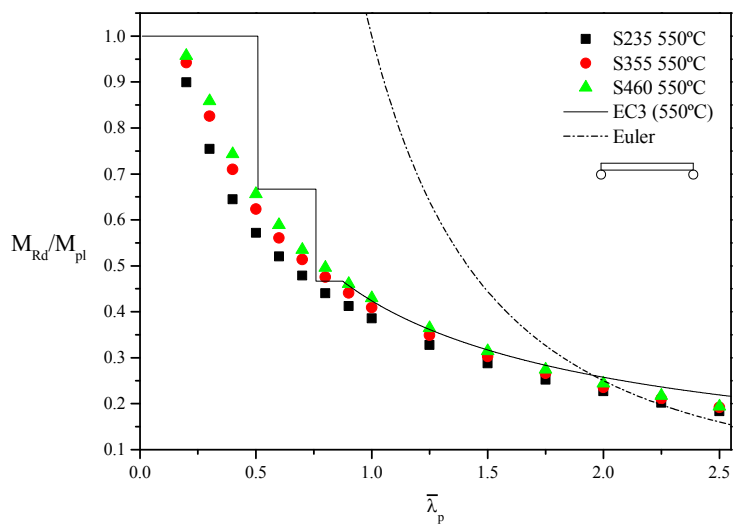
In Figure 2.20 results of the ultimate strength of an internal plate under bending are shown for various steel grades and different temperatures.



a) 350°C



b) 450°C



c) 550°C

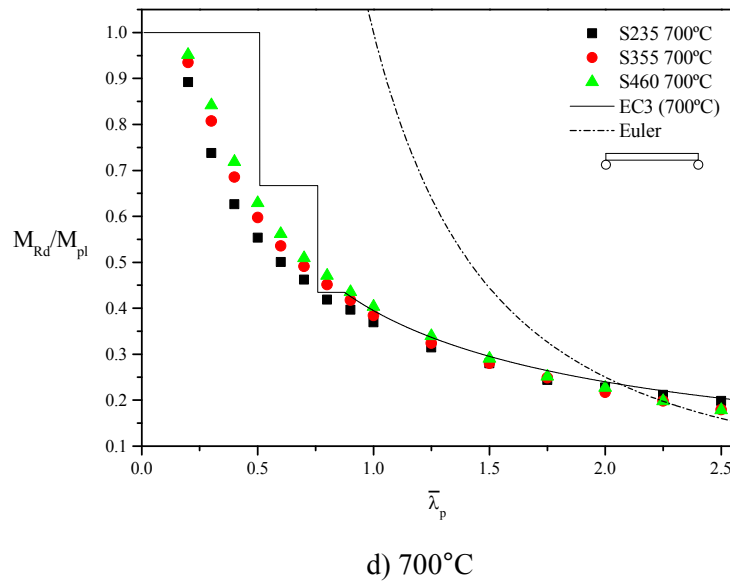


Figure 2.20: Ultimate strength of a plate simply supported in 4 sides at elevated temperatures under bending.

At elevated temperatures the bending resistance for the different plate classification regarding the local buckling according to the Eurocode 3 for the limits in Table 2.2, is defined by:

$$M_{fi,Rd} = \begin{cases} M_{pl,fi,Rd} = W_{pl,y} k_{y,\theta} f_y / \gamma_{M,fi} & \bar{\lambda}_p \leq 0.508 \\ M_{el,fi,Rd} = W_{el,y} k_{y,\theta} f_y / \gamma_{M,fi} & 0.508 < \bar{\lambda}_p \leq 0.759 \\ M_{eff,fi,Rd} = W_{eff,y} k_{0.2p,\theta} f_y / \gamma_{M,fi} & \bar{\lambda}_p > 0.759 \end{cases} \quad (2.12)$$

where $M_{pl,fi,Rd}$, $M_{el,fi,Rd}$ and $M_{eff,fi,Rd}$ are the plastic bending resistance, elastic bending resistance and the effective bending resistance respectively of a plate at elevated temperatures, $k_{y,\theta}$ and $k_{0.2p,\theta}$ are the reduction factors from Part 1-2 of Eurocode 3 for the steel at elevated temperatures as shown in Figure 2.4. From the results of Figure 2.20 it can be observed that the obtained numerical results follow the design curve of the Eurocode 3 for non-dimensional slenderness values higher than the corresponding Class 4 limit ($\bar{\lambda}_p = \bar{\lambda}_{p,\theta} > 0.759$), however, this curve fails to predict the ultimate bending resistance of plates with non-dimensional slenderness values lower than this Class 4 limit. Being non-conservative for non-dimensional slenderness lower than $\bar{\lambda}_p = \bar{\lambda}_{p,\theta} < 0.759$. It is also noticeable the inexistence of almost any post-critical resistance, just for higher values of the

non-dimensional slenderness $\bar{\lambda}_p > (\approx 2.0)$. As mentioned before, there is also some influence of the steel grade on the plate ultimate strength of the plates.

Again it is possible to see a plateau in the EC3 curve since the reduction factor for the plate buckling resistance only starts to decrease for internal elements in bending for $\bar{\lambda}_p = 0.874$ (see equation (2.2)).

2.4 New proposal

From the results obtained in the last section it is clear that a new design method to take into account the ultimate plate strength at elevated temperatures is needed. A new proposal for a design curve that better fits the numerical results obtained has been developed. This design curve has been calibrated as close as possible to the existing design curve of the Eurocode 3 by introducing the factors α_θ and β_θ on the expressions of Part 1-5 of Eurocode 3 (see equations (2.5) and (2.6)), hence the influence of the imperfections is taken into account as in the original formulas developed by Winter and additionally the non-linear steel constitutive law at elevated temperatures is also accounted for, furthermore by using the factor ε_θ (see Table 2.5) steel grade is also taken into account in this new proposal.

Table 2.5: Coefficients to be used in equations (2.13) and (2.14).

Internal compression elements	Outstand compression elements
$\alpha_\theta = 0.9 - 0.315 \frac{k_{0.2p,\theta}}{\varepsilon_\theta k_{y,\theta}}$	$\alpha_\theta = 1.1 - 0.630 \frac{k_{0.2p,\theta}}{\varepsilon_\theta k_{y,\theta}}$
$\beta_\theta = 2.3 - 1.1 \frac{k_{0.2p,\theta}}{k_{y,\theta}}$	$\beta_\theta = 2 - 1.1 \frac{k_{0.2p,\theta}}{k_{y,\theta}}$
$\varepsilon_\theta = 0.85\varepsilon = 0.85\sqrt{235/f_y}$	

This proposal is intended to be used only for cross-sections with a classification of Class 3 or Class 4. This proposal has also the advantage of taking the necessary allowances in order to use the strength at 2% total strain instead of the 0.2% proof strength, leading to much more economic cross-sections.

For internal compression elements the following expressions is proposed:

$$\rho_{\theta} = \frac{(\bar{\lambda}_p + \alpha_{\theta})^{\beta_{\theta}} - 0.055(3 + \psi)}{(\bar{\lambda}_p + \alpha_{\theta})^{2\beta_{\theta}}} \leq 1.0 \quad (2.13)$$

and for outstand compression elements is proposed:

$$\rho_{\theta} = \frac{(\bar{\lambda}_p + \alpha_{\theta})^{\beta_{\theta}} - 0.188}{(\bar{\lambda}_p + \alpha_{\theta})^{2\beta_{\theta}}} \leq 1.0 \quad (2.14)$$

The coefficients to be used in equations (2.13) and (2.14) are given in Table 2.5. Conservatively, to avoid having temperature-dependent effective cross-sections, the values of α_{θ} and β_{θ} to be considered in equations (2.13) and (2.14), can be obtained for a temperature of $\theta_a = 700^{\circ}C$ being the respective values given in the Table 2.6.

Table 2.6: Coefficients to be used in equations (2.13) and (2.14) by conservatively adopting a steel temperature of $\theta_a = 700^{\circ}C$.

Internal compression elements	Outstand compression elements
$\alpha_{\theta} = 0.9 - \frac{0.205}{\varepsilon_{\theta}}$	$\alpha_{\theta} = 1.1 - \frac{0.412}{\varepsilon_{\theta}}$
$\beta_{\theta} = 1.583$	$\beta_{\theta} = 1.283$
$\varepsilon_{\theta} = 0.85\varepsilon = 0.85\sqrt{235/f_y}$	

For instance, the compression resistance of outstand plates is obtained according to:

$$N_{fi,Rd} = \begin{cases} Ak_{y,\theta}f_y / \gamma_{M,fi} & \bar{\lambda}_p \leq 0.456 \\ A_{eff}k_{y,\theta}f_y / \gamma_{M,fi} & \bar{\lambda}_p > 0.456 \end{cases} \quad (2.15)$$

where the steel strength at 2% total strain at elevated temperatures $k_{y,\theta}f_y$ is used.

For internal plates the compression resistance is given by equation (2.14) but the transition value of the non-dimensional slenderness is 0.569 instead of 0.456.

In Figure 2.21 and Figure 2.22 the design curves for outstand and internal elements under compression obtained with the new proposal are shown respectively for different temperatures, and in Figure 2.23 the respective curves for internal elements under bending are depicted.

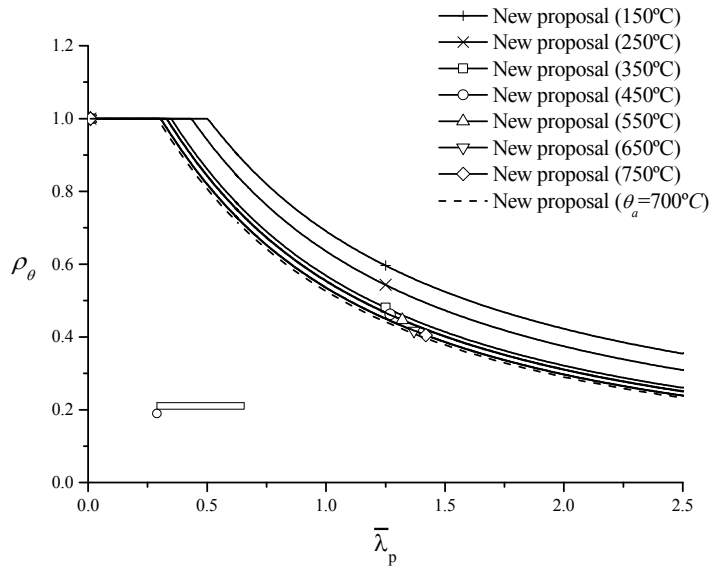


Figure 2.21: New proposed design curves for outstand elements under compression for steel grade S355.

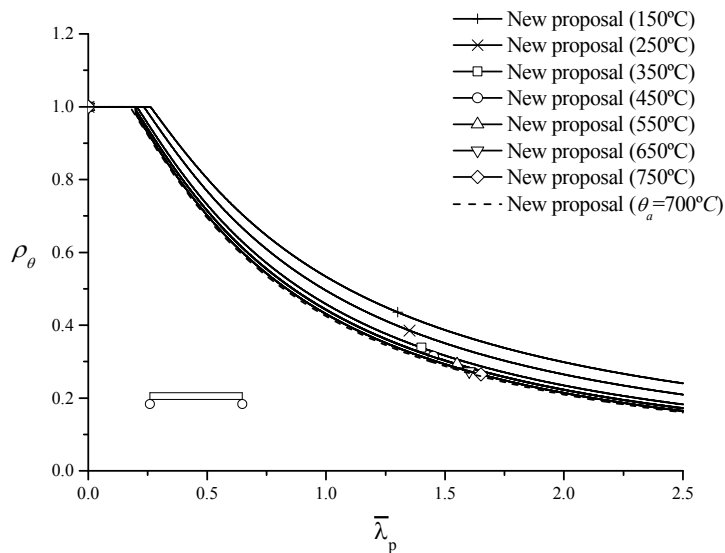


Figure 2.22: New proposed design curves for internal elements under compression for steel grade S355.

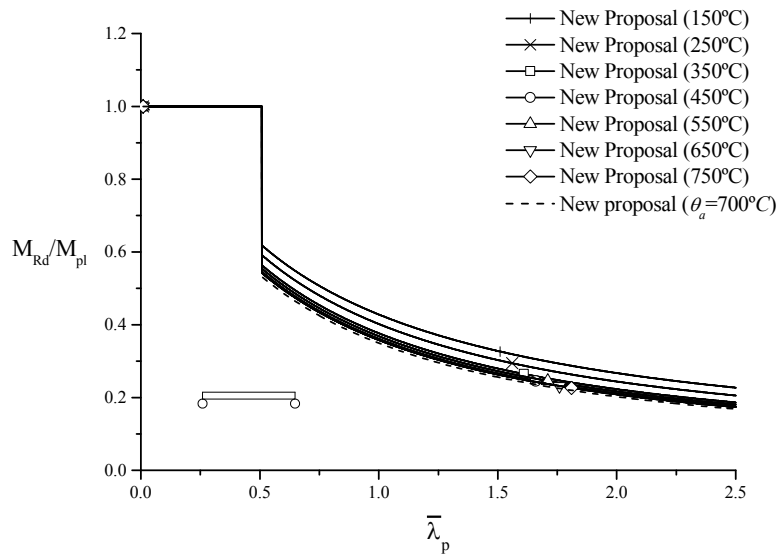


Figure 2.23: New proposed design curves for internal elements under bending for steel grade S355.

In these figures, a comparison with conservatively adopting a constant temperature of $\theta_a = 700^\circ\text{C}$ is also highlighted. The actual design curves of Eurocode 3 as defined by equations (2.10) and (2.11) considering different temperatures are shown in Figure 2.24 and Figure 2.25 for an outstand and an internal plate element under compression respectively and in Figure 2.26 for an internal plate element under bending (see equation (2.12)). In each figure it is also shown the new design curve considering a temperature of $\theta_a = 700^\circ\text{C}$.

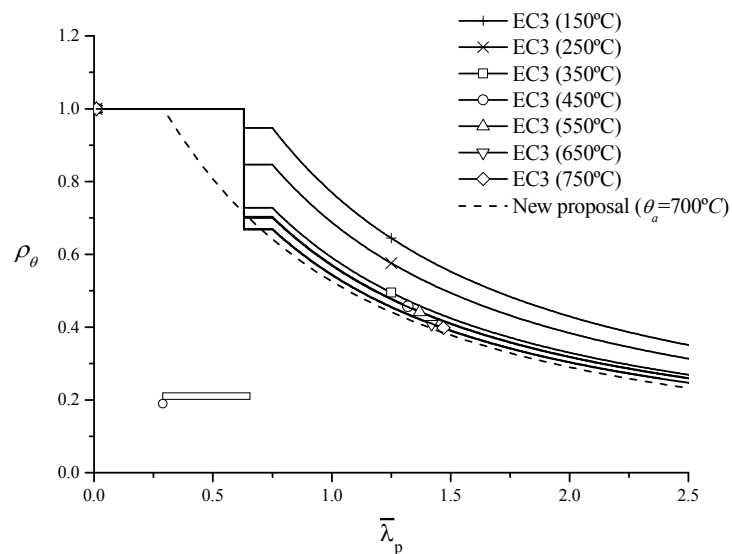


Figure 2.24: Comparison of the new simplified proposal with the actual design curves of Eurocode 3 for outstand elements under compression for steel grade S355.

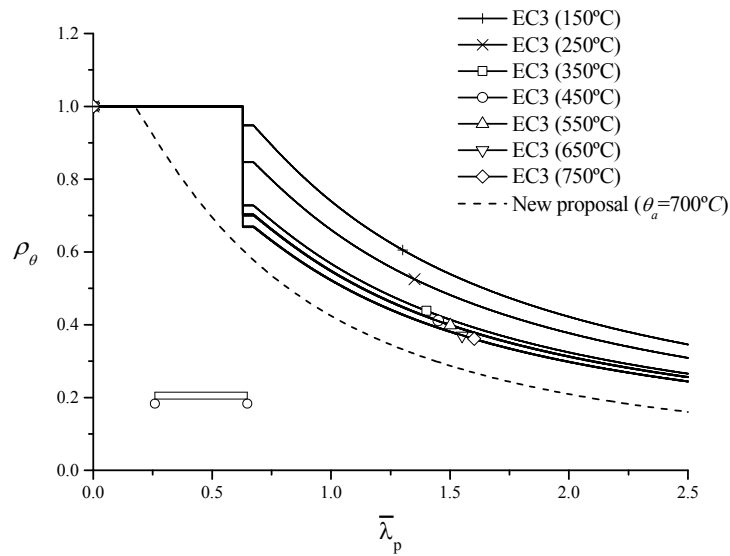


Figure 2.25: Comparison of the new simplified proposal with the actual design curves of Eurocode 3 for internal elements under compression for steel grade S355.

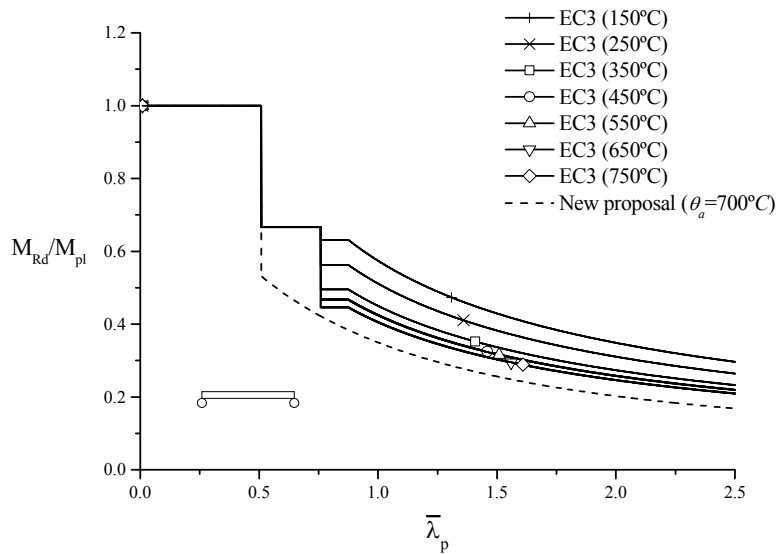


Figure 2.26: Comparison of the new simplified proposal with the actual design curves of Eurocode 3 for internal elements under bending for steel grade S355.

It can be seen that the curve of the new proposal with $\theta_a = 700^\circ C$ is safe and conservative regarding the actual existing design curves of the Eurocode 3. For steel temperatures below $350^\circ C$ this curve is very conservative, however these are very low temperatures and elements with such critical temperatures are not expected to be common in fire design.

2.4.1 Results for plates under compression

In Figure 2.27, Figure 2.28 and Figure 2.29 the numerical results are compared with the new proposal for outstand plates in compression for the steel grades S235, S355 and S460 respectively, for the temperatures of 350°C, 450°C, 550°C and 700°C.

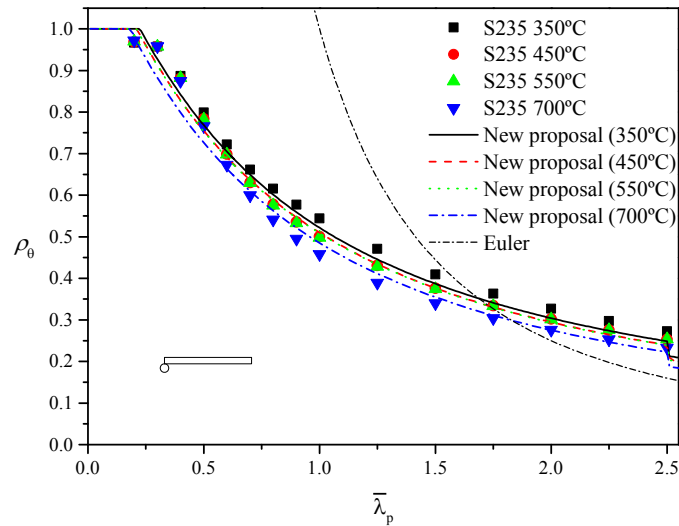


Figure 2.27: Results of numerical study of simply supported plates on 3 sides at elevated temperature for steel grade S235 under compression and comparison to the new proposal.

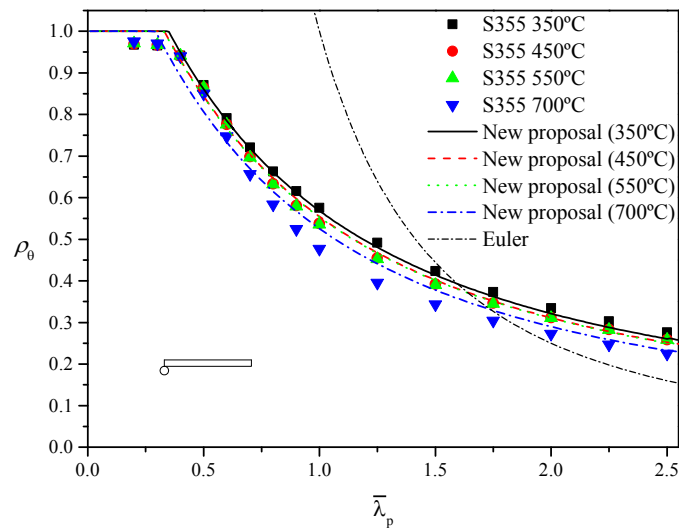


Figure 2.28: Results of numerical study of simply supported plates on 3 sides at elevated temperature for steel grade S355 under compression and comparison to the new proposal.

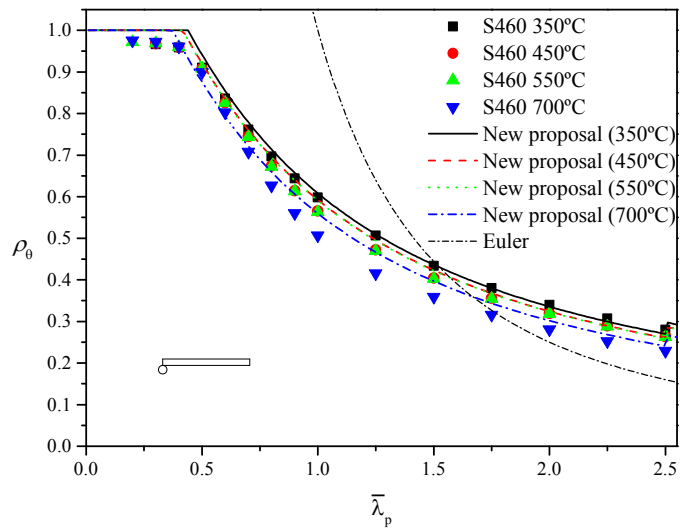


Figure 2.29: Results of numerical study of simply supported plates on 3 sides at elevated temperature for steel grade S460 under compression and comparison to the new proposal.

It can be seen that there is a good agreement between the obtained numerical results and the new proposal for the design curve.

For an internal plate, the numerical results are compared with the new proposal for the design curve at elevated temperatures for the steel grades S235, S355 and S460 in the figures Figure 2.30, Figure 2.31 and Figure 2.32 respectively.

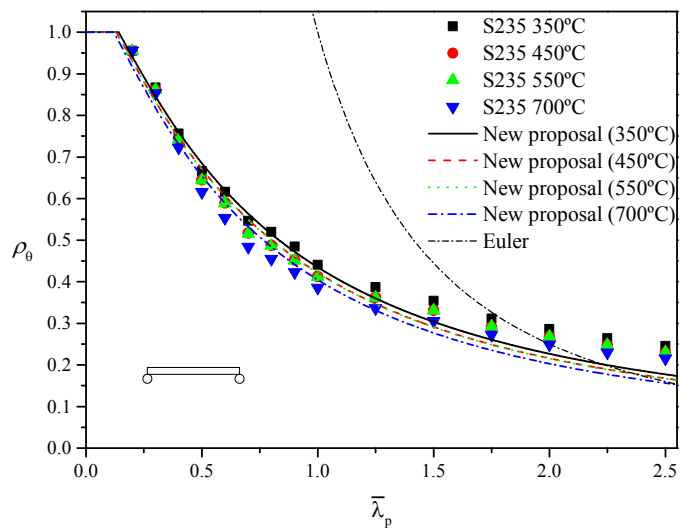


Figure 2.30: Results of numerical study of simply supported plates on 4 sides at elevated temperature for steel grade S235 under compression and comparison to the new proposal.

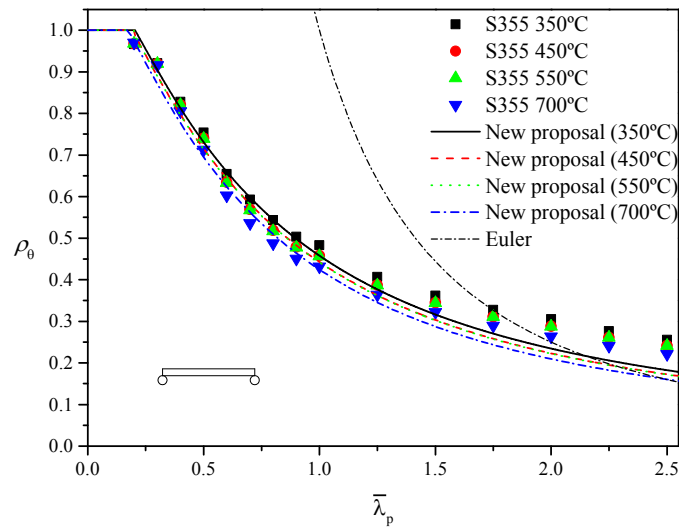


Figure 2.31: Results of numerical study of simply supported plates on 4 sides at elevated temperature for steel grade S355 under compression and comparison to the new proposal.

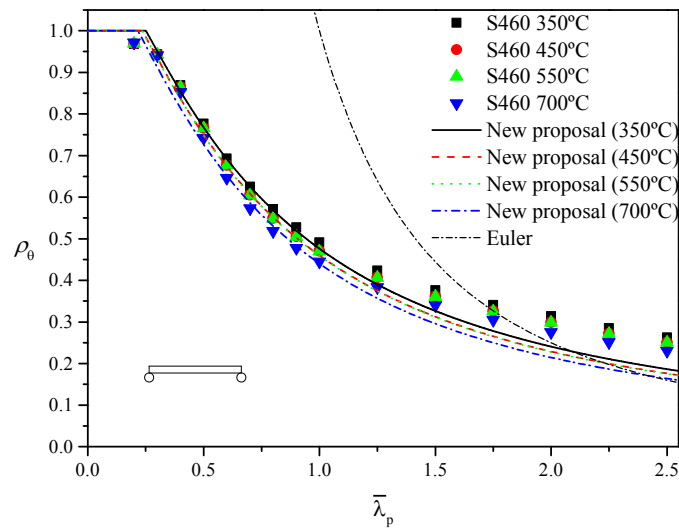


Figure 2.32: Results of numerical study of simply supported plates on 4 sides at elevated temperature for steel grade S460 under compression and comparison to the new proposal.

Again it can be observed a good correlation between the numerical results and the new proposal for the internal plates under compression.

2.4.2 Results for plates under bending

In this section the results of the bending resistance of internal plates are compared for various steel grades and different temperatures with the new proposal. The bending resistance of the plate is obtained according to:

$$M_{fi,Rd} = \begin{cases} M_{pl,fi,Rd} = W_{pl,y} k_{y,\theta} f_y / \gamma_{M,fi} & \bar{\lambda}_p \leq 0.508 \\ M_{eff,fi,Rd} = W_{eff,y} k_{y,\theta} f_y / \gamma_{M,fi} & \bar{\lambda}_p > 0.508 \end{cases} \quad (2.16)$$

where $M_{pl,fi,Rd}$ is the plastic bending resistance and $M_{eff,fi,Rd}$ is the effective bending resistance obtained with the section modulus $W_{eff,y}$ calculated with the reduction factor for the local buckling according to equation (2.13) of the new proposal. Notice that $M_{eff,fi,Rd}$ is calculated with the steel strength at a 2% total strain at elevated temperatures $k_{y,\theta} f_y$.

In Figure 2.33, Figure 2.34 and Figure 2.35 the results are shown for the steel grades S235, S355 and S460 respectively.

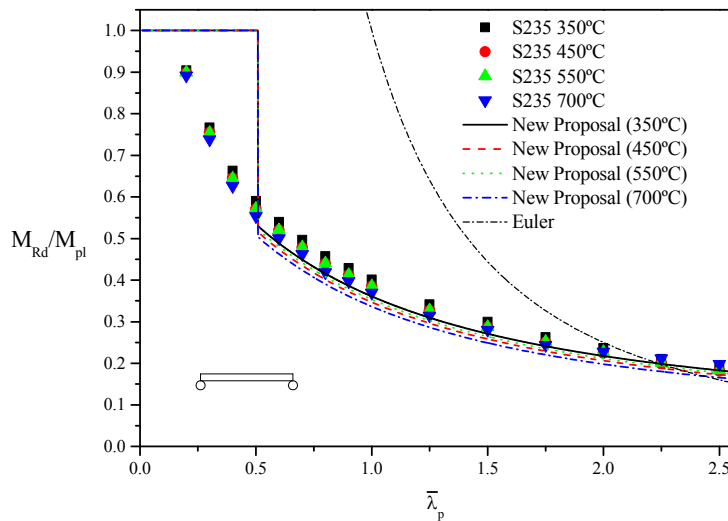


Figure 2.33: Results of numerical study of simply supported plates on 4 sides at elevated temperature for steel grade S235 under bending and comparison to the new proposal.

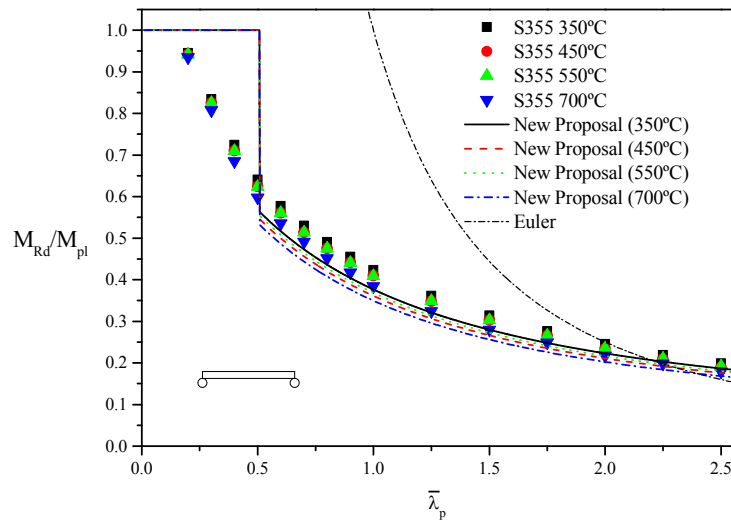


Figure 2.34: Results of numerical study of simply supported plates on 4 sides at elevated temperature for steel grade S355 under bending and comparison to the new proposal.

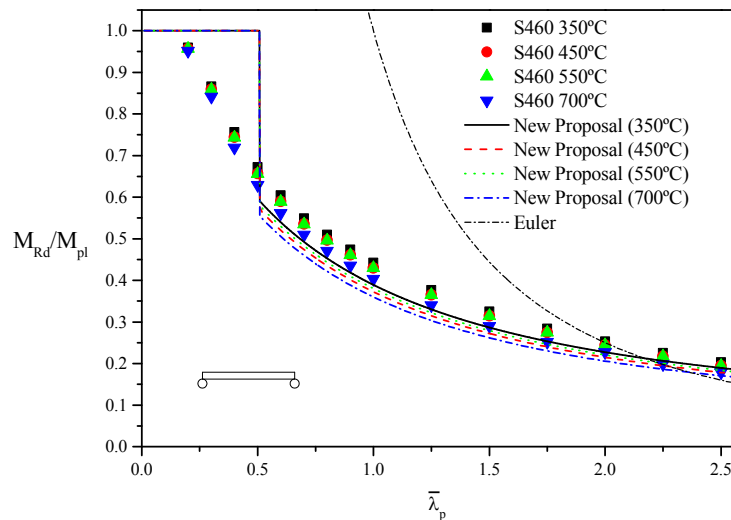


Figure 2.35: Results of numerical study of simply supported plates on 4 sides at elevated temperature for steel grade S460 under bending and comparison to the new proposal.

It can be observed a good agreement between the numerical results obtained and the new proposal for internal plates under bending for non-dimensional slenderness in the range of Class 3 and Class 4 ($\bar{\lambda}_p > 0.598$) where this new proposal is intended to be applied. It worth be mentioned that for non-dimensional slenderness limits of Class 1 and Class 2

($\bar{\lambda}_p < 0.598$) the results are still non-conservative and the same behaviour is observed at normal temperature (see Figure 2.15). This question however has not been addressed in this study.

2.5 Conclusions

Local buckling is a major concern when designing slender cross-sections. The existing design rules for taking into account local buckling and calculate the ultimate strength of steel plates at elevated temperatures have proven to be misleading and new expressions have been developed. On the basis of a numerical parametric study of several steel plates at elevated temperatures, considering different support conditions, loading cases and steel grades, it was possible to compare the results with the existing design curves for the ultimate plate strength and to calibrate new expressions for internal and outstand elements that have a better correlation with the obtained results. At normal temperature, the comparison of the numerical results with the existing design curves for calculating the ultimate strength of the steel plates according to Eurocode 3 shows that there is good agreement between them. It was also possible to conclude that the residual stresses influence the ultimate strength capacity of the plates at normal temperature while at elevated temperatures their effect is negligible. Concerning the steel grade, it was observed that the influence at elevated temperatures is more meaningful than at normal temperature. Due to the considerable reduction of strength and stiffness that occurs in the fire exposed plates, the post-critical resistance is also limited, but both the Eurocode design rules and the new proposal made within this study have a good agreement with the results for plates with high non-dimensional slenderness where this behaviour is more important.

At elevated temperatures, for the plates where local buckling needs to be taken into account in the determination of the cross-sectional resistance, the existing design rules of Eurocode 3 show good agreement with the obtained numerical results. For plates with lower non-dimensional slenderness, especially in the range of Class 3, the Eurocode 3 however fails to predict the ultimate strength of these plates and may lead to overestimation of the cross-sectional resistance, by using the new proposal in this study this limitation is corrected. On the other hand, using these new expressions to calculate the effective width of the plates and consequently the effective cross-section properties leads to a more realistic design.

Accordingly, the necessary allowances for local buckling have been taken into account considering the strength at a total strain of 2% instead of using the 0.2% proof strength as recommended in the Annex E of Part 1-2 of Eurocode 3. This overcomes the limitation of Eurocode 3 that assumes that every plate will buckle, when the cross-sections is classified as Class 4.

The new expressions are temperature dependant leading to a variation on the effective cross-section properties under fire situation and although the method herein proposed can be implemented with relatively ease of computational effort if compared with the actual design rules, it was also demonstrated that a simplified proposal can be used instead by considering a constant steel temperature of $\theta_a = 700^\circ C$. It worth be mentioned that this simplification can lead to over conservative results for steel temperatures of $\theta_a \leq 250^\circ C$, however these are very low temperatures and elements with such critical temperatures are not commonly used with respect to the usual degree of utilization of the elements.

References

- [2.1] CEN, “EN 1993-1-1, Eurocode 3: Design of steel structures - Part 1-1: General rules and rules for buildings.” European Committee for Standardisation, Brussels, 2005.
- [2.2] Knobloch M., Fontana M., “Strain-based approach to local buckling of steel sections subjected to fire,” *Journal of Constructional Steel Research*, vol. 62, no. 1–2, pp. 44–67, January 2006.
- [2.3] Renaud C., Zhao B., “Investigation of simple calculation method in EN 1993-1-2 for buckling of hot rolled class 4 steel members exposed to fire,” in *Fourth International Workshop “Structures in Fire,”* Aveiro, Portugal, 2006.
- [2.4] Quiel S. E., Garlock M. E. M., “Calculating the buckling strength of steel plates exposed to fire,” *Thin-Walled Struct.*, vol. 48, no. 9, pp. 684–695, September 2010.
- [2.5] CEN, “EN 1993-1-5, Eurocode 3 - Design of steel structures - Part 1-5: Plated structural elements.” European Committee for Standardisation, Brussels, 2006.
- [2.6] CEN, “EN 1993-1-2, Eurocode 3: Design of steel structures - Part 1-2: General rules - Structural fire design.” European Committee for Standardisation, Brussels, 2005.
- [2.7] Ranby A., “Structural fire design of thin walled steel sections,” *Journal of Constructional Steel Research*, vol. 46, no. 1–3, pp. 303–304, April 1998.
- [2.8] Ala-Outinen T., Myllymäki J., “Local Buckling of RHS Members at Elevated Temperatures,” Espoo, Finland, 1995.
- [2.9] Yang K., Chen S., Lin C., Lee H., “Experimental study on local buckling of fire-resisting steel columns under fire load,” *Journal of Constructional Steel Research*, vol. 61, no. 4, pp. 553–565, April 2005.
- [2.10] Yang K.-C., Lee H.-H., Chan O., “Performance of steel H columns loaded under uniform temperature,” *Journal of Constructional Steel Research*, vol. 62, no. 3, pp. 262–270, March 2006.
- [2.11] Yang K.-C., Lee H.-H., Chan O., “Experimental study of fire-resistant steel H-columns at elevated temperature,” *Journal of Constructional Steel Research*, vol. 62, no. 6, pp. 544–553, June 2006.

- [2.12] Franssen J.-M., “SAFIR, A Thermal/Structural Program for Modelling Structures under Fire,” *Engineering Journal, A.I.S.C.*, vol. 42, no. 3, pp. 143–158, 2005.
- [2.13] Von Karman T., Sechler E. E., Donnell L. H., “The strength of Thin Plates in Compression,” *Transactions of the American Society of Mechanical Engineers*, vol. 54, p. 53, 1932.
- [2.14] Winter G., “Strength of Thin Steel Compression Flanges,” *Transactions of the American Society of Mechanical Engineers*, vol. 112, p. 527, 1947.
- [2.15] CEN, “Publication N1664E - Corrigendum to EN 1993-1-5 Eurocode 3 : Design of steel structures -Part 1-5 : Plated structural elements,” 2009.
- [2.16] Talamona D., Franssen J.-M., “A Quadrangular Shell Finite Element for Concrete and Steel Structures Subjected to Fire,” *Journal of Fire Protection Engineering*, vol. 15, no. 4, pp. 237–264, November 2005.
- [2.17] CEN, “EN 1090-2: Execution of steel structures and aluminium structures - Part 2 : Technical requirements for steel structures.” European Committee for Standardisation, Brussels, 2008.
- [2.18] CEA, “CAST 3M is a research FEM environment; its development is sponsored by the French Atomic Energy Commission <<http://www-cast3m.cea.fr/>>.” 2012.
- [2.19] Couto C., Vila Real P., Lopes N., “RUBY - an interface software for running a buckling analysis of SAFIR models using Cast3M.” University of Aveiro, 2013.
- [2.20] ECCS, *Manual on Stability of Steel Structures. Publication No. 22.* European Convention for Constructional Steelwork Technical Committee No. 8, 1976.
- [2.21] ECCS, *New lateral torsional buckling curves k_{LT} - numerical simulations and design formulae.* European Convention for Constructional Steelwork Technical Committee No. 8, 2000.
- [2.22] ECCS, *Ultimate limit state calculation of sway frames with rigid joints. Publication No. 33.* European Convention for Constructional Steelwork Technical Committee No. 8, 1984.
- [2.23] Pauli J., Knobloch M., Fontana M., “On the local buckling behaviour of steel columns in fire,” in *8th fib PhD Symposium in Kgs. Lyngby, Denmark*, 2010, vol. 1.

- [2.24] FIDESC4, “Fire Design of Steel Members with Welded or Hot-rolled Class 4 Cross-sections, Grant Agreement RFSR-CT-2011-00030 (2011-2014),” 2014.
- [2.25] Hricák J., Jandera M., Wald F., “*Local buckling of Class 4 cross-sections at elevated temperatures.*” in Benchmark studies - Experimental validation of numerical models in fire engineering, C. E. Wald F., Burgess I., Kwasniewski L., Horová K., Ed. CTU Publishing House, Czech Technical University in Prague, pp. 21 – 33, 2014.
- [2.26] Wang W., Kodur V., Yang X., Li G., “Experimental study on local buckling of axially compressed steel stub columns at elevated temperatures,” *Thin-Walled Structures*, vol. 82, pp. 33–45, September 2014.

Chapter 3 Cross-sections

Chapter outline

- 3.1. Introduction
- 3.2. Design provisions to take local buckling into account in the cross-sectional resistance according to Eurocode 3
 - 3.2.1. Cross-section classification
 - 3.2.2. The effective width method from Eurocode 3
 - 3.2.3. Code provisions for local buckling at elevated temperatures
- 3.3. New proposal to calculate the effective width at elevated temperatures
- 3.4. Simple design methods to calculate the cross-sectional resistance at elevated temperatures
- 3.5. Numerical model
 - 3.5.1. Material properties
 - 3.5.2. Support conditions
 - 3.5.3. Loading
 - 3.5.4. Imperfections
- 3.6. Numerical study
 - 3.6.1. Cross-sections
 - 3.6.2. Results and comparison to simple design methods
 - 3.6.2.1. Elements in compression
 - 3.6.2.2. Elements in bending about the major-axis
 - 3.6.3. Statistical investigation of the proposed methodologies
- 3.7. Comparison with experimental results
- 3.8. Conclusions
- References

Abstract In this chapter, the resistance of slender I-shaped cross-sections, where local buckling has a predominant role in the ultimate capacity, is investigated at elevated temperatures. A numerical study considering several cross-sections submitted to compression or bending about the major-axis is performed using a finite element analysis software. The results are compared with the existing formulae available in Part 1-2 of the Eurocode 3 showing that they need to be improved. For Class 3 cross-sections, it is observed that the existing rules lead to unsafe results because local buckling occurs at elevated temperatures prior to the development of the elastic bending resistance or the gross cross-section compression resistance. For Class 4 cross-sections, the results show that these rules are not adequate because it is recommended for the design yield strength of steel the use of the 0.2% proof strength even if the cross-section has plates not prone to local buckling. A new methodology to account for the local buckling in steel I-sections at elevated temperatures is presented based on the expressions developed in the previous chapter to calculate the effective width of thin plates at elevated temperatures. According to this new methodology, an effective cross-section is calculated for Class 3 and Class 4 cross-sections and the yield strength at 2% total strain is used for Class 4 cross-sections as recommended by the Eurocode 3 for the other section classes. Finally, it is demonstrated that this methodology leads to good results when compared against numerical and experimental results.

3.1 Introduction

Slender cross-sections when submitted to compression stresses are prone to local buckling that prevents the attainment of the yield stress in the compressed parts of the cross-section thus affecting their ultimate capacity. At normal temperature, according to Eurocode 3 [3.1] these cross-sections are classified as Class 4 – the highest class – and Part 1-5 [3.2] provides two methods to take local buckling into account, namely the effective width method that leads to a reduced cross-section and the reduced stress method.

At elevated temperatures, Part 1-2 of Eurocode 3 [3.3] suggests for Class 4 cross-sections a default critical temperature of 350 °C if no fire design is made, which means that even for a requirement of 15 minutes of fire resistance, passive fire protection should normally be used for current profiles. Alternatively, the informative Annex E of Part 1-2 of Eurocode 3 suggests the use of a reduced cross-section calculated with the effective width method using the steel properties at normal temperature and for the design yield strength of steel the 0.2% proof strength ($f_{0.2p,\theta}$, see Figure 3.1).

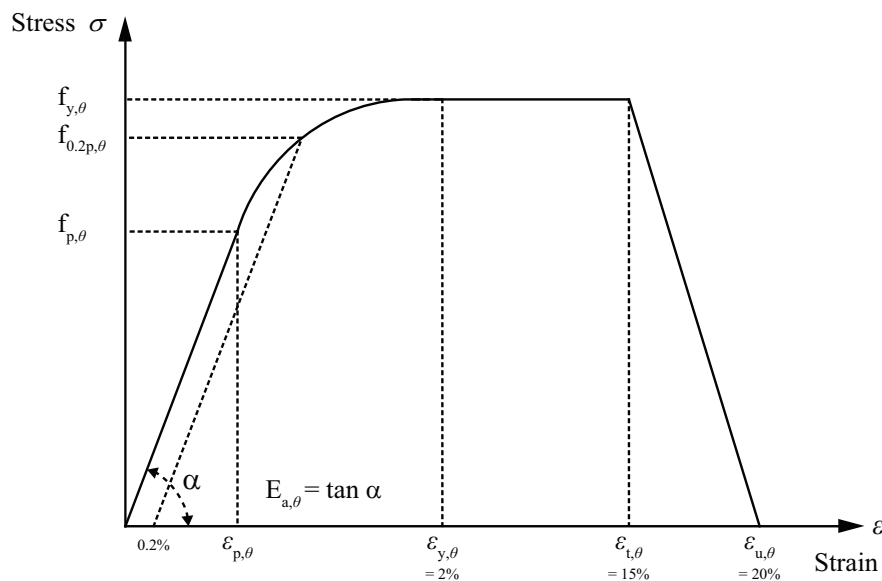


Figure 3.1: Stress-strain relationship for carbon steel at elevated temperatures [3.4].

Previous investigations of Fontana and Knobloch [3.5], Renaud and Zhao [3.6] and Quiel and Garlock [3.7] demonstrated that this methodology is too conservative. Hence, the need of more realistic formulae to account for the local buckling at elevated temperatures. Studies have been done previously within the scope of one research project [3.8], for welded or hot-

rolled Class 4 steel members. However, these type of studies are limited and cover only, for example, the buckling of Class 4 steel columns [3.5, 3.9–3.11] or are related to other types of steel, for example stainless steels [3.12], for which the constitutive laws differ from carbon steel. In Figure 3.2, an example of column showing local buckling from a test performed at elevated temperatures at the University of Liège is shown.



Figure 3.2: Example of column showing local buckling from a test performed at elevated temperatures at the University of Liège (taken from[3.13]).

In this work, a parametric investigation based on the finite element analysis using the software SAFIR [3.14] is made to assess the resistance of several slender cross-sections in bending and compression. In line with previous investigations by other authors, the obtained results show that the existing formulae of Part 1-2 of Eurocode 3 could be improved. For Class 3 cross-sections, it is observed that the existing rules lead to unsafe results because local buckling occurs at elevated temperatures prior to the development of the elastic bending resistance or the gross cross-section compression resistance. For Class 4 cross-sections, the results obtained show that the use of the 0.2% proof strength as the design yield strength for the whole cross-section is very conservative, especially if they contain also plates with inferior classes, i.e. without local buckling.

To overcome these inconsistencies and limitations, a new methodology to calculate the cross-sectional resistance of slender cross-sections at elevated temperatures is presented in this work. Accordingly, an effective cross-section is calculated for Class 3 and Class 4 cross-sections based on the expressions developed in the previous chapter to calculate the effective width of thin plates at elevated temperatures [3.15] and the yield strength at 2% total strain is used for Class 4 as recommended in Eurocode 3 for the other section classes. A comparison of the predicted cross-sectional capacity using the proposed methodology against numerical and experimental results shows the considerable advantages as well as the validity and accuracy of this proposal.

3.2 Design provisions to take local buckling into account in the cross-sectional resistance according to Eurocode 3

I-shaped cross-sections can be considered as an assembly of plates often referred as internal (webs) and outstand (flanges) elements. If the width-to-thickness ratios of these plates are high, they are normally referred to as slender and may buckle when submitted to compression, preventing the attainment of the yield strength in one or more parts of the cross-section, thus reducing the resistance of the cross-section and consequently the load bearing capacity of the structural members. To account for this phenomenon, the cross-section is classified as a function of the width-to-thickness ratio of its plates and this issue is addressed in subsection 3.2.1. In order to consider local buckling in the design, a reduced cross-section can be used, this method being referred in the literature as the effective width method. The rules to calculate effective width of plates are indicated in Part 1-5 [3.2] and are described in subsection 3.2.2. The code provisions to take local buckling into account at elevated temperatures are presented in subsection 2.3. In the section 3.3, the expressions developed in Chapter 2 to calculate the effective width of thin plates at elevated temperatures, which are used later in this study, are presented.

3.2.1 Cross-section classification

In Eurocode 3, four classes (Classes 1 to 4) of cross-sections are defined in respect to how the local buckling affects the load bearing capacity of the members, with a higher class denoting a higher influence of the local buckling on resistance. According to the definition

of Eurocode 3, Class 1 cross-sections are those that can form a plastic hinge with the rotation capacity required from plastic analysis without reduction of the resistance. Class 2 cross-sections are those that can develop their plastic moment resistance, but have limited rotation capacity because of local buckling. Class 3 cross-sections are those in which the stress in the extreme compression fibre of the steel member assuming an elastic distribution of stresses can reach the yield strength, but local buckling is liable to prevent development of the plastic moment resistance. Finally, Class 4 cross-sections are those in which local buckling will occur before the attainment of yield strength in one or more parts of the cross-section. Cross-section classification is illustrated in Figure 3.3 for a beam submitted to a point load at mid span.

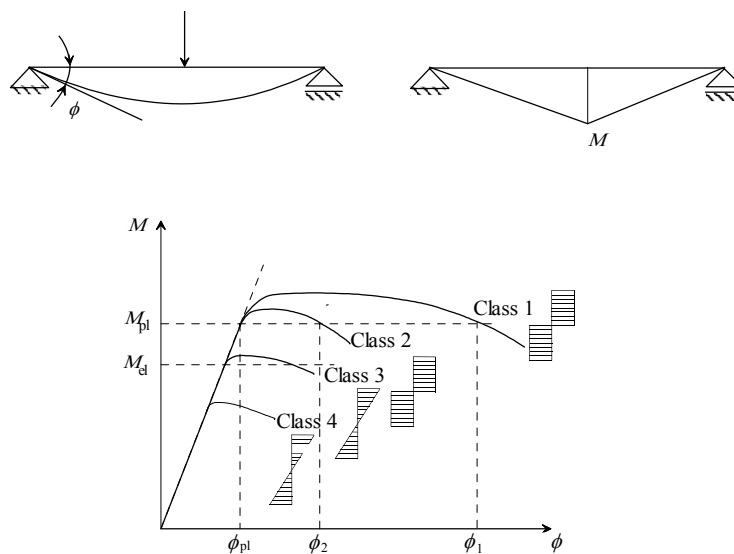


Figure 3.3: Moment-rotation curves for different cross-section classification (adapted from [3.4]).

The limits for each class, are defined in Part 1-1 of Eurocode 3 [3.1] in terms of the width-to-thickness ratio (b/t), also referred as the plate slenderness. For a steel plate to belong to a determined class, the slenderness limit is shown in Table 3. 1, where at normal temperature for carbon steel the parameter ε is defined by:

$$\varepsilon = \sqrt{235 / f_y} \text{ with } f_y \text{ in MPa.} \quad (3.1)$$

The cross-section overall classification is then given by the plate with higher class.

Table 3.1: Slenderness limits (b/t) for the plates for cross-sectional classification at normal temperature.

Element	Class 1	Class 2	Class 3
Outstand element (flange) submitted to compression	9ε	10ε	14ε
Internal element (web) submitted to compression	33ε	38ε	42ε
Internal element (web) submitted to bending	72ε	83ε	124ε

At elevated temperatures, the cross-section classification follows the same procedure and the same width-to-thickness limits as for normal temperature, but the Young's modulus and the yield strength are dependent on the temperature. For carbon steel the parameter at elevated temperatures is given by [3.4] (see equation (3.6)).

$$\begin{aligned}\varepsilon &= \sqrt{\frac{235}{f_{y,\theta}}} \sqrt{\frac{E_\theta}{210000}} = \sqrt{\frac{k_{E,\theta}}{k_{y,\theta}}} \sqrt{\frac{235}{f_y}} \sqrt{\frac{E}{210000}} \quad \text{with } f_y \text{ and } E \text{ in MPa.} \\ &= \sqrt{\frac{k_{E,\theta}}{k_{y,\theta}}} \sqrt{\frac{235}{f_y}} \approx 0.85 \sqrt{\frac{235}{f_y}}\end{aligned}\quad (3.2)$$

where $k_{E,\theta}$ is the reduction factor for the Young modulus at elevated temperatures and $k_{y,\theta}$ is the reduction factor for the steel yield strength at elevated temperatures.

The ratio $\sqrt{k_{E,\theta}/k_{y,\theta}}$ is plotted in Figure 3.4 as a function of the temperature. Eurocode 3 recommends that the ratio $\sqrt{k_{E,\theta}/k_{y,\theta}}$ be replaced by a constant value of 0.85, which is a kind of a mean value of that ratio as shown in Figure 3.4.

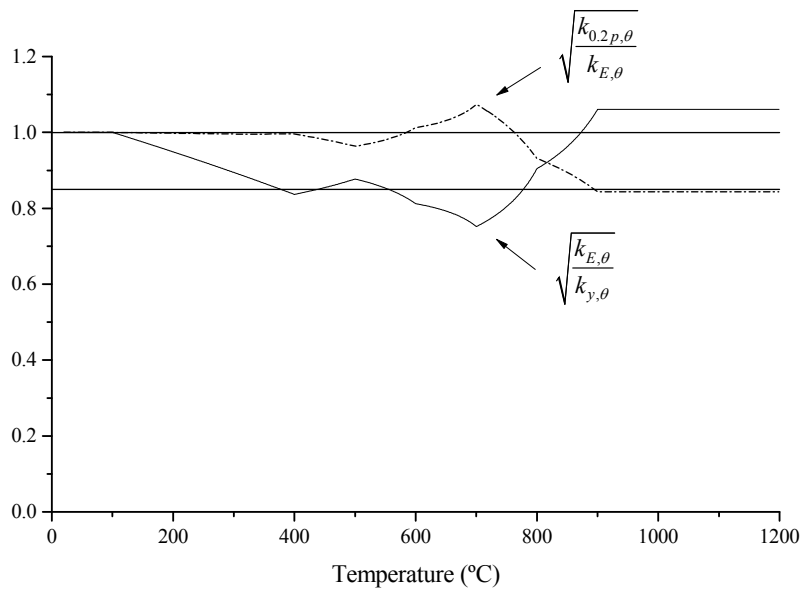


Figure 3.4: Ratios $\sqrt{k_{E,\theta}/k_{y,\theta}}$ and $\sqrt{k_{0.2p,\theta}/k_{E,\theta}}$ as a function of the temperature.

With this simplification, the cross-sectional classification is independent of the temperature.

On this subject, Renaud and Zhao [3.6] point out that it would be more consistent to classify the cross-sections as for normal temperature, instead of using those recommendations, since the square root of the reduction factors for the steel strength using the 0.2% proof strength $k_{0.2p,\theta}$ and for the Young modulus $k_{E,\theta}$ at elevated temperatures is close to one as shown in Figure 3.4. This would be more in accordance with the recommendation given in Annex E of Part 1-2 of Eurocode 3 regarding Class 4 cross-sections at elevated temperatures. But, on the other hand, the experimental results of Ala-Outinen and Myllymäki [3.16], Yang et al. [3.17–3.19] and more recently of Correia and Rodrigues [3.20], show that local buckling occurs even for cross-sections with plates with inferior classes (Class 1 - Class 3) for elevated temperatures. This suggests that is advisable to use a smaller value of the parameter ε , i.e. $\varepsilon = 0.85\sqrt{235/f_y}$ instead of $\varepsilon = \sqrt{235/f_y}$. Despite its importance, investigation on the classification of cross-sections at elevated temperatures is out of the scope of this study and the present guidelines of Eurocode 3 on this matter are followed.

3.2.2 The effective width method from Eurocode 3

The first expressions to calculate the effective width of simply supported plates, and the concept itself, were originally developed by von Karman [3.21] and then adapted by Winter [3.22] to account for the influence of the geometrical imperfections and the residual stresses on the decrease of the load bearing capacity of the plates. Similar expressions, are included in Part 1-5 of Eurocode 3, which gives the reduction factor for the plate buckling resistance for internal elements under compression as [3.23]

$$\rho = \begin{cases} \rho = 1 & \text{for } \bar{\lambda}_p \leq 0.5 + \sqrt{0.085 - 0.055\psi} \\ \frac{\bar{\lambda}_p - 0.055(3 + \psi)}{\bar{\lambda}_p^2} & \text{for } \bar{\lambda}_p > 0.5 + \sqrt{0.085 - 0.055\psi} \end{cases} \quad (3.3)$$

and for outstand elements under compression by

$$\rho = \begin{cases} \rho = 1 & \text{for } \bar{\lambda}_p \leq 0.748 \\ \frac{\bar{\lambda}_p - 0.188}{\bar{\lambda}_p^2} & \text{for } \bar{\lambda}_p > 0.748 \end{cases} \quad (3.4)$$

where $\bar{\lambda}_p$ is the non-dimensional slenderness of a plate given by [3.4]

$$\bar{\lambda}_p = \sqrt{\frac{f_y}{\sigma_{cr}}} = \sqrt{\frac{f_y}{k_\sigma \frac{\pi^2 E t^2}{12(1-\nu^2)b^2}}} = \frac{b/t}{\sqrt{k_\sigma} \sqrt{\frac{\pi^2}{12(1-\nu^2)}}} \frac{1}{\sqrt{\frac{E}{f_y}}} = \frac{b/t}{28.4\varepsilon\sqrt{k_\sigma}} \quad (3.5)$$

Where, σ_{cr} is the elastic critical plate buckling stress, k_σ is the buckling coefficient of the plates which takes into account the different boundary conditions and the stress pattern applied to the plates and

$$\varepsilon = \sqrt{\frac{235}{f_y}} \sqrt{\frac{E}{210000}} \quad \text{with } f_y \text{ and } E \text{ in MPa} \quad (3.6)$$

equations (3.3) and (3.4) are plotted in Figure 3.5 and the values of k_σ are given in Part 1-5 of Eurocode 3 in the Table 4.1 for internal elements and Table 4.2 for outstand elements, or can be found in the literature. Knowing ρ , the effective width is given by $b_{eff} = \rho \times b$.

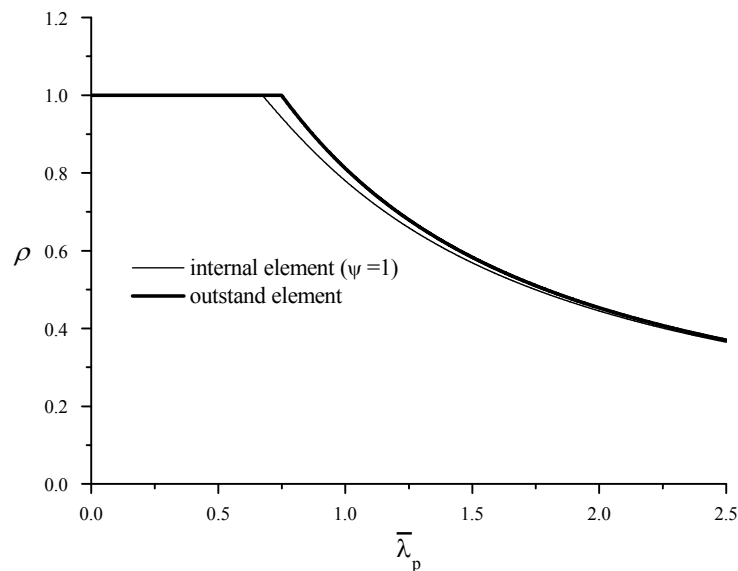


Figure 3.5: Plate reduction factor for internal and outstand elements.

3.2.3 Code provisions for local buckling at elevated temperatures

As mentioned previously, to account for local buckling at elevated temperatures, Part 1-2 of Eurocode 3, suggests for Class 4 cross-sections a default critical temperature of 350°C if no other calculation is made, which normally is conservative. Additionally some further guidance is given in Annex E for the fire design of this type of cross-sections. It is stated that i) the effective cross-section be determined with the effective width method as for normal temperature, i.e. using the material properties at normal temperature and (ii) to use the simple calculation methods with the design value for the steel yield strength as the 0.2% proof strength ($f_{0.2p,\theta}$) instead of the stress at 2% total strain ($f_{y,\theta}$), as normally used in the fire design of other cross-sectional classes. These recommendations are based essentially on the early work of Ranby [3.24] who has demonstrated that this methodology is safe, and leads to accurate results for determining the ultimate load of thin plates susceptible to local buckling at elevated temperatures. In fact, at elevated temperatures, the reduction factor for

plate buckling would be, according to equations (3.3) and (3.4), $\rho_\theta = \rho_\theta(\bar{\lambda}_{p,\theta})$ with the corresponding non-dimensional slenderness at elevated temperatures, given by

$$\bar{\lambda}_{p,\theta} = \sqrt{\frac{f_{y,\theta}}{\sigma_{cr,\theta}}} = \sqrt{\frac{k_{0.2p,\theta}}{k_{E,\theta}}} \sqrt{\frac{f_y}{\sigma_{cr}}} \cong 1.0 \sqrt{\frac{f_y}{\sigma_{cr}}} = \bar{\lambda}_p \quad (3.7)$$

The ratio $\sqrt{k_{0.2p,\theta} / k_{E,\theta}}$ is almost equal to 1.0 as shown in Figure 3.4, and since $\bar{\lambda}_{p,\theta} \cong \bar{\lambda}_p$, equations (3.3) and (3.4) show that it can be considered $\rho_\theta = \rho$. However, this is an inconsistent approach. If under an arbitrary loading, a cross-section has Class 4 plates (elements) and other plates with inferior classes, using a reduced stress to calculate the ultimate load capacity of every plate leads to unrealistic results. Take, for example, an element submitted to pure bending about the major-axis with a regular I-shaped cross-section with Class 1 or 2 flanges and Class 4 web. In this case using the 0.2% proof strength in the whole section due to the web classification is very restrictive because in these types of cross-sections it is usual that around 80% of the bending resistance is provided by the flanges that will have no local buckling problems. This is exemplified further in this study, but one can refer to Figure 3.19 where the moment-rotation curve for a beam in bending is shown for a cross-section with Class 2 flanges and Class 4 web, for the different temperatures the results of the finite element analysis are more than 20% above the ultimate capacity predicted by Eurocode 3.

On the other hand, there is an inconsistency pointed out by Renaud and Zhao in [3.6] regarding the reduction factors for the 0.2% proof strength at elevated temperatures, $k_{0.2p,\theta}$, given in the Table E.1 of Part 1-2 of Eurocode 3. These values do not correspond to the ones calculated according to the stress-strain relationship of steel at elevated temperatures given in the same norm, and it is unknown to the author where the values given in the Part 1-2 of Eurocode 3 come from. The values of $k_{0.2p,\theta}$ that are used in this study correspond to the ones that are calculated according to the stress-strain relationship of carbon steel at elevated temperatures for the case of the steel grade S355, as adopted in the French National Annex of Eurocode 3.

3.3 New proposal to calculate the effective width at elevated temperatures

Due to the limitations aforementioned, new expressions for the plate reduction factor (ρ) have been developed in Chapter 2 (see also [3.15]) in order to replace the use of the design yield strength corresponding to the 0.2% proof strength ($f_{0.2p,\theta}$) with the stress for 2% total strain ($f_{y,\theta}$). The proposed design curves have been calibrated using a format as closer as possible to the existing design curve of Eurocode 3 by introducing the factors α_θ and β_θ on the expressions of Part 1-5 of Eurocode 3 (see equations (3.3) and (3.4)).

According to this proposal, for internal compression elements the following expression is proposed in Chapter 2:

$$\rho_\theta = \frac{(\bar{\lambda}_p + \alpha_\theta)^{\beta_\theta} - 0.055(3 + \psi)}{(\bar{\lambda}_p + \alpha_\theta)^{2\beta_\theta}} \leq 1.0 \quad (3.8)$$

and for outstand compression elements is proposed in Chapter 2:

$$\rho_\theta = \frac{(\bar{\lambda}_p + \alpha_\theta)^{\beta_\theta} - 0.188}{(\bar{\lambda}_p + \alpha_\theta)^{2\beta_\theta}} \leq 1.0 \quad (3.9)$$

The coefficients to be used in equations (3.8) and (3.9) are given in Table 3.2 (see Chapter 2).

Table 3.2: Coefficients to be used in equations (3.8) and (3.9).

Internal compression elements	Outstand compression elements
$\alpha_\theta = 0.9 - 0.315 \frac{k_{0.2p,\theta}}{\varepsilon_\theta k_{y,\theta}}$	$\alpha_\theta = 1.1 - 0.630 \frac{k_{0.2p,\theta}}{\varepsilon_\theta k_{y,\theta}}$
$\beta_\theta = 2.3 - 1.1 \frac{k_{0.2p,\theta}}{k_{y,\theta}}$	$\beta_\theta = 2 - 1.1 \frac{k_{0.2p,\theta}}{k_{y,\theta}}$
$\varepsilon_\theta = 0.85\varepsilon = 0.85\sqrt{235 / f_y}$	

A simplified proposal is investigated in this study based on the assumption that the influence of the temperature on the range of the critical temperatures usually expectable for steel members (from 350°C to 750°C) are negligible (see Figure 3.6 and Figure 3.7), leading to a simpler yet accurate design. According to this simplified proposal for internal compression elements the following expression is proposed:

$$\rho = \frac{\left(\bar{\lambda}_p + 0.9 - \frac{0.26}{\varepsilon}\right)^{1.5} - 0.055(3 + \psi)}{\left(\bar{\lambda}_p + 0.9 - \frac{0.26}{\varepsilon}\right)^3} \leq 1.0 \quad (3.10)$$

and for outstand compression elements is proposed:

$$\rho = \frac{\left(\bar{\lambda}_p + 1.1 - \frac{0.52}{\varepsilon}\right)^{1.2} - 0.188}{\left(\bar{\lambda}_p + 1.1 - \frac{0.52}{\varepsilon}\right)^{2.4}} \leq 1.0 \quad (3.11)$$

with $\varepsilon = \sqrt{235 / f_y}$. In this study, equations (3.8) and (3.9) when used are referred as “Full Proposal” and equations (3.10) and (3.11) when used are referred as “Simple Proposal”. In Figure 3.6, a comparison is made between the “Full Proposal” for different temperatures and the “Simple Proposal” for internal elements and in Figure 3.7 for outstand elements in compression for the steel grade S355.

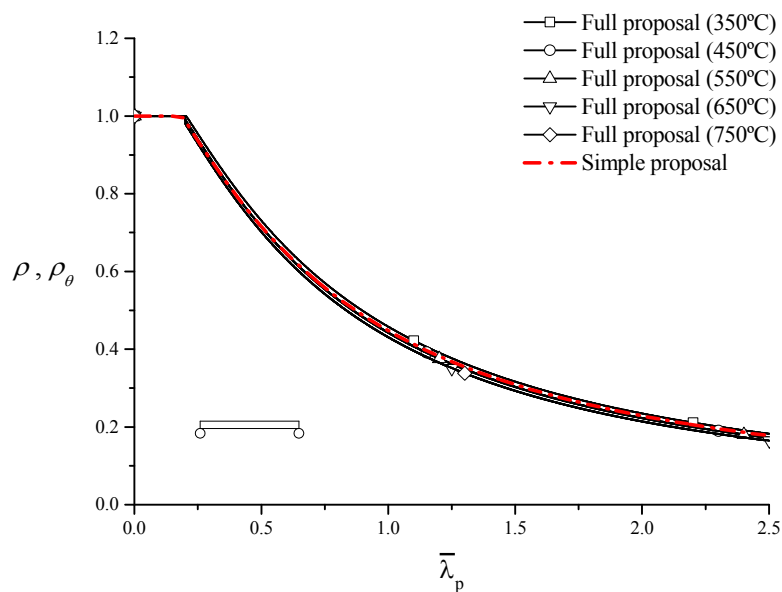


Figure 3.6: Comparison between the Full proposal and Simple proposal for internal elements (steel grade S355).

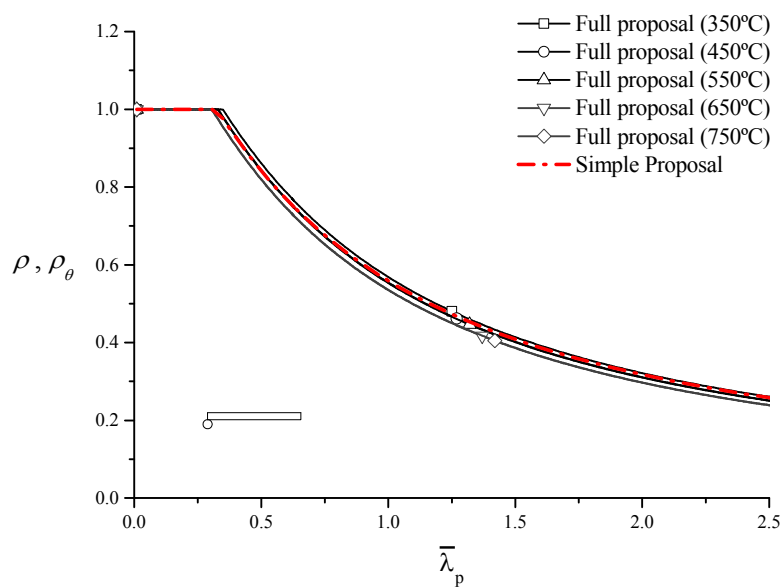


Figure 3.7: Comparison between the Full proposal and Simple proposal for outstand elements (steel grade S355).

3.4 Simple design methods to calculate the cross-sectional resistance at elevated temperatures

According to Eurocode 3, the compression resistance of a cross-section can be determined at elevated temperatures using clause 4.2.3.2 of Part 1-2 assuming that no flexural buckling will occur. Additionally, if the cross-section is classified as Class 4, clause 4.2.3.6 of Part 1-2 of Eurocode 3 applies, and an effective cross-section area (A_{eff}) must be calculated as mentioned in subsection 2.3 of this chapter. In Table 3.3, the summary of the Eurocode 3 methodology to calculate the cross-sectional resistance is given where A and A_{eff} refer to the gross and effective cross-section areas respectively. In this table, $\gamma_{M,fi}$ is the safety factor for the fire situation.

Table 3.3: Summary of methodologies to calculate the cross-sectional compression resistance at elevated temperatures.

Methodology	Cross-section classification at elevated temperatures	Simple design method to calculate the compression resistance at elevated temperatures	Determination of the effective cross-section area A_{eff}
Eurocode 3 Part 1.2	Class 1, Class 2 and Class 3	$N_{c,fi,t,Rd} = Ak_{y,\theta}f_y / \gamma_{M,fi}$	Not applicable
	Class 4	$N_{c,fi,t,Rd} = A_{eff}k_{0.2p,\theta}f_y / \gamma_{M,fi}$	According to Part 1-5 of Eurocode 3 (see subsection 3.2.3)
New proposal	Class 1 and Class 2	$N_{c,fi,t,Rd} = Ak_{y,\theta}f_y / \gamma_{M,fi}$	Not applicable
	Class 3 and Class 4	$N_{c,fi,t,Rd} = A_{eff}k_{y,\theta}f_y / \gamma_{M,fi}$	Full proposal: Eqs. (3.8) and (3.9) Simple Proposal: Eqs. (3.10) and (3.11) (see section 3.3)

According to the new proposed methodology to assess the cross-sectional compression capacity at elevated temperatures (see Table 3.3), an effective cross-section is calculated for Class 3 and Class 4 using equations (3.8) and (3.9) for the “Full Proposal” and equations (3.10) and (3.11) for the “Simple Proposal”, given in section 3.3. Accordingly, the

reduction factor for the design yield stress at elevated temperatures $k_{y,\theta}$ is used instead of $k_{0.2p,\theta}$ for all the cross-section classes.

The methodologies to calculate the cross-sectional resistance of members in bending at elevated temperatures ($M_{fi,t,Rd}$) according to both Eurocode 3 (clause 4.2.3.3) and the new methodology are summarized in Table 3.4. In this table, $W_{pl,y}$ refers to the plastic section modulus for Class 1 and Class 2 members and $W_{el,y}$ to the elastic section modulus for Class 3 members. $W_{eff,min,y}$ refers to the minimum effective section modulus for Class 4 members, if Eurocode 3 is used or for Class 3 and Class 4 in the case of the new proposal.

Table 3.4: Summary of methodologies to calculate the cross-sectional bending resistance at elevated temperatures.

Methodology	Cross-section classification at elevated temperatures	Simple design method to calculate the beam bending resistance at elevated temperatures	Determination of the minimum effective section modulus $W_{eff,min,y}$
Eurocode 3 Part1.2	Class 1 and Class 2	$M_{fi,t,Rd} = W_{pl,y} k_{y,\theta} f_y / \gamma_{M,fi}$	Not applicable
	Class 3	$M_{fi,t,Rd} = W_{el,y} k_{y,\theta} f_y / \gamma_{M,fi}$	Not applicable
	Class 4	$M_{fi,t,Rd} = W_{eff,min,y} k_{0.2p,\theta} f_y / \gamma_{M,fi}$	According to Part 1-5 of Eurocode 3 (see subsection 3.2.3)
New proposal	Class 1 and Class 2	$M_{fi,t,Rd} = W_{pl,y} k_{y,\theta} f_y / \gamma_{M,fi}$	Not applicable
	Class 3 and Class 4	$M_{fi,t,Rd} = W_{eff,min,y} k_{y,\theta} f_y / \gamma_{M,fi}$	Full proposal: Eqs. (3.8) and (3.9) Simple Proposal: Eqs. (3.10) and (3.11) (see subsection 3.3)

3.5 Numerical model

In this section, the numerical model used to investigate the accuracy of the proposed methodologies to calculate the ultimate capacity of slender cross-sections at elevated temperatures is presented. For the numerical models, geometric and material non-linear analyses with imperfections (GMNIA) with shell finite elements were used. The finite element model was implemented using the software SAFIR, which has been developed specifically for the analysis of structures in case of fire [3.14]. The capability of SAFIR to model local buckling with shell elements was validated by Talamona and Franssen [3.25]. The members were discretized into several quadrangular shell elements with four nodes and six degrees of freedom (3 translations and 3 rotations). The SAFIR shell elements adopt the Kirchhoff's theory formulation with a total co-rotational description. The steel material law is a two-dimensional constitutive relation with the von Mises yield surface according to the non-linear stress-strain formulae of Eurocode 3 and the respective reduction factors at elevated temperatures. The integration on the shell element follows a Gauss scheme with 2×2 points on the surface and 4 points through the thickness. The temperature has been considered uniform along the cross-section so that a comparison between the numerical results and the simple design equations is possible. The cross-sectional resistance at elevated temperatures was determined by firstly increasing the temperature to the desired value and then applying an increasing load until the failure is reached. A mesh sensitivity study has been performed and the solution converged for the members discretized into 100 divisions on the length, 10 divisions on the flange width and 22 divisions of the web height. Additionally, for the cases where the ratio between the flange width and the web height is close to one the divisions on the flange width were doubled. The length of the members was set as 10 times the web height. The numerical model has been validated against experimental results in a previous work [3.15] (see Chapter 2).

3.5.1 Material properties

S235, S355 and S460 steel grades were considered in the numerical investigations, with a yield strength at normal temperature of 235 MPa, 355 MPa and 460 MPa respectively, a modulus of elasticity of 210 GPa at normal temperature and a Poisson's ratio of 0.3.

3.5.2 Support conditions

Single span members were considered with the boundary conditions defined in order to determine the axial compression resistance and flexural bending resistance about the major-axis. For compression members, fully-fixed supports were considered in one end and free in the other, the displacements were also restrained in the transversal direction (U_y) and vertical direction (U_z) in the intersection of the web with the flange as illustrated in Figure 3.8. For members in bending about the major-axis, fork-supports were considered in both ends restraining the transversal displacements (U_y) along the web and restraining the vertical displacements (U_z) in the lower flange. Additionally, the transversal displacements (U_y) were also restrained in the upper flange in this case.

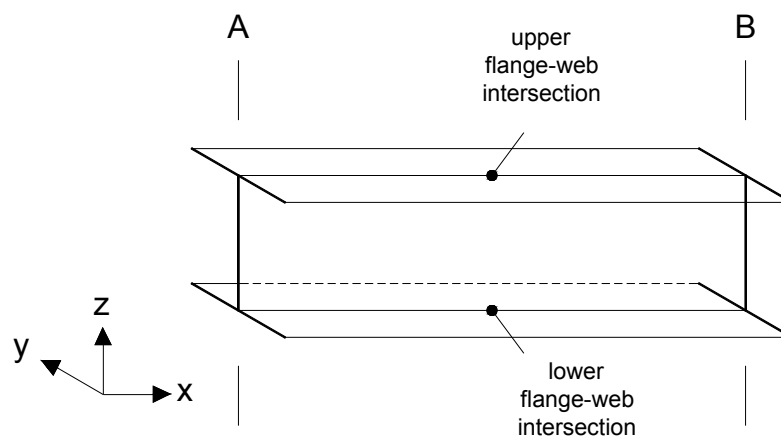


Figure 3.8: Illustration of the numerical model.

3.5.3 Loading

The loads were modelled by applying distributed loads (by means of nodal forces) on the flanges and on the web as indicated in Figure 3.9 for each loading case. To avoid numerical problems, an additional layer of shell elements with higher thickness was used in the extremities of the structural elements to apply the loads that correspond to the applied end moments or the axial compression force.

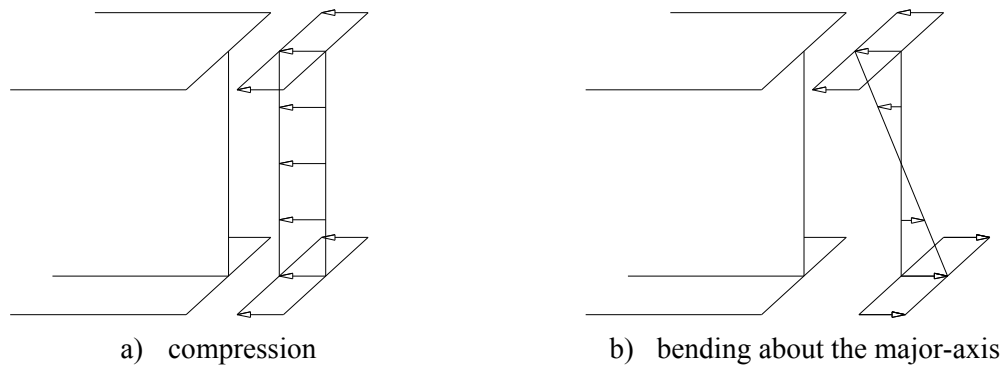


Figure 3.9: Load modelling.

3.5.4 Imperfections

In terms of geometrical imperfections, the recommendations of Part 1-5 of Eurocode 3 [3.2] were followed. The geometrical imperfections were introduced in the models by scaling the first eigenmode with an amplitude corresponding to 80 % of the geometric fabrication tolerances given in the EN 1090-2 [3.26]. Accordingly, the amplitude was considered as $b/100$ where b is the web height or the flange width depending on the location of the most displaced node of the eigenmode. Additionally, if the maximum displaced node was in the web, an amplitude of at least 4 mm was considered, as recommended in the norm. For both models, the residual stresses were not considered because their effect at elevated temperatures is negligible in the ultimate cross-sectional resistance [3.15].

3.6 Numerical study

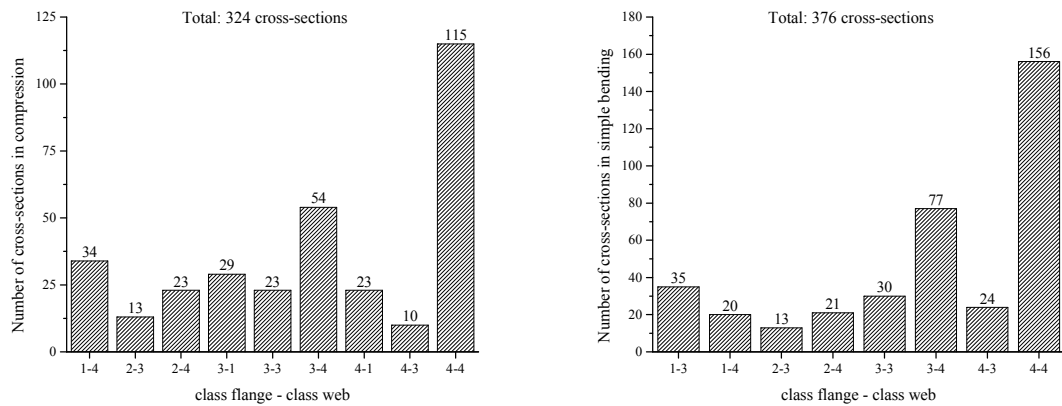
An extensive numerical study was conducted to investigate the ultimate capacity of several I-shaped cross-sections under compression and bending about the major-axis when exposed to fire. The numerical model described in section 3.5 was used. The cross-sections that were used in this numerical study are described in subsection 3.6.1. The steel grades S235, S355 and S460 were considered. The temperatures chosen were 350, 450, 550 and 700°C and considered constant in the whole cross-section to allow direct comparison with the simplified design methods. The results obtained are presented in subsection 3.6.2 and it is demonstrated that the existing methodology of Eurocode 3 to predict the ultimate capacity of cross-sections prone to local buckling when exposed to elevated temperatures needs to be improved. On the other hand, the comparison of the results with the methodologies proposed in this chapter

demonstrates their validity and improvements towards a better prediction of the cross-sectional capacity at elevated temperatures. This conclusion is also supported by the statistical investigation presented in subsection 3.6.3.

3.6.1 Cross-sections

In this section, the definition and classification of cross-sections used in the numerical study are indicated. The cross-sections were defined in order to have a large set of results and to cover different cases of cross-section classification (see Subsection 3.2.1). A total of 324 cross-sections submitted to compression and 376 cross-sections submitted to bending about major-axis with different width-to-thickness ratios of their plates were investigated. The choice of the cross-section dimensions was based on the ones used in current practice as well as extreme geometries in order to cover a wider scope of application. The web height (h_w) was defined as 450, 634, 817 and 1000 mm for the compression cases and 450, 1000 and 2000 mm for the bending cases. The flange width (b_f) was defined as 150, 157, 184, 200 and 450 mm for the compression cases and as 150, 300 and 420 mm for the bending cases. For the compression cases, the thickness of the web (t_w) and flanges (t_f) was chosen in order to cover the ranges of Class 2, Class 3 and Class 4 and for the bending cases to cover Class 3 and Class 4 and the frontier between these two classification limits. Finally, the different configurations of web and flange geometries were combined in order to have cross-sections classified as Class 3 and Class 4 with various combinations of flange and web classifications. Figures 3.10 – 3.11 show the different combinations of the cross-sections used in this parametric study.

In Figure 3.12, the number and classification of cross-sections grouped by class of flange and web are shown.



a) cross-sections submitted to compression

b) cross-sections submitted to bending about major-axis

Figure 3.12: Number and classification of cross-sections used in the numerical study.

3.6.2 Results and comparison to simple design methods

Herein, the results obtained for the cross-section resistance with Finite Element Analysis (FEA) are compared with the simple design methods defined in Section 3.4 for elements in compression and bending about the major axis. It is demonstrated that the actual methodology of EN1993-1-2 needs to be improved and that the methods provided in this chapter lead to accurate and safer prediction of the cross-sectional resistance.

3.6.2.1 Elements in compression

In Figure 3.13, the results obtained with FEA are compared with the simplified design methods of EN1993-1-2, through the ratio between the resistance obtained with FEA ($N_{fi,Rd,FEA}$) and with simplified methods of EN1993-1-2 ($N_{fi,Rd,EC3}$) calculated according to Table 3.3. A value higher than 1.0 means that the resistance predicted by the EN1993-1-2 is higher than that obtained with FEA and therefore the results are unsafe. A value less than 1.0 means the results are safe when compared to the numerical results.

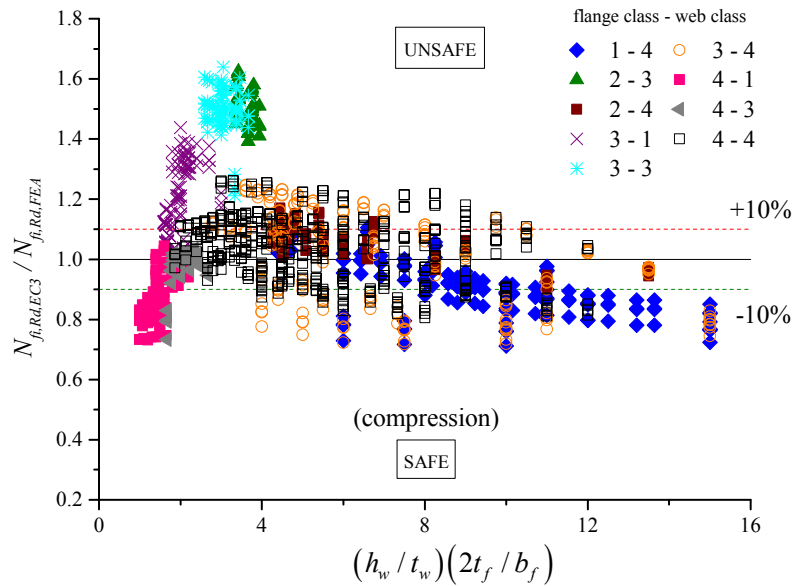


Figure 3.13: Cross-sectional resistance of Class 3 and Class 4 members submitted to compression at elevated temperatures. Comparison between FEA and Part 1-2 of Eurocode 3.

It is shown that for Class 3 profiles the current simple design methods of Part 1-2 of Eurocode 3 give higher resistance than the obtained numerically (results are unsafe) while for Class 4 the predicted capacity is less than those obtained numerically (results are conservative). For Class 3 members, observation of the failure mode shows that local buckling occurs preventing the cross-section to reach the full resistance. This is exemplified in Figure 3.14 for a Class 3 profile (I450×18+450×30, steel grade S460), where it can be seen the deformed shape at collapse where local buckling in the web and in the flanges is evident.

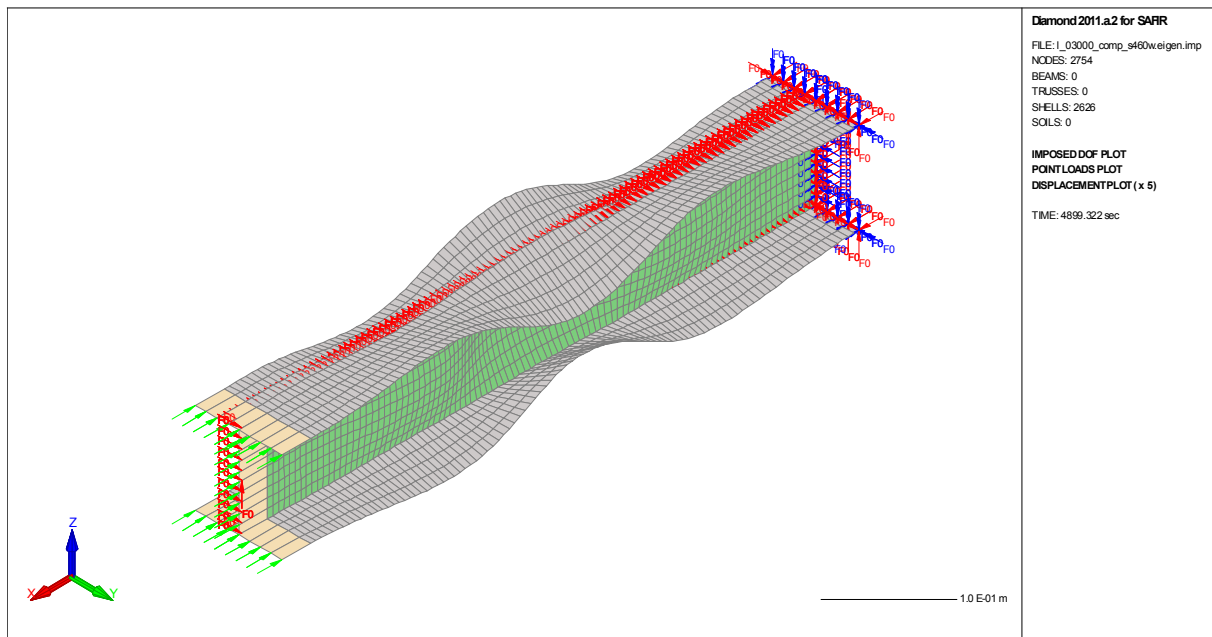


Figure 3.14: Deformed shape ($\times 5$) at the collapse for a Class 3 profile (I450 \times 18+450 \times 30, steel grade S460) at 450°C.

Although it can be argued that the classification limits could be changed at elevated temperatures in order to classify these cross-sections as Class 4, results obtained for Class 4 cross-sections are also not satisfactory, therefore this possibility was not addressed in this study. This is supported by Figure 3.13 where it is clear that the resistance of Class 4 cross-sections is underestimated, especially if they have plates with an inferior class (see, for instance, the data points of 1-4 cases, representing Class 1 flanges and Class 4 web). In these cases, local buckling is unlikely to happen in the non-Class 4 plates but their additional reserve of resistance is not considered because of the use of the 0.2% proof strength as the design yield stress. This is reinforced by Figure 3.15, where is shown that the deformed shape at collapse for a Class 4 cross-section with Class 1 flanges and in this case local buckling in the flanges was not observed.

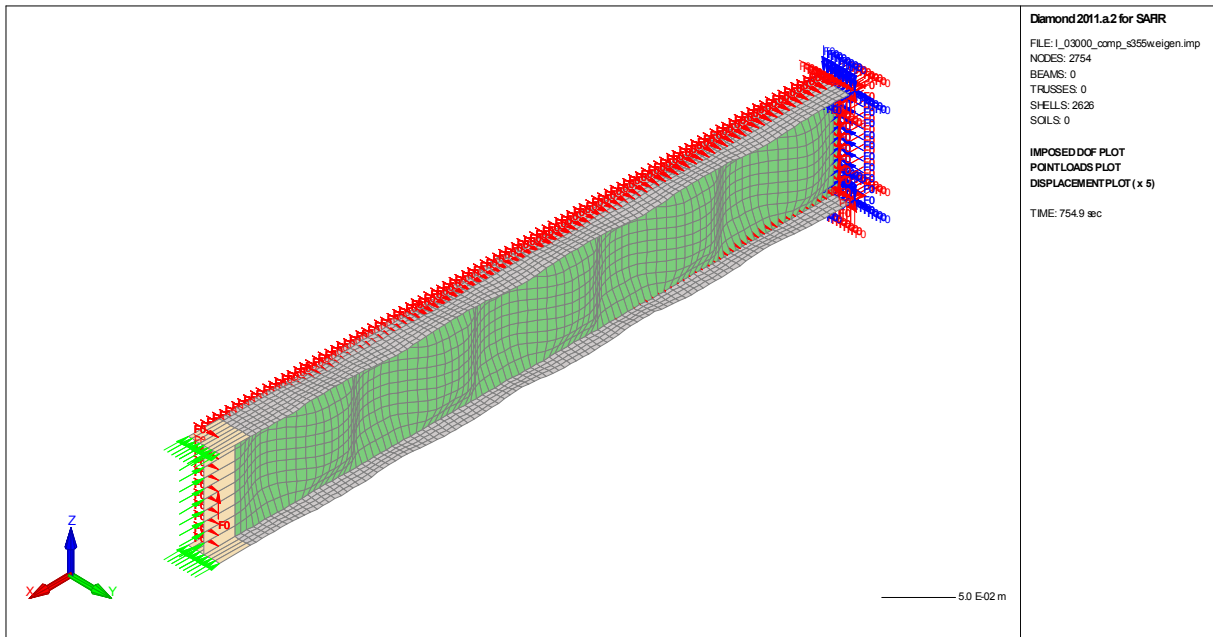


Figure 3.15: Deformed shape ($\times 5$) at the collapse for a Class 4 cross-section but with Class 1 flanges (I450 \times 4+150 \times 11, steel grade S235) at 450°C.

In Figure 3.16, the Full Proposal method presented in this chapter (see Table 3.3) is employed to predict the cross-sectional resistance in accordance with Table 3.3.

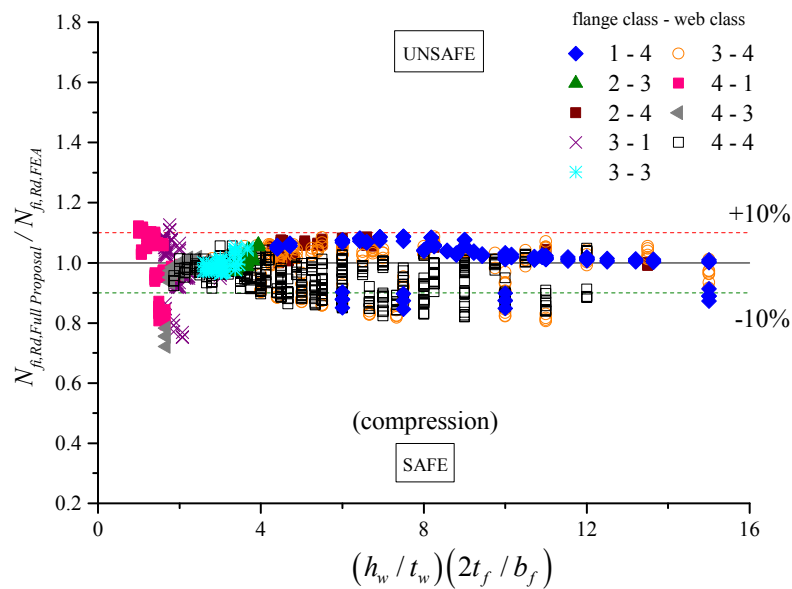


Figure 3.16: Cross-sectional resistance of Class 3 and Class 4 members submitted to compression at elevated temperatures. Comparison between FEA and the Full Proposal.

Results show that the Full Proposal is an accurate methodology to estimate the cross-sectional resistance since a better agreement with the FEA numerical investigation is obtained.

The validity of using the Simple Proposal (see Table 3.3) was also investigated and compared to the FEA results. Figure 3.17 shows that, using the Simple Proposal leads also to safe, yet accurate results, although slightly on the safer side than the Full Proposal as expectable.

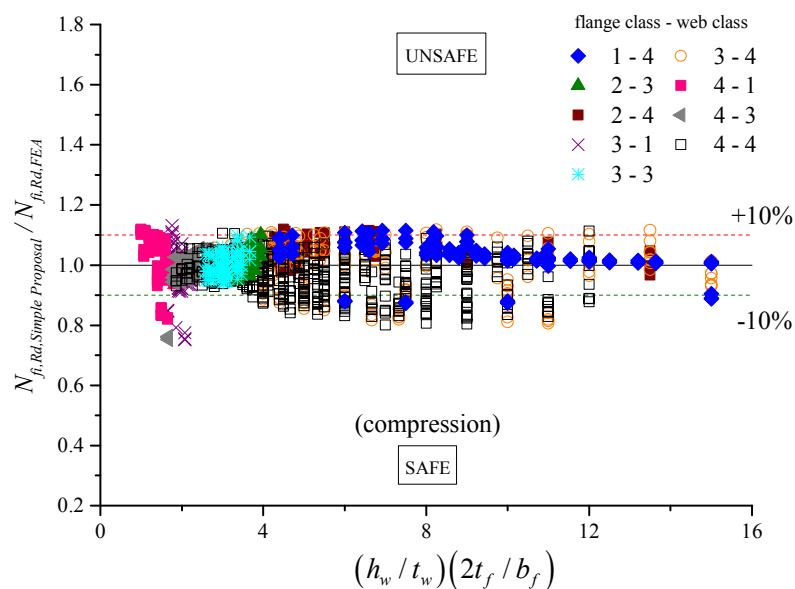


Figure 3.17: Cross-sectional resistance of Class 3 and Class 4 members submitted to compression at elevated temperatures. Comparison between FEA and the Simple Proposal.

3.6.2.2 Elements in bending about the major-axis

In Figure 3.18, the results obtained with FEA are compared with the simplified design methods of EN1993-1-2, through the ratio between the bending resistance obtained with FEA ($M_{fi,Rd,FEA}$) and with simplified methods of EN1993-1-2 ($M_{fi,Rd,EC3}$) calculated according to Table 3.4. A value higher than 1.0 means that the resistance predicted by the EN1993-1-2 is higher than that obtained with FEA and therefore the results are unsafe, a value less than 1.0 means the results are safe.

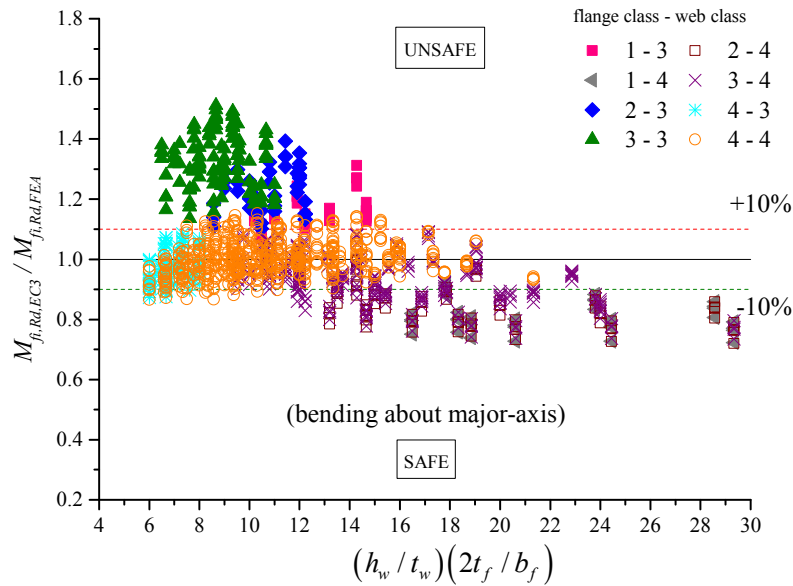
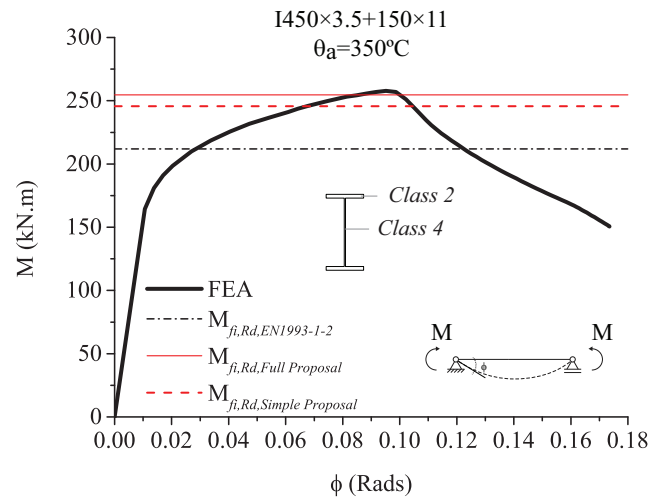
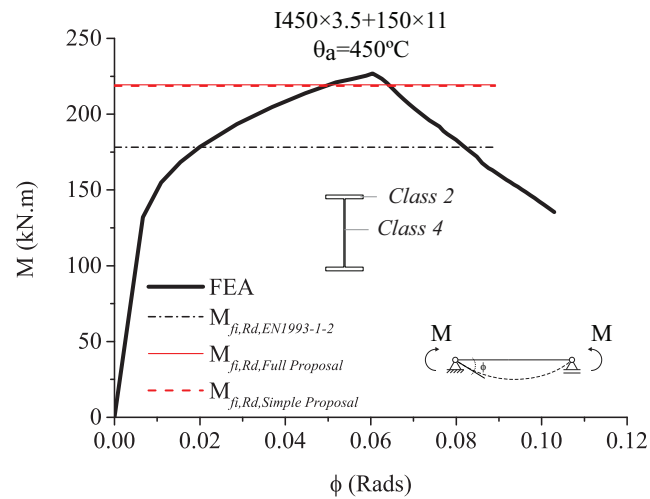


Figure 3.18: Cross-sectional resistance of Class 3 and Class 4 I-shaped profiles under bending about the major axis at elevated temperatures. Comparison between FEA and Part 1-2 of Eurocode 3.

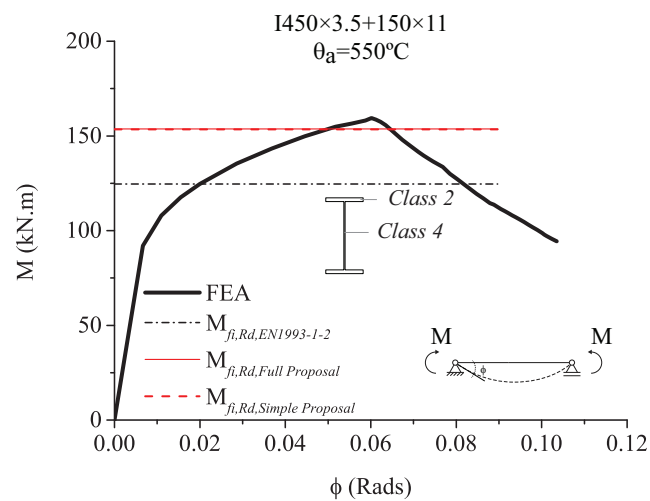
The results show that the prediction of the bending resistance according to Part 1-2 of Eurocode 3 needs to be improved. For beams with Class 4, it is observed that the resistance is underestimated especially for members with cross-sections with non-Class 4 flanges. See for example the 1-4 and 2-4 points in Figure 3.18, which represent cross-sections with Class 1 or Class 2 flanges and Class 4 web. As mentioned before, it is usual that, in these cases, around 80% of the bending resistance is provided by the flanges. If flanges are Class 1 or Class 2, they will not have local buckling, but since the actual simple design method of Part 1-2 of Eurocode 3 suggests the use of $k_{0,2p,\theta}$ for the whole cross-section (see Table 3.4), a considerable amount of resistance is not taken into account. It was observed that for some cases this could be as much as 30% less. Figure 3.19 shows the moment-rotation curve of a beam with a cross-section with Class 2 flange and Class 4 web for different temperatures, with the results again indicating the same conclusions.



a) 350°C



b) 450°C



c) 550°C

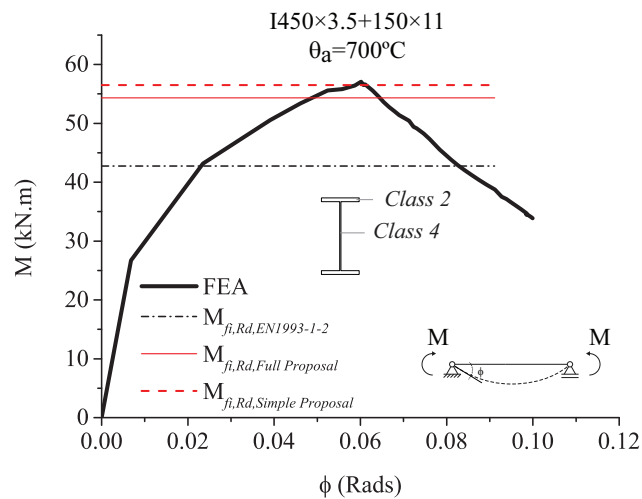
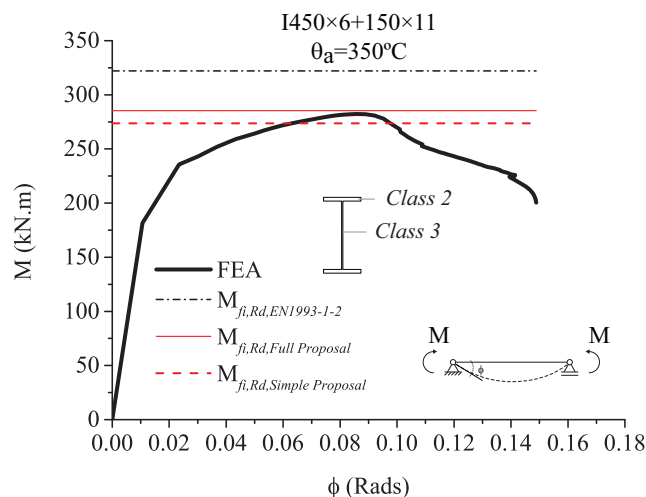


Figure 3.19: Moment-rotation curve at elevated temperatures for an element submitted to bending about the major-axis with a cross-section classified as Class 4 with a fully effective flange (with $h_w = 450$ mm, $b_f = 150$ mm, $t_w = 3.5$ mm and $t_f = 11$ mm). Steel grade S355.

On the other hand, beams with Class 3 cross-sections (1-3, 2-3 and 3-3 in Figure 3.18) have less resistance than the simple design methods predict. In the same way as for members in compression, these beams have local buckling problems that prevent the elastic bending resistance to be attained. This is shown in Figure 3.20, where the moment-rotation curve is depicted for a beam with Class 3 cross-section at different temperatures.



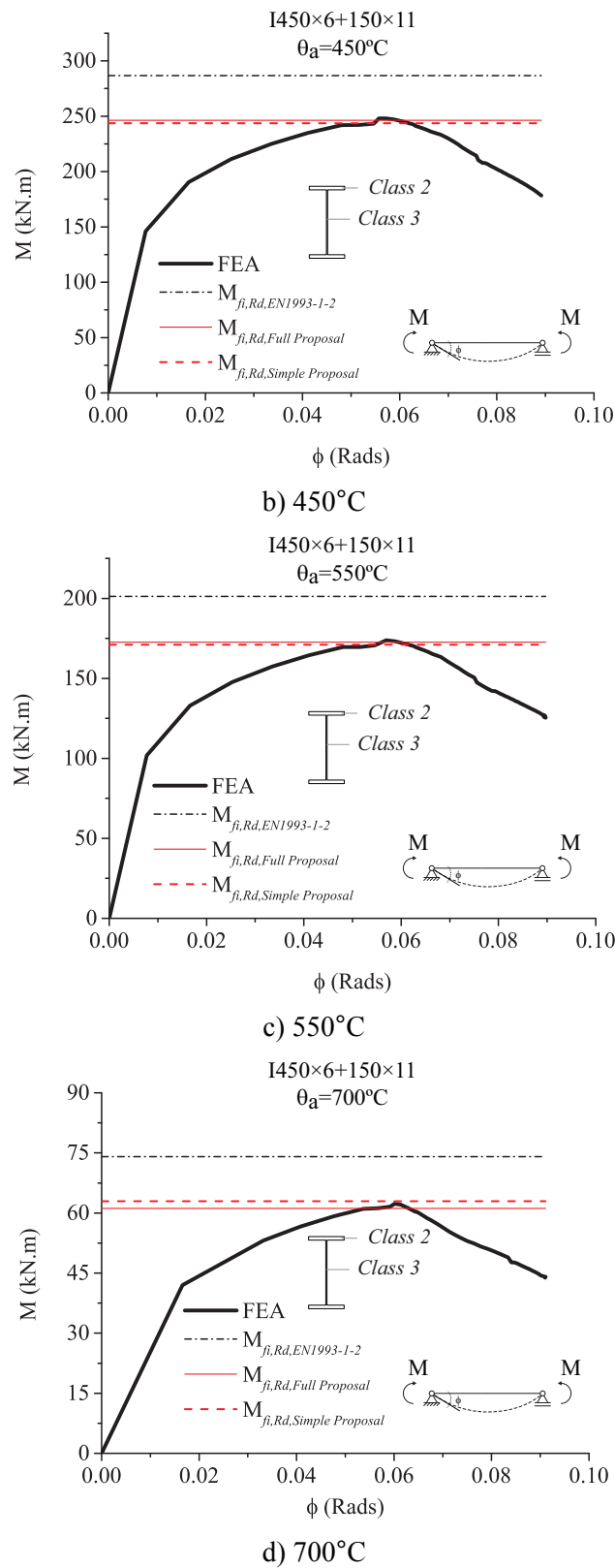


Figure 3.20: Moment-rotation curve at high temperatures for an element submitted to bending about major-axis with Class 3 cross-section ($h_w=450$ mm, $b_f=150$ mm, $t_w=6$ mm and $t_f=11$ mm).

Steel grade S355.

The new approach proposed in this study, improves the actual design method of the EN1993-1-2. In Figure 3.21, the results obtained with the FEA and with the Full Proposal as described in Table 3.4 are shown and in Figure 3.22, a comparison is made between the numerical results and the Simple Proposal.

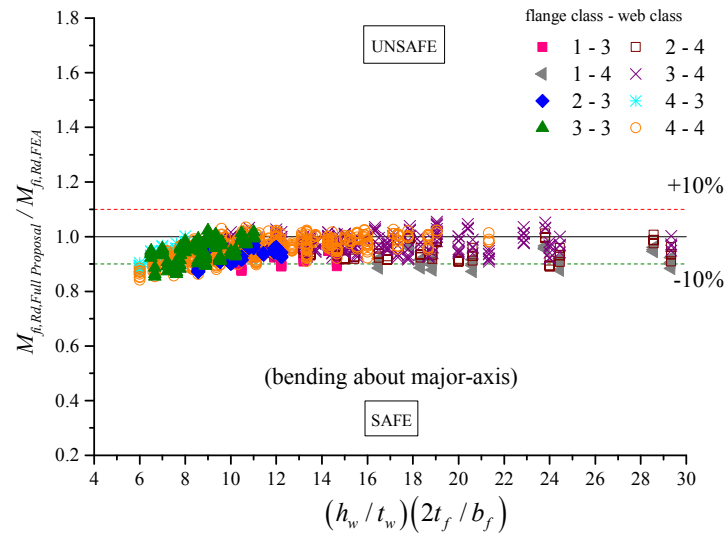


Figure 3.21: Cross-sectional resistance of Class 3 and Class 4 I-shaped profiles under bending about the major axis at elevated temperatures. Comparison between FEA and the Full Proposal.

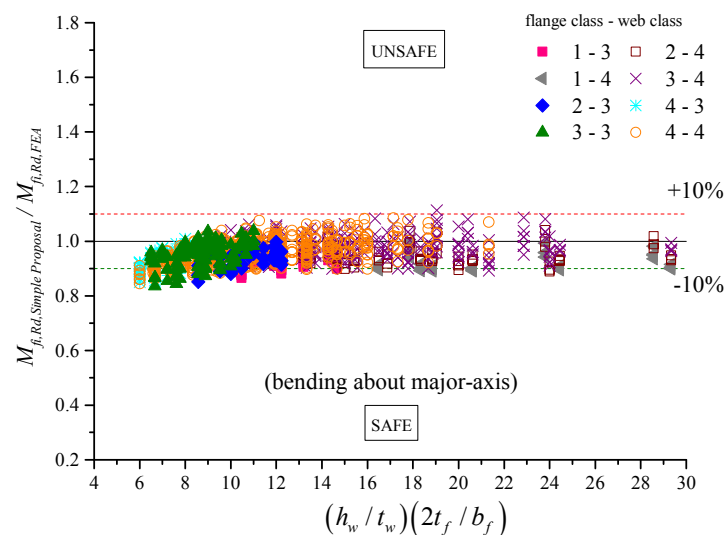


Figure 3.22: Cross-sectional resistance of Class 3 and Class 4 I-shaped profiles under bending about the major axis at elevated temperatures. Comparison between FEA and the Simple Proposal.

A better correlation between the numerical results obtained by means of FEA calculations and the new proposed methodologies to calculate the cross-sectional resistance is observed. It is concluded that adopting these approaches leads to a safer and economic design of steel beams with Class 3 and Class 4 cross-sections in fire conditions. This is also demonstrated in Figures 3.19-3.20 where the moment-rotation curves are depicted for a beam with Class 4 cross-section (with Class 2 flange) and for a beam with Class 3 cross-section (with Class 2 flange) respectively. It is also demonstrated that the Simple Proposal leads to safe and accurate results.

3.6.3 Statistical investigation of the proposed methodologies

In this section, a statistical investigation was performed. For each cross-section, the mean value μ and the standard deviation s of the results were calculated from:

$$\mu = \frac{\sum_{i=1}^n x_i}{n} \quad (3.12)$$

$$s = \sqrt{\frac{\sum_{i=1}^n (x_i - \mu)^2}{n-1}} \quad (3.13)$$

where for each methodology, x_i is given for compression members as

$$x_i = \frac{N_{c,fi,Rd,Simplified}}{N_{c,fi,Rd,FEA}} \quad (3.14)$$

and $N_{c,fi,Rd,Simplified}$ is the value obtained with the simplified design methods according to Table 3.3 and $N_{c,fi,Rd,FEA}$ is the value obtained with SAFIR. For members in bending x_i is calculated according to

$$x_i = \frac{M_{fi,Rd,Simplified}}{M_{fi,Rd,FEA}} \quad (3.15)$$

where $M_{f_i,Rd,Simplified}$ is the value obtained with the simplified design methods according to Table 3.4 and $M_{f_i,Rd,FEA}$ is the value obtained with SAFIR.

The results from the simplified methods are deemed safe if they lead to values of x_i lower than the unity and unsafe for values higher than one.

For compression, a total of $n = 324 \times 4 = 1296$ cases were studied representing the 324 cross-sections analysed and considering the different steel grades (see Figure 3.10), for 4 different temperatures. For bending about the major-axis, $n = 376 \times 4 = 1504$ cases were studied representing the 376 cross-sections analysed considering the different steel grades (see Figure 3.11) and also 4 different temperatures.

The results of this statistical study are shown in Table 3.5 for the mean value and standard deviation of the results. The results for the three methodologies considered, namely i) Eurocode 3, the ii) Full Proposal and the iii) Simple Proposal for calculating the cross-sectional effective properties and the corresponding resistance of the elements under compression and bending are shown.

Table 3.5: Statistical results for each of the methodologies.

	Members in compression		Members in bending	
	Mean	Standard deviation	Mean	Standard deviation
	(μ)	(s)	(μ)	(s)
i) Eurocode 3	1.106	0.200	1.007	0.123
ii) Full proposal	0.989	0.063	0.950	0.034
iii) Simple proposal	0.997	0.067	0.955	0.038

Table 3.5 shows that, the statistical investigation supports the conclusions drawn before. The existing design method of Eurocode 3 is the one that leads to more unsafe and scattered results with a mean value higher than 1.0 for the studied cases. On the other hand, both the Full Proposal and the Simple Proposal, in turn, lead to results with better agreement with those obtained with FEA investigation.

3.7 Comparison with experimental results

In this section, the Full Proposal and the Simple Proposal described in section 3.3 are used to predict the cross-sectional capacity of different cases that were tested experimentally. The reduced number of experimental investigation on the behaviour of I-shape cross-sections at elevated temperatures, found in the literature is noticeable. Nonetheless, Wang et al. [3.27] conducted experimental investigation on steel stub columns with Class 4 cross-sections at elevated temperatures and within the European Research Project FIDESC4 [3.13], Hricák *et al.* [3.28], tested four laterally restrained beams to evaluate the bending resistance of Class 4 cross-sections at elevated temperatures. These tests were used to validate the proposed methodologies in this study. For the column cases, two cross-sections were tested, namely 234×6+250×8 (Test 1) and 300×6+200×8 (Test 2), whose flanges and webs in compression are classified as Class 4 at elevated temperatures. The specimens were heated at 450°C and 650°C. For the laterally restrained beams, the experiments were conducted on two different cross-sections also for the temperatures 450°C and 650°C. The first cross-section (Test 3 - 656×4+250×12) has a Class 4 web and a Class 3 flange and the second cross-section (Test 4 - 830×5+300×8) has a web and flange of Class 4. A summary of the results obtained and the comparison to the predicted resistance using the methodologies proposed in this chapter are presented in Table 3.6. The provisions indicated in Table 3.3 and Table 3.4 were used to predict the compression and bending resistance about the major-axis respectively for the Full Proposal and Simple Proposal. The results of these calculations, as well as the ratio of experimentally evaluated resistance over the calculated results using the proposed methodologies are also summarized in Tables 3.6 and 3.7.

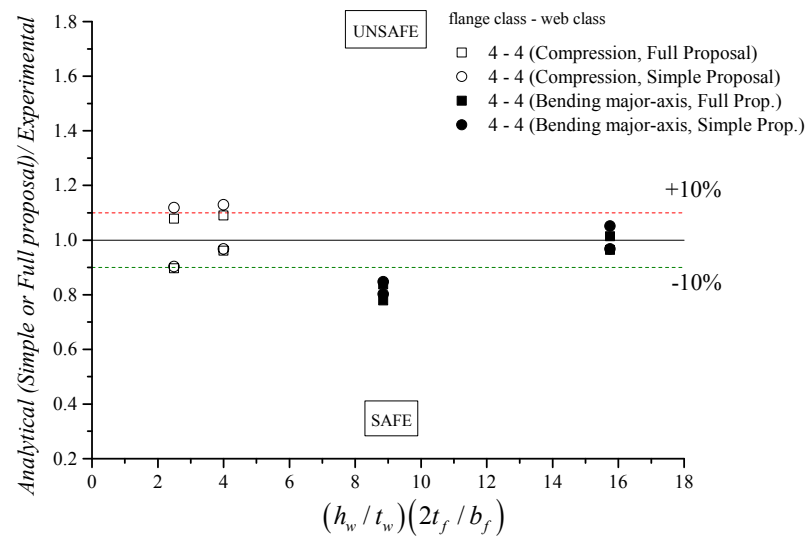
Table 3.6: Comparison of the proposed methodologies against experimental results [3.27] for compression.

Designation	Cross-section ($h_w \times t_w + b_f \times t_f$)	$f_{y,20^\circ\text{C}}$ (flange) (MPa)	$f_{y,20^\circ\text{C}}$ (web) (MPa)	θ (°C)	Exp. (1) (kN)	Full proposal (2) (kN)	(2)/(1)	Simple Proposal (3) (kN)	(3)/(1)	EC3 (4) (kN)	(4)/(1)
Test 1	234×6+250×8	306.3	321.9	450	930	834	0.90	840	0.90	914	0.98
				650	295	318	1.08	330	1.12	342	1.16
Test 2	300×6+200×8	306.3	321.9	450	830	798	0.96	803	0.97	890	1.07
				650	280	305	1.09	316	1.13	333	1.19

Table 3.7: Comparison of the proposed methodologies against experimental results [3.28] for bending about major-axis.

Designation	Cross-section ($h_w \times t_w + b_f \times t_f$)	$f_{y,20^\circ\text{C}}$ (flange) (MPa)	$f_{y,20^\circ\text{C}}$ (web) (MPa)	θ ($^\circ\text{C}$)	Exp. (1) (kN.m)	Full proposal (2) (kN/kN.m)	(2)/(1)	Simple Proposal (3) (kN.m)	(3)/(1)	EC3 (4) (kN.m)	(4)/(1)
Test 3	656×4+250×12	424	392	450	558	538	0.96	540	0.97	537	0.96
					202	205	1.01	212	1.05	201	1.00
Test 4	830×5+300×8	338	378	450	424	355	0.84	359	0.85	377	0.89
				176	137	0.78	141	0.80	141	0.80	

The results indicated in the tables are plotted in the charts of Figure 3.23 and Figure 3.24, for the New Proposal and for Eurocode 3 provisions respectively, with the values above the line that divide the chart deemed unsafe and safe otherwise.

**Figure 3.23:** Comparison between the New proposal (Full and Simple) and experimental results from other authors [3.27, 3.28].

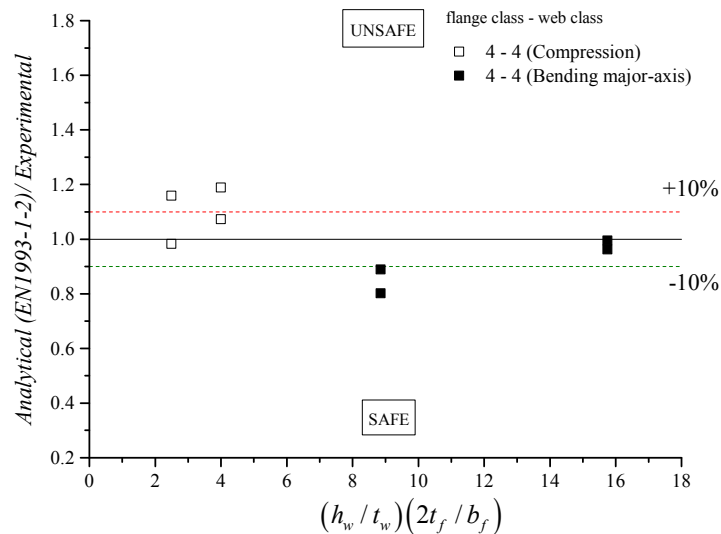


Figure 3.24: Comparison between Part 1-2 of Eurocode 3 (EN1993-1-2) provisions and experimental results from other authors [3.27, 3.28].

It can be observed a good correlation between the experimental results and the predicted values using the new simplified methodologies proposed in this chapter. For most of the cases, the predicted results are lower than the ones obtained experimentally. For both proposals, three cases are on the unsafe side with a maximum of 9% and 13% difference respectively for the Full and Simple proposal but within the acceptable range as they refer to specimens heated at 650°C where it is more difficult to control the tests. Thus, it is demonstrated that both the Full Proposal and the Simple Proposal are methodologies that can be used to predict the ultimate capacity of cross-sections prone to local buckling at elevated temperatures, providing a reasonable method to calculate the cross-sectional resistance suitable for design and consistent with the current state of practice. The comparison of Eurocode 3 actual provisions with the experimental results also shows similar agreement. Unfortunately, these test results do not show the main advantages of using the new methodologies comparatively to the actual Eurocode 3 methodology as observed previously in this work.

3.8 Conclusions

In this chapter, the resistance of several cross-sections where local buckling can occur under axial compression and bending was investigated at elevated temperatures. A numerical study with the FEA software SAFIR was conducted for a significant number of cross-sections, and a comparison to the actual design methodology of EN1993-1-2 was made. It was possible to conclude that the actual provisions of the EN1993-1-2 to calculate the cross-sectional resistance leads to both very conservative and unsafe results when compared to the numerical results obtained in FEA. Three reasons are highlighted. First, the effect of the temperature on the local buckling at elevated temperatures is not correctly taken into account when considering the effective properties determined based on the material properties at normal temperature. Secondly, local buckling occurs prior to what is currently assumed especially for Class 3 cross-sections. Third, considering the 0.2 % proof strength as the design yield strength, for the whole cross-section is restrictive if the cross-section has non-Class 4 elements. Therefore, a new methodology to calculate the resistance of cross-sections with local buckling at elevated temperatures is provided in this study. Based on the effective width expressions at elevated temperatures previously developed [3.15] (see Chapter 2), which are presented in this study, the effects of local buckling in case of fire are better accounted for in the resulting effective cross-section. Using this effective cross-section, the use of the strength at a total 2% strain – $f_{y,\theta}$, as the design yield strength when calculating the resistance of members with Class 4 cross-section is recommended. With this, the additional resistance provided by the plates that do not have local buckling is taken into consideration, leading to an economic yet safe design. On the other hand, it was shown that for Class 3 cross-sections at elevated temperatures, local buckling occurs prior to the attainment of the yield strength in one or more parts of the cross-section. Despite the possibility of considering these cross-sections as Class 4, and the consequent change in the width-to-thickness limits used in the classification, in this study, the use of an effective cross-section also for members with Class 3 cross-sections was proposed.

Regarding the determination of the effective cross-section, two proposals were developed. A Full Proposal, for which the effective cross-section is temperature dependent, meaning that the designer needs to calculate an effective cross-section for each temperature, which represents the more rigorous approach to the issue of dealing with local buckling at elevated

temperatures. A Simple Proposal was also developed, which is not temperature dependent allowing the designer to perform prompt calculations yet safe and accurate. The accuracy and validity of two proposals for calculating the effective cross-sections were confirmed and both approaches lead to a safer and economic design. This was also confirmed by the statistical investigation performed and the comparison with experimental results.

References

- [3.1] CEN, “EN 1993-1-1, Eurocode 3: Design of steel structures - Part 1-1: General rules and rules for buildings.” European Committee for Standardisation, Brussels, 2005.
- [3.2] CEN, “EN 1993-1-5, Eurocode 3 - Design of steel structures - Part 1-5: Plated structural elements.” European Committee for Standardisation, pp. 1–53, Brussels, 2006.
- [3.3] CEN, “EN 1993-1-2, Eurocode 3: Design of steel structures - Part 1-2: General rules - Structural fire design.” European Committee for Standardisation, Brussels, 2005.
- [3.4] Franssen J.-M., Vila Real P., *Fire design of steel structures*. ECCS : Ernst & Sohn, 2010.
- [3.5] Knobloch M., Fontana M., “Strain-based approach to local buckling of steel sections subjected to fire,” *Journal of Constructional Steel Research*, vol. 62, no. 1–2, pp. 44–67, January 2006.
- [3.6] Renaud C., Zhao B., “Investigation of simple calculation method in EN 1993-1-2 for buckling of hot rolled class 4 steel members exposed to fire,” in *Fourth International Workshop “Structures in Fire,”* Aveiro, Portugal 2006.
- [3.7] Quiel S. E., Garlock M. E. M., “Calculating the buckling strength of steel plates exposed to fire,” *Thin-Walled Structures*, vol. 48, no. 9, pp. 684–695, September 2010.
- [3.8] Directorate-General for Research and Innovation, “Fire safety of industrial halls and low-rise industrial buildings, Contract No 7210-PR/378,” European Commission, Brussels, Belgium, 2005.
- [3.9] Fontana M., Knobloch M., “Local buckling behaviour and strain-based effective widths of steel structures subjected to fire,” in *Third International Workshop “Structures in Fire,”* Ottawa, Canada, 2004.

- [3.10] Fontana M., Knobloch M., “Elements with nonlinear stress-strain relationships subjected to local buckling,” in *Proceedings of ICMS 2006 Conference*, 2006.
- [3.11] Pauli J., Knobloch M., Fontana M., “On the local buckling behaviour of steel columns in fire,” in *8th fib PhD Symposium in Kgs. Lyngby, Denmark*, 2010.
- [3.12] Lopes N., Vila Real P., Simões da Silva L., Franssen J.-M., “Numerical Modelling of Thin-Walled Stainless Steel Structural Elements in Case of Fire,” *Fire Technology*, vol. 46, pp. 91–108, 2010.
- [3.13] FIDESC4, “Fire Design of Steel Members with Welded or Hot-Rolled Class 4 Cross-Section, RFCS-CT-2011-00030, 2011-2014, Techinal Report No.5,” 2014.
- [3.14] Franssen J.-M., “SAFIR, A Thermal/Structural Program for Modelling Structures under Fire,” *Engineering Journal, A.I.S.C.*, vol. 42, no. 3, pp. 143–158, 2005.
- [3.15] Couto C., Vila Real P., Lopes N., Zhao B., “Effective width method to account for the local buckling of steel thin plates at elevated temperatures,” *Thin-Walled Structures*, vol. 84, pp. 134–149, November 2014.
- [3.16] Ala-Outinen T., Myllymäki J., “Local Buckling of RHS Members at Elevated Temperatures,” Espoo, Finland, 1995.
- [3.17] Yang K., Chen S., Lin C., Lee H., “Experimental study on local buckling of fire-resisting steel columns under fire load,” *Journal of Constructional Steel Research*, vol. 61, no. 4, pp. 553–565, April 2005.
- [3.18] Yang K.-C., Lee H.-H., Chan O., “Performance of steel H columns loaded under uniform temperature,” *Journal of Constructional Steel Research*, vol. 62, no. 3, pp. 262–270, March 2006.
- [3.19] Yang K.-C., Lee H.-H., Chan O., “Experimental study of fire-resistant steel H-columns at elevated temperature,” *J. Constr. Steel Res.*, vol. 62, no. 6, pp. 544–553, June 2006.

- [3.20] Correia A. J. P. M., Rodrigues J. P. C., “Fire resistance of steel columns with restrained thermal elongation,” *Fire Safety Journal*, vol. 50, pp. 1–11, May 2012.
- [3.21] Von Karman T., Sechler E. E., Donnell L. H., “The strength of Thin Plates in Compression,” *Transactions of the American Society of Mechanical Engineers*, vol. 54, p. 53, 1932.
- [3.22] Winter G., “Strength of Thin Steel Compression Flanges,” *Transactions of the American Society of Mechanical Engineers*, vol. 112, p. 527, 1947.
- [3.23] CEN, “Publication N1664E - Corrigendum to EN 1993-1-5 Eurocode 3 : Design of steel structures -Part 1-5 : Plated structural elements,” European Committee for Standardisation, Brussels, Belgium, 2009.
- [3.24] Ranby A., “Structural fire design of thin walled steel sections,” *Journal of Constructional Steel Research*, vol. 46, no. 1–3, pp. 303–304, April 1998.
- [3.25] Talamona D., Franssen J.-M., “A Quadrangular Shell Finite Element for Concrete and Steel Structures Subjected to Fire,” *Journal of Fire Protection Engineering*, vol. 15, no. 4, pp. 237–264, November 2005.
- [3.26] CEN, “EN 1090-2: Execution of steel structures and aluminium structures - Part 2 : Technical requirements for steel structures.” European Committee for Standardisation, Brussels, Belgium, 2008.
- [3.27] Wang W., Kodur V., Yang X., Li G., “Experimental study on local buckling of axially compressed steel stub columns at elevated temperatures,” *Thin-Walled Structures*, vol. 82, pp. 33–45, September 2014.
- [3.28] Hricák J., Jandera M., Wald F., “*Local buckling of Class 4 cross-sections at elevated temperatures.*” in Benchmark studies - Experimental validation of numerical models in fire engineering, C. E. Wald F., Burgess I., Kwasniewski L., Horová K., Ed. CTU Publishing House, Czech Technical University in Prague, pp. 21 – 33, 2014.

Chapter 4 Beams

Chapter outline

- 4.1 Introduction
- 4.2 Lateral-torsional buckling of beams with Class 3 and 4 cross-section at elevated temperatures
 - 4.2.1 Eurocode 3 Part 1-2
 - 4.2.2 Using a new methodology to calculate the cross-sectional resistance
- 4.3 Numerical model
- 4.4 Comparison of FEA results with actual beam design curve of the Eurocode 3
- 4.5 Parametric Study
 - 4.5.1 The Effective Section Factor concept and its influence
 - 4.5.2 Temperature influence
 - 4.5.3 Residual stresses influence
 - 4.5.4 Steel grade influence
 - 4.5.5 Depth-to-width ratio influence
- 4.6 New design curve
- 4.7 Non-uniform bending diagrams
 - 4.7.1 Uniformly distributed load
 - 4.7.2 End-moments
- 4.8 Conclusions
- References

Abstract An extensive numerical study is performed to investigate the lateral-torsional buckling of steel beams with slender cross-sections in case of fire. The influence of local buckling is analysed and the numerical results are compared with the simplified design methods of Part 1-2 of Eurocode 3 for the case of beams with Class 1 and 2 cross-sections. It is demonstrated that the actual provisions of Eurocode 3 Part 1-2 are unreliable. A parametric study is carried out to investigate the influence of several parameters on the resistance of laterally unrestrained steel beams with slender cross-sections in case of fire: the effective section factor, the temperature, the steel grade, the depth (h)-to-width (b) ratio (h/b) and the residual stresses. Based on the parametric study a proposal for a new design curve is made for beams with slender cross-sections in case of fire taking into account the influence of local buckling by grouping the response of beams into different ranges of effective section factor. The capacity predicted by the simplified methods using the proposed design curve leads to an improved yet safe design method when compared to the results of the finite element analysis. Finally, it is demonstrated that factor “ f ” which was developed for Class 1 and 2 cross-sections, could be used to account for non-uniform bending diagrams if it is limited to a certain value.

4.1 Introduction

This chapter deals with the lateral-torsional buckling (LTB) behaviour of laterally unrestrained steel beams with slender cross-sections in case of fire. Slender cross-sections are comprised of plates with high width-to-thickness ratio (slenderness) and for that reason are prone to local buckling. Studies about the influence of local buckling in the LTB are very scarce under fire situation since LTB has been mainly studied for beams with cross-sections without local buckling instability. Bailey et al. [4.1] numerically investigated the LTB of unrestrained steel beams, and concluded that both British code and the Eurocode, at that time, overestimated the limiting temperatures for unrestrained simple beams in fire resistance calculations. Vila Real and Franssen [4.2] performed a numerical study, and proposed a design curve for LTB of steel beams. This design curve was later adopted in the final version of the Eurocode 3 Part 1-2 (EN 1993-1-2) [4.3]. The experimental investigation of Vila Real et al. [4.4] and later Mesquita et al. [4.5] carried out on the LTB of steel beams at elevated temperature was used to validate the proposed method by Vila Real and Franssen [4.2]. Vila Real et al. [4.6, 4.7] also studied the influence of the residual stresses in the LTB of steel beams, and they concluded that for Class 1 members is negligible, and widen his initial proposal to account for other loading types. An improved proposal for the lateral-torsional buckling of unrestrained steel beams subjected to elevated temperatures was later presented by Vila Real et al. [4.8]. In this publication the influence of the loading type, the steel grade, the pattern of the residual stresses (hot-rolled or welded sections) and the ratio h/b , between the depth h and the width b of the cross-section on the resistance of the beam was addressed through an extensive numerical study. Based on this study, a proposal to include a factor to account for other loading cases (the factor “ f ”) as well as a severity factor for the influence of the steel grade in the current design method of Part 1-2 was presented. Dharma and Tan [4.9] proposed two alternatives approaches to the current design method of Eurocode 3 Part 1-2 based on numerical investigation to calculate the lateral-torsional buckling resistance in case of fire. They proposed an Alternative approach to address the discontinuity between the design method at high temperature and the one at room temperature; and an approach based on the Rankine formula that enables the failure temperature to be determined directly, without an iterative procedure as required in the EN1993-1-2 design method. In the referred studies, the beams were considered uniformly

heated and the influence of other temperature distribution was not addressed. On this subject, Yin and Wang [4.10] have numerically investigated the effects of several design factors on the lateral-torsional buckling bending moment resistance of a steel I-beams submitted to non-uniform temperature distributions. A proposal was made for a modification to the lateral-torsional buckling slenderness of the beam to account with the non-uniform distribution of the temperature along the cross-section, however only the variation of the temperature in the depth of cross-section was considered. Later, Zhang et al. [4.11] analysed the LTB behaviour of beams subjected to localized fires and concluded that the failure temperature may be considerably lower than that of uniformly heated beams. Further investigation on the LTB resistance on non-uniformly heated beams should be done but it is out of the scope of the present study. More recently, numerical investigation by Lopes and Vila Real [4.12] on Class 4 stainless steel beams was performed. The influence of the geometrical imperfections (local, global and both) and the residual stresses was analysed at high temperatures and it was concluded that they are relevant for the determination of the ultimate load and therefore should be considered according to the expected collapse mode.

Apart from [4.12], which comprises a study for stainless steel members, none of the remaining studies deal with slender cross-sections prone to local buckling and its influence on the LTB resistance of beams. The Eurocode 3 [4.13] classifies these cross-sections, where local buckling prevents the yield strength of being reached in the compressed parts of the cross-sections, as Class 4, the highest class. Furthermore, in the establishment of the design rules of Eurocode 3 [4.3] in case of fire (Part 1-2), it was assumed that the simple design methods were adequate to design beams with Class 4 cross-sections if the recommendations of the Annex E of that norm were followed. In this Annex E of Part 1-2 of the Eurocode 3, it is suggested the use of an effective cross-section determined as for normal temperature and the use of 0.2% proof strength ($f_{0.2p,\theta}$, see Figure 4.1) for the design yield strength. Thus, the influence of the local buckling is accounted for by reducing the cross-sectional capacity, by reducing the effective area and considering a small value of the yield strength.

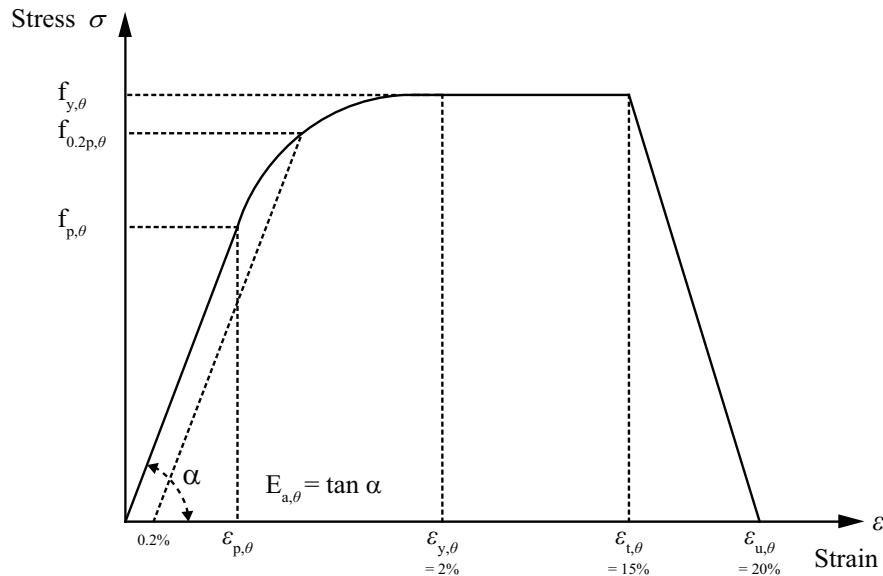


Figure 4.1: Stress-strain relationship for carbon steel at elevated temperatures [4.14].

It must be noted that these recommendations of Annex E are based essentially in the early work of Ranby [4.15] who studied Class 4 plates at elevated temperature. On this matter, the same conclusions were reached in the previous chapters of this thesis [4.16–4.18] for cross-sections built up exclusively of plates classified as Class 4 but demonstrated that for Class 4 cross-sections with non-Class 4 plates these recommendations lead to inaccurate results. Additionally, it was demonstrated also that the local buckling prevents the elastic bending resistance of being reached even in Class 3 cross-section. Thus, the load bearing capacity of the members with such cross-sections is affected and needs to be investigated.

In this chapter, an extensive numerical investigation is performed by finite element analysis (FEA) to study the influence of the local buckling on the LTB resistance of beams with Class 3 and Class 4 cross-sections under fire conditions. The effect of the temperature, residual stresses, steel grade and the depth-to-width (h/b) on the LTB resistance of beams with slender cross-sections are also detailed. It is demonstrated that using a new methodology to calculate the cross-section resistance developed in the previous chapters [4.16–4.18] together with the Eurocode 3 Part 1-2 beam design curve leads to an improvement on the results compared to FEA calculations. However, it is observed this design curve should be slightly changed for Class 3 and Class 4 cross-sections and a proposal for a new design curve is made. Accordingly, an effective section factor is proposed to group the behaviour of beams with slender cross-sections in a way that the interaction between

local and lateral-torsional buckling may be accounted for in case of fire. With this, better agreement between the simplified design methods and the numerical results is achieved leading to an improved yet safe design method.

4.2 Lateral-torsional buckling of beams with Class 3 and 4 cross-section at elevated temperatures

4.2.1 Eurocode 3 Part 1-2

According to Part 1-2 of the Eurocode 3, the resistance of laterally unrestrained beams in bending at elevated temperature should be verified according to the equation (4.1) for members with Class 3 cross-section and according to equation (4.2) for Class 4 cross-sections.

$$M_{b,fi,t,Rd} = \chi_{LT,fi} W_{el,y} k_{y,\theta} f_y / \gamma_{M,fi} \quad (4.1)$$

$$M_{b,fi,t,Rd} = \chi_{LT,fi} W_{eff,min,y} k_{0.2p,\theta} f_y / \gamma_{M,fi} \quad (4.2)$$

with $W_{el,y}$ being the elastic section modulus, $W_{eff,y,min}$ the section modulus of the effective cross-section calculated with the same rules as for normal temperature. $k_{y,\theta}$ and $k_{0.2p,\theta}$ are the reduction factors for effective yield strength and the design strength of Class 4 cross-sections both relative to f_y . f_y is the design yield strength and its respective safety factor for fire design situation is $\gamma_{M,fi}$. As it can be seen, the difference between equations (4.1) and (4.2) is the use of the effective section modulus ($W_{eff,y}$) and the steel 0.2% proof strength ($f_{0.2p,\theta} = k_{0.2p,\theta} f_y$) in equation (4.2), whereas in equation (4.1) the elastic section modulus of the gross cross-section ($W_{el,y}$) and the yield strength ($f_{y,\theta} = k_{y,\theta} f_y$) are used. The reduction factor for LTB in the fire design situation is determined by

$$\chi_{LT,fi} = \frac{1}{\phi_{LT,\theta} + \sqrt{\phi_{LT,\theta}^2 - \bar{\lambda}_{LT,\theta}^2}} \quad (4.3)$$

and

$$\phi_{LT,\theta} = 0.5 \left[1 + \alpha \bar{\lambda}_{LT,\theta} + \bar{\lambda}_{LT,\theta}^2 \right] \quad (4.4)$$

With the imperfection factor given by

$$\alpha = 0.65\varepsilon = 0.65\sqrt{235/f_y} \quad (4.5)$$

with the non-dimensional slenderness at elevated temperatures given by equation (4.6) for Class 3 cross-sections and equation (4.7) for Class 4 cross-sections.

$$\bar{\lambda}_{LT,\theta} = \bar{\lambda}_{LT} \sqrt{k_{y,\theta} / k_{E,\theta}} \quad (4.6)$$

$$\bar{\lambda}_{LT,\theta} = \bar{\lambda}_{LT} \sqrt{k_{0.2p,\theta} / k_{E,\theta}} \quad (4.7)$$

with

$$\bar{\lambda}_{LT} = \sqrt{W_{y,\min} f_y / M_{cr}} \quad (4.8)$$

where $W_{y,\min}$ is the elastic section modulus $W_{el,y}$ for Class 3 cross-sections or the effective section modulus $W_{eff,y,\min}$ for Class 4 cross-section. $k_{E,\theta}$ is the reduction factor for the *Young modulus* at elevated temperature given in EN1993-1-2 and M_{cr} is the elastic critical moment given in the literature, based on gross cross-sectional properties and taking into account the loading conditions, the real moment distribution and the lateral restraints.

4.2.2 Using a new methodology to calculate the cross-sectional resistance

According to the methodology developed in Chapter 3 [4.17, 4.18] to assess the cross-sectional resistance of Class 3 and Class 4 cross-sections, the equation (4.9) should be used to check the resistance of laterally unrestrained beams in bending at elevated temperature.

In this proposal it is used the reduction factor $k_{y,\theta}$ for Class 4 sections as for the other cross-sections, instead of the reduction factor $k_{0.2p,\theta}$.

$$M_{b,fi,t,Rd} = \chi_{LT,fi} W_{new,eff,y} k_{y,\theta} f_y / \gamma_{M,fi} \quad (4.9)$$

with $\chi_{LT,fi}$ given in equation (4.3) but considering the non-dimensional slenderness at elevated temperatures as

$$\bar{\lambda}_{LT,\theta} = \bar{\lambda}_{LT} \sqrt{k_{y,\theta} / k_{E,\theta}} \quad (4.10)$$

The new effective section modulus – $W_{new,eff,y}$ – is calculated according to the Simple proposal from Chapter 3. Accordingly, the same principles as for normal temperature are used but considering the plate reduction factors for internal compression elements as

$$\rho = \frac{\left(\bar{\lambda}_p + 0.9 - \frac{0.26}{\varepsilon} \right)^{1.5} - 0.055(3 + \psi)}{\left(\bar{\lambda}_p + 0.9 - \frac{0.26}{\varepsilon} \right)^3} \leq 1.0 \quad (4.11)$$

and for outstand compression elements as

$$\rho = \frac{\left(\bar{\lambda}_p + 1.1 - \frac{0.52}{\varepsilon} \right)^{1.2} - 0.188}{\left(\bar{\lambda}_p + 1.1 - \frac{0.52}{\varepsilon} \right)^{2.4}} \leq 1.0 \quad (4.12)$$

with $\varepsilon = \sqrt{235 / f_y}$ and the plate non-dimensional slenderness as [4.17–4.19]:

$$\bar{\lambda}_p = \frac{b/t}{28.4\varepsilon\sqrt{k_\sigma}} \quad (4.13)$$

4.3 Numerical model

The finite element model used in this work was implemented using the software SAFIR, which has been developed specifically for the analysis of structures in case of fire [4.20]. Geometric and material non-linear analysis with imperfections (GMNIA) using shell finite element models were carried out. The capability of SAFIR to model local buckling with shell elements was validated by Talamona and Franssen [4.21]. The beams were modelled using shell elements with four nodes and six degrees of freedom (3 translations and 3 rotations). These shell elements adopt the Kirchoff's theory formulation with a total co-rotational description. A study on the mesh sensitivity was performed and the solution has converged for the members discretized with 100 divisions per 10.0 m on the length, 10 divisions on the flange width and 22 divisions of the web height. This mesh was used in this study. For the steel material model it was adopted a two-dimensional constitutive relation with the von Mises yield surface according to the non-linear stress-strain formulae of the Eurocode 3 (see Figure 4.1) and the respective reduction factors at elevated temperatures ($k_{y,\theta}$, $k_{p,\theta}$ and $k_{E,\theta}$). The integration on the shell elements is made with a Gauss scheme with 2×2 points on the surface and 4 points through the thickness were defined. The temperature has been considered uniform along the cross-section and along the beam so that a comparison between the numerical results and the simple design equations is possible. Single span members with fork supports as boundary conditions were modelled. Vertical displacements (U_z) were prevented on both extremities of the beam (see Figure 4.2) on the lower flange and lateral displacements (U_y) were also prevented in both extremities along the web, on one extremity, the displacements along the axis of the beam (U_x) were also blocked.

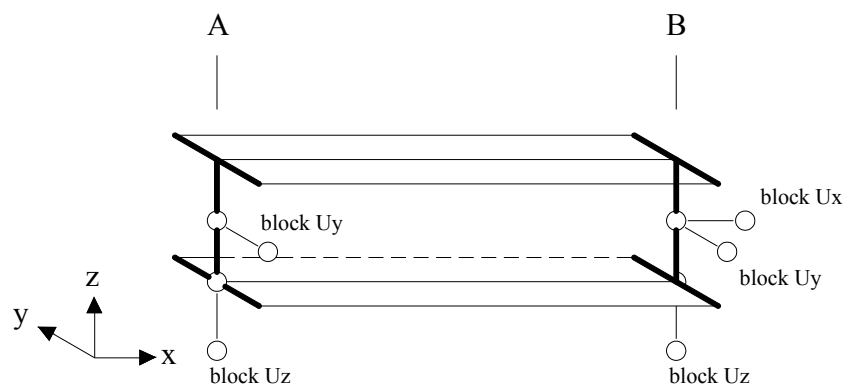


Figure 4.2: Illustration of the boundary conditions in the numerical model.

The loads were modelled by applying distributed loads (by means of nodal forces) on the flanges and on the web. The collapse load for the beam at elevated temperatures was determined by firstly increasing the temperature to the desired value and then applying an increasing load until the failure is reached. The geometric imperfections have been introduced in the model by changing the node coordinates to represent the worst scenario for the assessment of lateral-torsional buckling resistance of the beams. This has been considered as the shape given by the eigenmodes of a linear buckling analysis performed with the software Cast3M [4.22]. In accordance with the finite element method of analysis recommendations given in the Annex C of EN1993-1-5 [4.19] a combination of global and local modes (see Figure 4.3) has been used, where the lower mode has been taken as the leading imperfection and the other one reduced to 70%. The amplitude of the imperfections was considered as 80% of the geometric fabrication tolerances given in the EN1090-2 [4.23] as suggested in the same annex. That is, the global mode has been scaled to 80% of $L/750$ and the local mode to 80% of $b/100$ or 80% of $h_w/100$, where b is the flange width and h_w is the height of the web of the cross-section depending on which node occurred the maximum displacement for the local mode. The recommendation of the norm to consider at least 4 mm as the geometric fabrication tolerances for the web was also taken into account.

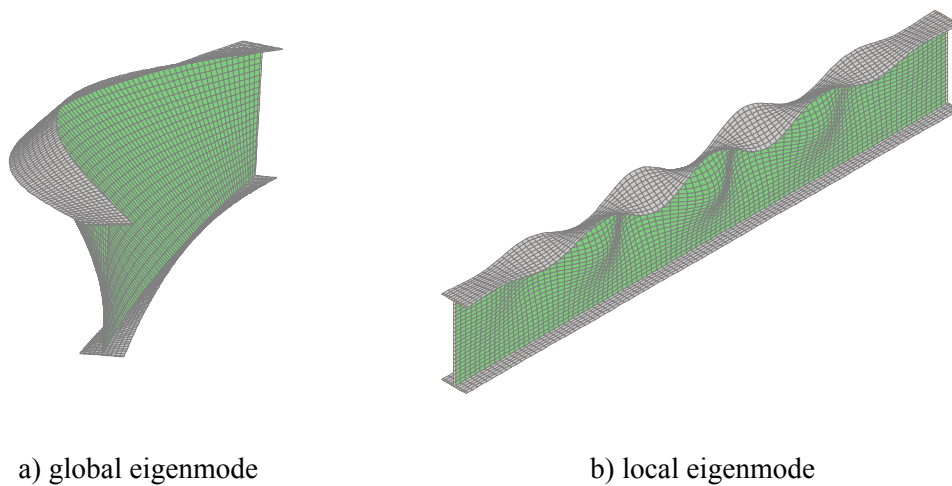


Figure 4.3: Shape of eigenmodes for imperfection consideration.

Residual stresses have been introduced in the numerical model with the stress pattern [4.24] depicted in Figure 4.4, the values adopted for the residual stresses are according to [4.24, 4.25] as used in a previous study [4.26].

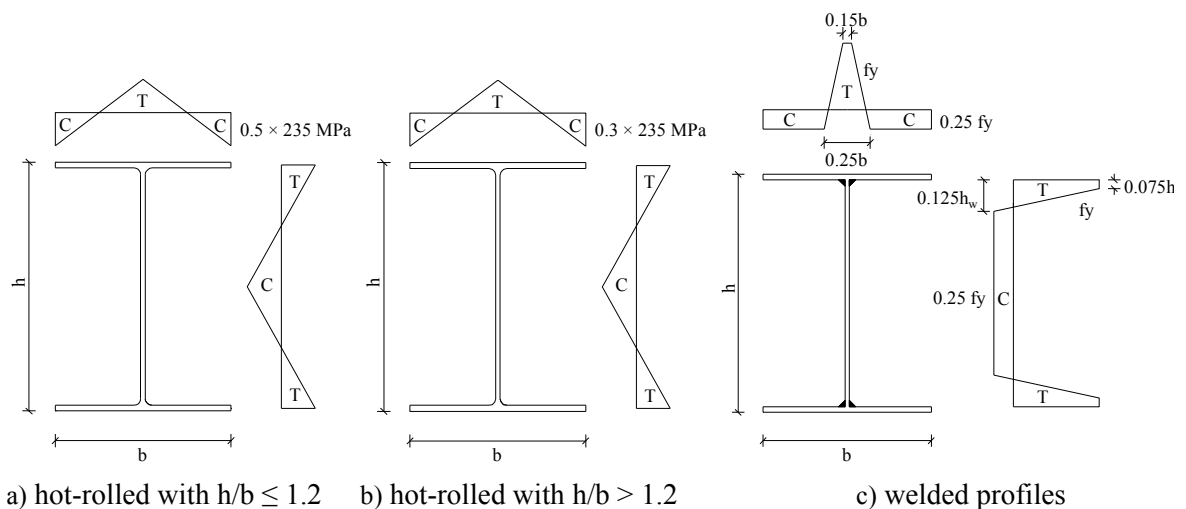


Figure 4.4: Pattern of the residual stresses considered in this study.

As mentioned already, the investigation on the ultimate capacity of laterally unrestrained beams with slender cross-sections in case of fire is very limited and experimental results are almost non-existent. On the scope of the European Research project FIDESC4 [4.27], three tests were performed on laterally unrestrained beams heated at elevated temperatures. The numerical model presented in this study was validated against those experimental tests and the results of this validation, as well as a mesh sensitivity study, are published in [4.28].

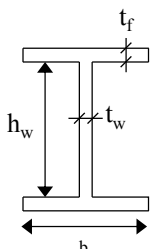
4.4 Comparison of FEA results with current beam design curve of the Eurocode 3

In this section, a comparison between the numerical results obtained in SAFIR and the actual beam design curve from Part 1-2 of the Eurocode 3 (see section 4.2) is made. Several slender cross-sections with Class 3 and Class 4 classification were considered in this study. The geometry of the cross-sections is indicated in Table 4.1, as well as the steel grade, temperatures and non-dimensional slenderness considered in the numerical study. Here, the cross-sectional resistance was calculated according to EN1993-1-2 as given by equation (4.14) for Class 3 cross-sections and equation (4.15) for Class 4 cross-sections.

$$M_{fi,Rd,EC3} = W_{el,y} k_{y,\theta} f_y / \gamma_{M,fi} \quad (4.14)$$

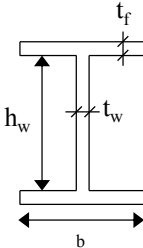
$$M_{fi,Rd,EC3} = W_{eff,y} k_{0.2p,\theta} f_y / \gamma_{M,fi} \quad (4.15)$$

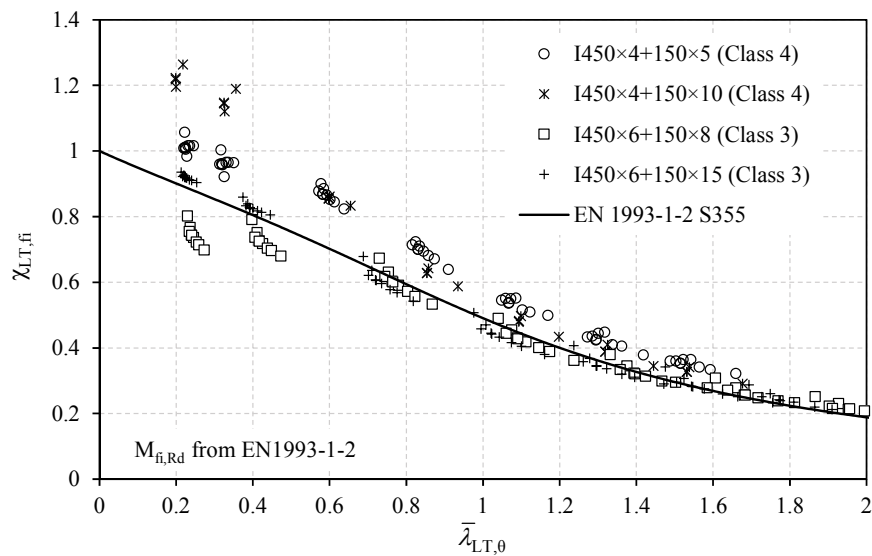
Table 4.1: Cases considered in the numerical study.

	Geometry $h_w \times t_w + b \times t_f$ (mm)	Flange thickness (t_f) (mm)	Steel grade	Temperatures	$\bar{\lambda}_{LT,0}$
	450×4+150× t_f	5, 6, 7, 8, 9, 10, 11, 12, 13, 14, 15	S235, S275, S355 and S460	350°C, 450°C, 550°C and 700°C	[0, 2]
	450×4+200× t_f	7, 8, 9, 10, 11, 12, 13, 14, 15, 16, 17, 18, 19, 20			
	450×4+250× t_f	8, 10, 11.5, 13, 15, 16.5, 18, 20, 21.5, 23, 25			
	450×6+150× t_f	8, 8.1, 8.2, 8.3, 8.4, 8.5, 9, 9.5, 10, 11.5, 13, 15, 16.5, 18, 20, 21.5, 23, 25			
	450×6+250× t_f	13, 13.5, 14, 14.5, 15, 15.5, 16, 18, 20, 23, 25			

For comparison purposes, Figure 4.5 shows the results obtained with the FEA simulations carried out with SAFIR and the actual beam design curve from Part 1-2 of Eurocode 3 (EN1993-1-2), for four cross-sections representing different classifications cases for the steel grade S355 (see Table 4.2).

Table 4.2: Geometry and classification of cross-sections in fire.

	Dimensions ($h_w \times t_w + b \times t_f$) (mm)	Steel grade	Classification in fire web – flange	Overall classification in fire
	450×6+150×15	S355	3 – 1	3
	450×4+150×10		4 – 3	4
	450×6+150×8		3 – 3	3
	450×4+150×5		4 – 4	4

**Figure 4.5:** Comparison of actual LTB design curve of EN1993-1-2 and FEA simulations.

From the figure, it is observed a distinct behaviour between Class 3 and Class 4 beams, more particularly for low slenderness range $\bar{\lambda}_{LT,\theta} \approx 0.2$ where the resistance of the beam is mainly governed by the cross-section capacity.

It is observed that for the beam with cross-section I450×6+150×8 (web Class 3 and flange Class 3), the EN1993-1-2 design curve over-predicts the beam capacity. For the cross-section with higher flange thickness (see I450×6+150×15, web Class 3 and flange Class 1), better agreement is achieved between the capacity predicted numerically and with EN1993-1-2. For Class 4 beams, the actual design curve underestimates the beam capacity, especially for the Class 3 flange case (I450×4+150×10). This particular case of cross-

sections with Class 4 web and Class 3 flange, is representative of the situations from which the designers may benefit more from using beams with slender cross-sections. For the intermediate beams with $\bar{\lambda}_{LT,\theta} \approx 1.0$ it is observed that for Class 3 cross-sections the curve is slightly unsafe. Furthermore, in Figure 4.6, the accuracy of EN1993-1-2 is compared for all the FEA simulations undertaken in this study as indicated in Table 4.1.

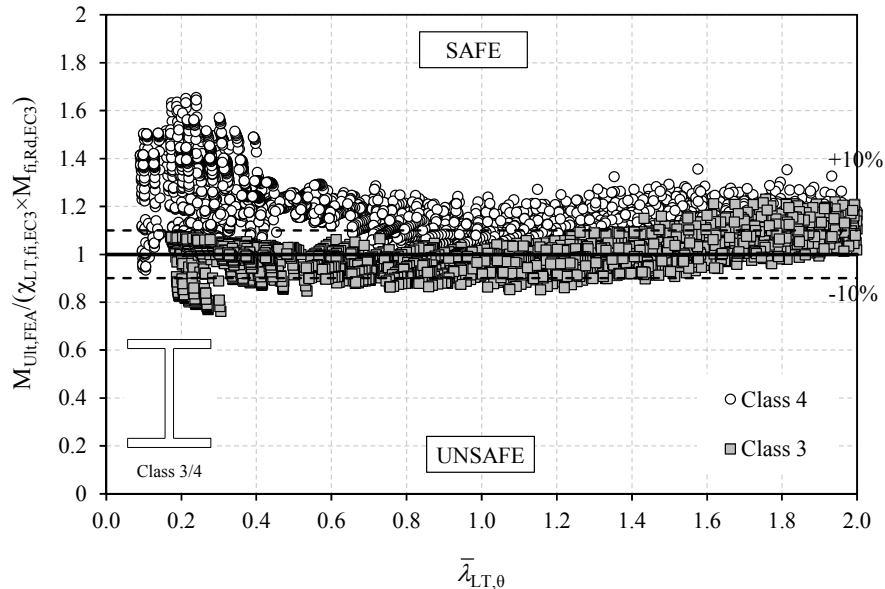


Figure 4.6: Accuracy of the LTB design curve from EN1993-1-2 compared to FEA results with cross-sectional resistance calculated according to EN1993-1-2.

The results obtained show the same pattern as for the cases considered in Figure 4.5 with distinct results attained for Class 3 and Class 4 beams. Here, for non-dimensional slenderness values of $\bar{\lambda}_{LT,\theta} \approx 0.2$, more than 60% of load bearing capacity is not considered for Class 4 beams while for Class 3 beams the EN1993-1-2 curve over predicts the capacity in more than 20%. On the subject of the resistance of slender cross-sections in case of fire, it was demonstrated in the previous chapter [4.16–4.18] that the cross-sectional resistance given by EN1993-1-2 formulae in comparison to FEA for Class 3 and Class 4 is inadequate because it underestimates the resistance of Class 4 cross-sections and overestimates the resistance of Class 3 cross-sections.

Since the cross-sectional capacity influences the LTB resistance of the beams it worth study the impact of using this new formulation. Thus, in Figure 4.7, the results obtained with FEA and considering the cross-sectional resistance predicted by Simple proposal, i.e. using

equation (4.9) are shown for the previous four analysed cases. It is noticed that results are now less scattered compared to those obtained with the actual provisions for the cross-sectional resistance of EN1993-1-2, given by equations (4.14) and (4.15).

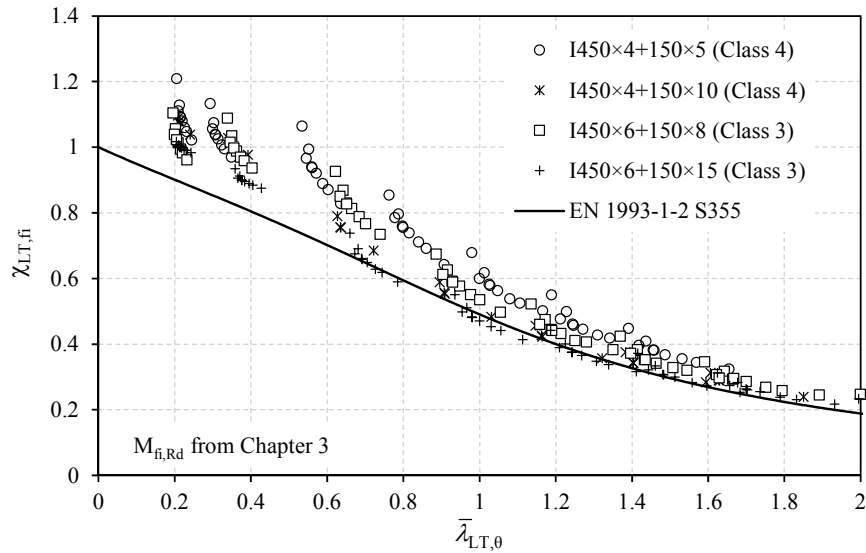


Figure 4.7: Comparison of actual LTB design curve of EN1993-1-2 with cross-sectional calculated according to Simple proposal from Chapter 3 (see equation (4.9)) and FEA simulations.

In Figure 4.8, the FEA results are plotted against the EN 1993-1-2 design curve combined with Simple proposal from Chapter 3 for the cross-sectional resistance.

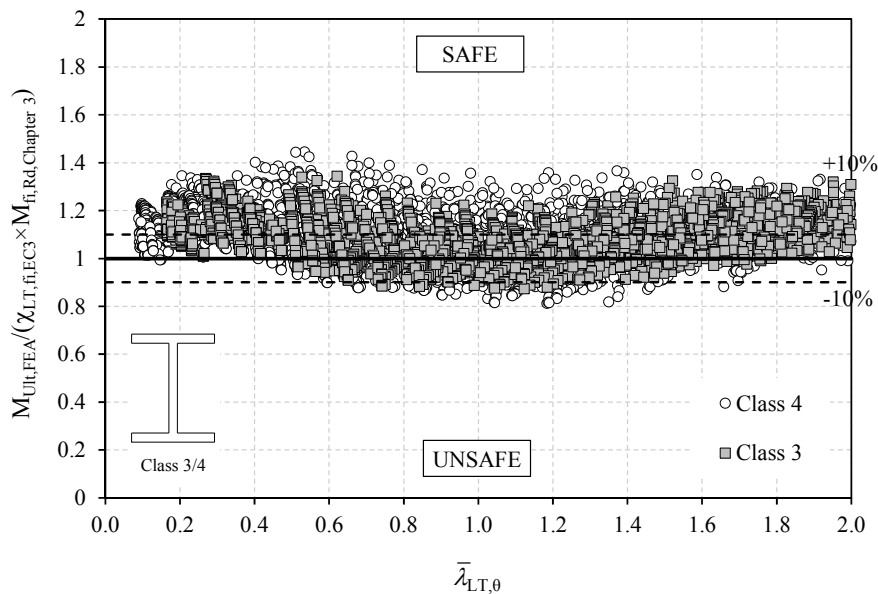


Figure 4.8: Accuracy of the LTB design curve from EN1993-1-2 compared to FEA results with cross-sectional resistance calculated according to Simple proposal from Chapter 3.

In this case, it is observed again that the deviation of the results is less comparatively to Figure 4.6 where the cross-sectional resistance was calculated according to EN 1993-1-2 provisions. For Class 3 beams the results are now mainly on the safe side with a maximum 10% on the unsafe side. For Class 4 beams there is less load-bearing capacity disregarded moving from a maximum 60% in Figure 4.6 towards 40% in Figure 4.8 for $\bar{\lambda}_{LT,\theta} \approx 0.2$. However in the particular case of Class 4 cross-sections, it is observed that for $\bar{\lambda}_{LT,\theta} > 0.5$ the use of the Simple proposal for the cross-sectional resistance developed in Chapter 3 increased the scatter of the results when compared to Figure 4.6, ranging from -20% to almost 30% for instance for $\bar{\lambda}_{LT,\theta} \approx 1.0$. Although improvements are seen by considering the Simple proposal made in Chapter 3 for the cross-sectional resistance, the actual LTB design curve of EN 1993-1-2, which was developed only for Class 1 and Class 2 beams [4.2, 4.4], could be improved to better predict the capacity of beams with slender cross-sections as shown in the remaining part of this study.

4.5 Parametric Study

In order to develop an improved design curve for beams with slender cross-sections at elevated temperatures, a parametric study was performed to investigate the influence of various parameters using the numerical model described in section 4.3. Here, only uniform bending moment distribution was considered. First, the effective section factor concept is presented and its influence on LTB capacity is demonstrated then the influence of the temperature, the residual stresses, the steel grade and the depth-to-width ratio was also investigated.

4.5.1 The Effective Section Factor concept and its influence

The load bearing capacity of beams with slender cross-sections is influenced by the interaction between the resistance to local buckling of the cross-sectional and the overall resistance of the beam to lateral-torsional buckling. In order to account with this interaction, it is here proposed to group the behaviour of the beams by considering an effective section factor s for the cross-section given by

$$s = W_{eff,y} / W_{el,y} \quad (4.16)$$

where $W_{eff,y}$ is the effective section modulus and $W_{el,y}$ is the elastic section modulus, both for the strong axis. From the results it were identified three different groups according to the interaction between the local buckling and the lateral-torsional buckling being high ($W_{eff,y}/W_{el,y} \leq 0.8$), moderate ($0.8 < W_{eff,y}/W_{el,y} \leq 0.9$) or small ($W_{eff,y}/W_{el,y} > 0.9$). In Figures 4.9 – 4.11 the numerical results are plotted for these ranges of effective section factor ratios. For ease of comparison, in these figures it is also plotted the EN1993-1-2 design curve for steel grade S355 as a reference line.

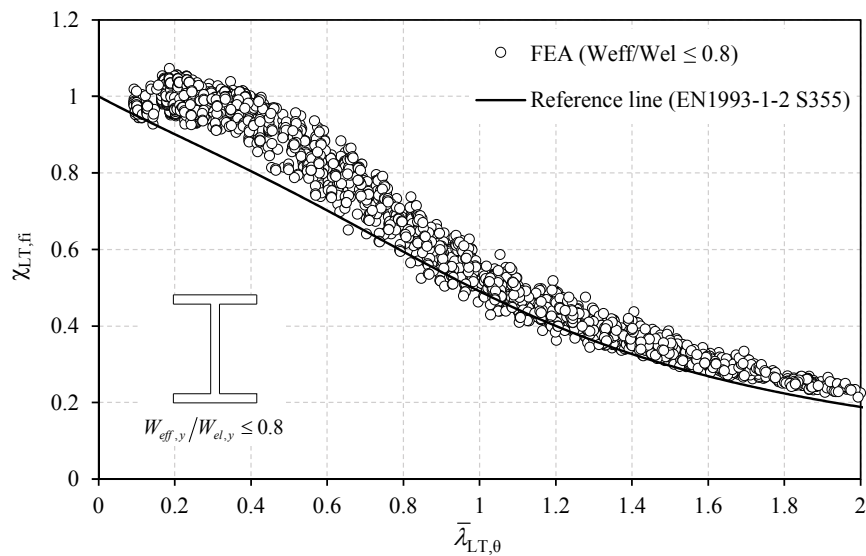


Figure 4.9: LTB behaviour of beams with effective section factor of $W_{eff,y}/W_{el,y} \leq 0.8$.

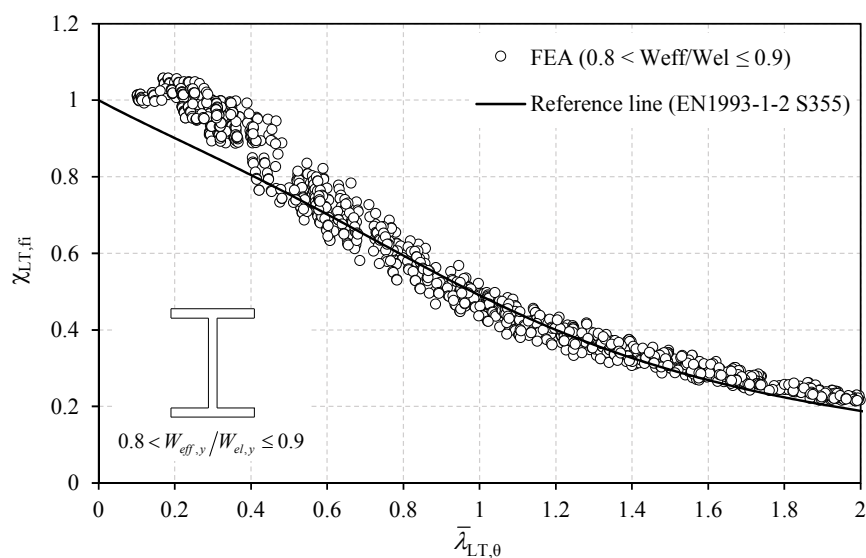


Figure 4.10: LTB behaviour of beams with effective section factor of $0.8 < W_{eff,y}/W_{el,y} \leq 0.9$.

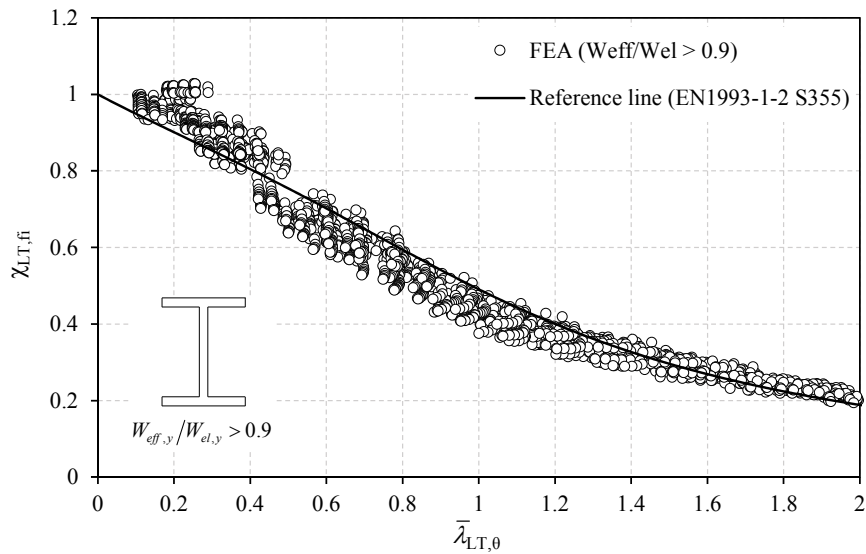


Figure 4.11: LTB behaviour of beams with effective section factor of $W_{eff,y}/W_{el,y} > 0.9$.

From these figures it can be observed different trends for the numerical results depending on the effective section factor and the following conclusions can be highlighted:

- For $W_{eff,y}/W_{el,y} \leq 0.8$, it is observed a plateau until $\bar{\lambda}_{LT,\theta} \approx 0.4$, meaning that until this slenderness the capacity of the beams is governed by the cross-sectional resistance. For higher slenderness ($\bar{\lambda}_{LT,\theta} > 0.4$), the capacity of the beam is reduced due to the interaction between the local buckling resistance of the cross-section and the lateral-torsional buckling resistance of the member. However, in this effective section factor range, cross-sections are more prone to local buckling and therefore its influence in the response of the beams is higher, when compared to the remaining ranges. For this purpose, the reduction on the overall load bearing capacity of the beams is also less in relative terms. For instance, the minimum values of the reduction factor for a slenderness of $\bar{\lambda}_{LT,\theta} \approx 1.0$, in Figure 4.9 is $\chi_{LT,\hat{f}} \approx 0.46$, for Figure 4.10 is $\chi_{LT,\hat{f}} \approx 0.42$ and in Figure 4.11 is $\chi_{LT,\hat{f}} \approx 0.37$, this represents a difference of approximately 10% in relative terms for each successive range.
- For $0.8 < W_{eff,y}/W_{el,y} \leq 0.9$, and comparing to the previous case, the effective section factor of the cross-section is higher (i.e. more effective) meaning the cross-section is less prone to local buckling and therefore the influence of local buckling in the overall response of the beams is less in relative terms. For this range, the plateau is

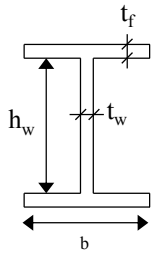
smaller and placed at $\bar{\lambda}_{LT,\theta} \approx 0.3$. After this slenderness, the reduction of resistance is more severe due to the greater influence of the lateral-torsional instability mode, when compared to local buckling, in the overall response of the beam.

- Finally, for $W_{eff,y}/W_{el,y} > 0.9$, the influence of the local buckling is even less compared to previous cases, and consequently the plateau is placed at $\bar{\lambda}_{LT,\theta} \approx 0.2$ and, as expected, the reduction of the load bearing capacity is even more severe when compared to the previous ranges of effective section factor because it is mainly influenced by the lateral-torsional buckling resistance of the beam.

4.5.2 Temperature influence

The influence of temperature values on the lateral-torsional buckling resistance of laterally unrestrained beams is analysed. The results obtained for four sections described in Table 4.3 are detailed here. The steel grade considered was the S355. The temperature distribution in the cross-section and along the member was considered uniform so that comparison between the numerical results and simple design equations is possible. The temperatures 350 - 700°C (in 50°C intervals) were used.

Table 4.3: Cross-sections considered in the study of the influence of the temperature on the LTB resistance.

	Dimensions ($h_w \times t_w + b \times t_f$) (mm)	Steel grade	Effective section factor $s = W_{eff,y}/W_{el,y}$
	450×6+150×15	S355	0.96
	450×4+150×10		0.85
	450×6+150×8		0.73
	450×4+150×5		0.60

In Figures 4.12 - 4.15, the results obtained for the various temperatures and for the cross-sections indicated in the Table 4.3 are shown.

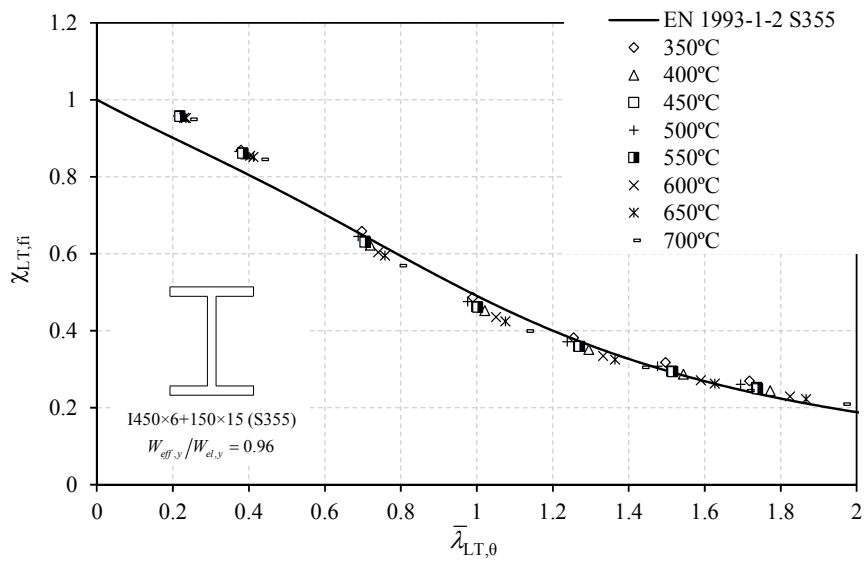


Figure 4.12: Influence of the temperature on the LTB resistance of the beams with cross-section 450×6+150×15, effective section factor $W_{eff,y}/W_{el,y} = 0.96$.

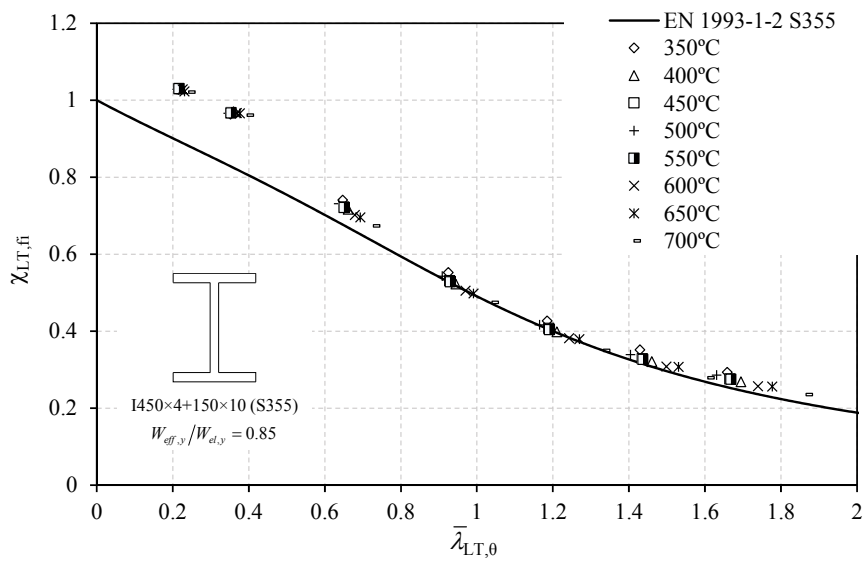


Figure 4.13: Influence of the temperature on the LTB resistance of the beams with cross-section 450×4+150×10, effective section factor $W_{eff,y}/W_{el,y} = 0.85$.

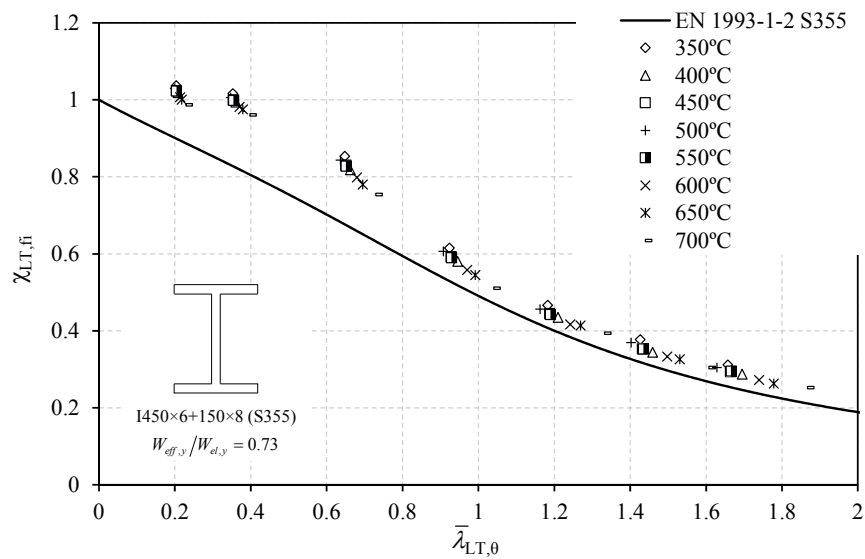


Figure 4.14: Influence of the temperature on the LTB resistance of the beams with cross-section 450x6+150x8, effective section factor $W_{eff,y}/W_{el,y} = 0.73$.

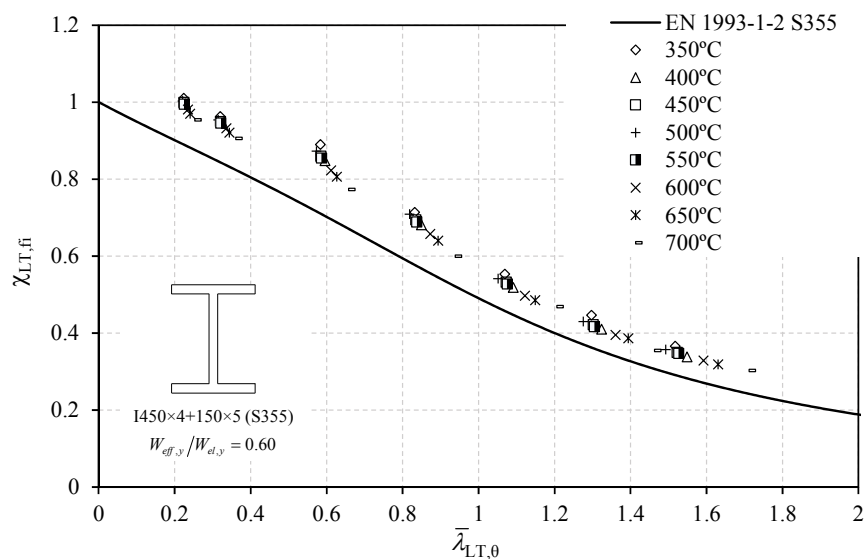
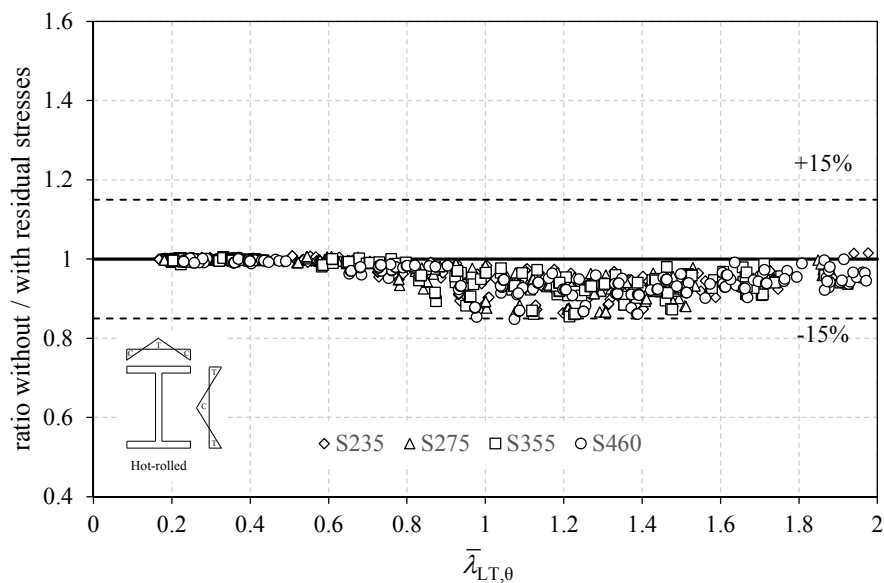


Figure 4.15: Influence of the temperature on the LTB resistance of the beams with cross-section 450x4+150x5, effective section factor $W_{eff,y}/W_{el,y} = 0.60$.

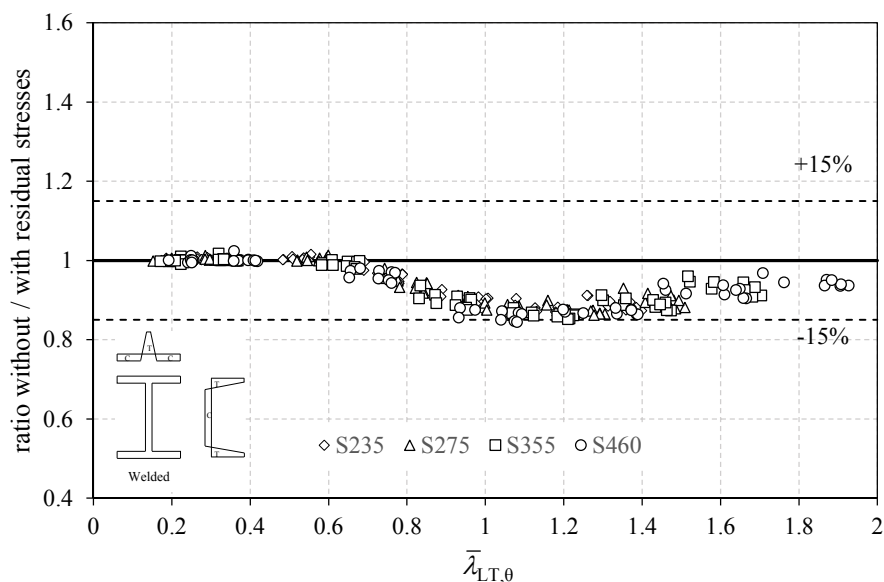
From figures 4.12 – 4.15 it can be concluded that LTB is not very much influenced by the temperature. For this reason, the actual beam design curve of Part 1-2 of Eurocode 3 is not dependent on the value of temperature.

4.5.3 Residual stresses influence

Here, the influence of the residual stresses on the ultimate capacity of laterally unrestrained beams is investigated for four different cross-sections described in Table 4.3. Welded and hot-rolled cases are considered with the patterns of residual stresses defined in Figure 4.4. Results are shown in Figure 4.16 and are presented as the ratio between the ultimate load obtained in FEA with and without residual stresses. Various steel grades and temperatures (350°C, 450°C, 550°C and 700°C) were considered.



a) Hot-rolled cross-sections



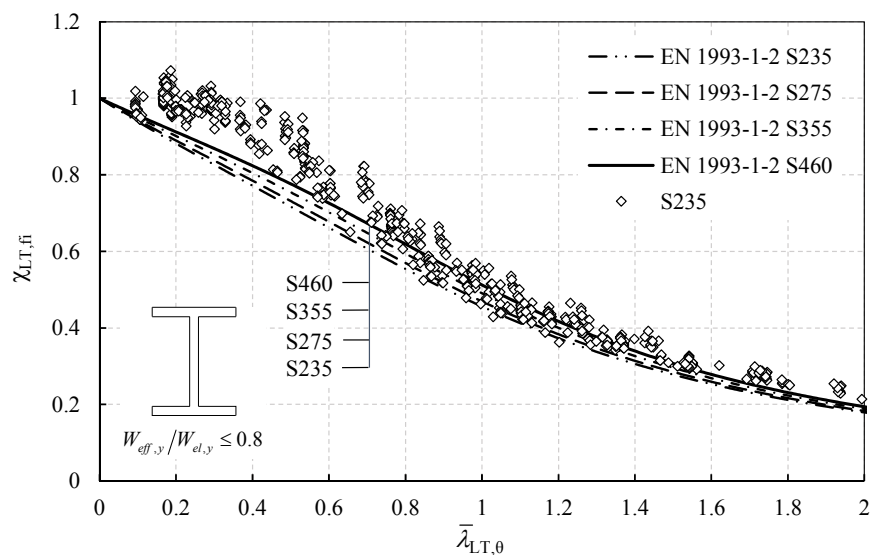
b) Welded cross-sections

Figure 4.16: Influence of the residual stresses on the LTB resistance of a) hot-rolled and b) welded beams with slender cross-section.

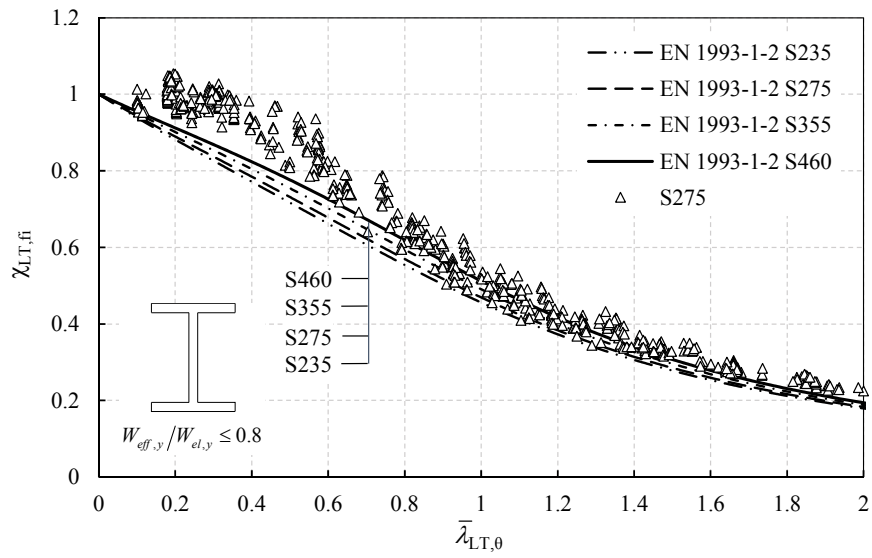
The residual stresses have an unfavourable influence on the LTB resistance of beams. In case of fire, this influence is less than that at normal temperature, since in case of fire the temperature causes a relaxation of the residual stresses and, therefore, a maximum 15% of reduction of the LTB resistance due to the residual stresses on beams with slender cross-sections is observed for both hot-rolled and welded cases. The reduction on the LTB resistance is higher for intermediate slenderness values $1.0 \leq \bar{\lambda}_{LT,\theta} \leq 1.4$ for both cases and for slenderness values of $\bar{\lambda}_{LT,\theta} \leq 0.4$ no influence is noticed of the residual stresses. Based on this comparison, it was decided to consider in the remaining part of this study, only the pattern corresponding to welded cross-sections depicted in Figure 4.4.

4.5.4 Steel grade influence

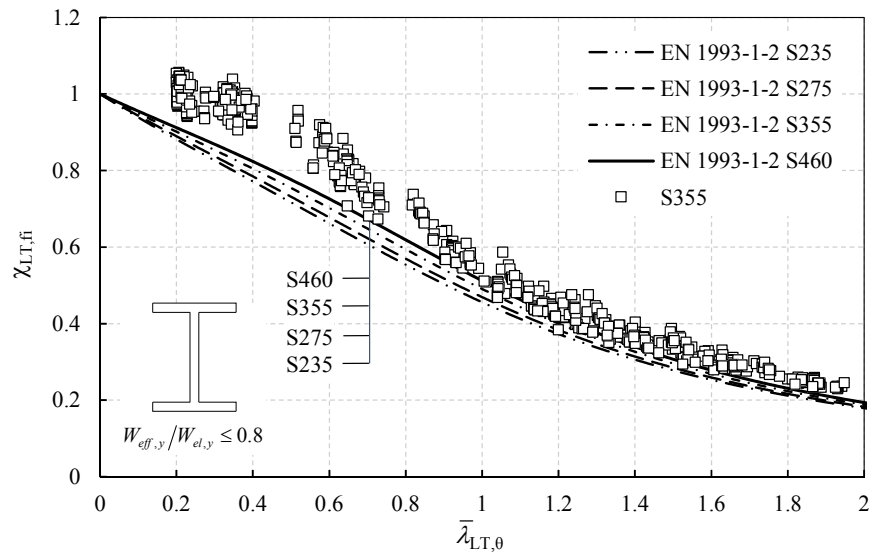
In this section, the influence of the steel grade is shown. Figure 4.17 a) – d) depict the numerical results obtained for all the profiles indicated in Table 4.1 with effective section factor of $W_{eff,y}/W_{el,y} \leq 0.8$ and steel grades S235, S275, S355 and S460 respectively. These steel grades have a yield strength at normal temperature of 235 MPa, 275MPa, 355 MPa and 460 MPa. For the purpose of comparison, the EN1993-1-2 design curves for each steel grades are plotted in all charts.



a) S235



b) S275



c) S355

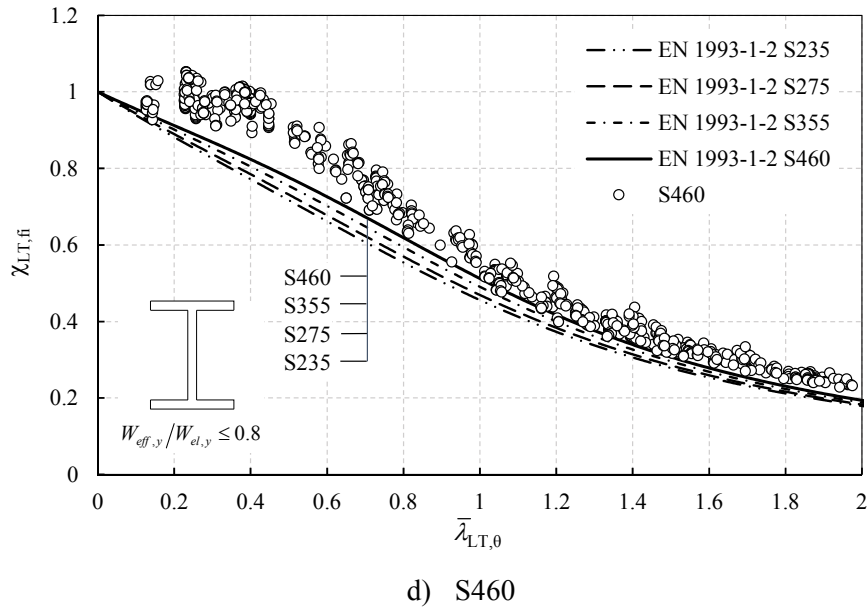


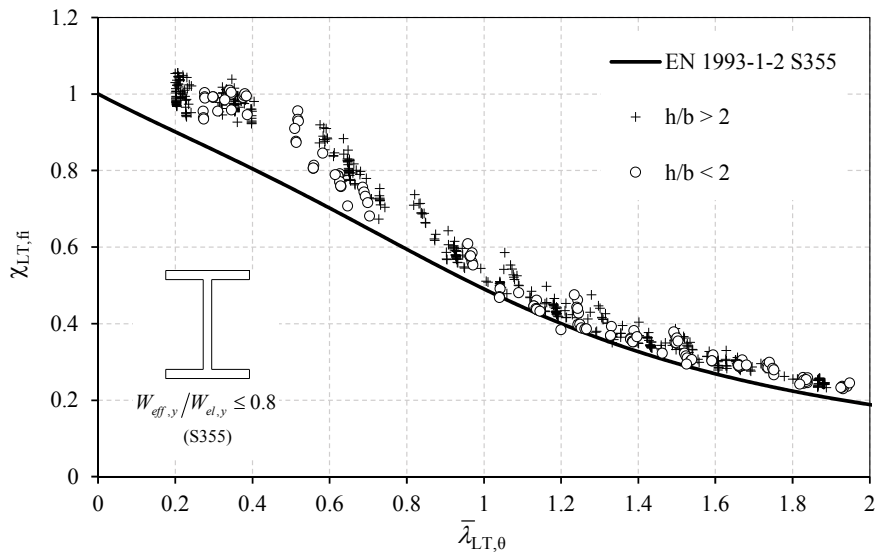
Figure 4.17: LTB behaviour of beams with effective section factor of $W_{eff,y}/W_{el,y} \leq 0.8$ for different steel grades.

From these figures, it is observed that the reduction of the beam capacity is dependent on the steel grade. The better the steel grade the less is the reduction of the lateral-torsional buckling resistance of a beam. For instance, for slenderness of $\bar{\lambda}_{LT,\theta} \approx 1.0$, the minimum value for the reduction factor on the steel S235 is about $\chi_{LT,fi} \approx 0.46$ (see Figure 4.17 a) while for S460 is about $\chi_{LT,fi} \approx 0.51$ (see Figure 4.17 d) which represents more than 10% increase of resistance in relative terms. This is in line with the actual provisions of the Eurocode 3 which take the effect of steel grade into account in the verifications of beams against lateral-torsional buckling through the parameter α (see equation (4.4)). Although it is not here shown to reduce the size of this chapter, similar results was obtained for other ranges of effective section factor.

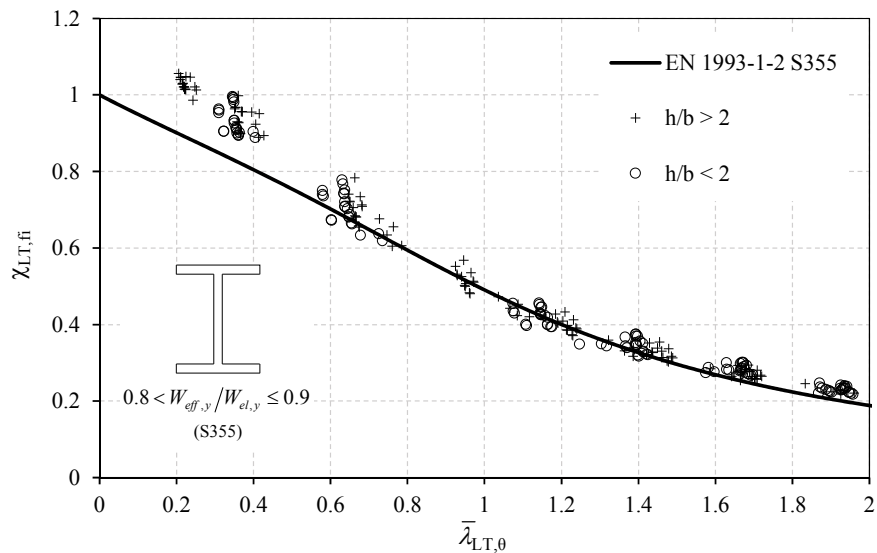
4.5.5 Depth-to-width ratio influence

The depth h to width b ratio (h/b) of a cross-section is used in Part 1-1 of Eurocode 3 to group the properties of the sections and take into account a variety of factors such as the torsional stiffness or the critical behaviour in plasticity as pointed out in [4.29]. At elevated temperatures, this influence was also observed for Class 1 profiles in [4.8] and a severity factor that takes into account the influence of the h/b ratio among other parameters was

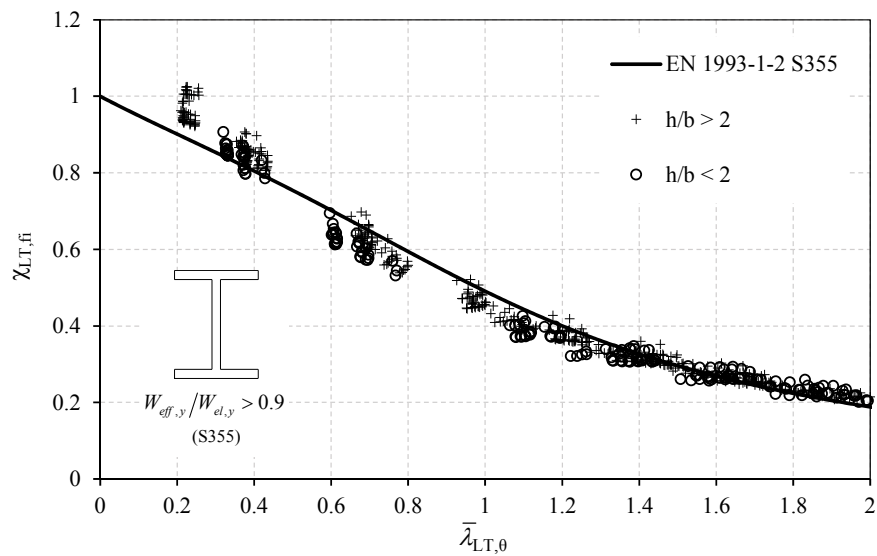
suggested in that publication. In this section, the influence of the depth-to-width ratio is investigated for a variety of slender cross-sections (see Table 4.1) considering different steel grades and temperatures (350°C, 450°C, 550°C and 700°C). Figure 4.18 shows the influence of the depth-to-width ratio for different ranges of effective section factor and steel grade S355.



a) Cross-sections with $W_{eff,y}/W_{el,y} \leq 0.8$.



b) Cross-sections with $0.8 < W_{eff,y}/W_{el,y} \leq 0.9$.



c) Cross-sections with $W_{eff,y}/W_{el,y} > 0.9$

Figure 4.18: Influence of the depth-to-width ratio on the LTB resistance of beams with different effective section factor. Steel grade S355.

From this figure, it is observed that influence of the depth-to-width ratio (h/b) is negligible for slender cross-sections. As depicted in these figures, no distinct behaviour between sections with $h/b < 2$ and $h/b > 2$ is noticed. Since this parameter accounts for the critical behaviour in plasticity and slender cross-sections are considered here, explains the absence of a different behaviour. Although it is not demonstrated in this chapter, similar trends were observed for other steel grades.

4.6 New design curve

Based on the parametric study performed in section 4.5, new design curves are proposed in this section. The improvements of using this new proposal in comparison to the actual design curve given in Part 1-2 of Eurocode 3 are also here demonstrated. The new design curves are dependent on the effective section factor (see subsection 4.5.1) and on the steel grade (see subsection 4.5.4), which were the main parameters influencing the lateral-torsional buckling behaviour of beams with slender cross-sections at elevated temperatures. As stated before, the influence of the steel grade was already taken into account in EN 1993-1-2 in the definition of the imperfection factor, using parameter $\varepsilon = \sqrt{235/f_y}$ (see equation (4.5)).

The proposed expressions are based on the actual design curve of Part 1-2 of Eurocode, given by equations (4.3) – (4.8) but considering

$$\phi_{LT,\theta} = 0.5 \left[1 + \alpha_{LT,new} (\bar{\lambda}_{LT,\theta} - \bar{\lambda}_{LT,0}) + \bar{\lambda}_{LT,\theta}^2 \right] \quad (4.17)$$

with the values of $\alpha_{LT,new}$ and $\bar{\lambda}_{LT,0}$ given in Table 4.4. Three different curves are proposed (L1, L2 and L3) depending on the effective section factor. Although as seen in subsection 4.5.1, plateaus ($\bar{\lambda}_{LT,0}$) of 0.4 and 0.3 would represent better the behaviour for the effective section factor $W_{eff,y} / W_{el,y} \leq 0.8$ and $0.8 < W_{eff,y} / W_{el,y} \leq 0.9$ respectively, a constant plateau of 0.2 was adopted for all the curves to simplify the proposal.

Table 4.4: Parameters for the new design curve of beams with slender cross-sections and criteria for selection.

Curve	Limits	$\alpha_{LT,new}$	$\bar{\lambda}_{LT,0}$
L1	$\frac{W_{eff,y}}{W_{el,y}} > 0.9$	$1.25\varepsilon = 1.25\sqrt{235 / f_y}$	0.2
L2	$0.8 < \frac{W_{eff,y}}{W_{el,y}} \leq 0.9$	$1.00\varepsilon = 1.00\sqrt{235 / f_y}$	0.2
L3	$\frac{W_{eff,y}}{W_{el,y}} \leq 0.8$	$0.75\varepsilon = 0.75\sqrt{235 / f_y}$	0.2

In the Figure 4.19, the proposed beam design curves L1, L2 and L3 are plotted for steel grade S235 and in Figure 4.20 it is depicted the variation of curve L1 with different steel grades.

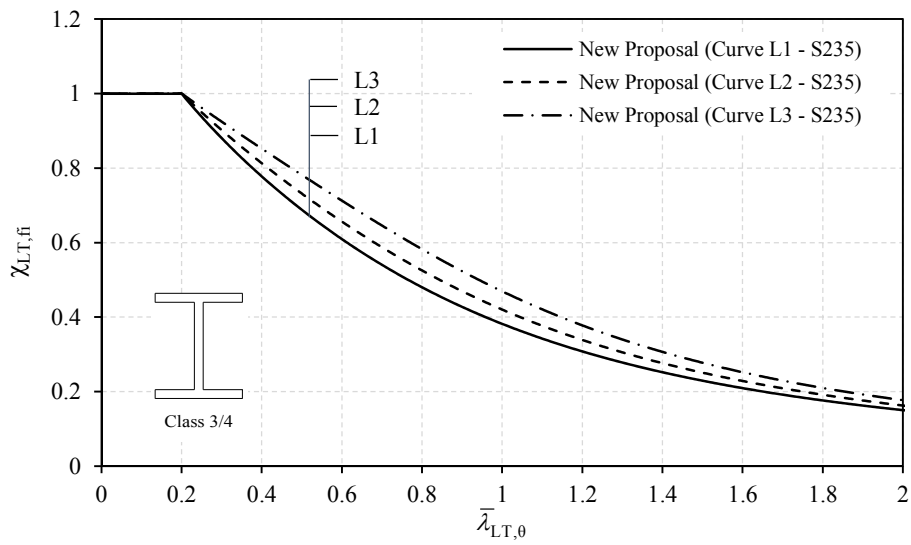


Figure 4.19: New design curve for beams with slender cross-sections at elevated temperatures (S235).

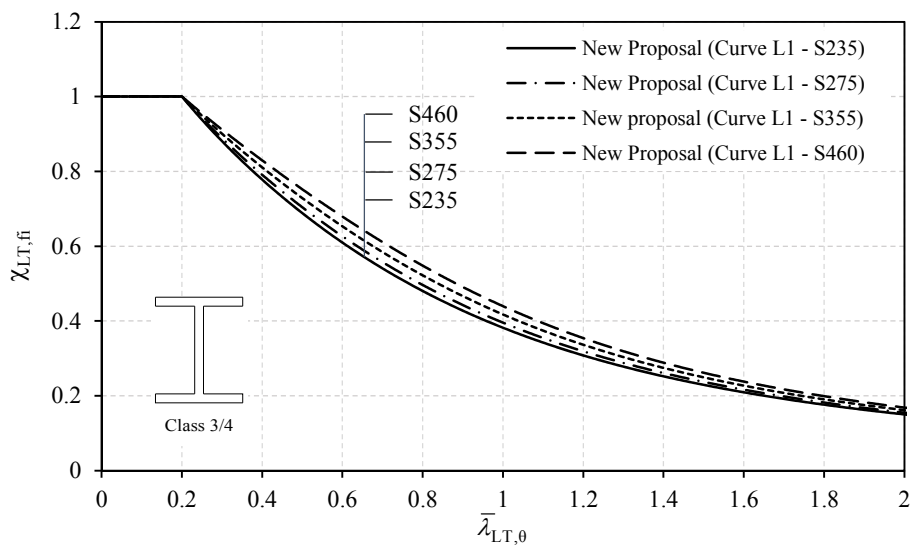


Figure 4.20: Variation of new design curve (L1) with the steel grade.

A comparison between the numerical results obtained and the new design curve proposed in this work are shown in Figure 4.21 - Figure 4.24 for the cross-sections indicated in Table 4.3.

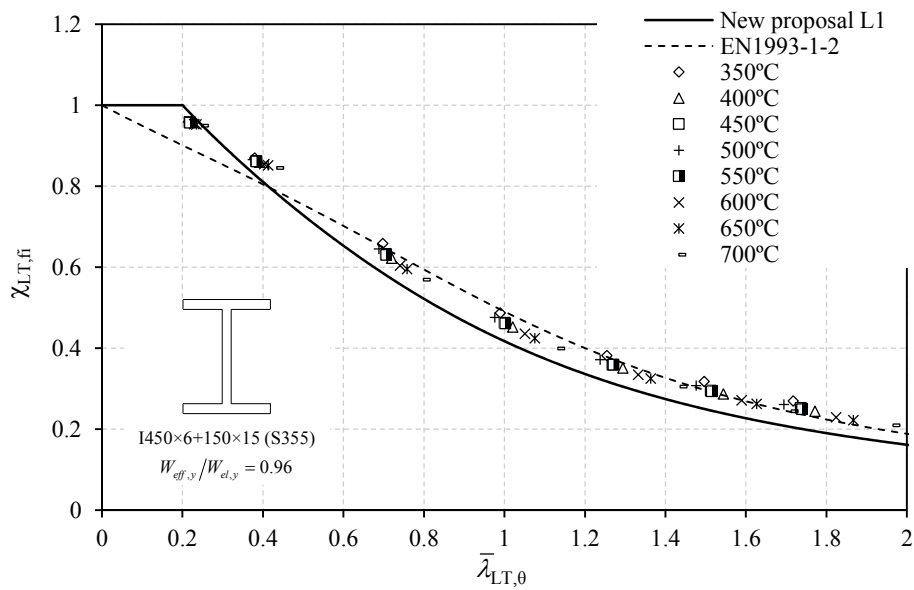


Figure 4.21: Comparison between the new design curve the beam with cross-section 450x6+150x15, effective section factor $W_{eff,y}/W_{el,y} = 0.96$.

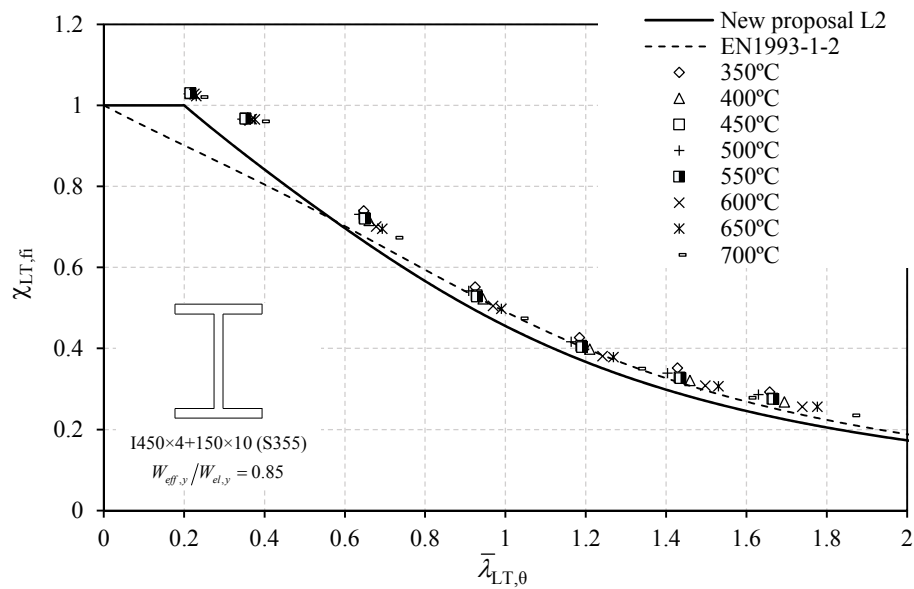


Figure 4.22: Comparison between the new design curve the beam with cross-section 450x4+150x10, effective section factor $W_{eff,y}/W_{el,y} = 0.85$.

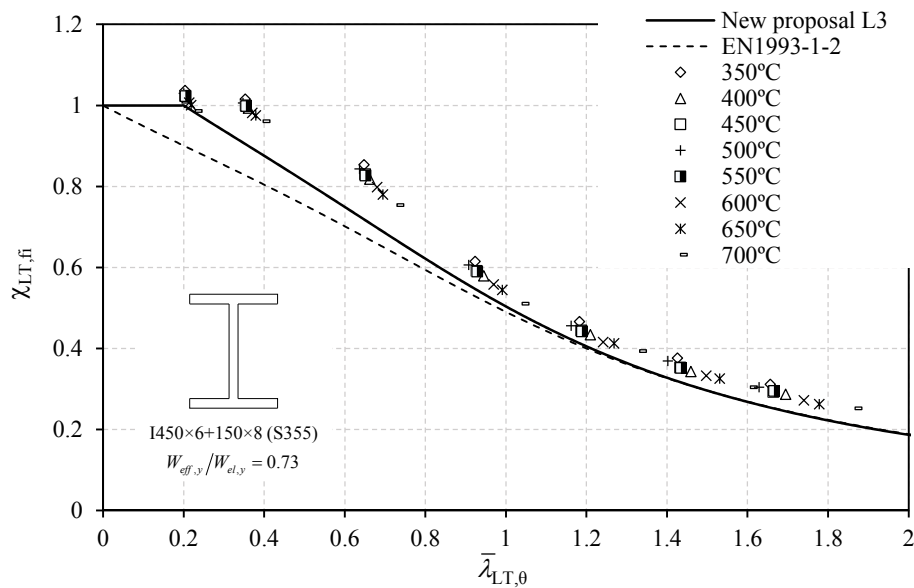


Figure 4.23: Comparison between the new design curve the beam with cross-section $450 \times 6 + 150 \times 8$, effective section factor $W_{eff,y}/W_{el,y} = 0.73$.

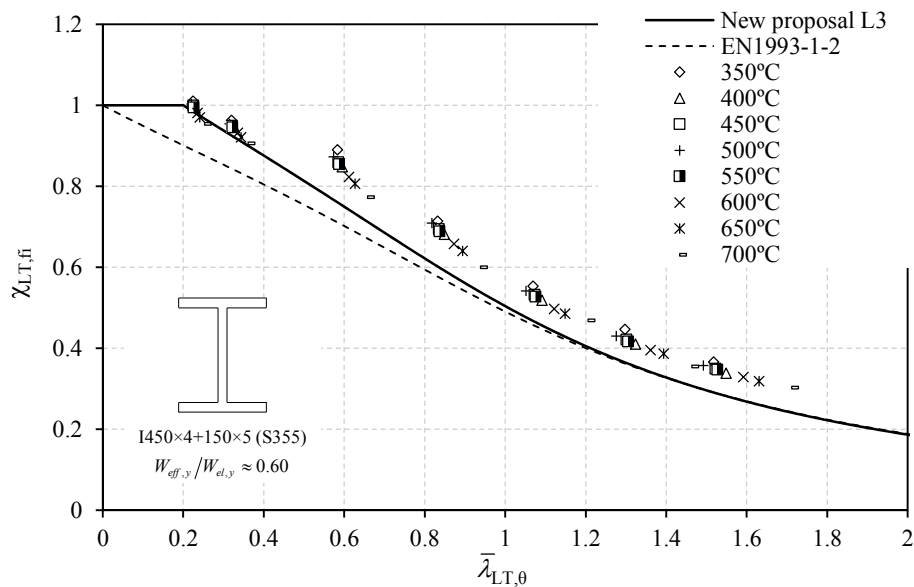


Figure 4.24: Comparison between the new design curve the beam with cross-section $450 \times 4 + 150 \times 5$, effective section factor $W_{eff,y}/W_{el,y} = 0.60$.

As it can be seen, there is closer agreement between FEA numerical results and the proposed design curves (represented by the solid line in the figures). The introduction of the plateau $\bar{\lambda}_{LT,0} = 0.2$ improves the accuracy of the proposal for small slenderness range $\bar{\lambda}_{LT,\theta} < 0.4$ when compared to EN 1993-1-2 (represented by the dashed line in the previous figures).

Since in practical terms the proposed design curves should be used together with the cross-sectional resistance calculated according to Simple proposal (see section 4.2.2), in Figure 4.25 its accuracy is presented.

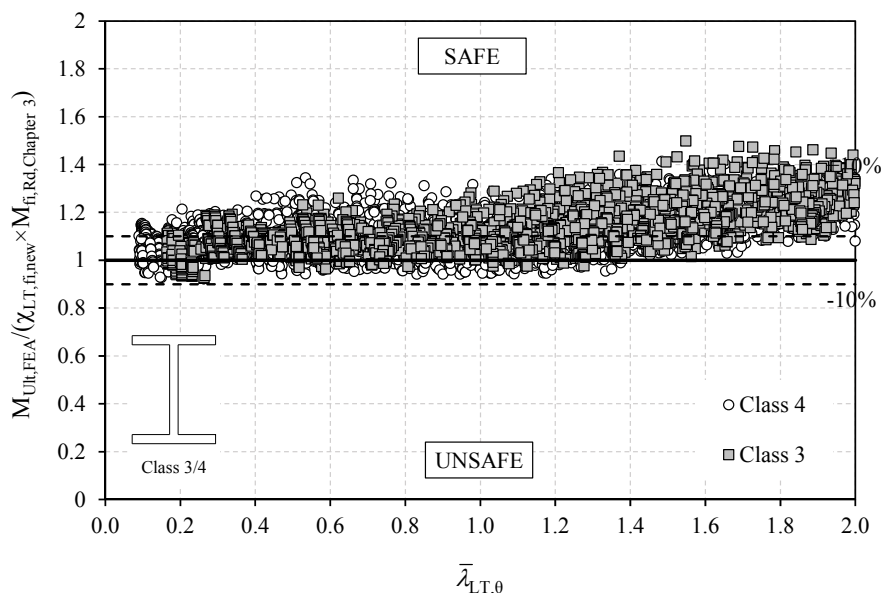


Figure 4.25: Accuracy of the new design curve compared to FEA results with cross-sectional resistance calculated according to Simple proposal from Chapter 3.

Figures 4.25 and 4.8 are comparable, i.e., the new proposal and the EN 1993-1-2 design curve respectively considering the cross-section resistance calculated with the Simple proposal from Chapter 3. It is observed from this comparison that results are less scattered when using the new proposal, especially for slenderness $\bar{\lambda}_{LT,\theta} \leq 1.0$, meaning that there is closer agreement between the numerical results and the proposal for the simplified design method. On the other hand, a large number of results for slenderness around $\bar{\lambda}_{LT,\theta} \approx 1.0$ lay on the unsafe side for the EN 1993-1-2 design curve. As observed in Figure 4.21 and Figure 4.22, these are mainly Class 3 and Class 4 cross-sections with an effective section factor tending towards the unity, i.e. are less prone to local buckling, this is corrected by considering curve L1 which is more conservative than that of EN 1993-1-2. With the new proposal, the beam capacity is better predicted and the safety of using simplified design methods increases (going from a minimum of -20% for EN1993-1-2 to -7% on the new proposal).

4.7 Non-uniform bending diagrams


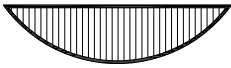



In this section, beams submitted to non-uniform bending diagrams are studied. The numerical model described in section 4.3 was used and cross-section $450 \times 4 + 150 \times t_f$ was considered. In this section, it was not possible to study the common case corresponding to a point load applied at mid-span due to web-buckling and other local phenomena that was observed prior to global instability. For this case, web stiffeners could have been considered to address this issue but such assumptions were out of the scope of this research programme. For the same reason, the distributed load case was modelled using nodal forces applied at the lower flange. Additionally, the numerical results where failure of the beams was mainly due to shear stresses were disregarded.


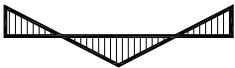

The inclusion of the factor “ f ” to take into account different loading cases on the lateral-torsional buckling response of the beams in case of fire was proposed in [4.8, 4.30] for Class 1 and 2 beams. The applicability of the formulae to Class 3 and 4 beams is investigated here. Accordingly, the factor “ f ” is defined as

$$f = 1 - 0.5(1 - k_c) \quad (4.18)$$

where k_c is a correction factor according to Table 4.5.

Table 4.5: Correction factors k_c .

Moment distribution	k_c
<div style="display: flex; justify-content: space-around;"> <div style="text-align: center;"> <p>M</p>  <p>$-1 \leq \psi \leq 1$</p> </div> <div style="text-align: center;"> <p>ψM</p>  </div> </div>	$0.6 + 0.3\psi + 0.15\psi^2$ but $k_c \leq 1$
	0.91
	0.90
	0.91

Moment distribution	k_c
	0.79
	0.73
	0.75

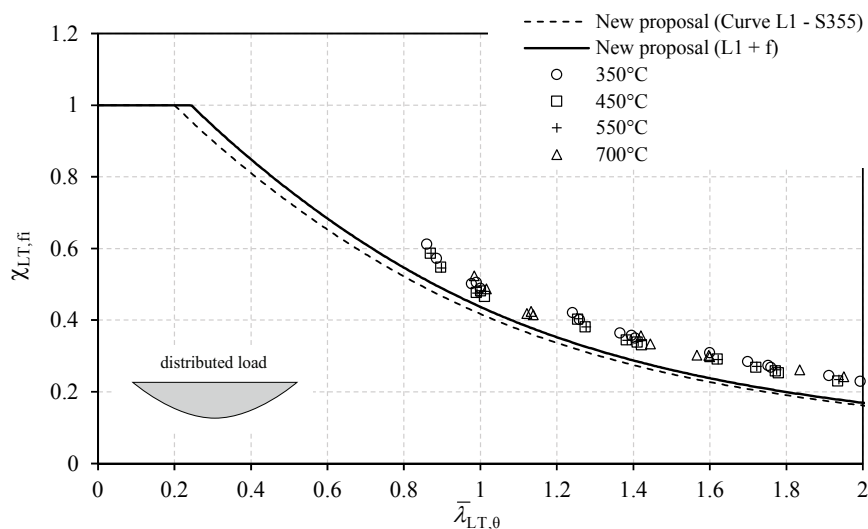
Note: for others bending diagrams $k_c = 1$.

Finally, the reduction factor to take lateral-torsional buckling into account is calculated as

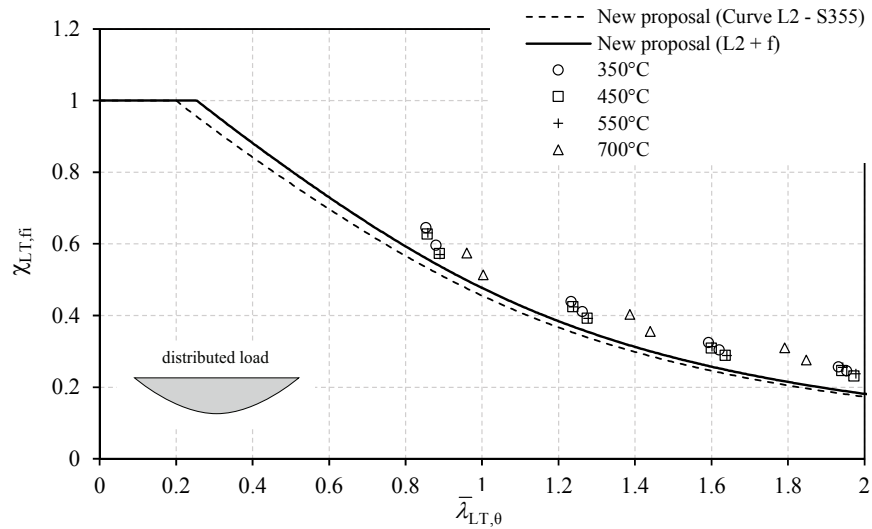
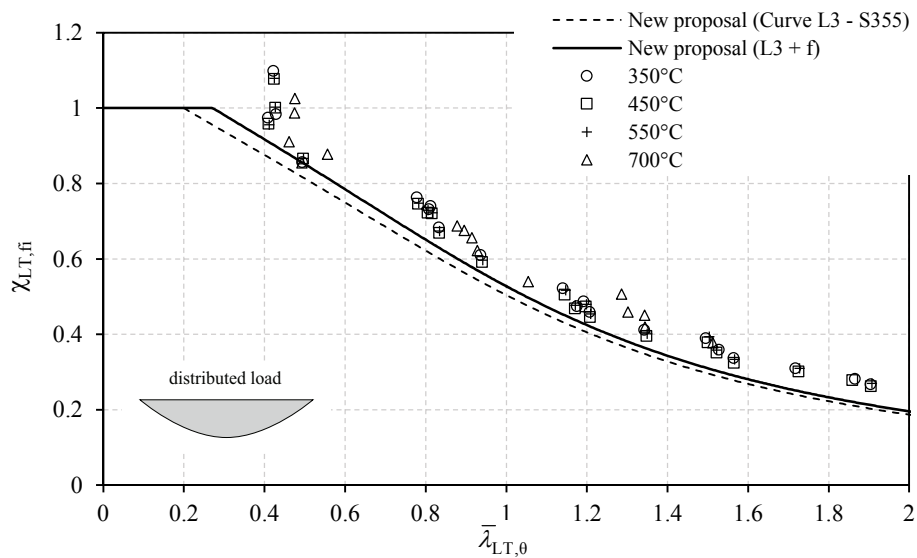
$$\chi_{LT,fi,mod} = \frac{\chi_{LT,fi}}{f} \tag{4.19}$$

4.7.1 Uniformly distributed load

In Figure 4.26, the results for uniformly distributed load are depicted for the different curves proposed (L1-L3) and considering the factor “ f ”. In this figure, the “New proposal (L# + f)” curve denotes the one corresponding to the calculation of $\chi_{LT,fi,mod}$ according to equation (4.19) with the factor “ f ” given in equation (4.18).



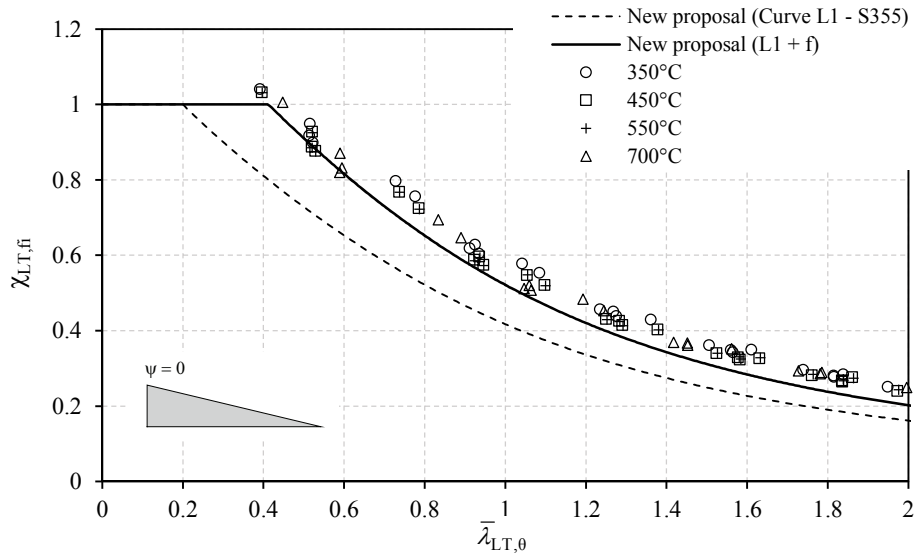
a) Cross-sections with $W_{eff,y}/W_{el,y} \leq 0.8$.

b) Cross-sections with $0.8 < W_{eff,y}/W_{el,y} \leq 0.9$.c) Cross-sections with $W_{eff,y}/W_{el,y} > 0.9$ **Figure 4.26:** Comparison of the new proposal with factor “ f ” for distributed load.

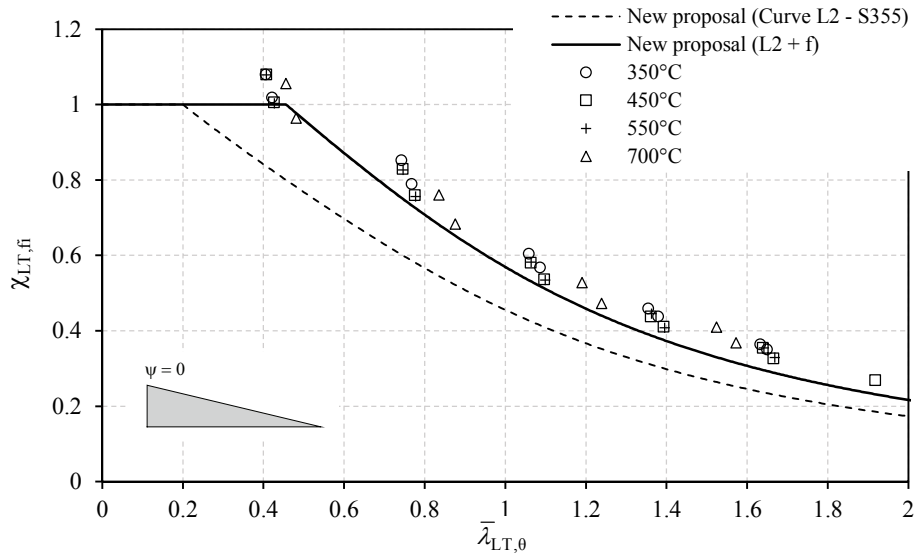
For this load case, the differences to the fundamental case of considering beams submitted to a constant bending moment are not much. It is observed that using the factor “ f ” in this case leads to some improvements and therefore it is recommended.

4.7.2 End-moments

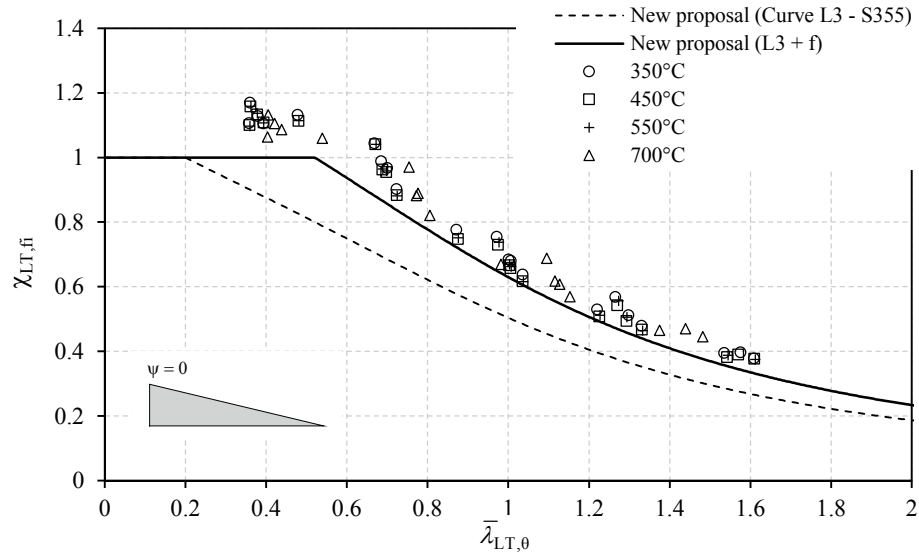
Here, beams submitted to end moments are analysed. Two cases are considered corresponding to triangular ($\psi = 0$) and bi-triangular ($\psi = -1$) bending moment and are depicted in Figure 4.27 and Figure 4.28 respectively.



a) Cross-sections with $W_{eff,y}/W_{el,y} \leq 0.8$.



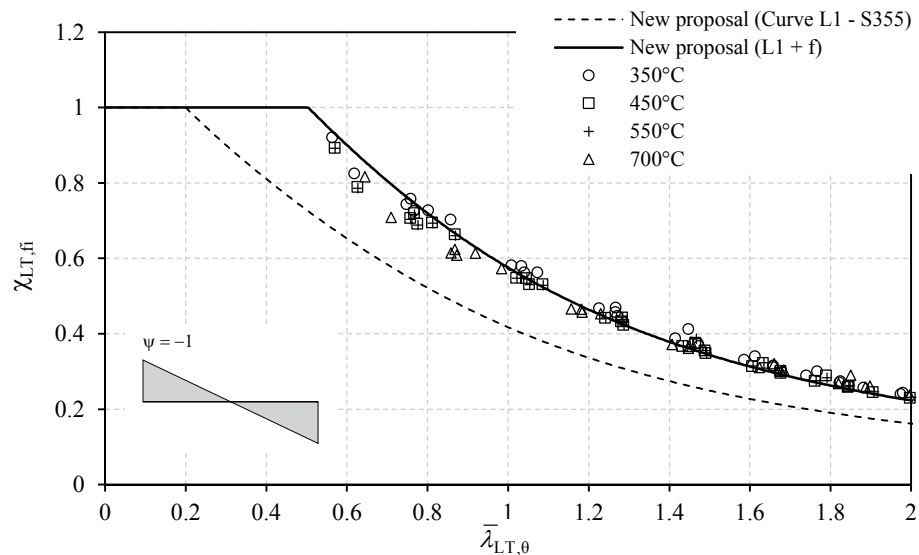
b) Cross-sections with $0.8 < W_{eff,y}/W_{el,y} \leq 0.9$.



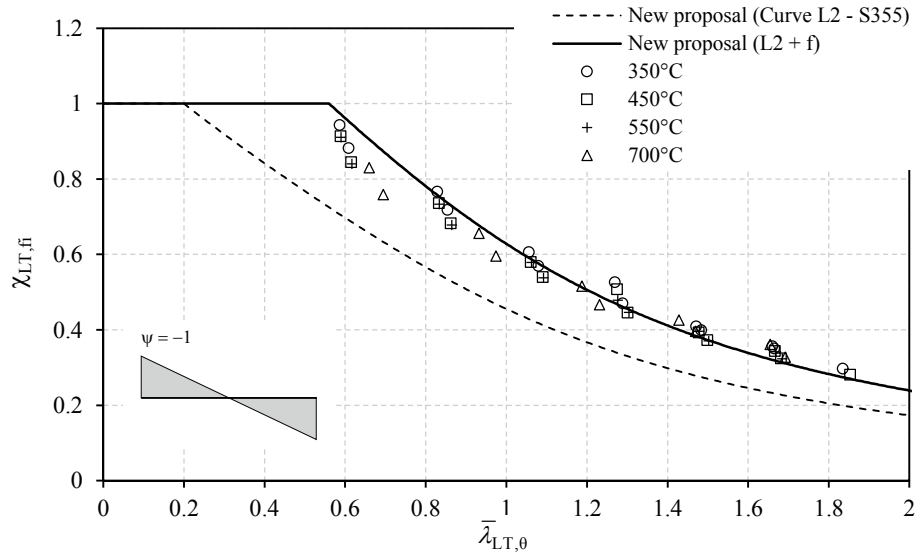
c) Cross-sections with $W_{eff,y}/W_{el,y} > 0.9$

Figure 4.27: Comparison of the new proposal with factor “ f ” for triangular bending moment.

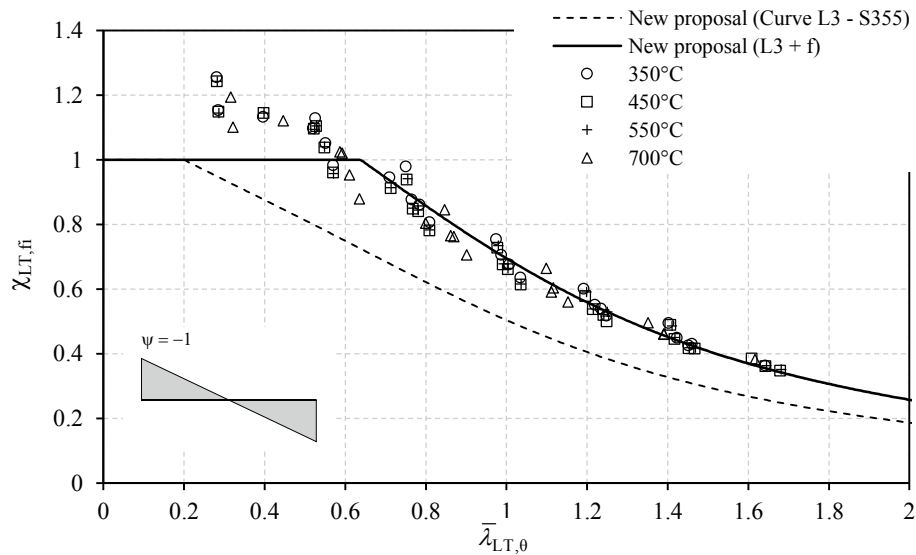
For the triangular bending diagram, it is observed that the inclusion of the factor “ f ” gives better prediction of the beam resistance and improvements are noticed and therefore it is recommended its use.



a) Cross-sections with $W_{eff,y}/W_{el,y} \leq 0.8$.



b) Cross-sections with $0.8 < W_{eff,y} / W_{el,y} \leq 0.9$.



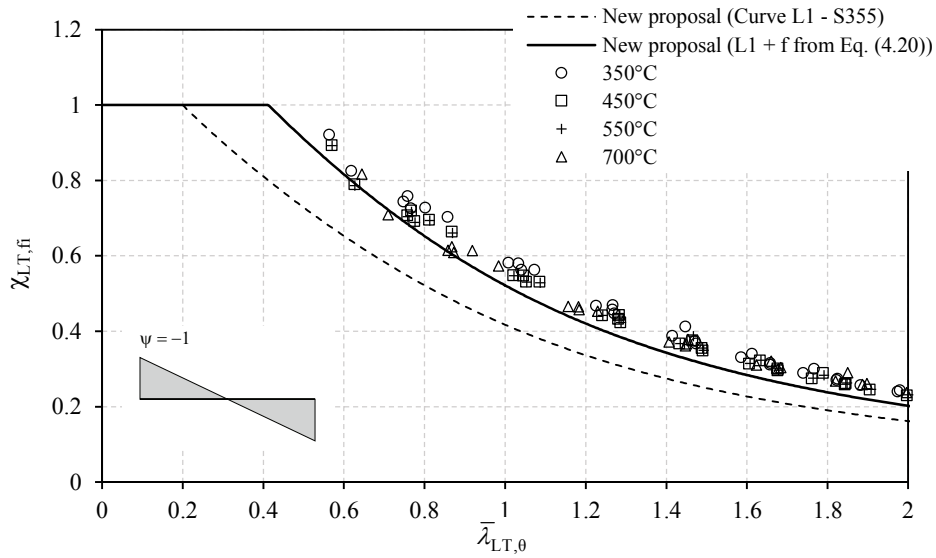
c) Cross-sections with $W_{eff,y} / W_{el,y} > 0.9$

Figure 4.28: Comparison of the new proposal with factor “ f ” for bi-triangular bending moment.

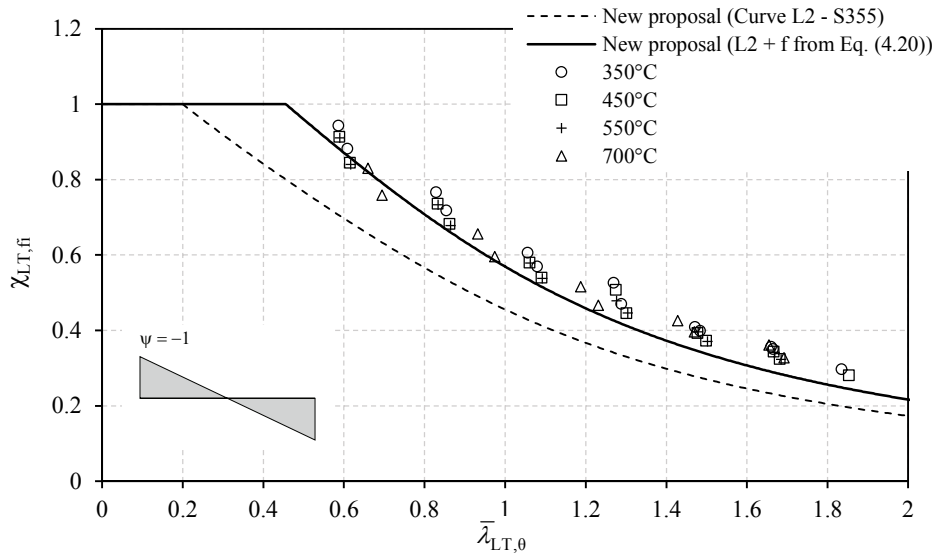
However, for the bi-triangular case, it is noticed that the curve does not fit the numerical results and several results lay on the unsafe side. In this case, it is observed that for slender cross-sections the interaction between local buckling and lateral-torsional buckling does not allow reaching the beam resistance as predicted by the factor “ f ” that was initially developed for Class 1 and 2 cross-sections. For that reason, it is proposed to use a limitation on the factor “ f ” to account with this. Accordingly, this factor should be given by

$$f = 1 - 0.5(1 - k_c) \text{ but } f \geq 0.8 \quad (4.20)$$

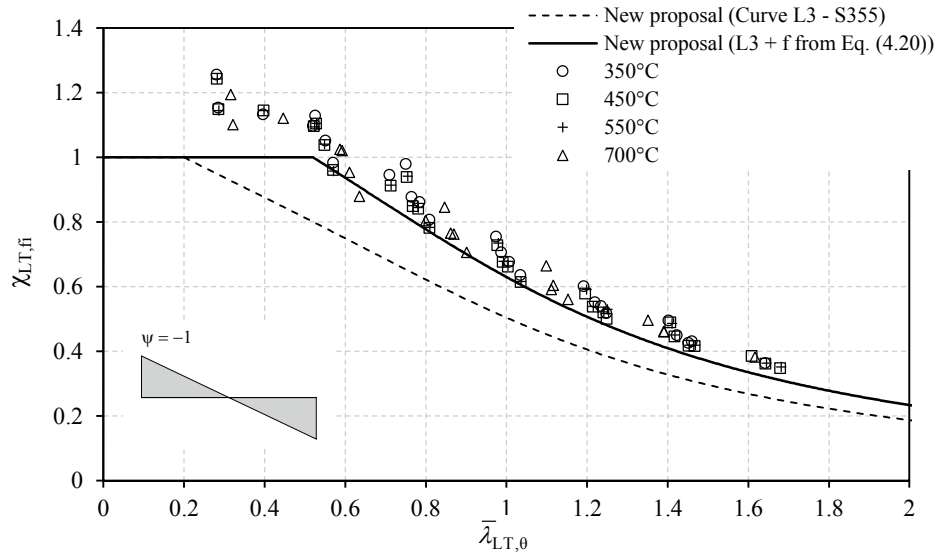
Figure 4.29 depicts the results using equation (4.20) for factor “ f ”.



a) Cross-sections with $W_{eff,y}/W_{el,y} \leq 0.8$.



b) Cross-sections with $0.8 < W_{eff,y}/W_{el,y} \leq 0.9$.



c) Cross-sections with $W_{eff,y}/W_{el,y} > 0.9$

Figure 4.29: Comparison of the new proposal with factor “ f ” modified for the bi-triangular bending moment case using equation (4.20).

As it can be seen, the proposed modification to factor “ f ” leads to better prediction of the beam resistance and almost all numerical results are now on the safe side.

4.8 Statistical evaluation

Tables 4.6 and 4.7 presents the statistical results for the comparison between the FEA results and the simplified methodologies to design beams against lateral-torsional buckling in fire situation considering uniform and non-uniform bending diagrams respectively. For each methodology, the mean value μ and the standard deviation s of the numerical results were calculated from:

$$\mu = \frac{\sum_{i=1}^n x_i}{n} \quad (4.21)$$

$$s = \sqrt{\frac{\sum_{i=1}^n (x_i - \mu)^2}{n-1}} \quad (4.22)$$

where for each methodology, x_i is given according to equation (4.23).

$$x_i = \frac{M_{b,fi,Rd,Simplified}}{M_{Ult,FEA}} \quad (4.23)$$

where $M_{b,fi,Rd,Simplified}$ represents the beam ultimate capacity calculated with simplified methodologies and $M_{Ult,FEA}$ the ultimate bending moment calculated with SAFIR. The LTB design curve and methodology used to calculate the cross-section resistance used to determine $M_{b,fi,Rd,Simplified}$ is indicated in the tables. A x_i greater than 1.0 represents an unsafe result, that is, the capacity predicted by SAFIR is lower than that obtained by the simplified methodology and vice-versa. The maximum unsafe result given in tables corresponds to the maximum deviation obtained with equation (4.23) and the number of unsafe results is the percentage of cases for which x_i is greater than 1.0.

Table 4.6: Statistical results of beams submitted to uniform bending diagrams.

LTB Design Curve	Cross-section Resistance ($M_{fi,Rd}$)	Number cases (n)	Mean (μ)	StdDev (s)	Max. Unsafe	Num. Unsafe
i) EN 1993-1-2	EN 1993-1-2	7707	0.92	10.87%	1.32	24.39%
ii) EN 1993-1-2	Simple proposal (Chapter 3)	7707	0.91	8.37%	1.23	16.70%
iii) New proposal	Simple proposal (Chapter 3)	7707	0.90	7.22%	1.08	6.53%

From Table 4.6 it is observed that 24,39% of unsafe results are obtained when considering the LTB design curve and $M_{fi,Rd}$ from EN 1993-1-2 (case i). If $M_{fi,Rd}$ is calculated according to Simple proposal from Chapter 3 (case ii), the number of unsafe results decreases to 16.70%. In addition, for both cases the maximum unsafe result is high (1.32 and 1.23) which demonstrates that the current design LTB curve from EN 1993-1-2, as mentioned previously in this chapter, is not adequate to design beams with slender cross-sections

against lateral-torsional buckling in fire situation. The proposed design method (case iii) gives 6.53% cases on the unsafe side with a maximum unsafe result of 1.08, meaning that the capacity predicted by the simplified methods gives a maximum 8% difference on the unsafe side comparatively to the FEA results.

Regarding beams submitted to non-uniform bending diagram, statistical results obtained for different methodologies are presented in Table 4.7.

Table 4.7: Statistical results of beams submitted to non-uniform bending diagrams.

LTB Design Curve	Cross-section Resistance ($M_{f,Rd}$)	Number cases (n)	Mean (μ)	StdDev (s)	Max. Unsafe	Num. Unsafe
i) New proposal		687	0.76	6.28%	n.a.	0.00%
ii) New proposal + f (equation 4.18)	Simple proposal (Chapter 3)	687	0.93	8.56%	1.18	19.21%
iii) New proposal + $f \geq 0.8$ (equation 4.20)		687	0.90	6.22%	1.07	4.80%

Table 4.7 shows that the new proposal (case i) is too much conservative (average value of 0.76) but is always safe sided. Considering factor “ f ” from equation (4.18) (case ii) the results now yield an average value of 0.93, however, 19.21% unsafe results are obtained with a maximum of 1.18. As it was demonstrated in section 4.7.2, this proposal is not adequate for bi-triangular bending diagram ($\psi = -1$). Finally, considering a limitation on the factor $f \geq 0.8$ (case iii), gives an average value of 0.90 with just 4.80% unsafe results and a maximum of 1.07, thus it is concluded that this proposal could be used to design beams with slender cross-sections submitted to non-uniform bending diagram in fire situation.

4.9 Conclusions

In this study, the behaviour of beams with slender cross-sections subjected to uniform bending moment was investigated with finite element analysis software SAFIR in case of fire. Shell finite elements were used and several Class 3 and Class 4 cross-sections, as well as different temperatures and different steel grades were considered. In the first instance, it

was observed that the actual fire design rules of Part 1-2 of Eurocode 3 for checking the lateral-torsional buckling resistance of beams with slender cross-sections could be improved. It was demonstrated that using the current methodology to calculate the cross-sectional resistance at elevated temperatures to check the LTB resistance of beams in case of fire according to Part 1-2 leads to inaccurate results. The comparison to FEA carried out in SAFIR, demonstrated that for small slenderness ranges of the beams the resistance was over predicted for Class 3 cross-sections and underestimated for Class 4 cross-sections. The methodology developed in Chapter 3 to calculate the cross-sectional capacity of Class 3 and Class 4 cross-sections was then used to check the accuracy of the existing beam design rule and improvements were noticed. Nonetheless, it was observed that the actual simplified methodology of EN 1993-1-2 could be improved to better account with the specific behaviour of beams with slender cross-sections.

A parametric study was performed to investigate the influence of several parameters on the LTB resistance of beams with slender cross-sections, namely the effective cross-section ratio $W_{eff,y}/W_{el,y}$, the temperature, the residual stresses, the steel grade and the depth-to-width ratio. From the studied parameters, it was found that the beam resistance depends on the effective ratio of the cross-section. Therefore, an effective section factor was proposed for this ratio $s = W_{eff,y}/W_{el,y}$ and different ranges were defined according to the influence of the local buckling on the lateral-torsional buckling resistance of beams: i) for $W_{eff,y}/W_{el,y} \leq 0.8$ it is high; ii) For $0.8 < W_{eff,y}/W_{el,y} \leq 0.9$ it is moderate and iii) for $W_{eff,y}/W_{el,y} > 0.9$ it is small.

Finally, a proposal for a new design curve including the effective section factor was proposed and validated against numerical results. The new proposal allows for better prediction of the capacity of beams with slender cross-sections against lateral-torsional buckling in case of fire. Additionally, for non-uniform bending diagrams, it was concluded that the factor “ f ” could be used together with the new proposal to account with the effect of the loading case providing that this factor is limited to $f \geq 0.8$.

References

- [4.1] Bailey C., Burgess I., Plank R., “The Lateral-torsional Buckling of Unrestrained Steel Beams in Fire,” *Journal of Constructional Steel Research*, vol. 36, no. 2, pp. 101–119, 1996.
- [4.2] Vila Real P., Franssen J.-M., “Numerical modeling of lateral-torsional buckling of steel I-Beams under fire conditions - Comparison with eurocode 3,” *Journal of Fire Protection Engineering*, 2001.
- [4.3] CEN, “EN 1993-1-2, Eurocode 3: Design of steel structures - Part 1-2: General rules - Structural fire design.” European Committee for Standardisation, Brussels, Belgium, 2005.
- [4.4] Vila Real P. M. M., Piloto P. A. G., Franssen J.-M., “A new proposal of a simple model for the lateral-torsional buckling of unrestrained steel I-beams in case of fire: experimental and numerical validation,” *Journal of Constructional Steel Research*, vol. 59, no. 2, pp. 179–199, February 2003.
- [4.5] Mesquita L. M. R., Piloto P. a. G., Vaz M. a. P., Vila Real P. M. M., “Experimental and numerical research on the critical temperature of laterally unrestrained steel I beams,” *Journal of Constructional Steel Research*, vol. 61, no. 10, pp. 1435–1446, October 2005.
- [4.6] Vila Real P. M. ., Lopes N., Simões da Silva L., Franssen J.-M., “Lateral-torsional buckling of unrestrained steel beams under fire conditions: improvement of EC3 proposal,” *Computers & Structures*, vol. 82, no. 20–21, pp. 1737–1744, August 2004.
- [4.7] Vila Real P. M. M., Cazeli R., Simões da Silva L., Santiago a., Piloto P., “The effect of residual stresses in the lateral-torsional buckling of steel I-beams at elevated temperature,” *Journal of Constructional Steel Research*, vol. 60, no. 3–5, pp. 783–793, March 2004.
- [4.8] Vila Real P. M. M., Lopes N., Simões da Silva L., Franssen J.-M., “Parametric analysis of the lateral–torsional buckling resistance of steel beams in case of fire,” *Fire Safety Journal*, vol. 42, no. 6–7, pp. 416–424, September 2007.

-
- [4.9] Dharma R. B., Tan K.-H., “Proposed design methods for lateral torsional buckling of unrestrained steel beams in fire,” *Journal of Constructional Steel Research*, vol. 63, no. 8, pp. 1066–1076, August 2007.
- [4.10] Yin Y. Z., Wang Y. C., “Numerical simulations of the effects of non-uniform temperature distributions on lateral torsional buckling resistance of steel I-beams,” *Journal of Constructional Steel Research*, vol. 59, no. 8, pp. 1009–1033, Aug. 2003.
- [4.11] Zhang C., Gross J. L., McAllister T. P., “Lateral torsional buckling of steel W-beams subjected to localized fires,” *Journal of Constructional Steel Research*, vol. 88, pp. 330–338, September 2013.
- [4.12] Lopes N., Vila Real P. M. M., “Class 4 stainless steel I beams subjected to fire,” *Thin-Walled Structures*, vol. 83, pp. 137–146, 2014.
- [4.13] CEN, “EN 1993-1-1, Eurocode 3: Design of steel structures - Part 1-1: General rules and rules for buildings.” European Committee for Standardisation, Brussels, 2005.
- [4.14] Franssen J.-M., Vila Real P., *Fire design of steel structures*. ECCS : Ernst & Sohn, 2010.
- [4.15] Ranby A., “Structural fire design of thin walled steel sections,” *Journal of Constructional Steel Research*, vol. 46, no. 1–3, pp. 303–304, April 1998.
- [4.16] Couto C., Vila Real P., Lopes N., Zhao B., “A new design method to take into account the local buckling of steel cross-sections at elevated temperatures,” in *8th International Conference on Structures In Fire*, Shanghai, China, June 2014.
- [4.17] Couto C., Vila Real P., Lopes N., Zhao B., “Effective width method to account for the local buckling of steel thin plates at elevated temperatures,” *Thin-Walled Structures*, vol. 84, pp. 134–149, November 2014.
- [4.18] Couto C., Vila Real P., Lopes N., Zhao B., “Resistance of steel cross-sections with local buckling at elevated temperatures,” *Journal of Constructional Steel Research*, vol. 109, pp. 101–114, June 2015.
- [4.19] CEN, “EN 1993-1-5, Eurocode 3 - Design of steel structures - Part 1-5: Plated structural elements.” European Committee for Standardisation, pp. 1–53, Brussels, 2006.

- [4.20] Franssen J.-M., “SAFIR, A Thermal/Structural Program for Modelling Structures under Fire,” *Engineering Journal, A.I.S.C.*, vol. 42, no. 3, pp. 143–158, 2005.
- [4.21] Talamona D., Franssen J.-M., “A Quadrangular Shell Finite Element for Concrete and Steel Structures Subjected to Fire,” *Journal of Fire Protection Engineering* vol. 15, no. 4, pp. 237–264, November 2005.
- [4.22] CEA, “CAST 3M is a research FEM environment; its development is sponsored by the French Atomic Energy Commission <<http://www-cast3m.cea.fr/>>,” 2012.
- [4.23] CEN, “EN 1090-2: Execution of steel structures and aluminium structures - Part 2 : Technical requirements for steel structures.” European Committee for Standardisation, Brussels, Belgium, 2008.
- [4.24] ECCS, *Ultimate limit state calculation of sway frames with rigid joints. Publication No. 33.* European Convention for Constructional Steelwork Technical Committee No. 8, 1984.
- [4.25] ECCS, *Manual on Stability of Steel Structures. Publication No. 22.* European Convention for Constructional Steelwork Technical Committee No. 8, 1976.
- [4.26] ECCS, *New lateral torsional buckling curves k_{LT} - numerical simulations and design formulae.* European Convention for Constructional Steelwork Technical Committee No. 8, 2000.
- [4.27] FIDESC4, “Fire Design of Steel Members with Welded or Hot-Rolled Class 4 Cross-Section, RFCS-CT-2011-00030, 2011-2014,” 2014.
- [4.28] Prachar M., Lopes N., Couto C., Jandera M., Vila Real P., Wald F., “Lateral torsional buckling of Class 4 Steel Plate Girders Under Fire Conditions: Experimental and Numerical Comparison,” in *Benchmark studies - Experimental validation of numerical models in fire engineering*, C. E. Wald F., Burgess I., Kwasniewski L., Horová K., Ed. CTU Publishing House, Czech Technical University in Prague, pp. 21 – 33, 2014.
- [4.29] Taras A., Greiner R., “New design curves for lateral–torsional buckling—Proposal based on a consistent derivation,” *Journal of Constructional Steel Research*, vol. 66, no. 5, pp. 648–663, May 2010.

- [4.30] Lopes N., Vila Real P., Simões da Silva L., Franssen J.-M., “Lateral-torsional buckling on carbon steel and stainless steel beams with lateral loads plus end moments in case of fire,” in *proceedings of the 6th International Conference on Structures in Fire SiF'10*, 2010.

Chapter 5 Beam-columns

Chapter outline

- 5.1 Introduction
 - 5.2 The code provisions of Part 1-2 of Eurocode 3
 - 5.3 Numerical study
 - 5.3.1 Numeric model
 - 5.3.2 Geometric and material imperfections
 - 5.3.3 Cases studied
 - 5.4 Results
 - 5.4.1 In-plane behaviour
 - 5.4.2 Calibration of in-plane interaction factor
 - 5.4.3 Out-of-plane behaviour
 - 5.4.4 Calibration of out-of-plane interaction factor
 - 5.5 Statistical evaluation
 - 5.6 New proposal according to the developments of this thesis
 - 5.7 Conclusions
- References

Abstract In this chapter, the behaviour of steel beam-columns with Class 4 cross-section is numerically investigated in case of fire. The accuracy of the simplified methods stated in Part 1-2 of Eurocode 3 is analysed and its safety level is determined. More than 6000 numerical simulations have been carried out, considering in-plane and out-of-plane buckling, several member lengths, different temperatures as well as different bending moment diagram and load ratios. Local and global geometrical imperfections as well as residual stresses have been considered in the numerical simulations. It was possible to conclude that the interaction curve of Part 1-2 of Eurocode 3 is inconsistent for the in-plane direction giving both unsafe and very conservative results. For the out-of-plane direction, the interaction curve demonstrated to be very conservative mainly because the reduction factor for the lateral-torsional buckling is too severe for bending diagrams other than that of uniform bending. Regarding the accuracy of the interaction factors predicted by the formulae, modifications are proposed in this work that lead to reduction of the number of unsafe results. Finally, a new proposal for the interaction curve is presented according to the developments in this thesis and its accuracy and validity is demonstrated by comparison to the numerical results.

5.1 Introduction

The structural elements subjected to axial compression and bending are normally designated as beam-columns. For beam-columns at normal temperature, two methods exist in Part 1-1 of the Eurocode 3 [5.1], to evaluate the safety of the members resulting from the work of two different groups in the framework of the European convention for constructional steelwork (ECCS) Technical Committee 8 (TC8 – Stability). The two methods called the “Level 1” and “Level 2” beam-column interaction formulae [5.2–5.4] replaced the beam-column interaction formulae present in the previous ENV version of the Eurocode 3 Part 1-1 [5.5] that proven to be very conservative.

In case of fire, Part 1-2 of the Eurocode 3 [5.6] adopts the same format as the ENV version making the necessary modifications to account for the yield stress and the modulus of elasticity values at high temperatures. The buckling reduction factors for flexural buckling and Lateral Torsional Buckling (LTB) in fire were also included and when LTB is prevented, the beam-column interaction curves are the results from the studies of Talamona et al. [5.7, 5.8]. Numerical studies carried out by Vila Real et al. [5.9, 5.10], Lopes et al. [5.11] and Knobloch et al. [5.12] evaluated the safety and accuracy of the current methods available in the EN1993-1-1 adapted to elevated temperatures for the fire design of beam-columns and concluded that additional changes had to be made in order to use them. Several researches were then conducted to investigate the influence of different parameters on the behaviour of steel beam-columns in fire. Experimental investigations of Kodur and Dwaikat [5.13], conducted on beams that behave as beam-columns due to the compressive forces originated from the thermal restraint allowed to conclude that the fire scenario, load level, degree of end-restraint and high-temperature creep have significant influence on the behaviour of beams under fire conditions. Dwaikat et al. [5.14] investigated beam-columns that develop a thermal gradient through their depth when exposed to fire and conclude that the plastic resistance to combinations of axial load and moment was also affected by the thermal gradients influencing the location of the most critical section. Quiel et al. [5.15] evaluated the adequacy of different methodologies to predict the capacity and response caused by non-uniform thermal gradients through the depth of beam-columns. A simplified approach to predict the axial and moment capacity is made by Dwaikat and Kodur in [5.16] for the cases where a thermal gradient is developed.

However, in these studies, local buckling was not covered. In the numerical investigations beam-finite elements were used which do not capture the plate instability and therefore only Class 1 or 2 cross-sections were analysed. In the experimental investigation, local buckling was out of the scope of the aforementioned studies. Consequently, the behaviour of Class 4 members submitted to combined moment and axial loads has not yet been studied at elevated temperatures and the safety and accuracy of the existing rules of Part 1-2 of Eurocode 3 has not yet been established. It is unclear how the interaction between flexural buckling and lateral torsional buckling together with local buckling affects the load bearing capacity of the members in case of fire.

This chapter presents a numerical study of the behaviour of steel I-shaped Class 4 beam-columns subjected to combined axial and in-plane bending moment under fire conditions. A parametric study at elevated temperatures was done using shell finite elements with the software SAFIR [5.17, 5.18] by performing geometrically and materially nonlinear analyses with imperfections included (GMNIA). Several member lengths, cross-section geometries and different axial and bending moment ratio with and without lateral displacements allowed (restriction to out-of-plane displacements). A comparison of the obtained numerical results and the interaction curves of EN1993-1-2 show that for members with Class 4 cross-sections the existing formulae are safe and conservative. Mainly because the existing design curves for beams and columns with Class 4 cross-sections need to be improved. It is demonstrated that new interaction curves can be used based on the numerical results leading to a safer and economic design of steel I-shaped profiles with Class 4 cross-section at elevated temperatures, on the assumption that the design curves for beams and columns are correctly calibrated.

5.2 The code provisions of Part 1-2 of Eurocode 3

According to Part 1-2 of EC3 [5.6], the design buckling resistance at time t for a member without lateral restraints and with a Class 4 cross section subject to combined bending and axial compression in fire situation should be verified by satisfying the interaction curve defined by equations (5.1a) and (5.1b) for doubly symmetric cross-sections. These are the equations (4.21c) and (4.21d) respectively of Part 1-2 of EC3 adapted for Class 4, i.e., considering the effective cross-sectional properties.

$$\frac{N_{fi,Ed}}{\chi_{\min,fi} A_{eff} k_{0.2p,\theta} \frac{f_y}{\gamma_{M,fi}}} + \frac{k_y M_{y,fi,Ed}}{W_{eff,y,\min} k_{0.2p,\theta} \frac{f_y}{\gamma_{M,fi}}} + \frac{k_z M_{z,fi,Ed}}{W_{eff,z,\min} k_{0.2p,\theta} \frac{f_y}{\gamma_{M,fi}}} \leq 1 \quad (5.1a)$$

$$\frac{N_{fi,Ed}}{\chi_{z,fi} A_{eff} k_{0.2p,\theta} \frac{f_y}{\gamma_{M,fi}}} + \frac{k_{LT} M_{y,fi,Ed}}{\chi_{LT,fi} W_{eff,y,\min} k_{0.2p,\theta} \frac{f_y}{\gamma_{M,fi}}} + \frac{k_z M_{z,fi,Ed}}{W_{eff,z,\min} k_{0.2p,\theta} \frac{f_y}{\gamma_{M,fi}}} \leq 1 \quad (5.1b)$$

with $N_{fi,Ed}$, $M_{y,fi,Ed}$ and $M_{z,fi,Ed}$ the design axial force, design bending moment about y-axis and z-axis respectively for fire situation; A_{eff} , $W_{eff,y,\min}$ and $W_{eff,z,\min}$ are respectively the effective area of the cross-section and the effective section modulus for y-axis and z-axis, $k_{0.2p,\theta}$ is the reduction factor for the 0.2% proof strength of steel at elevated temperatures, f_y is the steel yield strength and $\gamma_{M,fi}$ is the partial safety factor for fire situation. $\chi_{\min,fi}$ is the minimum reduction factor of the y-axis ($\chi_{y,fi}$) and z-axis ($\chi_{z,fi}$) for flexural buckling in the fire design situation and $\chi_{LT,fi}$ is the reduction factor for the lateral-torsional buckling in fire design situation. The interaction factors are defined according to equations (5.2) and (5.4), as following

$$k_y = 1 - \frac{\mu_y N_{fi,Ed}}{\chi_{y,fi} A_{eff} k_{0.2p,\theta} \frac{f_y}{\gamma_{M,fi}}} \leq 3 \quad (5.2)$$

and

$$\mu_y = (2\beta_{M,y} - 5)\bar{\lambda}_{y,\theta} + 0.44\beta_{M,y} + 0.29 \leq 0.8 \text{ but } \bar{\lambda}_{y,20^\circ\text{C}} \leq 1.1 \quad (5.3)$$

while

$$k_{LT} = 1 - \frac{\mu_{LT} N_{fi,Ed}}{\chi_{z,fi} A_{eff} k_{0.2p,\theta} \frac{f_y}{\gamma_{M,fi}}} \leq 1 \quad (5.4)$$

and

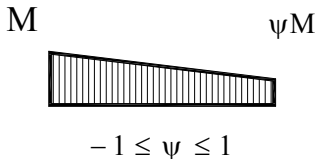

$$\mu_{LT} = 0.15\bar{\lambda}_{z,\theta} \beta_{M,LT} - 0.15 \leq 0.9 \quad (5.5)$$

The equivalent uniform moment factors $\beta_{M,LT}$ and $\beta_{M,y}$ are evaluated using the bending diagram corresponding to the major-axis - $M_{y,fi,Ed}$ and for the cases studied in this chapter are given in Table 5.1. In the previous equations $\bar{\lambda}_{y,\theta}$ and $\bar{\lambda}_{z,\theta}$ are the column non-dimensional slenderness of the y- and z-axis respectively for flexural buckling at elevated temperature, given by

$$\bar{\lambda}_{\theta} = \bar{\lambda} \sqrt{\frac{k_{0.2p,\theta}}{k_{E,\theta}}} \quad (5.6)$$

with $\bar{\lambda}$ the non-dimensional slenderness for flexural buckling at room temperature and $k_{E,\theta}$ the reduction factor for the slope of the linear elastic range at elevated temperature.

Table 5.1: Equivalent uniform moment factor for the cases studied.

Moment distribution	Equivalent uniform moment factor β_M
 <p style="text-align: center;">$-1 \leq \psi \leq 1$</p>	$\beta_M = 1.8 - 0.7\psi$
	$\beta_M = 1.3$

The type of cross-sections analysed in this work are normally submitted to in-plane loading and therefore only bending about the major-axis were considered, thus the terms related to the minor-axis (z) were disregarded.

5.3 Numerical study

A numerical investigation on the behaviour of members submitted to combined bending and axial compression was performed with the finite element method using the software SAFIR [5.17] in case of fire. Next, the used numerical model is described. In 5.3.2 the

geometric and material imperfections used are referred and in 5.3.3 the cases that have been studied are presented.

5.3.1 Numeric model

The beam-columns were discretized into several quadrangular shell elements with four nodes with six degrees of freedom (3 translations and 3 rotations) each. In SAFIR, these shell elements adopt the Kirchoff's theory formulation with a total co-rotational description. The material law is a two-dimensional constitutive relation with the von Mises yield surface. The integration on the shell element follows a Gauss scheme with 2×2 points on the surface and 4 points through the thickness. Since shell elements are used, the root fillet of the cross-sections has been disregarded in all the models. The shell finite element used in SAFIR and its ability to model local buckling has been validated by Talamona and Franssen [5.19, 5.20].

After a sensitivity analysis a mesh with 10 shell elements for the flange, 22 shell elements for the web and 100 shell elements along the length has been used. For the beam-columns with a span higher than 10 m the divisions on the length were doubled. The loads were applied to the model by means of nodal forces and to prevent numerical problems end-plates have been used. The so-called "fork-support" conditions have been considered in the model by restraining vertical displacements of the bottom flange and the out-of-the plane horizontal displacements of the web in the extremities of the beam as well as the rotation about the beam axis.

5.3.2 Geometric and material imperfections

The geometric imperfections have been introduced in the model by changing the node coordinates to represent the worst scenario for the assessment of beam-column resistance. This has been considered as the shape given by the eigenmodes of a linear buckling analysis (LBA) performed with the software Cast3M [5.21]. A tool was written in order to automate this process resulting in the software RUBY [5.22]. In accordance with the finite element method of analysis recommendations given in the Annex C of EN1993-1-5 [5.23], a combination of global and local modes (see Figure 5.1) has been used, where the lower mode has been taken as the leading imperfection and the other one reduced to 70%. The amplitude of the imperfections has been chosen as 80% of the fabrication tolerances given in the

EN1090-2 [5.24], as suggested in the same annex [5.23]. Consequently, the global mode has been scaled to 80% of $L/750$ and the local mode has been scaled either to 80% of $b/100$ if the maximum node displacement (in respect to the local mode) occurs in the flange or to 80% of $h_w/100$ if the maximum node displacement occurs in the web, whereas b is the flange width and h_w is the height of the web of the cross-section.

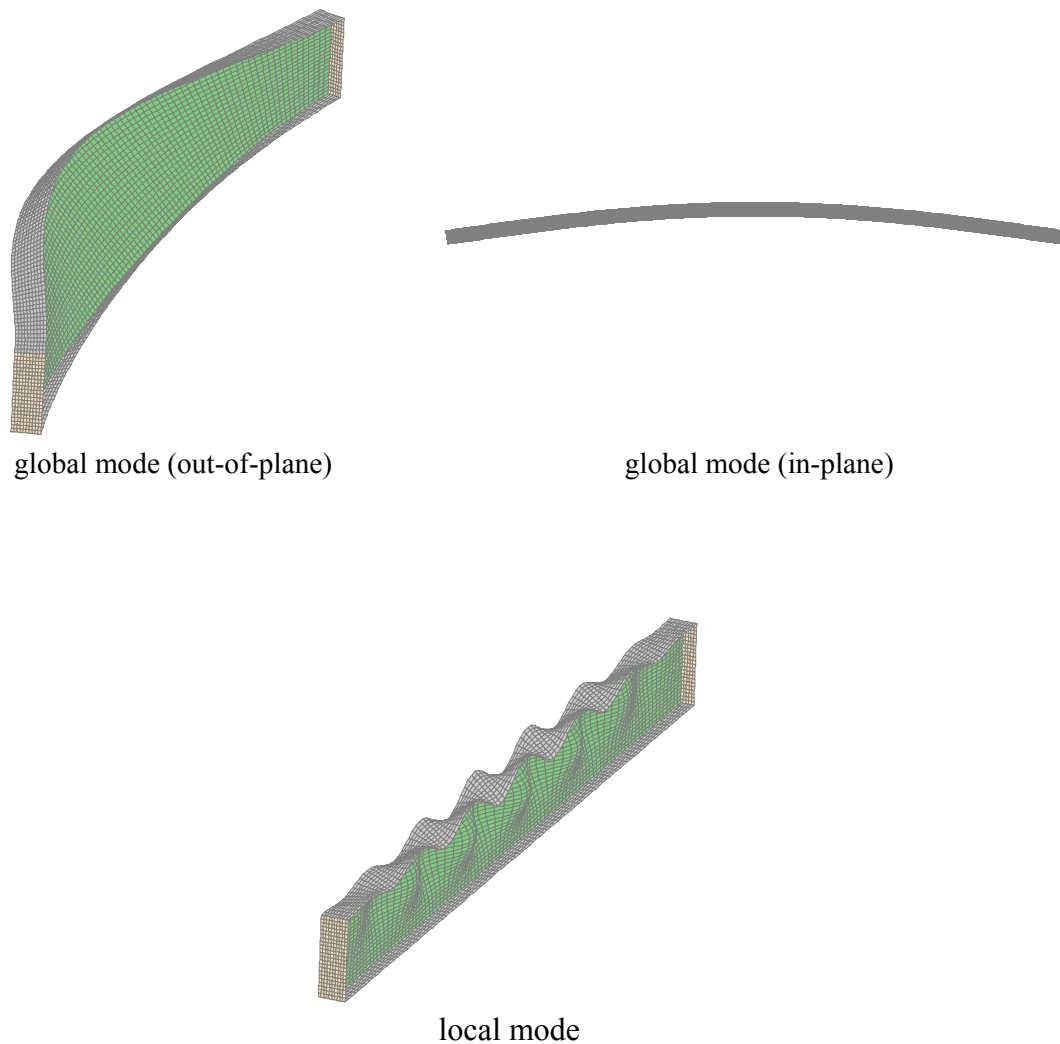


Figure 5.1: Buckling modes in a laterally unrestrained steel beam-column with Class 4 cross-section subjected to in-plane bending moment.

At elevated temperature, the effect of the residual stresses is small [5.25, 5.26]. In this study, only the residual stress diagram [5.27] that corresponds to welded cross-sections has been

used as depicted in Figure 4.4. The values adopted for the residual stresses are according to [5.27, 5.28] as used in a previous study [5.29].

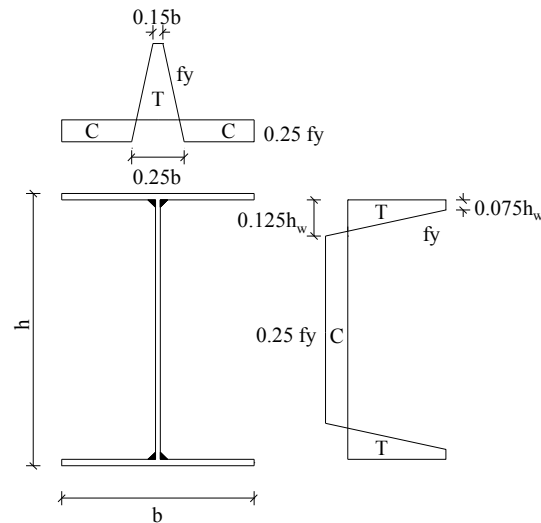






Figure 5.2: Pattern of the residual stresses considered in this study for welded profiles.

5.3.3 Cases studied

Different Class 4 cross-sections, member lengths, temperatures and ratios between the applied axial compression and bending moment were considered as shown in Table 5.2. The steel grade considered was the S355. The temperature was considered constant in the cross-section and along the member to allow direct comparison with the simplified methods of the Part 1-2 of Eurocode 3. Different moment distribution was also considered, with end-moments and distributed load. Two directions of buckling have been considered, the minor-axis buckling was considered as out-of-plane buckling and the buckling in the major-axis was considered as in-plane buckling. Since in the studied cases the web was slender (Class 4), it was not possible to study the common case corresponding to a point load applied at mid-span due to web-buckling and other local phenomena that was observed prior to global instability and being out of the scope of this research programme. The same was observed regarding the location of the application of the distributed load and it was only possible to investigate the case corresponding to the load applied in the lower flange. To study the other cases stiffeners to avoid local buckling would be needed and it was out of the scope of this study.

Table 5.2: Summary of the cases analysed (steel grade S355).

Cross-section ($h_w \times t_w + b \times t_f$) (mm)	Non-dimensional slenderness	Load ratios β (*)	Moment distribution	Temperature θ_a (°C)
450×4+150×5	$\bar{\lambda}_{y,\theta} = \{0.5, 1.0, 1.5\}$ $\bar{\lambda}_{z,\theta} = \{0.5, 1.0, 1.5, 2.25\}$	0.2; 0.4; 0.6; 0.8; (plus only axial force and only bending moment)**	$\psi = 1$ 	350, 450, 550, 650
450×4+150×7			$\psi = 0$ 	
450×4+150×10			$\psi = -1$ 	
450×4+250×5				
450×4+250×6				
450×4+250×12				
450×5+250×16				
1000×5+300×10				
1000×5+300×15				
1000×7+300×12				
1000×8+300×20				

* The ratio between the applied loads was defined as $N_{fi,Ed} / M_{y,fi,Ed} = (1 - \beta) / (\beta M_{y,fi,Rd} / N_{fi,Rd})$

** For the in-plane cases (bending about y-y), an additional ratio of 0.9 was also considered.

5.4 Results

Comparison between the results obtained numerically and using the predicted capacity of the interaction curves in equations (5.1a) and (5.1b) are presented here. Throughout this study, the values for the axial compression resistance $N_{fi,Rd}$ and the bending resistance about the major-axis $M_{y,fi,Rd}$ were obtained numerically with SAFIR. This procedure avoids the error associated with the determination of the cross-sectional resistance of Class 4 sections using simplified methods as demonstrated in Chapter 3 [5.30].

5.4.1 In-plane behaviour

The in-plane behaviour of the beam-columns is investigated numerically by considering the model described in 5.3.1 but restraining the out-of-plane (lateral) displacements by imposing the additional restraints in the flanges as depicted in Figure 5.3.

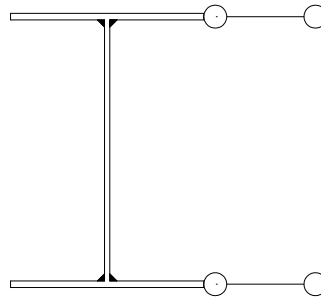


Figure 5.3: Additional lateral restraints added to the model to prevent the out-of-plane displacements.

equation (5.1a) was then employed considering the ultimate axial force and uniform bending moment given in SAFIR as the design loads. Results are plotted in Figure 5.4 against the non-dimensional slenderness $\bar{\lambda}_{y,\theta}$ and in Figure 5.5 against the ratio between the applied bending moment and the cross-sectional bending resistance $M / M_{y,f,Rd}$. In these figures, the line corresponding to the value 1 in the vertical axis defines the interaction curve. If the points, which represent the numerical results, are below the line it means the ultimate loads obtained numerically are below those predicted by equation (5.1a) and therefore are unsafe and safe otherwise.

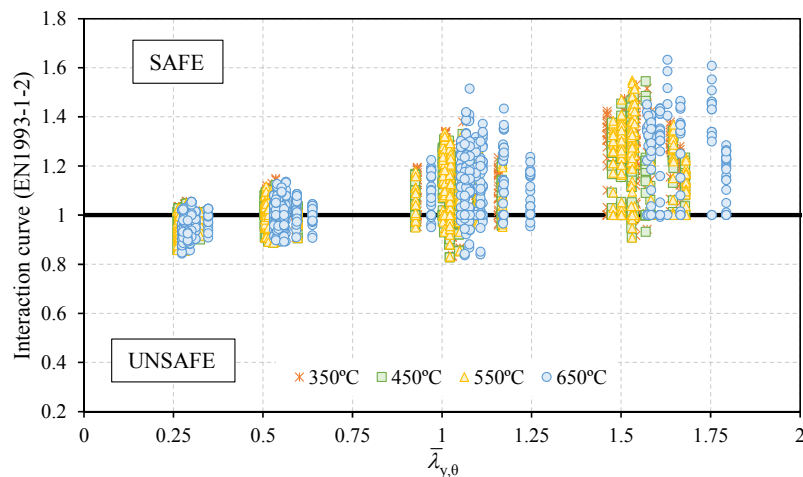


Figure 5.4: Comparison of interaction curve and the numerical cases studied for the in-plane behaviour in terms of non-dimensional slenderness.

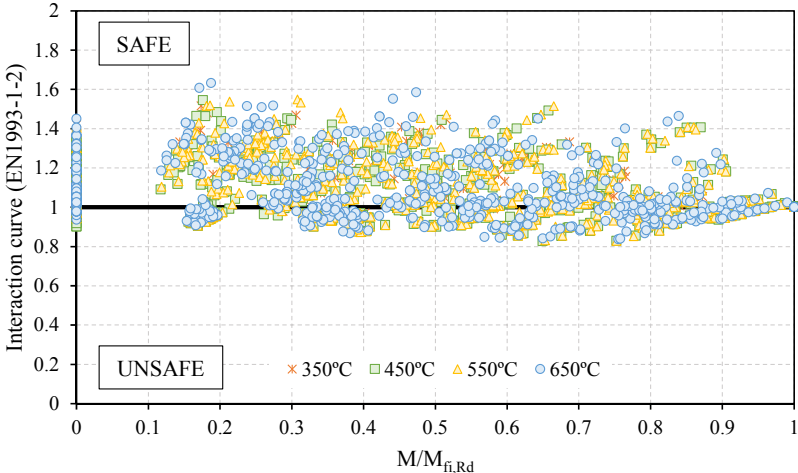


Figure 5.5: Comparison of interaction curve and the numerical cases studied for the in-plane behaviour in terms of the applied bending moment.

It is observed that the results are inconsistent with both unsafe and very conservative results obtained. Two reasons for this are pointed out: i) the reduction factor for the in-plane column buckling $\chi_{y,fi}$ calculated according to EN1993-1-2 demonstrates to be too severe for some cases and unsafe for others (see Figure 5.6) and ii) the interaction factor k_y calculated according to equation (5.2) depends on the factor μ_y calculated with equation (5.3) that gives unsafe results for the bi-triangular bending diagram ($\psi = -1$) as later shown in section 5.4.2.

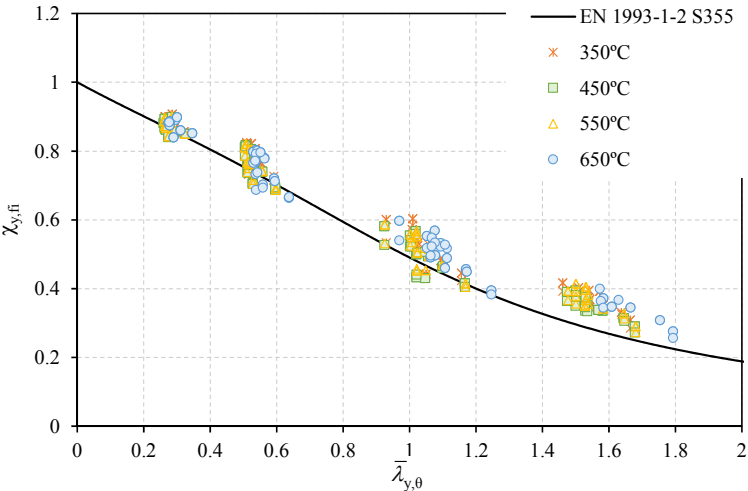


Figure 5.6: Comparison of the reduction factor for the column behaviour obtained numerically and according to EN1993-1-2.

To investigate the accuracy of the interaction curve but not considering the differences related to the calculation of reduction factors using the formulae from EN 1993-1-2, these reduction factors were determined numerically as

$$\chi_{y,fi} = \frac{N_{SAFIR,in-plane}}{N_{fi,Rd,SAFIR,CS}} \quad (5.7)$$

where $N_{SAFIR,in-plane}$ is the axial compression load at collapse for the in-plane direction of the member submitted only to an axial load and $N_{fi,Rd,SAFIR,CS}$ is the cross-sectional resistance obtained numerically with SAFIR (as in Chapter 3). The interaction curve with the reduction factor calculated with equation (5.7) is referred as “EN 1993-1-2 calibrated” later in Figures 5.9 – 5.11. By doing so, this curve corresponds to a theoretically interaction curve without the uncertainties associated with the cross-sectional resistance (see Chapter 3) and also without the uncertainties associated with the reduction factor for the flexural buckling according to 1.2 of Eurocode 3. Following this methodology, the safety level of the existing interaction factors used in equation (5.1a) are investigated. Figure 5.7 shows the comparison of the numerical results and the interaction curve defined in equation (5.1a) and calculating the reduction factor according to equation (5.7) and using, as the resistance moment of the cross-section, the corresponding value calculated with SAFIR.

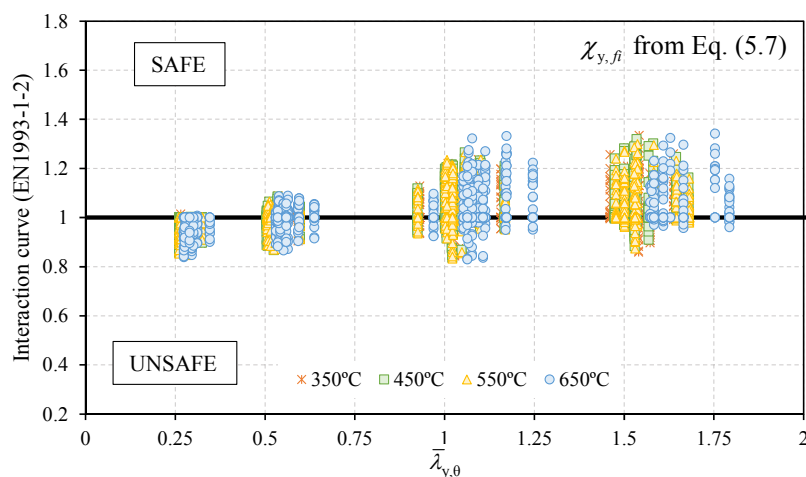


Figure 5.7: Comparison of interaction curves and the numerical cases studied.

5.4.2 Calibration of in-plane interaction factor

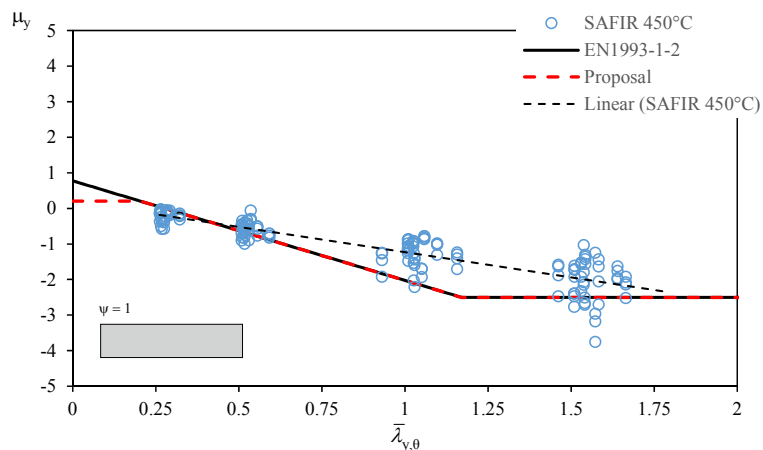
In order to reduce the number of unsafe results, the factor μ_y was calibrated following the same methodology adopted in [5.7]. According to the procedure adopted by Talamona, the following expression can be used to extract from each numerical simulation the value of μ_y , that fulfils equation (5.1a).

$$\mu_y = \frac{(M_{y,fi,Rd,SAFIR,CS} \cdot N_{SAFIR} - \chi_{y,fi} \cdot N_{fi,Rd,SAFIR,CS} \cdot M_{y,fi,Rd,SAFIR,CS} + \chi_{y,fi} \cdot N_{fi,Rd,SAFIR,CS} \cdot M_{SAFIR})}{N_{SAFIR} \cdot M_{SAFIR}} \quad (5.8)$$

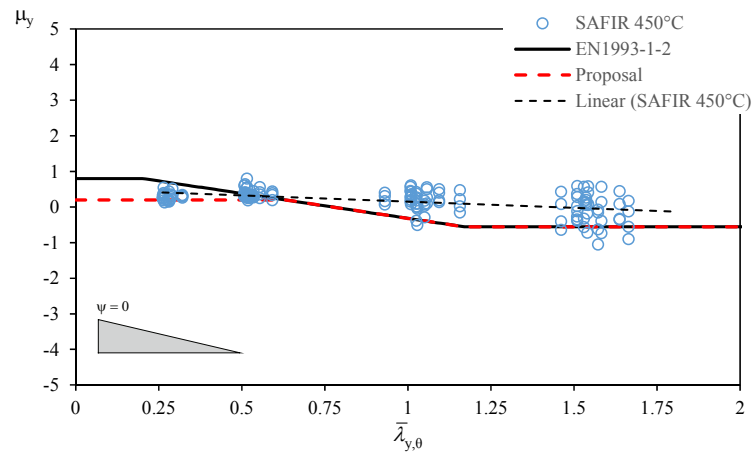
where $N_{fi,Rd,SAFIR,CS}$ and $M_{y,fi,Rd,SAFIR,CS}$ are respectively the numerical axial and moment resistance obtained with SAFIR and N_{SAFIR} and M_{SAFIR} are the ultimate axial load and moment given by SAFIR at collapse.

Figure 5.8 shows for a temperature of 450°C the evolution of μ_y as a function of the non-dimensional slenderness $\bar{\lambda}_{y,\theta}$ with the proposed modifications given by equation (5.9) denoted “Proposal”. “Linear (SAFIR 450°C)” denotes the linear trend line of the numerical results.

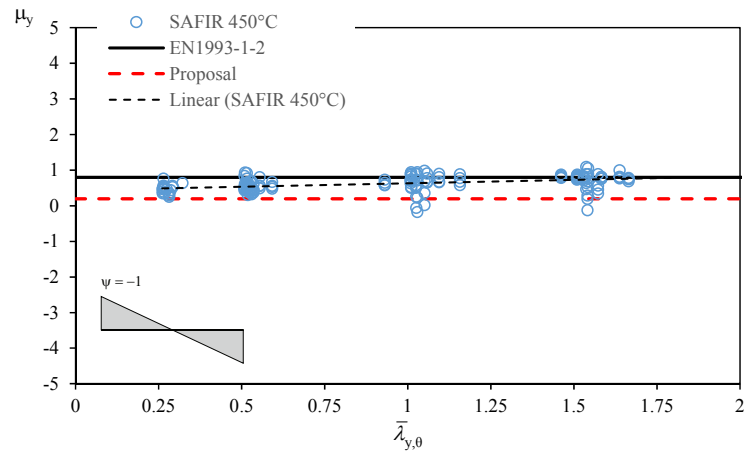
$$\mu_{y,proposal} = (2\beta_{M,y} - 5)\bar{\lambda}_{y,\theta} + 0.44\beta_{M,y} + 0.29 \leq 0.2 \text{ but } \bar{\lambda}_{y,20^\circ\text{C}} \leq 1.1 \quad (5.9)$$



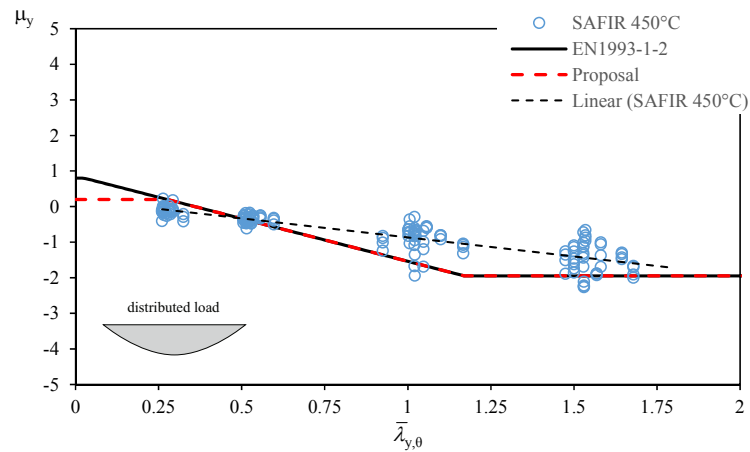
a) Uniform bending moment



b) Triangular bending moment



c) Bi-triangular bending moment



d) Distributed load

Figure 5.8: Calibration of the factor μ_y for the in-plane behaviour of beam-columns considering different loading cases at 450°C.

By using equation (5.9) instead of equation (5.3), a limit value of 0.2 is introduced that changes the response obtained especially for the beam-columns subjected to bi-triangular bending moment ($\psi = -1$) (see Figure 5.8c).

In Figure 5.9, results are shown for one beam-column, for different temperatures and the different procedures for the interaction curve including the one using μ_y given in equation (5.9) which is referred as “Eq. (5.1a) with $\mu_y = \text{new}$ ”. In Figure 5.10, the results for the same beam-column submitted to different moment distribution and considering a temperature of 450°C.

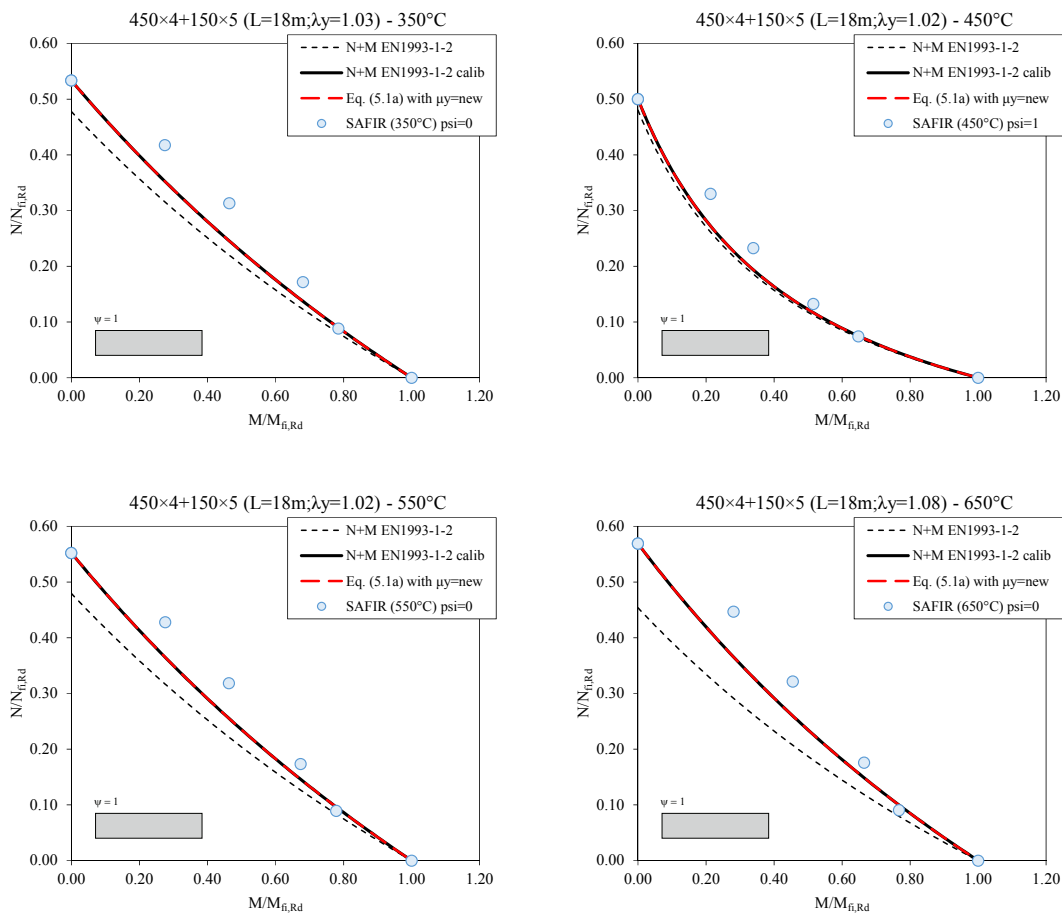


Figure 5.9: Interaction curves for a beam-column with $L=18\text{m}$ ($\bar{\lambda}_{y,\theta} \approx 1.0$) and cross-section $1450 \times 4 + 150 \times 5$ at elevated temperatures.

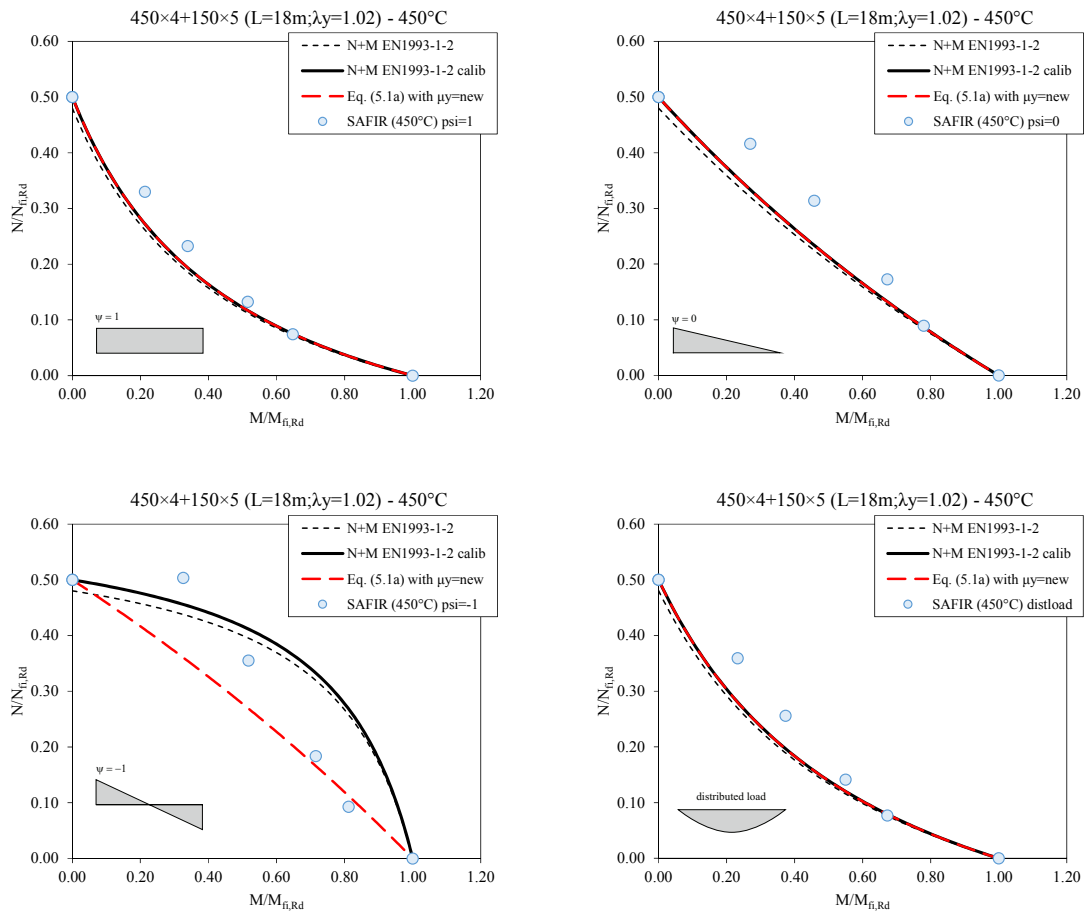


Figure 5.10: Interaction curves for different moment distribution for in-plane buckling.

It is demonstrated the improvements made with the proposed modification for the bi-triangular bending diagram ($\psi = -1$) in Figure 5.11.

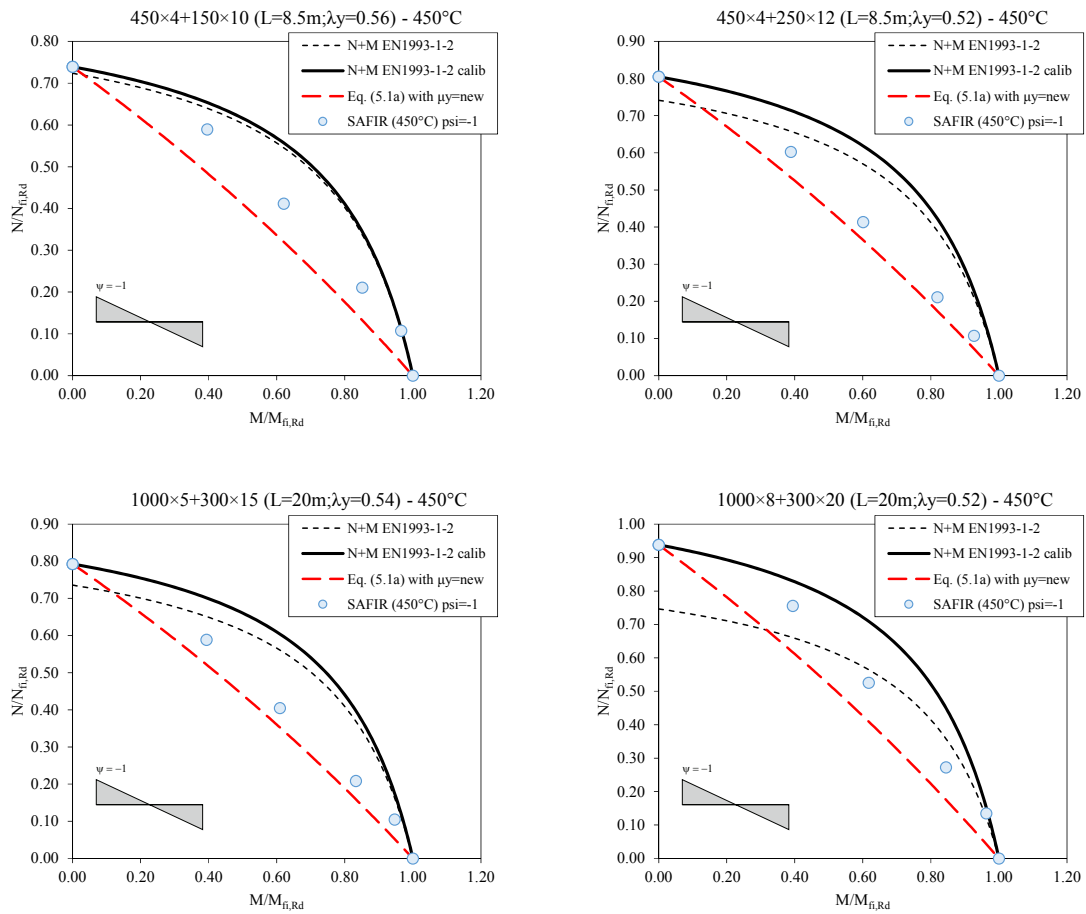


Figure 5.11: Improvement of the in-plane interaction curve for the bi-triangular cases.

In Figure 5.12, all the in-plane numerical results are plotted and compared with equation (5.1a) using μ_y from equation (5.9).

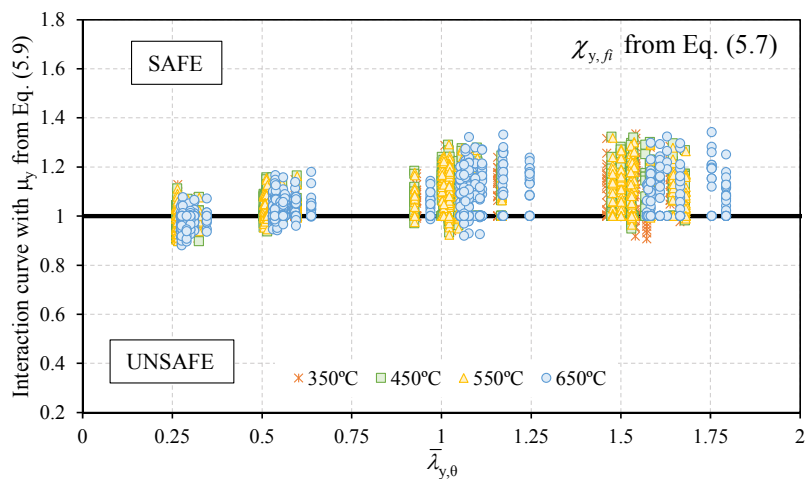


Figure 5.12: Comparison of interaction curves and the numerical cases studied considering μ_y from equation (5.9).

Some improvements are observed with less unsafe results while the same level of accuracy was maintained for the remaining results (see Section 5.5).

5.4.3 Out-of-plane behaviour

The out-of-plane behaviour of the beam-columns was investigated. Equation (5.1b) was used considering the ultimate axial load and bending moment given by SAFIR as the design loads. Results are plotted in Figure 5.13 against the non-dimensional slenderness $\bar{\lambda}_{z,\theta}$ and in Figure 5.14 against the ratio between the applied bending moment and the cross-sectional bending resistance $M / M_{y,fi,Rd}$. In these figures, the horizontal line at the value 1 in the vertical axis defines the interaction curve. If the points that represent the numerical results are below the line it means the ultimate loads obtained numerically are below those predicted by equation (5.1b) and therefore are unsafe or safe otherwise.

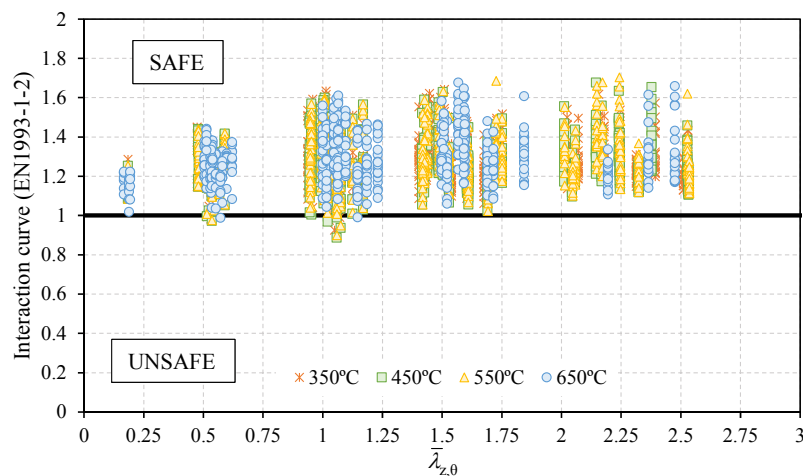


Figure 5.13: Comparison of interaction curve and the numerical cases studied for the out-of-plane behaviour in terms of non-dimensional slenderness.

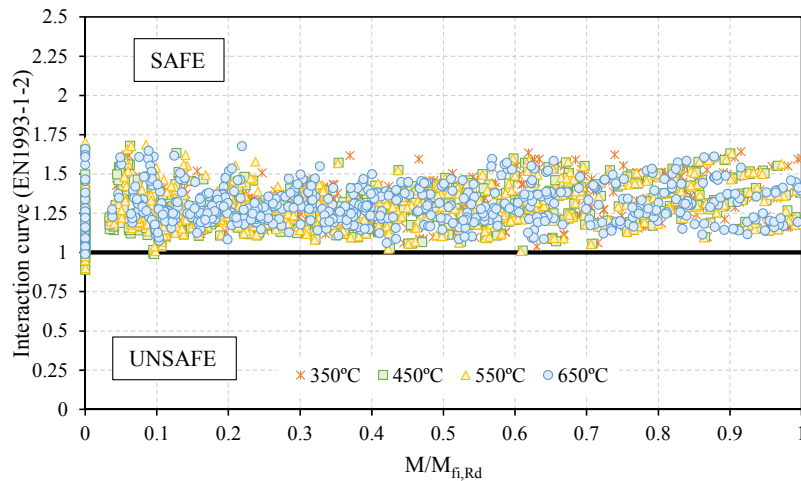


Figure 5.14: Comparison of interaction curve and the numerical cases studied for the out-of-plane behaviour in terms of the applied bending moment.

From Figures 5.13-5.14, it can be seen that the existing curve of Part 1-2 of EC3 for members with combined uniform bending moment and axial compression is very conservative, but this is mainly because the design curves for columns and beams are conservative. Figure 5.15 shows the comparison between the numerical results for members only submitted to axial compression and the column design curve of the EN 1993-1-2, where this is observed. Figure 5.16 shows the same comparison but for members submitted to bending in the major axis without any lateral restraints and the EN 1993-1-2 beam design curve. As shown in the previous chapter, the design curve of EN 1993-1-2 is much safe sided especially for triangular ($\psi = 0$) and bi-triangular ($\psi = -1$) cases.

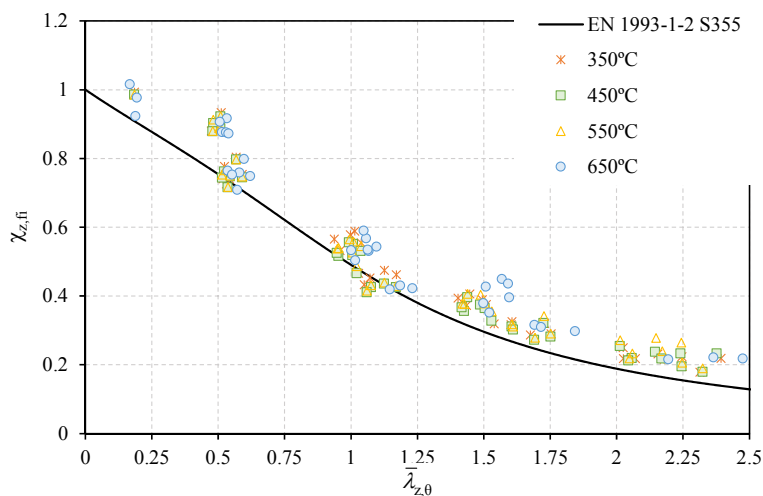


Figure 5.15: Comparison of the numerical results with the reduction factor for flexural buckling about the minor-axis.

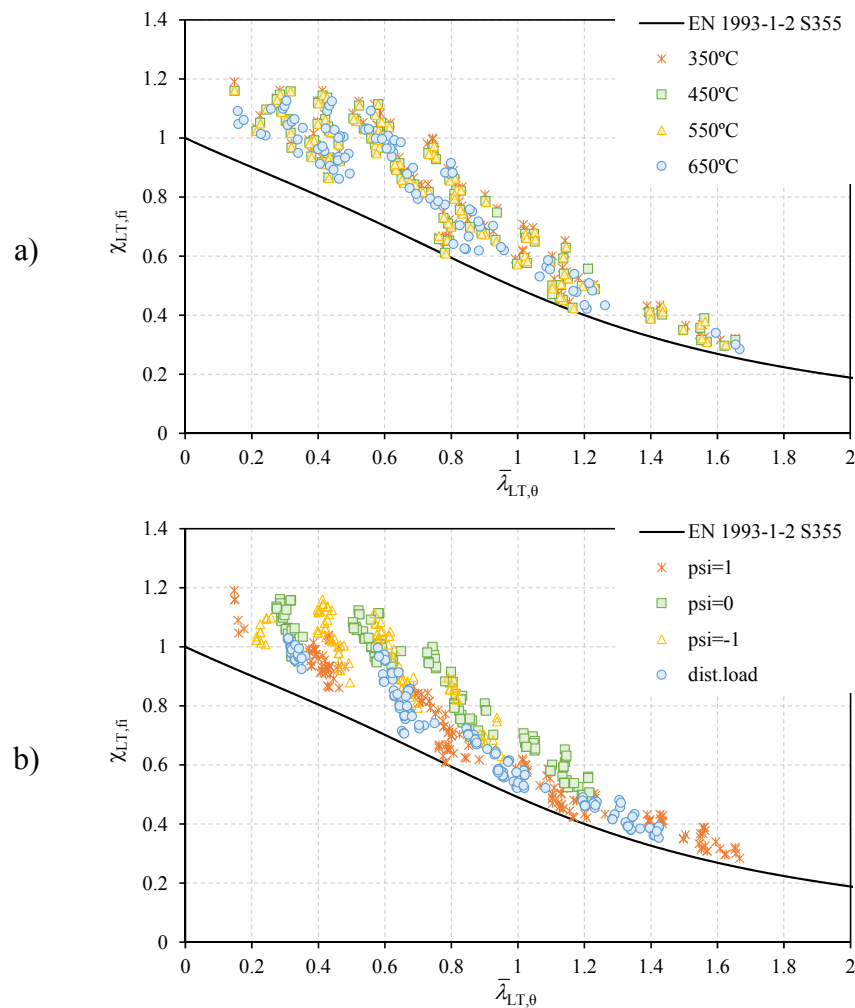


Figure 5.16: Comparison of the numerical results with the reduction factor for lateral-torsional buckling a) function of the temperature and b) function of the moment distribution.

As done for the in-plane direction (see section 5.4.1), the reduction factor for the flexural buckling in the minor-axis was numerically calculated as

$$\chi_{z,fi} = \frac{N_{SAFIR,out-of-plane}}{N_{fi,Rd,SAFIR,CS}} \quad (5.10)$$

where $N_{SAFIR,out-of-plane}$ is the axial compression load at collapse for the out-of-plane direction of the member submitted only to axial force and $N_{fi,Rd,SAFIR,CS}$ is the cross-sectional resistance obtained numerically with SAFIR. The reduction factor for lateral-torsional buckling, $\chi_{LT,fi}$, was calculated for the element submitted only to bending in the major axis, as

$$\chi_{LT,fi} = \frac{M_{SAFIR}}{M_{y,fi,Rd,SAFIR,CS}} \quad (5.11)$$

where M_{SAFIR} is the corresponding bending moment at the collapse of the member submitted only to bending moments and $M_{y,fi,Rd,SAFIR,CS}$ is the cross-sectional resistance calculated numerically with SAFIR. The interaction curve considering these reduction factors is referred as “EN 1993-1-2 calibrated” and corresponds to a theoretical interaction curve without the errors associated to the cross-sectional resistance and reduction factors calculated with the formulae provided by Part 1-2 of Eurocode 3. Following this methodology, the safety level of the existing interaction curve defined by equation (5.1b) is investigated by comparison to the numerical results obtained, as depicted in Figure 5.17.

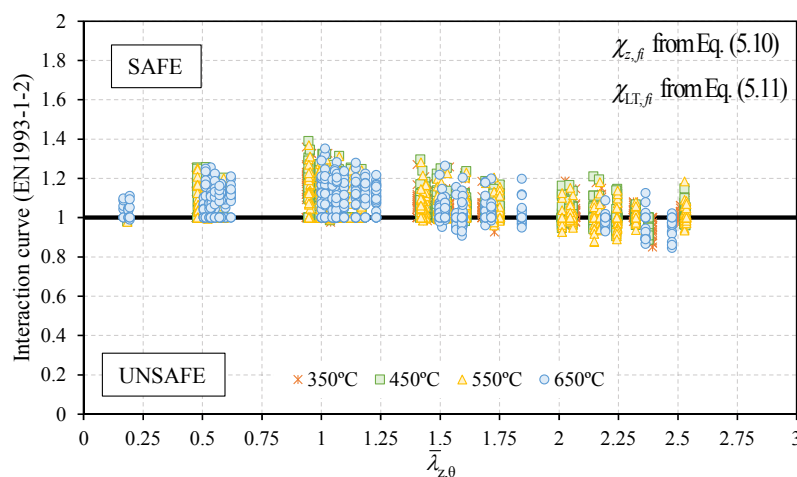


Figure 5.17: Comparison of interaction curves and the numerical cases studied with reduction factors according to equations (5.10) and (5.11).

It is observed that the interaction curve is slightly in the unsafe side (see the statistical evaluation on Section 5.5) for higher values of the non-dimensional slenderness. In the next section, modification to the current interaction factors is proposed in order to correct this deviation.

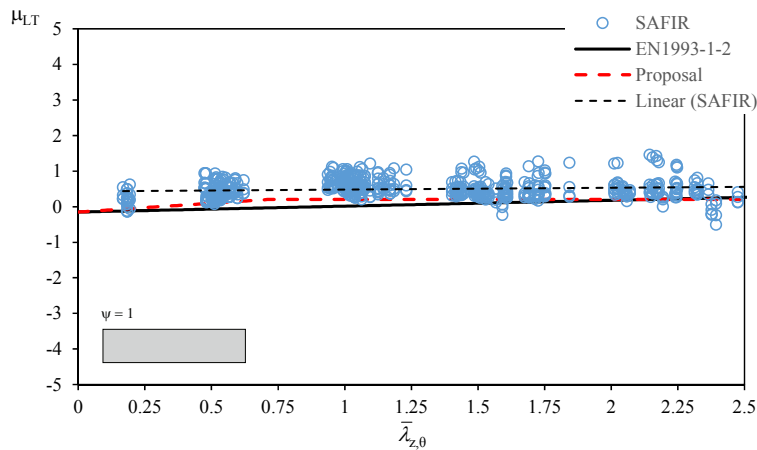
5.4.4 Calibration of out-of-plane interaction factor

Using the same methodology as done in Section 5.4.2, the following expression can be used to extract from each numerical simulation the value of μ_{LT} , that fulfils equation (5.1b).

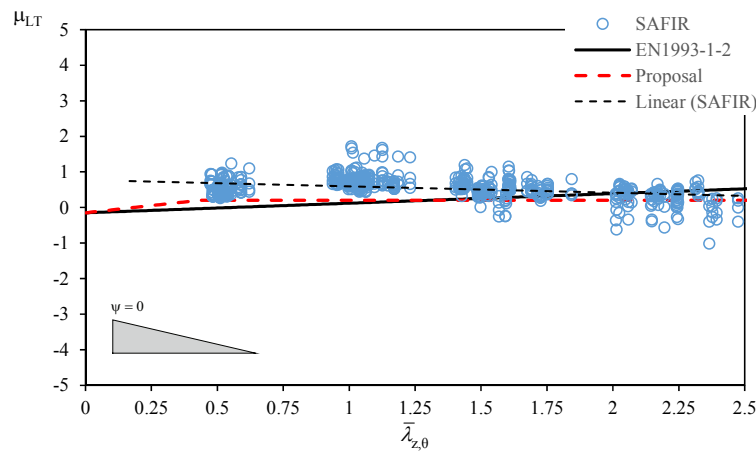
$$\mu_{LT} = (M_{SAFIR} \cdot N_{f_i, Rd, SAFIR, CS} \cdot \chi_{z, f_i} + M_{y, f_i, Rd, SAFIR, CS} \cdot N_{SAFIR} \cdot \chi_{LT, f_i} - M_{y, f_i, Rd, SAFIR, CS} \cdot N_{f_i, Rd, SAFIR, CS} \cdot \chi_{z, f_i} \cdot \chi_{LT, f_i}) \cdot \frac{1}{(M_{SAFIR} \cdot N_{SAFIR})} \quad (5.12)$$

Figure 5.18 shows the evolution of μ_{LT} as a function of the non-dimensional slenderness $\bar{\lambda}_{z, \theta}$ with the proposed modifications given by equation (5.13) denoted “Proposal” for different temperatures. In this figure, “Linear (SAFIR)” refers to the linear trend line of the numerical results.

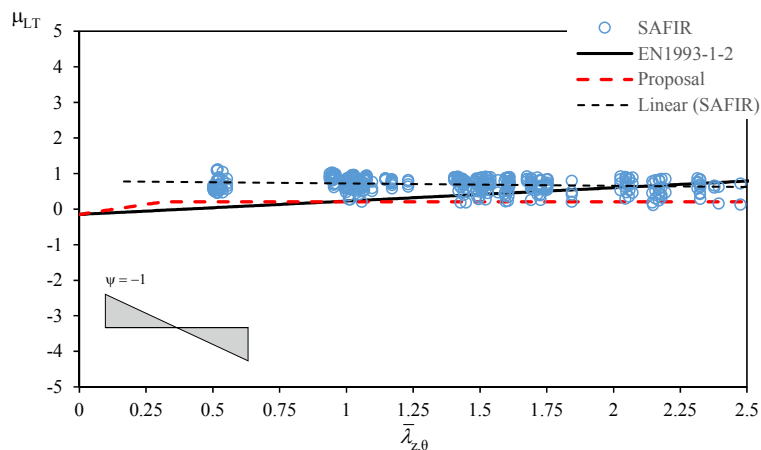
$$\mu_{LT, proposal} = 0.45 \bar{\lambda}_{z, \theta} \beta_{M, LT} - 0.15 \leq 0.2 \quad (5.13)$$



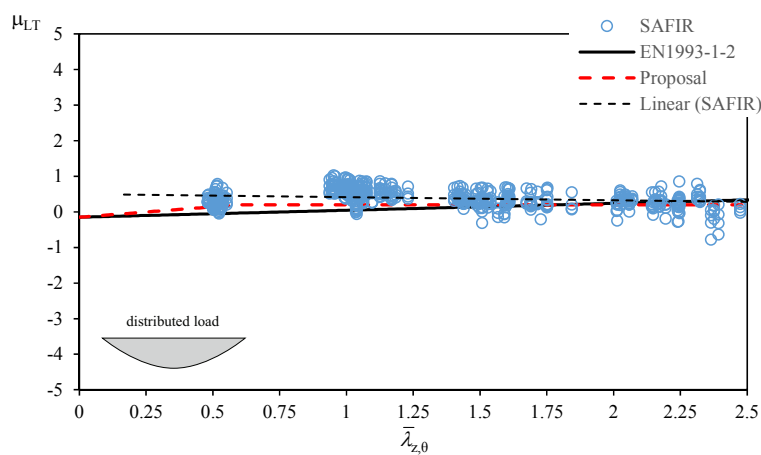
a) Uniform bending moment



b) Triangular bending moment



c) Bi-triangular bending moment



d) Distributed load

Figure 5.18: Calibration of the factor μ_{LT} for the out-of-plane behaviour of beam-columns considering different loading cases for different temperatures.

In Figure 5.19, results are shown for one beam-column and for different temperatures comparing the different procedures studied in this work for the interaction curve including the one using μ_{LT} given in equation (5.13) referred as “Eq. (5.1b) with $\mu_{LT} = \text{new}$ ”. In Figure 5.20, the same comparison is shown considering different moment distribution.

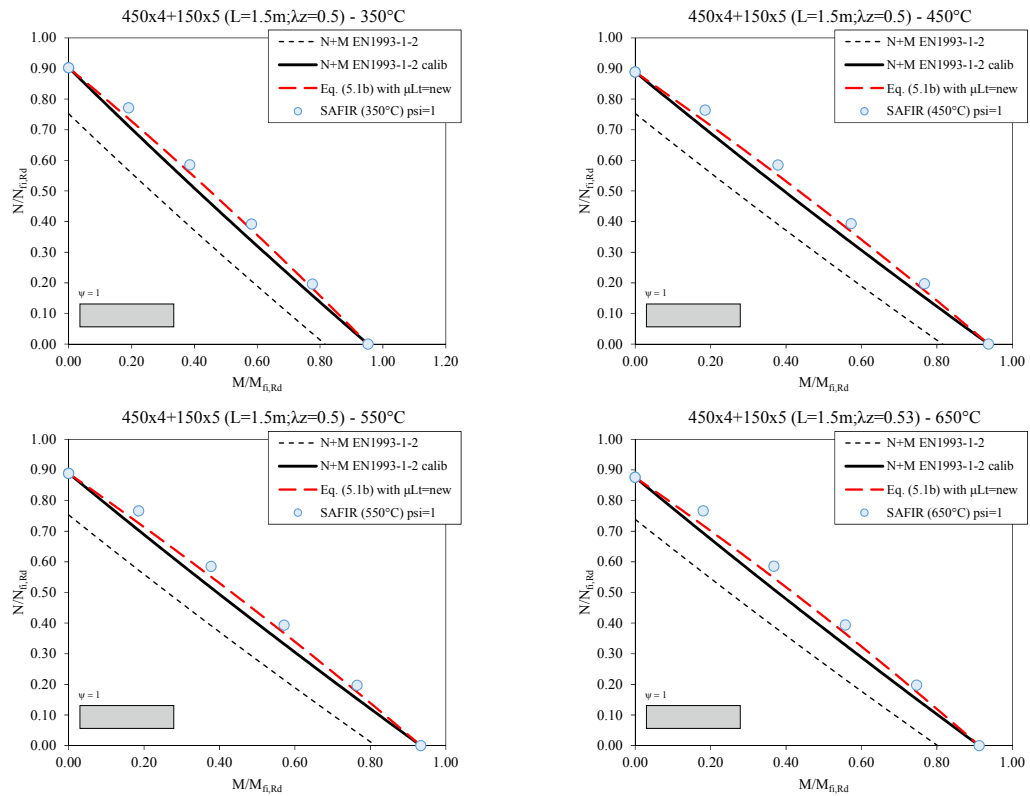


Figure 5.19: Interaction curves for a beam-column with $L=1.5\text{m}$ ($\bar{\lambda}_{z,\theta} \approx 0.50$) and cross-section I450×4+150×5 at elevated temperatures.

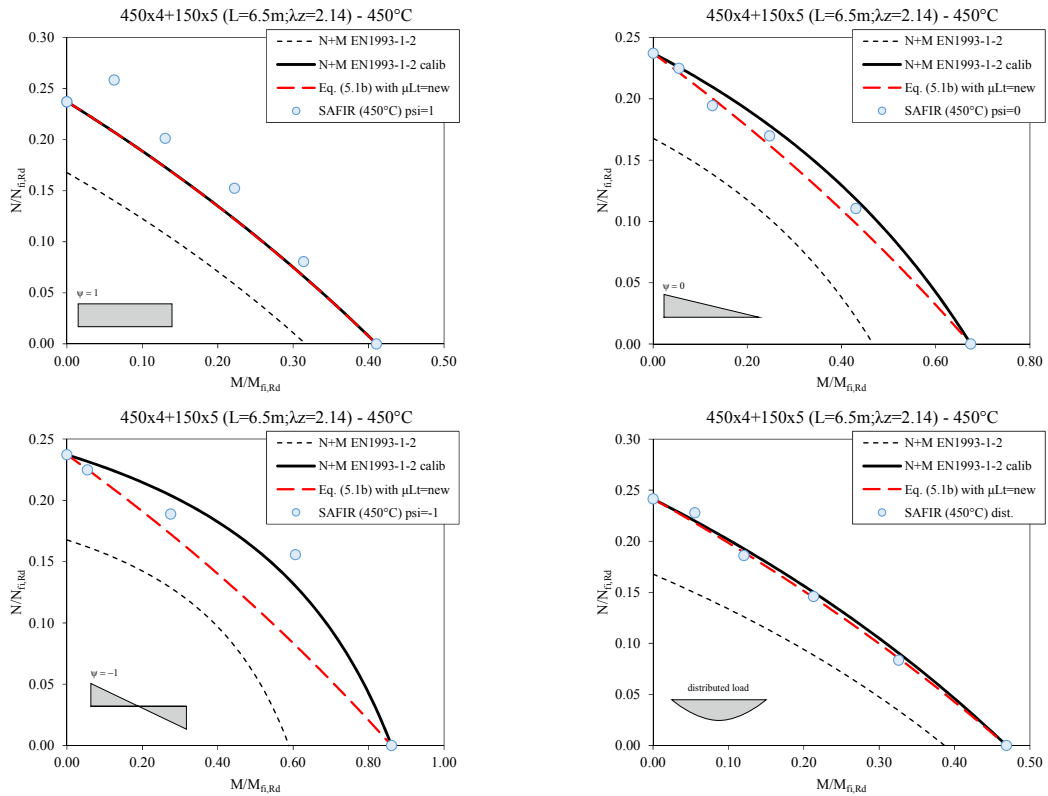


Figure 5.20: Interaction curves for different moment distribution for out-of-plane buckling.

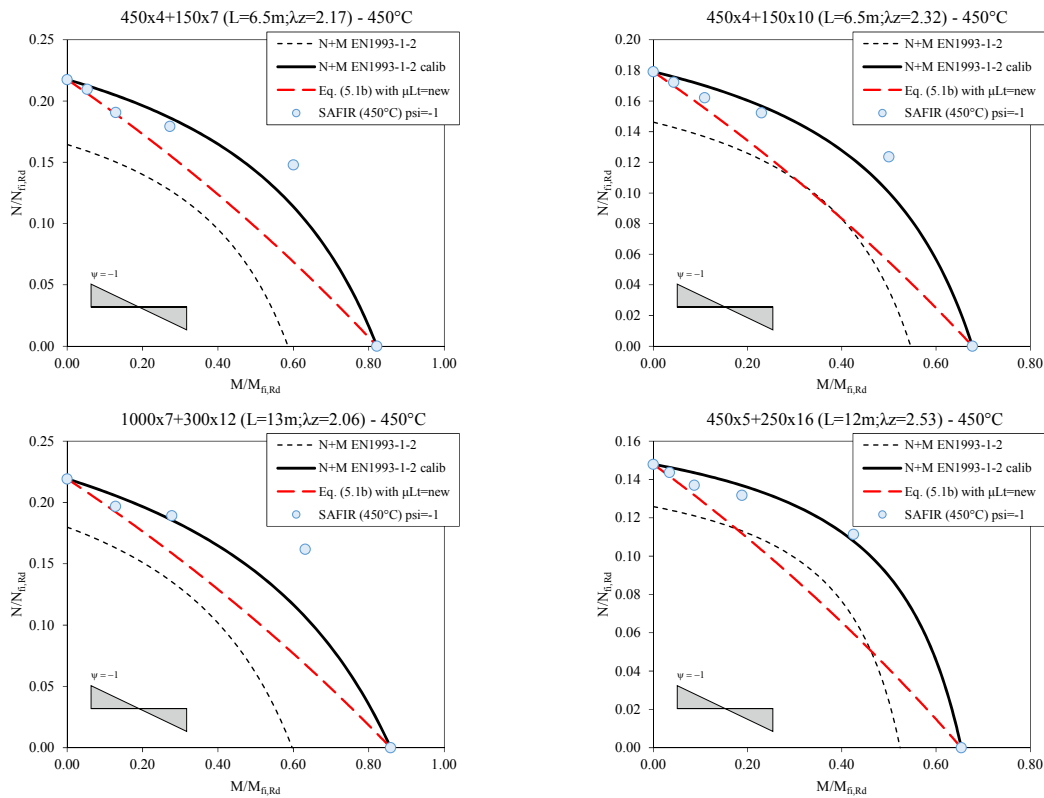


Figure 5.21: Improvements of the out-of-plane interaction curve for the bi-triangular cases.

With this proposal, improvements are introduced especially for the case of bi-triangular moment ($\psi = -1$), as depicted in Figure 5.21, that lead to the reduction of number of unsafe results (see Section 5.5).

In Figure 5.22, all the numerical results are plotted and compared with the interaction curve considering μ_{LT} from equation (5.13).

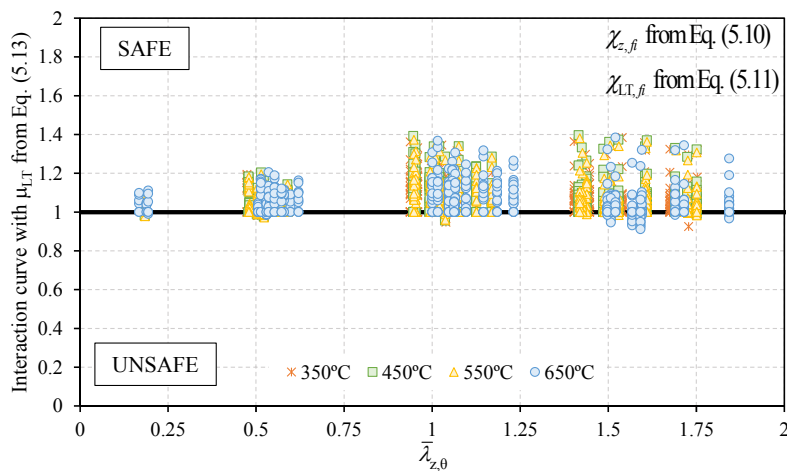


Figure 5.22: Comparison of interaction curve and the numerical cases studied using μ_{LT} from equation (5.13).

5.5 Statistical evaluation

Table 5.3 presents the statistical results for the beam-columns in fire situation for the various methods and both in-plane and out-of-plane directions. More than 3000 numerical simulations were considered for each direction. For each methodology, the mean value μ and the standard deviation s of the numerical results were calculated from:

$$\mu = \frac{\sum_{i=1}^n x_i}{n} \quad (5.14)$$

$$s = \sqrt{\frac{\sum_{i=1}^n (x_i - \mu)^2}{n - 1}} \quad (5.15)$$

where for each methodology, x_i is given according to equations (5.1a) and (5.1b) for in-plane or out-of-plane direction. Since in these expressions the ultimate loads obtained in SAFIR were considered as the design loads, a value higher than 1.0 yield a safe results. Accordingly, the maximum unsafe result is the maximum deviation obtained with equations (5.1a) and (5.1b). In this table, it is also indicated the percentage of unsafe results. For the EN1993-1-2 method, it can be seen that the standard deviation is high in both directions, with a considerable number of results unsafe for the in-plane buckling direction. In what concerns unsafe results in the in-plane direction, it was observed to be due to the EN1993-1-2 column design curve being slightly unsafe for some results (see Figure 5.6) and the expression for μ_y not being adequate for bi-triangular bending diagram (see 5.4.2). For the out-of-plane direction, the column design curve (see Figure 5.15) and beam design curve (see Figure 5.16) are mainly over-conservative in comparison to the numerical results, especially for the beam cases with triangular and bi-triangular bending diagrams, this leads to over-conservative results for the interaction curve with an average value of 1.29. For the methodologies where the reduction factors were calculated numerically (denoted “calibrated”) it is observed that the standard deviation is reduced, but the number of unsafe results also increases (from 25.72% to 29.14% for the in-plane direction and from 0.56% to 14.82% for the out-of-plane direction). To solve this, it were proposed modifications to

the interaction factors (μ_y and μ_{LT}) that reduce the number of unsafe results as seen for “ μ_y proposal” and “ μ_{LT} proposal” in the table.

Table 5.3: Statistical results of beam-columns in fire situation.

Direction	Methodology	Number cases (n)	Mean (μ)	StdDev (s)	Max. Unsafe	%Unsafe
In-plane	EN1993-1-2	3480	1.09	14.06%	0.83	25.72%
	EN1993-1-2 calibrated	3480	1.02	8.11%	0.83	29.14%
	μ_y proposal – equation (5.7)	3480	1.05	8.17%	0.88	12.53%
Out-of-plane	EN1993-1-2	3022	1.29	12.15%	0.89	0.56%
	EN1993-1-2 calibrated	3022	1.06	7.91%	0.84	14.82%
	μ_{LT} proposal – equation (5.12)	3022	1.06	7.72%	0.87	11.02%

5.6 New proposal according to the developments of this thesis

According to the developments of this thesis, the design buckling resistance at time t for a member without lateral restraints and with a Class 4 cross section subject to combined in-plane bending and axial compression in fire situation should be verified by satisfying the interaction curve defined by equations (5.13a) and (5.13b) for doubly symmetric cross-sections.

$$\frac{N_{fi,Ed}}{\chi_{\min,fi} A_{eff} k_{y,\theta} \frac{f_y}{\gamma_{M,fi}}} + \frac{k_y M_{y,fi,Ed}}{W_{eff,y,\min} k_{y,\theta} \frac{f_y}{\gamma_{M,fi}}} \leq 1 \quad (5.13a)$$

$$\frac{N_{fi,Ed}}{\chi_{z,fi} A_{eff} k_{y,\theta} \frac{f_y}{\gamma_{M,fi}}} + \frac{k_{LT} M_{y,fi,Ed}}{\chi_{LT,fi} W_{eff,y,\min} k_{y,\theta} \frac{f_y}{\gamma_{M,fi}}} \leq 1 \quad (5.13b)$$

with the effective properties A_{eff} and $W_{eff,y,\min}$ calculated according to the expressions given in Chapter 3, the reduction factor for the flexural buckling $\chi_{y,fi}$ and $\chi_{z,fi}$ according to the expressions of Eurocode 3 Part 1-2 but considering the new effective properties given in

Chapter 3, and the reduction factor for the lateral-torsional buckling $\chi_{LT,fi}$ as defined in Chapter 4 including the use of factor “ f ” to account for non-uniform bending diagrams.

The interaction factor k_y is calculated according to equation (5.14):

$$k_y = 1 - \frac{\mu_y N_{fi,Ed}}{\chi_{y,fi} A_{eff} k_{y,\theta} \frac{f_y}{\gamma_{M,fi}}} \leq 3 \quad (5.14)$$

and

$$\mu_y = (2\beta_{M,y} - 5)\bar{\lambda}_{y,\theta} + 0.44\beta_{M,y} + 0.29 \leq 0.2 \text{ but } \bar{\lambda}_{y,20^\circ\text{C}} \leq 1.1 \quad (5.15)$$

while k_{LT} is determined according to equation (5.16):

$$k_{LT} = 1 - \frac{\mu_{LT} N_{fi,Ed}}{\chi_{z,fi} A_{eff} k_{y,\theta} \frac{f_y}{\gamma_{M,fi}}} \leq 1 \quad (5.16)$$

with

$$\mu_{LT} = 0.45\bar{\lambda}_{z,\theta} \beta_{M,LT} - 0.15 \leq 0.2 \quad (5.17)$$

The equivalent uniform moment factors $\beta_{M,y}$ and $\beta_{M,LT}$ are given in Eurocode 3 Part 1-2. Table 5.3 presents the statistical results obtained using equations (5.13a) and (5.13b) to verify the buckling resistance of the numerical cases studied. In these results, the cross-section capacity has been calculated according to the simple proposal of Chapter 3 (see Tables 3.3 and 3.4).

Table 5.4: Statistical results for the new proposals.

Direction	Number cases (n)	Mean (μ)	StdDev (s)	MaxUnsafe	%Unsafe
In-plane equation (5.13a)	3480	1.17	13.94%	0.89	10.14%
Out-of-plane equation (5.13b)	3022	1.28	12.32%	0.91	0.89%

For sake of comparison, Table 5.5 presents the results obtained using the formulae of the Eurocode 3 Part 1-2. In this case, the cross-sectional resistance has been calculated with the actual formulae of the Eurocode 3 given in Tables 3.3 and 3.4 in Chapter 3.

Table 5.5: Statistical results according to Eurocode 3 Part 1-2.

Direction	Number cases (n)	Mean (μ)	StdDev (s)	MaxUnsafe	%Unsafe
In-plane equation (5.1a)	3480	1.13	15.72%	0.81	23.79%
Out-of-plane equation (5.1b)	3022	1.31	12.11%	0.97	0.13%

From the previous tables it is observed that the number of unsafe results reduced considerably from 23.79% to 10.14% for the in-plane direction and it is close for the out-of-plane direction (from 0.13% to 0.89%). For the in-plane direction, the average value increased 4% (from 1.13 to 1.17) but the standard deviation and the maximum unsafe result decreased, from 15.72% to 13.94% and from 0.81 to 0.89 respectively. For the out-of-plane direction, the improvements obtained with the new proposal are less noticeable, with the average decreasing from 1.31 to 1.28 and the maximum unsafe results from 0.97 to 0.91. Nonetheless, the proposals made in this thesis revealed to be safe and accurate when compared to the numerical results for the determination of the buckling resistance of slender beam-columns in case of fire.

5.7 Conclusions

In this chapter, the behaviour of beam-columns with Class 4 cross-section is investigated numerically. The accuracy of the existing interaction formulae of EN 1993-1-2 was analysed. The methodology of EN1993-1-2 is based on an interaction curve that can be divided into in-plane and out-of-plane direction. According to the obtained numeric results, this interaction curve proved to be very conservative for the out-of-plane direction but inconsistent for the in-plane direction. The main reason for this, is that for both cases it depends on the reduction factor for the column behaviour ($\chi_{y,fi}$ and $\chi_{z,fi}$) with the formulae

available in the EN 1993-1-2 for their calculation being conservative. However, for the particular case of in-plane direction with bi-triangular bending moment ($\psi = -1$) some unsafe results were observed for low slenderness of the member. Additionally, for the out-of-plane direction, lateral-torsional buckling (LTB) is accounted for by the appropriate reduction factor, $\chi_{LT,fi}$, which revealed to be very conservative, especially for the cases where the member is submitted to triangular and bi-triangular bending moment diagrams, $\psi = 0$ and $\psi = -1$, respectively. This has an accountable influence on the safety level of the interaction curve for the out-of-plane situation making it very conservative. In both cases, it is undeniable that the formulation of Part 1-2 of Eurocode 3 to calculate the beam-columns in case of fire will benefit from improved design rules for columns and beams.

In this chapter, the safety level of the interaction factors preconized in the beam-column formulae of EN1993-1-2 was also investigated removing the scatter associated with the reduction factors $\chi_{y,fi}$, $\chi_{z,fi}$ and $\chi_{LT,fi}$ by calculating them numerically. From the results of numerical investigation, it was observed that for beam-columns submitted to bi-triangular bending moments ($\psi = -1$), the current interaction factor lead to some unsafe results for both directions. Based on the same methodology used for the calibration of these factors when they were established in Part 1-2 of Eurocode 3, a new proposal has been made. These modifications allowed the reduction of the number of unsafe results while maintaining the same level of accuracy of the interaction curve.

Finally, it was presented the formulation of the interaction curve accounting with the developments in this thesis for the cross-section resistance (Chapter 3) and considering the $\chi_{LT,fi}$ calculated as in Chapter 4. The formulation proved to be safe and accurate for determining the resistance of beam-columns with slender cross-sections submitted to combine axial compression and bending about the major-axis in case of fire when compared to numerical results.

References

- [5.1] CEN, “EN 1993-1-1, Eurocode 3: Design of steel structures - Part 1-1: General rules and rules for buildings.” European Committee for Standardisation, Brussels, 2005.
- [5.2] Greiner R., “Background information on the beam-column interaction formulae at Level 1. Report # TC8-2001-002,” 2001.
- [5.3] Boissonnade N., Jaspart J.-P., Muzeau J.-P., Villette M., “Improvement of the interaction formulae for beam columns in Eurocode 3,” *Computers and Structures*, vol. 80, no. 27–30, pp. 2375–2385, November 2002.
- [5.4] Boissonnade N., Greiner R., Jaspart J.-P., “Rules for Member Stability in EN1993–1–1 Background documentation and design guidelines,” 2006.
- [5.5] CEN, “ENV 1993–1–1, Eurocode 3: Design of Steel Structures – Part 1–1: General rules and rules for buildings.” European Committee for Standardisation, Brussels, Belgium, 1992.
- [5.6] CEN, “EN 1993-1-2, Eurocode 3: Design of steel structures - Part 1-2: General rules - Structural fire design.” European Committee for Standardisation, Brussels, 2005.
- [5.7] Talamona D., “Flambement de poteaux métalliques sous charge excentrée à haute température (in French),” Thesis submitted to the University Blaise Pascal, Clermont–Ferrand, France, for the degree of Doctor of Philosophy in Civil Engineering. 1995.
- [5.8] Talamona D., Franssen J., “Stability of steel columns in case of fire: numerical modeling,” *Journal of Structural Engineering*, June 1997.
- [5.9] Vila Real P. M. M., Lopes N., Simoes da Silva L., Piloto P., Franssen J. M., “Towards a consistent safety format of steel beam-columns: application of the new interaction formulae for ambient temperature to elevated temperatures,” *Steel and Composite Structures*, vol. 3, no. 6, pp. 383–401, December 2003.
- [5.10] Vila Real P. M. M., Lopes N., Simões da Silva L., Piloto P., Franssen J.-M., “Numerical modelling of steel beam-columns in case of fire—comparisons with Eurocode 3,” *Fire Safety Journal*, vol. 39, no. 1, pp. 23–39, February 2004.

-
- [5.11] Lopes N., Simões da Silva L., Vila Real P. M. ., Piloto P., “New proposals for the design of steel beam-columns in case of fire, including a new approach for the lateral–torsional buckling,” *Computers & Structures*, vol. 82, no. 17–19, pp. 1463–1472, July 2004.
- [5.12] Knobloch M., Fontana M., Frangi A., “Steel beam-columns subjected to fire,” *Steel Construction*, vol. 1, no. 1, pp. 51–58, September 2008.
- [5.13] Kodur V. K. R., Dwaikat M. M. S., “Response of steel beam–columns exposed to fire,” *Engineering Structures*, vol. 31, no. 2, pp. 369–379, February 2009.
- [5.14] Dwaikat M. M. S., Kodur V. K. R., Quiel S. E., Garlock M. E. M., “Experimental behavior of steel beam–columns subjected to fire-induced thermal gradients,” *Journal of Constructional Steel Research*, vol. 67, no. 1, pp. 30–38, January 2011.
- [5.15] Quiel S. E., Garlock M. E. M., Dwaikat M. M. S., Kodur V. K. R., “Predicting the demand and plastic capacity of axially loaded steel beam–columns with thermal gradients,” *Engineering Structures*, vol. 58, pp. 49–62, January 2014.
- [5.16] Dwaikat M., Kodur V., “A simplified approach for evaluating plastic axial and moment capacity curves for beam–columns with non-uniform thermal gradients,” *Engineering Structures*, vol. 32, no. 5, pp. 1423–1436, May 2010.
- [5.17] Franssen J.-M., “SAFIR, A Thermal/Structural Program for Modelling Structures under Fire,” *Engineering Journal, A.I.S.C.*, vol. 42, no. 3, pp. 143–158, 2005.
- [5.18] Talamona D., Franssen J.-M., “A Quadrangular Shell Finite Element for Concrete and Steel Structures Subjected to Fire,” *Journal of Fire Protection Engineering* vol. 15, no. 4, pp. 237–264, November 2005.
- [5.19] Talamona D., Franssen J.-M., “New quadrangular shell element in SAFIR,” *First International Workshop "Structures in Fire"*, Copenhagen, Denmark, June, 2000.
- [5.20] Talamona D., Franssen J.-M., “Nonlinear thin shell finite element for steel and concrete structures subjected to fire: theoretical development,” *Journal of Applied Fire Science*, 2002.
- [5.21] CEA, “CAST 3M is a research FEM environment; its development is sponsored by the French Atomic Energy Commission <<http://www-cast3m.cea.fr/>>.” 2012.

- [5.22] Couto C., Vila Real P., Lopes N., “RUBY - an interface software for running a buckling analysis of SAFIR models using Cast3M.” University of Aveiro, 2013.
- [5.23] CEN, “EN 1993-1-5, Eurocode 3 - Design of steel structures - Part 1-5: Plated structural elements.” European Committee for Standardisation, pp. 1–53, Brussels 2006.
- [5.24] CEN, “EN 1090-2: Execution of steel structures and aluminium structures - Part 2 : Technical requirements for steel structures.” European Committee for Standardisation, Brussels, 2008.
- [5.25] Vila Real P. M. M., Cazeli R., Simões da Silva L., Santiago a., Piloto P., “The effect of residual stresses in the lateral-torsional buckling of steel I-beams at elevated temperature,” *Journal of Constructional Steel Research*, vol. 60, no. 3–5, pp. 783–793, March 2004.
- [5.26] Franssen J.-M., Schleich J.-B., Cajot L.-G., “A simple model for the fire resistance of axially-loaded members according to eurocode 3,” *Journal of Constructional Steel Research*, vol. 35, no. 1, pp. 49–69, 1995.
- [5.27] ECCS, *Ultimate limit state calculation of sway frames with rigid joints. Publication No. 33.* European Convention for Constructional Steelwork Technical Committee No. 8, 1984.
- [5.28] ECCS, *Manual on Stability of Steel Structures. Publication No. 22.* European Convention for Constructional Steelwork Technical Committee No. 8, 1976.
- [5.29] ECCS, *New lateral torsional buckling curves k_{LT} - numerical simulations and design formulae.* European Convention for Constructional Steelwork Technical Committee No. 8, 2000.
- [5.30] Couto C., Vila Real P., Lopes N., Zhao B., “Resistance of steel cross-sections with local buckling at elevated temperatures,” *Journal of Constructional Steel Research*, vol. 109, pp. 101–114, June 2015.

Chapter 6 Conclusions

Chapter outline

- 6.1 General description of the work developed
 - 6.2 Chapter 2 – Plates
 - 6.3 Chapter 3 – Cross-sections
 - 6.4 Chapter 4 – Beams
 - 6.5 Chapter 5 – Beam-Columns
 - 6.6 Future developments
- References

Abstract This final chapter presents a general description and the main findings of the work developed within the research programme of this thesis. The key conclusions as well as critical remarks are described for each chapter. To conclude, future developments and research guidelines are delineated and discussed.

6.1 General description of the work developed

The work done in this thesis aimed at the development of simplified design rules for steel members with H or I shape Class 4 cross-section in case of fire, with special focus on beams and beams-columns.

First the accuracy of the existing fire design rules given in the informative Annex E of Part 1-2 of Eurocode 3 [6.1] for members with Class 4 cross-sections were investigated. In Chapter 2, it was concluded that using the proposed methodology of Eurocode 3 to deal with Class 4 cross-sections, namely using the effective width method given in Part 1-5 of Eurocode 3 [6.2] with a reduced design value of the steel yield strength (corresponding to 0.2% proof strength) leads to inaccurate determination of the ultimate buckling strength of thin plates in case of fire. In Chapter 3, the capacity of Class 4 cross-sections was investigated and it was concluded that the Eurocode 3 method was underestimating the resistance of the cross-sections mainly because the additional reserve of resistance provided by non-Class 4 plates is not accounted for by the current methodology. Additionally, it was concluded from these two chapters that local buckling may occur prior to the full development of axial plastic resistance or elastic bending resistance, thus Class 3 cross-sections were also investigated and treated as if they were prone to local buckling. Chapters 4 and 5 deal with the behaviour of beams and beam-columns respectively with slender (Class 3 and 4) cross-sections. It was concluded that the design provisions of Eurocode 3 for beams and beam-columns, were mainly conservative. The current simple design methods of Part 1-2 of Eurocode 3 were developed for Class 1 and 2 cross-sections and, when applied to Class 3 and Class 4 cross-sections demonstrated to be inadequate and that it could be improved.

The need of improved design rules for members with Class 3 and 4 cross-sections is implicit, and was addressed throughout this work and a contribute for better fire design of members with slender cross-sections was presented. In Chapter 2 analytical expressions that allow for a closer prediction of the ultimate strength of thin-plates were developed and then used in Chapter 3 to provide a methodology to calculate the cross-sectional capacity in case of fire. This new methodology was later used to assess the accuracy of the existing design rules for beam and beams-columns and also as the basis for the development of new formulae.

In Chapter 4, for beams with slender cross-sections, new curves for the design against lateral-torsional buckling were proposed, these expressions account with the influence of the interaction between the lateral-torsional buckling and the local buckling through a parameter denominated as the effective section factor. The imperfection factor normally used in the lateral-torsional buckling design formulae was calibrated and defined as a function of the effective section factor and a plateau was also introduced into the design formulae.

Beam-columns with slender cross-sections were studied in Chapter 5. The failure in strong-axis (designated in this document as in-plane buckling) and the weak-axis (designated as out-of-plane buckling) was investigated. Although conservative results were obtained, a good fit between numerical results and the Eurocode 3 interaction curve was generally observed, the reason is that the reduction factors to account with the column behaviour (flexural buckling) and the beam behaviour (lateral-torsional buckling) are conservative and influence the accuracy of the beam-column interaction curve. If this accumulated error is eliminated, good correlation is obtained between the numerical results and the interaction formulae. Nonetheless, for the in-plane case, however, the numerical results were slightly unsafe for beam-columns submitted to bi-triangular bending diagram ($\psi = -1$) and so a modification to the interaction factors was proposed to account with this difference.

The particular conclusions and remarks for each chapter of the thesis are addressed in the next sections.

6.2 Chapter 2 – Plates

In Chapter 2 the behaviour at elevated temperatures of individual thin steel plates that form the slender cross-sections was addressed. The influence of local buckling in the ultimate load bearing capacity of the plates in case of fire was investigated by performing several analyses based on shell finite elements.

At normal temperature, it was concluded that the numerical results obtained with shell finite elements do fit well on the existing design expressions given in Part 1-5 of Eurocode 3 [6.2] to calculate the effective width of the plates and thus the ultimate resistance of the plates, except for the internal elements under compression. In this case, the design expressions may have been defined considering a less severe geometrical imperfection than that currently

recommended by Part 2 of EN 1090 [6.3]. This may lead to inaccurate estimation of the cross-sectional capacity at normal temperature and further studies should be done to confirm this.

In case of fire, as mentioned, the Eurocode 3 recommends for Class 4 plates the same equations as for normal temperature to calculate the effective width of the plates and the 0.2% proof strength as the design yield strength to assess their capacity. Good agreement with the numerical results was achieved with this method, however, for plates with lower non-dimensional slenderness, especially in the range of Class 3, the Eurocode 3 failed to predict the ultimate strength of these plates. Consequently, this leads to overestimation of the capacity of Class 3 cross-sections as observed in Chapter 3. On the other hand, considering a different yield stress for steel demonstrated to have impact on the cross-sectional capacity as seen in Chapter 4: the non-Class 4 plates provide additional resistance to the cross-section which is not accounted for by the current methodology of Eurocode 3, leading to the underestimation of the cross-sectional capacity.

In this chapter, expressions for the effective width method to account for the local buckling at elevated temperatures were developed. These new expressions enable for the calculation of the effective cross-section properties and resistance using the strength at a total strain of 2% as the steel design yield stress as done for the other classes. This led to a better agreement between FEA results and the expressions to calculate the cross-sectional resistance in Chapter 3.

The new expressions are temperature dependant resulting in a variation of the effective cross-section properties under fire situation and although the method herein proposed can be implemented with relatively ease of computational effort if compared with the actual design rules, it was also demonstrated that the proposal corresponding to a constant steel temperature of $\theta_a = 700^\circ C$ could be used as the lower bound for the effective properties. In Chapter 3, this simplification was further developed in order to have a consistent and simple design methodology to calculate the cross-sectional resistance.

Some remarks are noticed here. First it was observed that the geometric imperfections have a considerable influence on the ultimate resistance of the plates and in this case imperfections were considered according to EN 1090-2 [6.3] by following the recommendations of

Part 1-5 of Eurocode 3, thus other values of geometrical imperfection amplitude may lead to distinct behaviour and should be investigated. The second remark is related to the temperature distribution that was considered uniform. In this case, non-uniform distribution of temperatures may have a non-negligible influence in the ultimate capacity of the plates and could be addressed in the future. As a final remark on this chapter, although these expressions were developed for simply supported plates considered separately, other supports and loading conditions could have been considered, in theory, by an appropriate plate buckling factor. The most interesting part would have been to take into account with the interaction between the plates, as for instance, Seif and Schafer [6.4] have made, by developing expressions to calculate the plate buckling factor for several hot-rolled cross-sections. These principles in the future could be extended as well as to consider non-uniform temperature distributions within the cross-section which was not covered in this thesis.

To conclude, the expressions developed within this chapter allow for a better prediction of the ultimate capacity of thin-plates at elevated temperature and thus provide a better solution to account for local buckling in case of fire.

6.3 Chapter 3 – Cross-sections

In Chapter 3, the resistance of several cross-sections where local buckling can occur under axial compression and bending about the major-axis was investigated at elevated temperatures using shell finite elements. The expressions to calculate the effective width in case of fire developed in the previous chapter (Chapter 2) were used in the definition of a new methodology to calculate the cross-sectional capacity of sections prone to local buckling in case of fire.

As noted in the previous section, the actual provisions of Eurocode 3 Part 1-2 to calculate the cross-sectional resistance leads to simultaneous to very conservative and to unsafe results when compared to the numerical results. Three reasons were highlighted in this chapter. First, the effect of the temperature on the local buckling at elevated temperatures is not correctly taken into account when considering the effective properties determined based on the material properties at normal temperature. Secondly, local buckling occurs prior to what is currently assumed especially for Class 3 cross-sections. Third, considering the 0.2 % proof

strength as the design yield strength, for the whole cross-section is restrictive if the cross-section has non-Class 4 elements.

To overcome these limitations, a new methodology to calculate the resistance of cross-sections with local buckling at elevated temperatures was defined in this chapter based on the effective width expressions at elevated temperatures developed in Chapter 2. Accordingly, the influence of local buckling in the decrease of resistance in case of fire is better taken into account. It was concluded that using the effective cross-section determined with those expressions and the strength at a total 2% strain – $f_{y,\theta}$, as the design yield strength when calculating the capacity of slender cross-sections, the additional resistance provided by the plates that do not have local buckling is considered, leading to an economic yet safe design. On the other hand, it was shown that by calculating an effective cross-section for Class 3 cross-sections at elevated temperatures that the decrease of resistance due to local buckling is also accounted for in these cases. The possibility of considering these cross-sections as Class 4, and to study the modifications to limits used in the classification of the cross-sections could be addressed in the future and was not covered in this work.

In this chapter, only H and I shape cross-sections were investigated and regarding the bending direction only bending in strong-axis was considered. As mentioned in the previous section, the expressions developed in Chapter 2 to calculate the effective width are not limited to H and I shape cross-sections but, nonetheless, their validity should be confirmed and the work done in this chapter be extended to square and rectangular cross-sections. In terms of bending in the weak-axis, in Chapter 2 outstand plates submitted to bending were not investigated and that should be covered in the future.

Finally and to conclude, for sake of simplicity, two proposals were presented in this chapter to calculate slender cross-section's resistance in case of fire: a more complex yet rigorous approach which is temperature dependent, meaning that an effective cross-section has to be determined for each temperature, and a simplified proposal that does not depend on the temperature and enables prompt calculations yet safe and accurate.

6.4 Chapter 4 – Beams

In this chapter, the behaviour of laterally unrestrained beams with slender cross-sections was investigated. The aim was to study existing design provisions of Eurocode 3 to check the lateral-torsional buckling in case of fire and to develop improved design methods.

First, the actual provisions of Part 1-2 of Eurocode 3 for checking the lateral-torsional buckling resistance of beams with slender cross-sections were analysed. It was demonstrated that inaccurate results were obtained mainly due to the cross-sectional capacity being inconsistently calculated. This was in line with the previous chapters of the thesis, and by using the methodology developed in Chapter 3 to calculate the cross-section capacity improvements were observed.

Nonetheless, in this chapter an improved design method was developed. For that purpose, several parameters were investigated in order to attain their influence on the lateral-torsional buckling of beams with slender cross-sections in case of fire. It was found that the capacity of the beams was mainly influenced by the interaction between the local buckling and the lateral-torsional buckling and that it depended on the steel grade as well. For the first, an effective section factor was proposed for this ratio $s = W_{eff,y}/W_{el,y}$ and different ranges were defined according to the influence of the local buckling on the lateral-torsional buckling resistance of beams: i) for $W_{eff,y}/W_{el,y} \leq 0.8$ it is high; ii) for $0.8 < W_{eff,y}/W_{el,y} \leq 0.9$ it is moderate and iii) for $W_{eff,y}/W_{el,y} > 0.9$ it is small. In respect to the steel grade, the proposed design method accounts with this influence through the parameter \mathcal{E} which was already the case in the current design formulae of Eurocode 3.

In terms of the interaction between local buckling and lateral-torsional buckling, the proposed philosophy of dealing with such a complex subject by grouping the behaviour of beams into several ranges of effective section factor must be subject to some considerations. This factor is somehow analogous to the depth-to-width (h/b) ratio on the formulae at room temperature. In that case, The depth h/b ratio of a cross-section is used in Part 1-1 of Eurocode 3 to group the properties of the sections and take into account a variety of factors such as the torsional stiffness or the critical behaviour in plasticity as pointed out in [6.5]. In the future, this interaction could be further investigated and developed and at best have an

effective section factor that is dependent on other variables such as the second moment of area in the strong-axis and weak-axis (I_y and I_z , respectively) that lead to better allowance for the interaction between local buckling and lateral-torsional buckling.

In the final part of the chapter, the proposal was also compared with the use of the factor “ f ” to take into account different loading cases. This factor was originally developed for Class 1 and 2 beams and demonstrated to be rather accurate for beams submitted to uniform distributed loads and triangular bending moments ($\psi = 0$). For the bi-triangular case ($\psi = -1$) it was observed that the original proposal for the factor “ f ” lead to some unsafe results and a lower bound of $f \geq 0.8$ was proposed leading to better agreement between the results and the simplified design methods. A remark on this subject should be made, further investigation should be developed in order to understand better the influence of the loading on the capacity of beams with slender cross-sections. The case where the shear stress is higher and constant on the beam ($\psi = -1$) is the one that leads to higher discrepancy between the original proposal for factor “ f ”. Since cross-sections with slender webs are considered here, the interaction between the shear stresses and the bending moment may not be negligible and needs to be analysed in more detail. Also, for the bi-triangular case, only $\psi = -1$ has been considered and a limitation is proposed for $f \geq 0.8$. The 0.8 value corresponds to the factor “ f ” for $\psi = 0$. The practical implications of using this limit is that for bi-triangular bending moments ($\psi < 0$) the factor “ f ” remains unchanged and this may be too conservative for some situations.

Finally it was concluded that the new proposal developed in this chapter allows for better prediction of the capacity of beams with slender cross-sections against lateral-torsional buckling in case of fire.

6.5 Chapter 5 – Beam-Columns

This chapter focused on the behaviour of beam-columns with slender cross-section. A numerical investigation using shell finite elements was performed to evaluate the accuracy of existing interaction formulae of Eurocode 3.

The actual methodology of Part 1-2 of Eurocode 3 to check the resistance of members submitted to combine axial compression with bending in case of fire is based on an interaction curve that can be separated into in-plane and out-of-plane direction. For both directions, this methodology proved to be unreliable: for the in-plane direction (buckling in the strong-axis) both very conservative and unsafe results were obtained. For the first, the reason for such results is that the reduction factor for the column behaviour – $\chi_{y,fi}$ – provided in Part 1-2 of Eurocode 3 is already conservative in some cases and has a favourable influence on the interaction curve. For the latter, it was observed that the interaction factor when the beam-column is submitted to bi-triangular moments loading case ($\psi = -1$) was not adequate and lead to some unsafe results. This behaviour is in accordance with what was obtained in Chapter 4 for the beams: for the cases where the shear stresses are more important the resistance deviates more from the existing design methodologies. The interaction between the shear stresses and bending moments was not exploited in this thesis because it was out of the scope of the present research programme, however this subject should be addressed in the future and better formulae to take into account with this phenomenon should also improve the proposals made within this thesis. For the out-of-plane direction, the interaction curve also relies on the calculation of the reduction factor for the lateral-torsional buckling (LTB) which demonstrated in Chapter 4 to be very conservative especially for the cases where the member is submitted to triangular and bi-triangular bending moment diagrams, $\psi = 0$ and $\psi = -1$. This has an accountable influence on the safety level of the interaction curve for the out-of-plane situation, making it very conservative. Consequently, it was concluded that for both directions, the formulation of Part 1-2 of Eurocode 3 to calculate the beam-columns in case of fire could benefit with improved design rules for columns and beams.

In accordance with the last statement, in this chapter, the safety level of the current interaction curve was also analysed but considering the reduction factors $\chi_{y,fi}$, $\chi_{z,fi}$ and $\chi_{LT,fi}$ obtained numerically. This allowed to observe that for beam-columns submitted to bi-triangular bending moments ($\psi = -1$), that the current interaction factor lead to some unsafe results for both directions. Based on the same methodology used for the calibration of these factors [6.6] when they were established in Part 1-2 of Eurocode 3, a new proposal has been

made. These modifications allowed the reduction of the number of unsafe results while maintaining the same level of accuracy of the interaction curve.

This chapter contains also the formulation of a proposal for the interaction curve according to the developments of this thesis to check the buckling resistance of slender beam-columns submitted to combined axial compression and bending in the major-axis at elevated temperatures. It was concluded that this proposal leads to conservative results for the cases studied.

6.6 Future developments

As any research study, the present work is delimited in a time period. Several questions were left open in the present document. Although some general remarks have been highlighted in the previous section of the current chapter, here some guidelines for further work are described.

The subject of **cross-section classification in case of fire** should be further investigated. The developments on this thesis demonstrated that cross-sections with Class 3 were also prone to local buckling and it was suggested that an effective cross-section should be calculated also for these types of cross-sections. However, it could be studied the modifications for the classification limits for the cross-sections and the effective cross-section be determined only for Class 4 cross-sections.

The existing design provisions of Eurocode 3 recommend a critical temperature of 350°C to be considered if no additional calculation is performed to assess the resistance of the members with Class 4 cross-section. Following the research conducted in this thesis and the new design methods developed, investigation towards a **higher prescribed temperature** could be proposed and compared against numerical results.

Cross-sections with different shape, the proposed methods developed in this thesis were based mainly on I and H shape cross-sections. Numerical investigations considering other shapes of cross-sections, namely rectangular and square hollow sections could be addressed in the future.

The **interaction between shear force and bending moment** may influence the response of members with slender cross-section. Although the proposals made within this thesis may account with this influence, for instance in the limitation of the “ f ” factor for bi-triangular bending diagram ($\psi = -1$, see Chapter 4), further investigation should address this matter in the future.

The **effect of non-uniform temperature**, should be seen as a future improvement on the current proposals. It is unclear how the non-uniform temperature distribution along the plates, the cross-sections and the members affect the conclusions in this work. It is assumed that considering a constant temperature along the cross-section is the worst scenario for assessing the capacity of the members in case of fire so it is foreseen that a non-uniform temperature distribution may have a favourable influence that could be accounted for in the design formulae.

Finally, the **proposed methods to design beams against lateral-torsional buckling could be extended to room temperature design**. Following the same methodology used within this thesis, the development of a methodology to account with the interaction between local buckling and lateral-torsional buckling by means of an effective section factor at room temperature is possible.

References

- [6.1] CEN, “EN 1993-1-2, Eurocode 3: Design of steel structures - Part 1-2: General rules - Structural fire design.” European Committee for Standardisation, Brussels, 2005.
- [6.2] CEN, “EN 1993-1-5, Eurocode 3 - Design of steel structures - Part 1-5: Plated structural elements.” European Committee for Standardisation, Brussels, 2006.
- [6.3] CEN, “EN 1090-2: Execution of steel structures and aluminium structures - Part 2 : Technical requirements for steel structures.” European Committee for Standardisation, Brussels, Belgium, 2008.
- [6.4] Seif M., Schafer B. W., “Local buckling of structural steel shapes,” *Journal of Constructional Steel Research*, vol. 66, no. 10, pp. 1232–1247, October 2010.
- [6.5] Taras A., Greiner R., “New design curves for lateral–torsional buckling—Proposal based on a consistent derivation,” *Journal of Constructional Steel Research*, vol. 66, no. 5, pp. 648–663, May 2010.
- [6.6] Talamona D., “Flambement de poteaux métalliques sous charge excentrée à haute température (in French),” Thesis submitted to the University Blaise Pascal, Clermont–Ferrand, France, for the degree of Doctor of Philosophy in Civil Engineering. 1995.